Decoding insect feeding: identification of regulatory components mediating insect-specific defense responses in plants.

Dissertation

Zur Erlangung des akademischen Grades

doctor rerum naturalium (Dr. rer. nat.)

Vorgelegt dem Rat der Biologisch-Pharmazeutischen Fakultät

der Friedrich-Schiller-Universität Jena

von Paola Gilardoni

geboren am 30. Juli 1981

in Rosario, Argentinien.

Gutachter

1. Prof. Dr. Ian T. Baldwin

2. Prof. Dr. Ralf Oelmüller

3. Prof. Raquel Chan

Datum der öffentlichen Verteidigung: 02.09.2011

Table of contents

Table of contents

Chapter 1: General introduction

Nicotiana attenuata in its natural environment

Nicotiana attenuata is an annual plant native to the Great Basin desert in the southwestern USA that grows in post-fire environments. *N. attenuata* plants germinate in nitrogen-rich soils after the seeds are exposed to cues contained in wood smoke (Baldwin and Morse, 1994). This synchronized germination behavior creates strong intra-specific competition, and *N. attenuata* plants must allocate their resources to sustain rapid growth and maximize seed set. *N. attenuata* monocultures also experience high herbivore pressure. Presumably in order to maximize the efficiency of their defense while maintaining competitive growth, these plants have developed a complex system of induced responses to defend against or tolerate herbivory (Baldwin, 1998). In its natural habitat, *N. attenuata* is attacked by unpredictable herbivore communities, for example the piercing-sucking herbivores *Tupiocoris notatus* (mirid) and *Empoasca* spp. (leafhopper), the chewing herbivores *Diabrotica undecimpunctata tenella* (spotted cucumber beetle), *Epitrix hirtipennis and E. subcrinit* (flea beetles), *Spodoptera exigua* (beet armyworm) and larvae of the specialists *Manduca sexta* (tobacco hornworm) and *M. quinquemaculata* (tomato hornworm). *N. attenuata*'s short generation time (time between seed germination and production of flowers), the complexity of induced defenses, self-compatibility and amenability to transformation by inverted repeated RNA interference and virus induced gene silencing (VIGS) makes it a good model for ecological and molecular studies.

A

B

Figure 1. (A) *Nicotiana attenuata* plants in their natural habitat (Great Basin desert, USA). (B) *N. attenuata*'s main herbivore, *Manduca sexta*. Photo courtesy: D. Kessler.

Chapter 1

Plant defense responses

Plants respond to insect attack with a broad array of defenses which are generally divided into indirect and direct defenses. Indirect defenses are plant traits that attract predators and parasitoids of herbivores and thereby reduce the number of feeding herbivores (Kessler and Baldwin, 2002; Arimura et al., 2005). On the other hand, direct defenses comprise all plant traits that affect insect host selection and performance including thorns, thricomes, spines, antinutritive proteins, antidigestive proteins and toxic or deterrent secondary metabolites (Kessler and Baldwin, 2002; Chen, 2008). The term "secondary metabolites" is used to classify metabolites for which no role had yet been found in growth, photosynthesis, reproduction and/or development (Croteau, 2000). Based on their chemical structure and biosynthesis they can be classified into three major groups: 1) terpenes (e.g., mono-, sesqui-, di- and tri-terpenes, saponins), 2) phenolics (e.g., lignins, flavonoids, quinones), and 3) nitrogen-containing compounds (e.g., cyanogenic glycosides, glucosinolates, alkaloids; Croteau, 2000). Some antidigestive proteins interfere with insect digestive enzymes (proteases and amylases) and are thus termed protease and amylase inhibitors (Chen, 2008). In many plant species (e.g., tomato, tobacco, potato, soybean, cowpea) the induction of protease and amylase inhibitors is triggered in response to insect attack. Other antidigestive proteins disrupt the ephitelium of the insect digestive tract, including cystein proteases and lectins (Chen, 2008). Antinutritive proteins like amino acid deaminases and polyphenol oxidases decrease the nutritive value of plant tissues. For example, in tomato, arginase and threonine deaminase deplete the essential amino acids arginine and threonine in the midgut of *M. sexta* larvae and are induced upon *M. sexta* folivory (Chen et al., 2005). Polyphenol oxidases cross-link proteins and oxidize phenolic secondary metabolites to toxic quinones (Kessler and Baldwin, 2002).

Induced versus constitutive defense responses

Some plant defense traits are produced constitutively: for example, in *Arabidopsis thaliana*, glucosinolates are expressed in all tissues and only activated upon herbivory when they are hydrolyzed into toxic isothiocyanates and nitriles (Wittstock and Gershenzon, 2002). On the other hand, a plethora of defenses are synthesized or mobilized, i.e., induced only in response to plant tissue damage. For example, in solanaceous plants (e.g., tomato, tobacco, potato) serine protease inhibitors are induced

upon herbivory (Lawrence and Koundal, 2002), whereas in maize a cystein protease is induced after lepidopteran attack (Chen, 2008).

Among the best-studied toxic induced defenses is the alkaloid nicotine used by tobacco plants to effectively ward off generalist insects and browsing mammals. Nicotine has been extensively used as an insecticide because it binds to receptors of the excitatory neurotransmitter acetylcholine and is thereby toxic to all heterotrophs with neuromuscular junctions (Baldwin, 2001; Millar and Denholm, 2007). *M. sexta* feeding induces multiple other defenses including protease inhibitors (PIs) and secondary metabolites known as 17-hydroxygeranyl-linalool diterpene glycosides (HGL-DTGs). HGL-DTGs are a diverse group of terpenoid metabolites; and in *N. attenuata* a total of 11 structures were identified which differ from each other in their sugar moieties and the number of malonyl sugar esters (0-2) (Heiling, Schuman et al., 2010). Additionally, two phenylpropanoid-polyamine conjugates (PPCs), caffeoylputrescine (CP) and dicaffeoylspermidine (DCS), are induced upon herbivory and play important roles in *N. attenuata*'s defense response against herbivores (Kaur et al., 2010). When *N. attenuata* plants are engineered to produce reduced amounts of these compounds (HGL-DTGs, nicotine, PPCs and PIs) they become severely compromised in their capacity to survive *M. sexta* attack, and *M*. *sexta* larvae grow larger (Steppuhn et al., 2004; Zavala et al., 2004; Jassbi et al., 2008; Kaur et al., 2010). Thus these secondary metabolites are required to mount a full defense response against *M. sexta*.

Additionally to its cocktail of direct defenses, *N*. *attenuata*, like many plants, emits a bouquet of volatile organic compounds (VOCs) upon herbivory (Kessler and Baldwin, 2002). Herbivore-induced VOCs can function as an indirect defense, attracting predators and parasitoids of herbivores to their prey feeding on the attacked plant. Well-described examples are the blend of VOCs release by plants in response to the attack different lepidopteran species including *S. exigua*, *M. sexta* and *Heliothis virescens* among others (Tumlinson and Lait, 2005; Kessler and Baldwin, 2002). Green leaf volatiles (GLVs, C_6-alcohols and –aldehydes) emitted by *N. attenuata* plants in response to *M. sexta* herbivory attract the generalist predator *Geocoris* spp (Allmann and Baldwin, 2010). An additional plant indirect defense is the production of extrafloral nectar rich in carbohydrates and

proteins. Extrafloral nectar production is induced upon herbivory and it is a nutritious reward for predators of herbivores like wasps, ants and spiders (Heil et al., 2001).

Regulation of defense responses

Plant hormones, or phytohormones, are small signaling molecules with a broad and complex, yet specific action spectrum which often exert their effects at low concentrations. They are known to regulate plant growth, development and responses to biotic and abiotic stress (Davies, 1995; Nemhauser et al., 2006; Bari and Jones, 2009). “Classic” phytohormones with long-known roles in plant development and stress responses are auxins, cytokinins, ethylene (ET), abscisic acid (ABA) and gibberellins (Bari and Jones, 2009); additionally, jasmonates (JAs, derivatives of jasmonic acid [JA]), salicylic acid (SA), and brassinosteroids have been more recently demonstrated as phytohormones (Bari and Jones, 2009). In plant-herbivore interactions, the production of induced defenses is tightly controlled by the fine-tuned orchestration of signal transduction pathways, especially those of JAs, SA and ET. JAs are key players in the orchestration of the plant defense response against herbivores, while the role of ET and SA in herbivore-induced responses is to modulate the JA-dependent defense response via cross-signaling mechanisms (see “Cross-signaling between JAs, SA and ET in plant defense responses”; Reymond and Farmer, 1998; Bari and Jones, 2009).

Oxylipins

Oxylipins are a diverse group of biologically active compounds, including the JAs, derived from the metabolism of polyunsaturated fatty acids (PUFAs; Howe and Schilmiller, 2002). Oxylipin biogenesis in plants is stimulated by diverse stresses including wounding, insect and pathogen attack, and proceeds through distinct enzymatic activities that generate different oxygenated derivatives (Howe and Schilmiller, 2002; Farmer et al., 2003). In one of the first induced chemical reactions, 13-lipoxygenases (13-LOXs) introduce molecular oxygen to the PUFAs linoleic (18:2) and linolenic acid (18:3), converting them to 13-hydroperoxides. In leaves, 13-hydroperoxides serve as substrates for two major biosynthetic pathways induced by wounding and insect herbivory: 1) the

allene oxide synthase (AOS) pathway and; 2) the hydroperoxide lyase (HPL) pathway, both of which begin in the chloroplast.

The allene oxide synthase (AOS) branch transforms 13-hydroperoxides to 12-oxo-phytodienoic acid (12-OPDA) which in the peroxisome is subjected to 3 rounds of β-oxidation to yield jasmonic acid (JA; Schaller et al., 2004). JA is conjugated to isoleucine (Ile) by JAR enzymes (JAR4 and JAR6 in *N. attenuata;* Staswick and Tiryaki, 2004; Wang et al., 2007) to produce the active signal molecule JA-Ile (Fonseca et al., 2009). JA-Ile binds to the SCF^{coi1} (for Skp1-Cullin-F-box) E3 ubiquitin ligase complex, causing the degradation of JAZ (jasmonate-ZIM domain) repressor proteins and permitting the transcription of jasmonate-elicited genes (Fonseca et al., 2009; Yan et al., 2009). Alternatively, JA may be modified by conjugation to amino acids, sugars or methyl groups; these compounds together with 12-OPDA and JA-Ile are collectively defined as jasmonates (JAs; Schaller et al., 2004). JAs mediate plant defense responses to many herbivores including caterpillars, spider mites, thrips, phloem-feeders, beetles and also to necrotrophic pathogens (Bari and Jones, 2009). In tomato, spider mite and western flower thrip feeding is increased when plants are unable to produce JAs and consequently impair in the accumulation of protease inhibitors (PI; Li et al., 2002). Arabidopsis, the legume *Medicago truncatula* and *N. attenuata* require a functional jasmonate pathway to mount a full defense response against the chewing herbivores *S. littoralis* or *Pieris rapae* and phloem-feeders (Bodenhausen and Reymond, 2007; Gao et al., 2007).

In the hydroperoxide lyase (HPL) branch, HPL cleaves 13-hydroperoxides to generate the green leaf volatiles (GLVs) hexanal and (3*Z*)-hexenal and (9*Z*)-traumatin (12-oxo-9*Z*-dodecenoic acid; Vick and Zimmerman, 1976). GLVs and (9*Z*)-traumatin may be further modified, isomerized or conjugated (Grechkin, 2002). The role of GLVs as chemical cues during herbivore and pathogen attack has been extensively studied both biochemically and functionally (Croft et al., 1993; Baldwin, 2010). However, less attention has been paid to the metabolism and signaling capacities of the C_{12} derivatives of the HPL pathway. **In Manuscript III, I contributed to the study of the fluxes and metabolism of C_{12} derivatives of the HPL pathway in *N. attenuata* plants after wounding and *M. sexta* OS elicitation**.

Salicylic acid

Salicylic acid (SA) can be synthesized in the chloroplast or in the cytosol from cinnamic acid by two possible pathways (Vlot et al., 2009). In one, a side-chain decarboxylation of cinnamic acid produces benzoic acid, which undergoes a 2-hydroxylation event to yield SA (Lee et al., 1995). Alternatively, cinnamic acid is first 2-hydroxylated to *o*-coumaric acid and then decarboxylated to SA (Lee et al., 1995). Post-synthesis, SA undergoes several modifications such as glycosilation, methylation and amino acid conjugation (Loake and Grant, 2007). SA is involved in responses to biotic and abiotic stresses, as well as growth and developmental processes such as seed germination, photosynthesis, thermogenesis and flowering (Rivas-San Vicente and Plasencia, 2011). SA is also required for establishing systemic acquired resistance (SAR) and thus plays a crucial role in the elicitation of defense responses against biotrophic pathogens such as the production of pathogenesis-related (PR) proteins (Ryals, 1996). For example, in tobacco, infection with the tobacco mosaic virus (TMV) increases SA levels and PR gene expression (Vlot et al., 2009). Similarly, SA levels are highly increased in cucumber after inoculation with tobacco necrosis virus or *Pseudomonas syringae*, and this is followed by SAR development (Vlot et al., 2009).

Ethylene

The biosynthesis of ethylene (ET) occurs in the cytoplasm with the conversion of *S*-adenosyl-methionine (*S*-AdoMet) to ACC (1-aminocyclopropane-1-carboxylic acid) by ACC synthase (ACS, 1-aminocyclopropane-1-carboxylic acid synthase). Finally, ACC is oxidized by ACC oxydase (ACO) to produce ethylene (Wang et al., 2002). ET plays a key role in physiological and developmental processes including seed germination, root, shoot and flower development, fruit ripening, leaf senescence and stress responses (Wang et al., 2002; von Dahl and Baldwin, 2007; Yang et al., 2008). In plant-herbivore interactions, ET is a modulator of the responses triggered by JA (von Dahl and Baldwin, 2007).

Cross-signaling between JAs, SA and ET in plant defense responses.

Although JAs play the prominent role in the induction of defense responses against necrotrophic pathogens and chewing insects in plants, SA and ET can either positively or negatively modulate jasmonate-induced defense responses, and JAs may also positively or

negatively affect responses moderated by SA an ET (Doherty et al., 1988; Doares et al., 1995; O'Donnell et al., 1996; Reymond and Farmer, 1998; Stotz et al., 2002; Zarate et al., 2007; Diezel et al., 2009; Pieterse et al., 2009). In tomato, it has been shown that the SA produced upon pathogen infection inhibits the accumulation of JA-induced protease inhibitors (PI; Doares et al., 1995). In contrast, ET and JA are required for the wound induction of PI genes in tomato; and this positive regulation of PI genes is suppressed by exogenous application of SA (O'Donnell et al., 1996). In *Nicotiana sylvestris,* the jasmonate- or wound-induced nicotine accumulation is prevented by applying methyl-salicylate (Me-SA) to wounds (Baldwin et al., 1997). A classic example of JAs suppressing SA is the production of the phytotoxin coronatine by *P. psyringae* which mimics JA-Ile and suppress SA-dependent plant defense responses, thus allowing bacteria to overcome the plant defense responses. In Arabidopsis, the non-expressor of PR1 (NPR1) is an important regulator of SA-JA cross-talk, though the final defense response depends on ET (Leon-Reyes et al., 2009). Feeding by thrips which do not induce ET requires NPR1 for the SA-mediated suppression of JA responses, whereas *Alternaria brassicicola* (a necrotrophic pathogen) which induces JA and ET bypasses the NPR1 requirement (Leon-Reyes et al., 2009). In *N. attenuata*, NPR1 plays the opposite role by negatively regulating SA production (independently of ET emission), allowing the unfettered elicitation of JA-mediated defenses against herbivores (Rayapuram and Baldwin, 2007). Additionally, in Arabidopsis, the transcription factors WRKY70 and WRKY62 regulate the SA-mediated suppression of JA responses (Li et al., 2004). Moreover, in Arabidopsis, enhanced disease susceptibility 4 (EDS4) functions in SA-dependent defense gene expression after *P. syringae* infection, and *eds4* mutants display enhanced expression of the JA- and ET-dependent defensin gene PDF1.2 (Gupta et al., 2000).

In *N. attenuata* plants the relative production of JAs, SA and ET is herbivore-specific and both plants and insects try to adjust or prevent, respectively, the induction of defense responses. For example, when *N. attenuata* leaves are elicited with OS of the generalist *S. exigua,* it induces the accumulation of SA to levels higher than those induced by OS of the specialist *M. sexta*, whereas *M. sexta* induces the accumulation of higher levels of JA and ET; the lower SA levels in *M. sexta* OS-elicited plants are a consequence of elevated ET levels (Diezel et al., 2009). *N. attenuata* defense responses were attenuated after *S.*

exigua elicitation when compared to those after *M. sexta* elicitation. Previous studies have shown that after *M. sexta* folivory, *N. attenuata* plants accumulate secondary metabolites such as nicotine, phenolics and PI, the accumulation of which depends on jasmonate production and is modulated by ethylene (von Dahl and Baldwin, 2007). For example, nicotine accumulation is stimulated by JA and repressed by ET (Winz et al., 2001); whereas PI synthesis depends on the synergistic action of JA and ET signaling cascades (von Dahl and Baldwin, 2007).

Plant perception of insect attack

A wide variety of plant species are able to trigger and tailor defense and tolerance responses against lepidopteran larval folivory after perception of elicitors (HAEs: herbivore associated elicitors) present in the oral secretions (OS) of the larvae (Tumlinson and Lait, 2005; Schmelz et al., 2009; Bonaventure et al., 2011). HAEs are diverse in chemical structure and are usually specific to a particular plant-insect association (Bonaventure et al., 2011). HAE perception induces a plant-specific cocktail of direct and indirect defenses (see “Plant defense responses”) as well as tolerance responses (Schwachtje and Baldwin, 2008) against insect feeding. When perceived by the plants, HAEs induce the production of the phytohormones ET and JAs which in turn activate herbivore-specific defense response (Schmelz et al., 2009).

The first HAE identified was the fatty acid-amino acid conjugate (FAC) *N*-(17-hydroxylinolenoyl)-L-Glu or volicitin, isolated from the OS of beet armyworm (*S. exigua)* larvae feeding on *Zea mays* plants (Alborn et al., 1997). Subsequently, many chemically diverse HAEs were identified in the OS of herbivorous species including enzymes, e.g., glucose oxidase (Musser et al., 2002), sulfated α-hydroxy fatty acids termed caeliferins (Alborn et al., 2007), fragments of cell walls (e.g., oligogalacturonides) and peptides released from digested plant proteins (e.g., the proteolytic fragments of chloroplastic ATP synthase γ-subunit, termed inceptins (Schmelz et al., 2006).

FACs belong to a widely distributed family of HAEs present in the OS of a large number of lepidopteran larvae and elicit herbivore-specific responses in several plant

species including maize (*Zea mays*), soybean (*Glycine max*), eggplant (*Solanum melongena*), black nightshade (*S. nigrum*) and wild tobacco (*N. attenuata;* Alborn et al., 1997; Bonaventure et al., 2011). The main FAC present in *S. exigua* OS is volicitin (*N*-(17-hydroxylinolenoyl)-L-Glu); in *S. litura* OS it is *N*-linolenoyl-L-glutamine rather than volicitin (Yoshinaga et al., 2010). *M. sexta* OS comprises primarily *N*-linolenoyl-L-glutamate (18:3-Glu), *N*-linoleoyl-L-glutamate (18:2-Glu) and *N*-linolenoyl-L-glutamine (18:3-Gln; Halitschke et al., 2001; Diezel et al., 2009).

The role of FACs in caterpillar physiology is not fully understood. In 1974, Collatz and Mommsen found that hydrolysis of the digestive fluids from several insects (crickets, spiders and crayfish) yielded fatty acids and amino acids (Collatz and Mommsen, 1974). Based on this observation they suggested that these compounds could act as emulsifiers of dietary fat. Recently, it has been demonstrated that glutamine-containing FACs are stored forms of glutamine used for the assimilation of nitrogen by the developing lepidopteran larvae (Yoshinaga et al., 2010).

Early signaling events after FAC perception

Since the isolation of volicitin in the OS of *S. exigua* (Alborn et al., 1997) little progress has been made in the identification of the signal transduction mechanisms utilized by plants to respond to HAEs. Two important questions are still unanswered: 1) how are FACs perceived? and 2) what are the molecular mechanisms underlying FAC perception? It has been shown that volicitin induces the depolarization of the plasma membrane of lima bean leaves (Maffei et al., 2004) and that a plasma membrane protein binds to violicitin in *Zea mays* (Truitt et al., 2004).

FACs are major components in the OS of *M. sexta* larvae and are necessary and sufficient to induce most of the defense responses triggered by *M. sexta* larvae feeding on *N. attenuata* plants (Halitschke et al., 2001). One of the earliest known molecular events induced by OS and FACs in *N. attenuata* is the activation of two mitogen-activated protein kinases, SIPK (salicylic acid-induced protein kinase) and WIPK (wound-induced protein kinase; Wu et al., 2007), together with NPR1 (non-expressor of PR1; Kallenbach et al.,

2010). Transcript levels of SIPK and WIPK are rapidly (within 60 min) and transiently (decline within 120 min) induced after elicitation (Wu et al., 2007). Reduced activity of SIPK and WIPK results in reduced expression of the transcription factors WRKY3 and 6 (Skibbe et al., 2008). To identify novel molecular players of the FAC-/ *M. sexta* OS-induced signal transduction pathway, genome-wide transcriptome studies using "open-architecture" approaches such as differential display PCR (DDRT-PCR) and cDNA- amplified fragment-length polymorphism (cDNA-AFLP) have been performed using *N. attenuata* plants (Hermsmeier et al., 2001; Schittko et al., 2001; Halitschke et al., 2003). Taken together, these studies identified ~ 250 transcripts that were differentially regulated either after 24 h of *M. sexta* larval feeding or after 1 h of multiple sequential events of OS elicitation. Some of the genes identified in these studies have been demonstrated to participate in insect defense mechanisms (Kang et al., 2006; Lou and Baldwin, 2006; Schwachtje et al., 2006). The fast development of high-throughput gene sequencing in combination with new "open-architecture" techniques for quantification of gene expression has opened-up the possibility of performing genome-wide transcriptome studies in organisms from which no massive nucleotide sequence information is yet available as in the case of *Nicotiana attenuata*. Serial analysis of gene expression (SAGE) is a technique that allows absolute quantification of mRNA abundance by quantifying the relative frequencies of individual short (13 nt) transcripts signatures (tags; Velculescu et al., 1995). Further development of the SAGE technique allowed the generation of 26 nt tags (SuperSAGE; Matsumura et al., 2005) which substantially improved the annotation of tags when aligned with sequences in public nucleotide databases (Matsumura et al., 2003). In the SuperSAGE technique the detection of transcripts is proportionally correlated to the scale of DNA sequencing and in combination with next generation sequencing (NGS) allows for the detection and analysis of very low-abundance transcripts (frequently encoding for regulatory components; Matsumura et al., 2005). **In Manuscript I, I identified genes encoding for potential regulatory components of the FAC-mediated responses using the SuperSAGE technique in combination with next generation sequencing (NGS)**. In line with the search for novel molecular players, I quantified the early changes (within 30 min) in the transcriptome of *N. attenuata* plants after a single event of 18:3-Glu elicitation. I concentrated on low-abundance transcripts that were rapidly and transiently induced after

18:3-Glu elicitation and compared these transcripts with those induced by wounding. **In Manuscript II, I characterized a G-type lectin receptor-like kinase, LecRK1, identified by SuperSAGE as a putative regulatory factor of the FACs signal transduction pathway in *N. attenuata***.

Objectives of the thesis:

1. Identify genes encoding for potential regulatory components of the FAC-mediated responses in *N. attenuata*.

2. Characterize the role of the *N. attenuata* G-type lectin receptor-like kinase 1 gene (Na*LecRK1*) in the plant's response to *M. sexta herbivory*.

3. Understand the fluxes and metabolism of C_{12} derivatives of the HPL pathway in *N. attenuata* plants after *M. sexta* herbivory.

Chapter 2: Manuscript overview

Manuscript 1

SuperSAGE analysis of the *Nicotiana attenuata* transcriptome after fatty acid-amino acid elicitation (FAC): Identification of early mediators of insect responses.

Paola A. Gilardoni, Stefan Schuck, Ruth Jüngling, Björn Rotter, Ian T. Baldwin and Gustavo Bonaventure.

Published in *BMC Plant Biology* 10: 66 (2010).

In Manuscript I, we analyzed the early changes in the transcriptome of *Nicotiana attenuata* after FAC elicitation using the SuperSAGE technique combined with 454 sequencing. We identified two regulatory genes involved in insect-specific mediated responses in plants. Moreover, we provided a foundation for the identification of additional novel regulators associated with this process.

P. Gilardoni and G. Bonaventure planned and performed the experiments, analyzed the data and wrote the manuscript. S. Shuck helped to analyzed data. R. Jüngling and B. Rotter carried out experiments and analyzed the data. I.T. Baldwin participated in the design and coordination of the study and helped to draft the manuscript.

Chapter 2

Manuscript 2

The *Nicotiana attenuata* Na*LecRK1* gene suppresses the salicylic acid-mediated inhibition of induced defense responses during *Manduca sexta* herbivory.

Paola A. Gilardoni, Christian Hattenhausen, Ian T. Baldwin and Gustavo Bonaventure.

Submitted to the Plant Cell Journal, PLANTCELL/2011/088229.

In Manuscript II, we functionally characterized a G-type receptor-like kinase (NaLecRK1) involved in *Nicotiana attenuata* defense response against *Manduca sexta*. We demonstrated that NaLecRK1 is essential to suppress the insect-mediated salicylic acid (SA) burst that inhibits the induction of critical defense metabolites.

P. Gilardoni carried out all the experiments, analyzed the data and drafted the manuscript. C. Hettenhausen characterized and provided the ov-nahg plants. I.T. Baldwin participated in the design and coordination of the study and helped to draft the manuscript. G. Bonaventure conceived of the study, participated in its design and coordination and helped to draft the manuscript.

Chapter 2

Manuscript 3

C_{12} derivatives of the hydroperoxide lyase pathway are produced by product recycling through lipoxygenase-2 in *Nicotiana attenuata* leaves.

Mario Kallenbach, Paola A. Gilardoni, Silke Allmann, Ian T. Baldwin and Gustavo Bonaventure.

Accepted for publication in *New Phytologist* (2011).

In Manuscript III, we studied the fluxes and metabolism of C_{12} derivatives of the HPL pathway in *Nicotiana attenuata* plants after wounding and *Manduca sexta* OS elicitation. The quantification of these metabolites was achieved by the development of a new liquid chromatography–mass spectrometry／mass spectrometry (LC-MS／MS) method. We reveal new aspects of the biogenesis of C_{12} derivatives of the HPL pathway and rise new hypothesis for possible roles of these metabolites in the regulation of stress responses.

M. Kallenbach carried out the experiments, analyzed the data and helped to draft the manuscript. P. Gilardoni carried out experiments. S. Allmann provided the data for the characterization of ir-hpl plants. I.T. Baldwin participated in the design and coordination of the study and helped to draft the manuscript. G. Bonaventure conceived of the study, participated in its design and coordination and helped to draft the manuscript.

Chapter 3:

SuperSAGE analysis of the *Nicotiana attenuata* transcriptome after fatty acid-amino acid elicitation (FAC): Identification of early mediators of insect responses.

Manuscript 1

Gilardoni *et al. BMC Plant Biology* 2010, **10**:66
http://www.biomedcentral.com/1471-2229/10/66

BMC Plant Biology

RESEARCH ARTICLE Open Access

SuperSAGE analysis of the *Nicotiana attenuata* transcriptome after fatty acid-amino acid elicitation (FAC): identification of early mediators of insect responses

Paola A Gilardoni[1], Stefan Schuck[1], Ruth Jüngling[2], Björn Rotter[2], Ian T Baldwin[1], Gustavo Bonaventure[1*]

Abstract

Background: Plants trigger and tailor defense responses after perception of the oral secretions (OS) of attacking specialist lepidopteran larvae. Fatty acid-amino acid conjugates (FACs) in the OS of the *Manduca sexta* larvae are necessary and sufficient to elicit the herbivory-specific responses in *Nicotiana attenuata*, an annual wild tobacco species. How FACs are perceived and activate signal transduction mechanisms is unknown.

Results: We used SuperSAGE combined with 454 sequencing to quantify the early transcriptional changes elicited by the FAC *N*-linolenoyl-glutamic acid (18:3-Glu) and virus induced gene silencing (VIGS) to examine the function of candidate genes in the *M. sexta-N. attenuata* interaction. The analysis targeted mRNAs encoding regulatory components: rare transcripts with very rapid FAC-elicited kinetics (increases within 60 and declines within 120 min). From 12,744 unique Tag sequences identified (UniTags), 430 and 117 were significantly up- and down-regulated ≥ 2.5-fold, respectively, after 18:3-Glu elicitation compared to wounding. Based on gene ontology classification, more than 25% of the annotated UniTags corresponded to putative regulatory components, including 30 transcriptional regulators and 22 protein kinases. Quantitative PCR analysis was used to analyze the FAC-dependent regulation of a subset of 27 of these UniTags and for most of them a rapid and transient induction was confirmed. Six FAC-regulated genes were functionally characterized by VIGS and two, a putative lipid phosphate phosphatase (LPP) and a protein of unknown function, were identified as important mediators of the *M. sexta-N. attenuata* interaction.

Conclusions: The analysis of the early changes in the transcriptome of *N. attenuata* after FAC elicitation using SuperSAGE/454 has identified regulatory genes involved in insect-specific mediated responses in plants. Moreover, it has provided a foundation for the identification of additional novel regulators associated with this process.

Background

Nicotiana attenuata is an annual native to Southwestern USA that germinates from seed banks in response to factors in wood smoke after fires [1]. Because of this germination behavior and a strong intra-specific competition, *N. attenuata* allocates resources primarily to sustain rapid growth and seed setting and as a consequence, it has developed a large number of induced defense responses to ward off the unpredictable attacks from herbivores [2]. Hence, when *N. attenuata* is attacked by insect folivores, an extensive reprogramming of its transcriptome, proteome and metabolome takes place [3-5]. Previous studies estimated that more than 500 *N. attenuata* genes respond to *Manduca sexta* larval feeding [6] and demonstrated that the plant readjusts its metabolism for *de novo* synthesis of direct and indirect defense responses and to induce tolerance mechanisms [7-9]. Activation of these defensive mechanisms requires energy and resources from primary metabolism and involves therefore a complex rearrangement of resource allocation in the plant, including altered photosynthesis and sink/source relations [5]. How plants decode insect feeding and trigger defense and tolerance responses is starting to be understood.

* Correspondence: gbonaventure@ice.mpg.de
[1]Max Planck Institute for Chemical Ecology, Department of Molecular Ecology, Hans Knöll Str. 8, 07745 Jena, Germany

For example, a SnRK1 kinase complex has been found to regulate tolerance mechanisms associated to the leaf/root partition of photoassimilates [9] and two MAPKs, WIPK and SIPK (Wound-induced and Salicylate-Induced Protein Kinases, respectively), were shown to be critical for the induction of direct defense responses in *N. attenuata* [10].

Herbivore attack induces in plants the coordinated activation of several signal cascades including those of jasmonic acid (JA), salicylic acid (SA), and ethylene (ET) [11]. Among them, JA plays a major and essential role in the induction of a large number of the plant's protective responses against insect herbivory and wounding [12,13]. Thus, having JA as a common signal, a large number of the plant responses to these two stimuli overlap, however, plants can differentiate between mechanical damage and insect herbivory to tailor their responses. The perception of components in the oral secretions (OS) of feeding larvae is one mechanism by which plants can decode insect feeding. Fatty acid-amino acid conjugates (FAC) are major components in the OS of *M. sexta* larvae and they are necessary and sufficient to induce most of the defense responses triggered by feeding *M. sexta* caterpillar in *N. attenuata* [14]. Hence, previous studies suggest the existence of central herbivore-activated regulators in *N. attenuata* leaves, which, in turn, are regulated by minute amounts of FACs in the insect's OS. Disentangling the effect of mechanical tissue damage and FAC elicitation will provide critical information on how plants control changes in its metabolism to more efficiently reduce the negative fitness consequences of herbivore attack.

One of the earliest known molecular events differentially induced by OS and FACs in tobacco is the activation of WIPK and SIPK. Activation of these protein kinases occur within the first minutes after wounding [15] and the activation is enhanced several-fold by applying *M. sexta* OS to wounds [10]. Importantly, not only their activities but also SIPK and WIPK transcript levels are rapidly (within 60 min) and transiently induced after elicitation [10,15], indicating that these regulators are under positive feedback control at the transcriptional level. One of the early targets of the FAC signal transduction pathway in *N. attenuata* is the *WRKY6* gene. Its transcript levels are also rapidly and transiently induced after wounds have been supplemented with *M. sexta* OS or synthetic FACs but only marginally by mechanical damage alone [16]. This rapid and transient kinetic of mRNA accumulation is characteristic of regulatory components and differs from that showed by, for example, transcripts encoding for defense components (e.g., protease inhibitors) which is characterized by a slower and more persistent rate of mRNA accumulation, reaching maximum levels after hours to days [8]. However, not all regulatory components are under positive feedback control at the transcriptional level: the *Coronatine Insensitive 1* (*COI1*) gene is an example in the JA transduction pathway [17]. However, some of the recently identified JAZ proteins that interact with COI1 and participate in JA-Ile perception are rapidly and transiently induced at the mRNA level by wounding in Arabidopsis [18].

The rapid advances in high throughput sequencing capacity in combination with new "open-architecture" techniques for quantification of gene expression has opened the possibility of performing genome-wide transcriptome studies in organisms from which massive nucleotide sequence information is not yet available. Serial analysis of gene expression (SAGE) is a technique that allows for the absolute quantification of mRNA abundance by quantifying the relative frequencies of individual short (13 nt) transcripts signatures tags [19]. Further development of the technique allowed for the generation of 26 nt tags (SuperSAGE) [20] which substantially improved the annotation of tags when aligned to sequences in public nucleotide databases [21]. With these techniques, the detection of transcripts is proportionally correlated to the scale of DNA sequencing and their combination with next generation sequencing (NGS) allows for the detection and analysis of very low abundant transcripts (frequently encoding for regulatory components) which have been estimated to account for more than 90% of mRNAs in eukaryotic cells [20,22].

Here we used SuperSAGE in combination with NGS for the quantification of the early changes (within 30 min) occurring in the transcriptome of *N. attenuata* plants after a single event of 18:3-Glu elicitation. The major objective of the study was to identify genes encoding for potential regulatory components of the FAC-mediated responses by looking for low abundant transcripts that were rapidly and transiently induced after 18:3-Glu elicitation.

Results

Generation of SuperSAGE libraries from wounded and FAC elicited *N. attenuata* leaves

Two SuperSAGE libraries were generated from the second fully expanded leaf of *N. attenuata* plants either mechanically wounded or wounded and supplemented with 18:3-Glu as a single FAC elicitor. Leaf samples were harvested after 30 min of the treatments (Figure 1). Wounding is a prerequisite for FAC-elicitation; hence, analysis of wounded leaves was used to differentiate between genes regulated by mechanical damage from those regulated more specifically or deferentially by FACs. Additionally, elicitation by a single elicitor (18:3-Glu) and a single wound event were used to eliminate the effects of other OS components and repeated wounding on gene expression.

Gilardoni *et al. BMC Plant Biology* 2010, **10**:66
http://www.biomedcentral.com/1471-2229/10/66

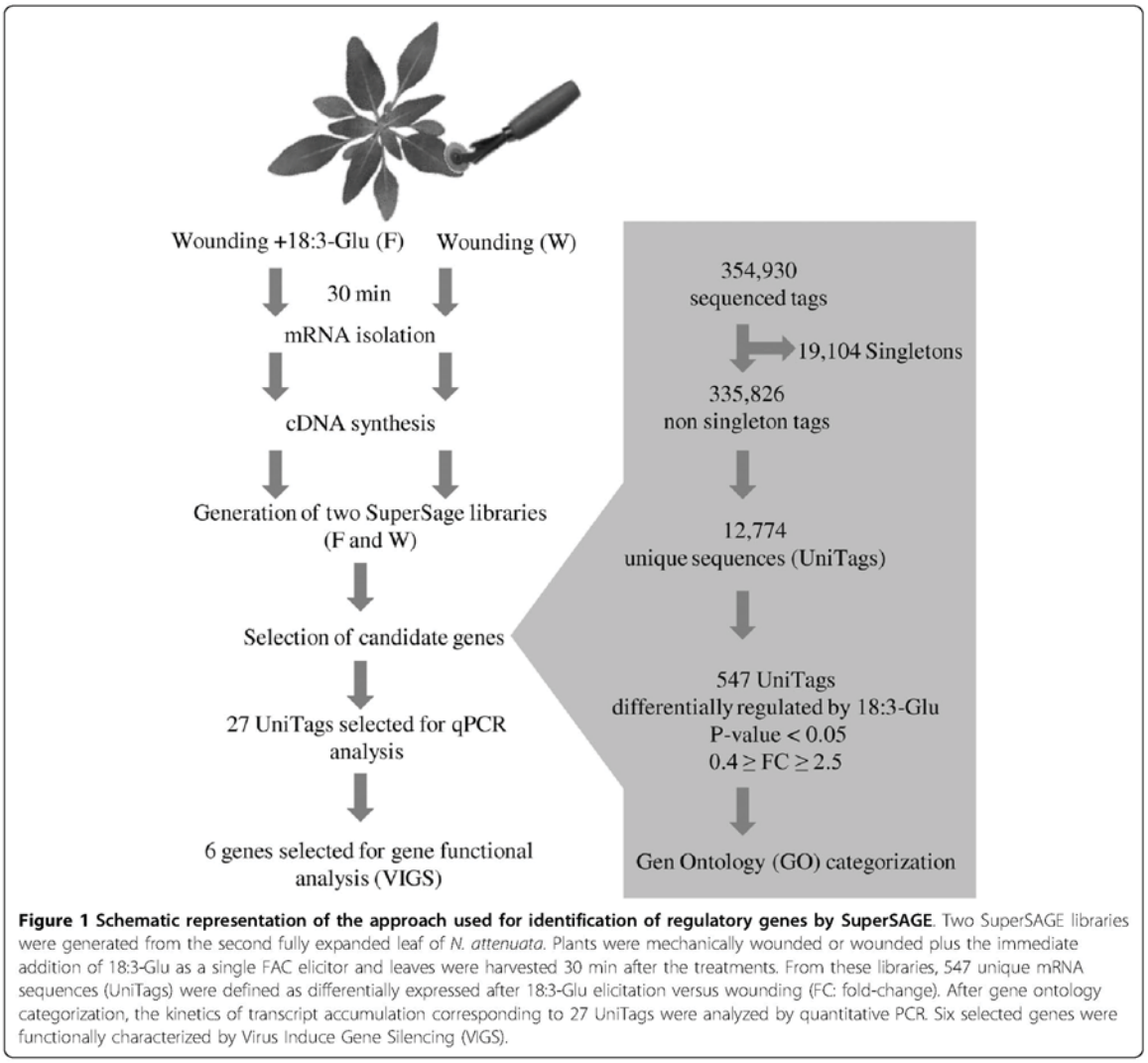

Figure 1 Schematic representation of the approach used for identification of regulatory genes by SuperSAGE. Two SuperSAGE libraries were generated from the second fully expanded leaf of *N. attenuata*. Plants were mechanically wounded or wounded plus the immediate addition of 18:3-Glu as a single FAC elicitor and leaves were harvested 30 min after the treatments. From these libraries, 547 unique mRNA sequences (UniTags) were defined as differentially expressed after 18:3-Glu elicitation versus wounding (FC: fold-change). After gene ontology categorization, the kinetics of transcript accumulation corresponding to 27 UniTags were analyzed by quantitative PCR. Six selected genes were functionally characterized by Virus Induce Gene Silencing (VIGS).

The total number of SuperSAGE tags obtained after sequencing the libraries in a single 454 plate and eliminating i) incomplete reads, ii) twin-ditags, and iii) ditags without complete library-identification DNA linkers was 354,930; comprising 227,536 tags from the wounding (W) library and 127,394 from the FAC-elicited (F) library (Table 1). These tags represented 31,878 unique sequences with 19,104 (11,951 in the W library and 7,153 in the F library) detected only once (singletons) in the combined libraries, and 12,774 detected at least twice in the combined libraries (Table 1). These latter tags are referred as UniTags throughout the manuscript [22] and will be considered for further analysis. Singletons represented thus ~60% of unique sequences, in agreement with previous studies [21,22]. The complete SuperSAGE dataset is available in Additional file 1 (see also Accession numbers).

Abundance of UniTags and annotation to public databases

The UniTags were first classified in abundance groups according to their number of copies [22]. UniTags present at ≤ 100, > 100 - ≤ 1,000, > 1,000 - ≤ 5,000 and >5,000 copies per million (copies.million^{-1}) were considered as low-, mid-, high- and very high-abundant tags, respectively (Table 1). The frequency distribution of the 12,774 UniTags showed that the number of copies in low and mid abundance groups (≤ 1,000 copies.million^{-1}) represented > 98% of the UniTags while high- and very high-abundant tags (>1,000

Gilardoni *et al. BMC Plant Biology* 2010, **10**:66
http://www.biomedcentral.com/1471-2229/10/66

Table 1 Features of the SuperSAGE libraries from wounded and 18:3-Glu elicited leaves

Library	W**	F**	Total	(%)
Sequenced tags	227,536	127,394	354,930	(100)
Number of unique transcripts (UniTags)	11,942	10,117	12,774	
Number of singletons	11,951	7,153	19,104	
Abundance classes of UniTags*				
Very high-abundant: > 5,000 copies.million^{-1}	24	22	46	(0.2)
High-abundant: > 1,000 - 5,000 copies.million^{-1}	127	133	260	(1.2)
Mid-abundant: 100 - 1,000 copies.million^{-1}	1,178	1,084	2,262	(10.2)
Low-abundant: < 100 copies.million^{-1}	10,613	8,878	19,491	(88.4)
Total	11,942	10,117		
Copy number of Tags in Abundance classes*				
Very high-abundant: > 5,000 copies.million^{-1}	2.34×10^5	2.34×10^5	4.68×10^5	(23.4)
High-abundant: > 1,000 - 5,000 copies.million^{-1}	2.36×10^5	2.43×10^5	4.80×10^5	(24.0)
Mid-abundant: 100 - 1,000 copies.million^{-1}	3.32×10^5	3.16×10^5	6.48×10^5	(32.4)
Low-abundant: < 100 copies.million^{-1}	1.98×10^5	2.07×10^5	4.05×10^5	(20.2)
Total	1.00×10^6	1.00×10^6		

* Values normalized to 1 million tags
** W: wounded; F: 18:3-Glu elicited

copies.million^{-1}) represented only 1.4% (Table 1). However, although the latter group represented only a small fraction of the 12,774 UniTags, together they accounted for ~47% of the total number of tag copies in both the W and F libraries (Table 1). These values were in agreement with previously reported data [23,24].

Annotation of the 12,774 UniTags using basic local alignments (BLASTN) gave 5,565 tags (43.6%) that matched with a maximum of 3 mismatches (score ≥ 46.1 or e-value ≤ 6.10^{-4}) to sequences deposited in GenBank plant nucleotide databases (Additional file 1 and Table 2). 78.8% of these 5,565 UniTags matched perfectly (26/26) with sequences in the databases while 8.4% did it with one mismatch (25/26), 6.5% with two mismatches (24/26) and 6.4% with three mismatches (23/26; Table 2). Moreover, 88% of the annotated UniTags matched sequences corresponding to *Nicotiana* spp, 5% to *Solanum* spp and 8% to other plant species (Table 2).

Table 2 Annotation of UniTags using GenBank DNA sequence databases

	No. of matches (total 26)					
	26	25	24	23	Total	(%)
Nicotiana spp	3,867	403	305	300	4,875	(88)
Solanum ssp	188	31	19	22	260	(5)
Other species	330	32	35	33	430	(8)
Total	4,385	466	359	355	5,565	(100)
(%)	(78.8)	(8.4)	(6.5)	(6.4)		

FAC elicitation induces differential expression of 547 UniTags

Statistically significant changes in tag copy number between the F and W libraries were analyzed by calculating a probability (*P*)-value according to [25] (see Materials and Methods for a brief description). Although small changes in expression levels may have biological significance [25], in this study we focused primarily on genes which showed strong changes in expression levels with arbitrary fold-change (FC) values ≥ 2.5 or ≤ 0.4 (FAC elicitation vs wounding). Based on the calculated (*P*)-values and using a 95% confidence level, 547 UniTags were identified as differentially expressed after FAC elicitation (Additional file 2). Among these UniTags, 430 had FC ≥ 2.5 and 117 FC ≤ 0.4 (F vs W; Figure 2a and Additional file 2). Most of the differentially expressed UniTags presented FC values between 0.2 and 10, with 29 and 24 UniTags presenting FC values ≥ 10 and ≤ 0.2, respectively (Figure 2b). The majority (98.6%) of the differentially up-regulated UniTags and all of the down-regulated UniTags corresponded to low- and mid-abundance groups (< 1,000 copies.million^{-1}; Figure 2c and Additional file 2), indicating that the strongest changes in expression levels occurred primarily in genes expressed at low to intermediate levels.

Assignment of differentially expressed UniTags to Gene Ontology (GO): biological and functional categories

To obtain gene function categories of the differentially expressed UniTags, gene ontology (GO) annotation was performed by BLASTX (using the corresponding annotated nucleotide sequences as queries) against the

Gilardoni *et al. BMC Plant Biology* 2010, **10**:66
http://www.biomedcentral.com/1471-2229/10/66

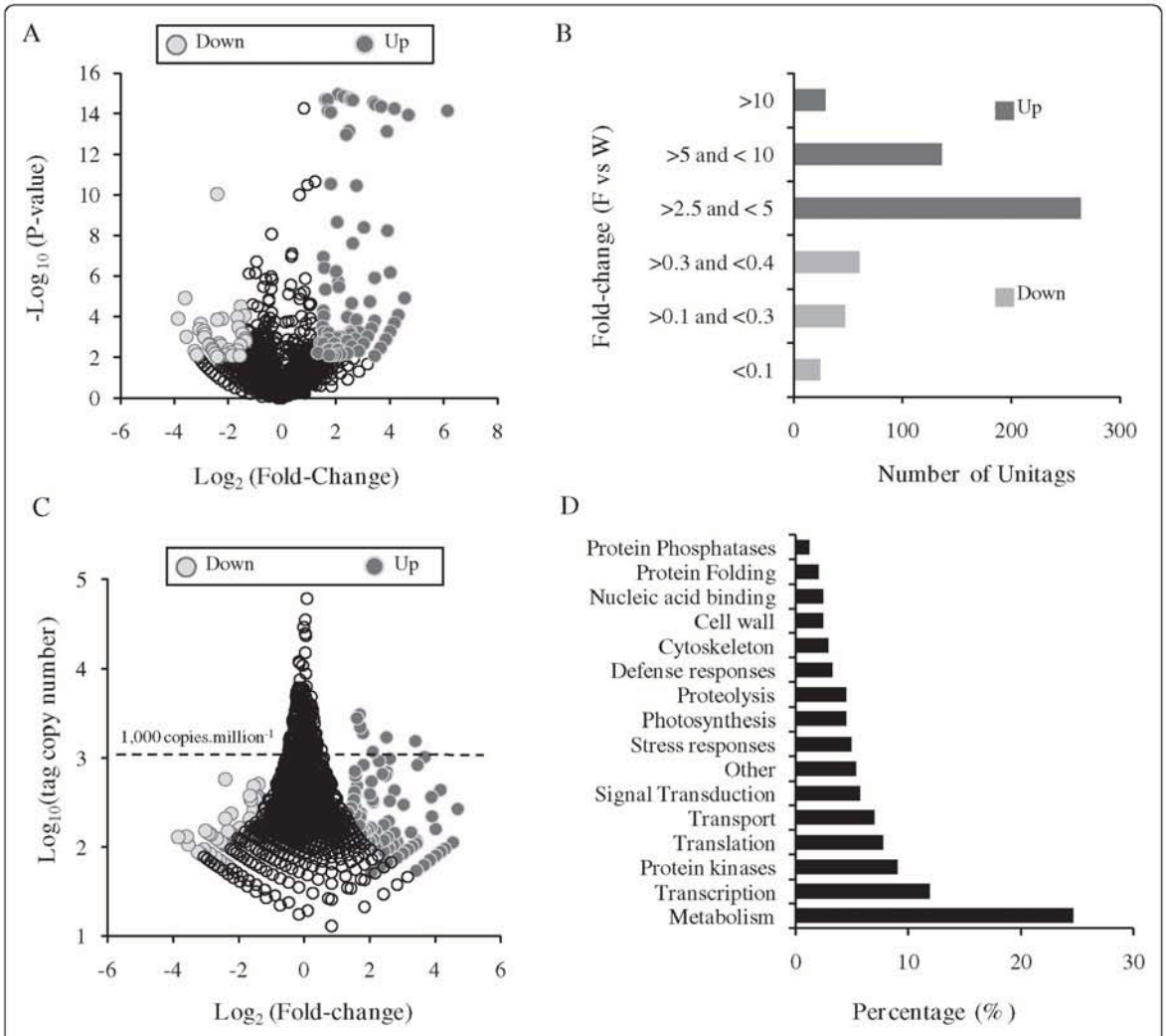

Figure 2 Analysis of differentially expressed UniTags. **A**, Volcano plot showing the Log_2(fold-change; F vs. W) versus Log_{10}(*P*-value) of 547 expressed UniTags. **B**, Fold change (F vs. W) distribution of the 547 differentially expressed UniTags. **C**, Distribution of the expressed UniTags based on the Log_2(Fold-change; F vs. W) versus Log_{10}(tag copy number). The dashed line corresponds to a threshold of 1,000 copies.million^{-1}. **D**, Distribution of 242 annotated UniTags in Gene Ontologiy (GO) categories based on Molecular Function and Biological Process.

non-redundant GenBank and UniProtKB/TrEMBL protein databases (Additional file 2). For this analysis, we used UniTags that showed a maximum of 2 mismatches (24/26) with entries in the GenBank nucleotide database (Additional file 1). Of the 547 differentially expressed UniTags, 349 had an associated nucleotide sequence and 323 matched to an amino acid sequence entry (e-value < 9.10^{-4}) in the GenBank and UniProtKB/TrEMBL databases (Additional file 2). GO annotations (biological processes and/or molecular function) could be assigned to 242 of these 323 UniTags with the remaining entries corresponding to uncharacterized proteins (Additional file 2).

Among the most prevalent GO biological processes, ~25% of the UniTags classified into metabolism, ~12% into regulation of gene expression (including transcription, nucleosome assembly and mRNA processing), ~10% into amino acid phosphorylation/dephosphorylation, ~8% into translation (including ribosome assembling), ~8% into defense and stress responses, ~7% into transport, ~6% into protein degradation and folding and ~6% into signal transduction components (Figure 2d). The preponderance of changes in transcripts corresponding to metabolism, signaling, transcription, translation and transport associated processes after 30 min of

Gilardoni et al. BMC Plant Biology 2010, 10:66
http://www.biomedcentral.com/1471-2229/10/66

18:3-Glu elicitation emphasized the fact that at this early time point a substantial reprogramming of the leaf metabolism is already in progress. Based on changes in metabolic genes, hallmarks of this reprogramming included an increased capacity for protein synthesis and the generation of C skeletons and reducing power (see Discussion). These changes in the expression of metabolic genes are consistent with a substantial shift in primary metabolism to support secondary metabolism and tolerance mechanisms [5] and are consistent with previous gene expression studies [3,6,26] (see Discussion). The identification of regulatory factors controlling these changes in metabolism and defense and tolerance processes against insects is one of the major challenges for the future and some potential candidates are described below.

Changes in the expression of UniTags/mRNAs encoding for regulatory components

The most prevalent GO molecular function with regulatory activity corresponded to transcriptional regulators and protein kinases, represented by 30 and 22 UniTags, respectively. The protein phosphatase category contained 3 UniTags, the signal transduction category 14 UniTags and the nucleic acid binding category 6 UniTags (Additional file 2). Thus, a total of 75 annotated UniTags corresponded to factors with potential regulatory function.

Among transcriptional regulators, UniTags corresponding to WRKY transcription factors (TFs) were the most predominant (seven UniTags) and Tag-995 was the most up-regulated (23 fold) after 18:3-Glu elicitation within this group. Other UniTags for WRKYs were up-regulated between 9 and 2.5 fold (Additional file 2). Within the WRKY domain containing family, a WIZZ TF (wound-induced leucine zipper zinc finger) [27] was up-regulated 7 fold. Other prevalent up-regulated TFs included AP2-like factors (three UniTags; up-regulated between 9 and 3 fold), RAV factors (two UniTags; up-regulated ~3 fold), ethylene-responsive element binding proteins (EREBP; two UniTags; up-regulated between 9 and 3 fold) and CCR4-NOT transcription complex proteins (two UniTags; up-regulated between 7 and 3 fold) (Additional file 2). Single up-regulated UniTags in this category corresponded to a bZIP TF (2.5 fold), HIS4 (2.5 fold), S1FA (7 fold), RNA polymerase II (RNAPII; 5.5 fold) and a sigma subunit for a plastidial RNA polymerase (7 fold). Among down-regulated transcriptional regulators were a GATA-1 zinc finger protein and RNA polymerase III (RNAPIII; Additional file 2).

Within the protein kinase and phosphatase classes, three UniTags corresponded to MAPK (two up-regulated between 4 and 2.5 fold and one down-regulated 10 fold), three to cell-wall associated kinases (WAK; up-regulated between 3.5 and 6 fold), two to BRASSINOSTEROID INSENSITIVE 1-associated receptor kinase 1 (BAK1; up-regulated between 9 and 3 fold) and three to protein phosphatase 2A (PP2A) and C (PP2C; two up-regulated ~3 fold and one down-regulated ~5-fold). In addition, this category contained a chloroplast precursor for *Arabidopsis* protein kinase 1 (APK1) [28] up-regulated ~7 fold, a shaggy-like kinase (up-regulated ~5 fold), and a cytokinin-regulated kinase 1 (CRK1; the most up-regulated, ~14 fold) and a calmodulin protein kinase 1 (up-regulated ~11 fold) among others (Additional file 2).

Within the signal transduction class, the most predominant UniTags corresponded to "Avr9/Cf-9 rapidly elicited proteins" (seven UniTags) up-regulated between 13 and 2.5 fold. Single up-regulated UniTags corresponded to a $Hs1^{pro-1}$-like protein (putative nematode resistance protein (NRP); 17.9 fold), SGT1 (3.6 fold), a lipid phosphate phosphatase (LPP; 5.4 fold) and an extra-large G protein (2.5 fold) were also contained in this category (Additional file 2).

Validation of the SuperSAGE data by qPCR

A subset of 27 differentially expressed UniTags (Table 3) was selected for further analysis based on the fulfillment of at least two of the following criteria: 1) strong and significant changes in their FC values (either up- or down-regulated, F vs W); 2) abundance of <1,000 copies.million^{-1} (as regulatory components are encoded by low abundant transcripts); 3) matched known regulatory components in the databases.

The selected UniTags were first elongated by amplification of their corresponding cDNAs and BLASTed against the GenBank plant nucleotide databases to confirm their identities. All of the elongated sequences (see "Accession numbers") matched to the same entries as the original 26 bp tags (data not shown). Secondly, the elongated sequences were used to design gene-specific primers to i) validate the SuperSAGE data and ii) to study the kinetic of mRNA induction by real time quantitative PCR (qPCR). Total RNA was extracted from both wounded and 18:3-Glu elicited leaves of WT plants after different times of the stimuli.

The accumulation of 20 mRNAs corresponding to the selected UniTags was consistent with a rapid increase (within 60 min) after FAC elicitation and a rapid decrease (within 120 min) to basal or lower levels after the stimuli (Figure 3 and Additional file 3 [Figure S1]). Interestingly, several transcripts showed either no or minimal induction by wounding, representing therefore genes activated almost specifically by FACs (e.g., 837, 995, 1844, 2815; Figure 3). For some transcripts mechanical damage induced an increase in their corresponding mRNA levels which was potentiated several

Gilardoni *et al. BMC Plant Biology* 2010, **10**:66
http://www.biomedcentral.com/1471-2229/10/66

Table 3 List of the 27 UniTags selected for qPCR and VIGS analysis[1]

Tag-Id	Tag sequence	FC	Protein Description
Tag-11166	CATGTGTCAAGCTGGAAAACTTGCCA	69.92	NM
Tag-4898	CATGCTGCTGGGACTCTCGTATACAG	25.78	NM
Tag-995	CATGAATTCAAGAAACAAGCCAACAA	23.31	ACJ04728.1| WRKY transcription factor
Tag-6642	CATGGCCAAGAGTACGTTCTCAAAGG	19.72	AAL08561.1| auxin-regulated protein
Tag-895	CATGAATGACACTAATGAATTCGTCG	19.72	NM
Tag-6205	**CATGGATCTACGCGTCAAAAATGCTT**	**17.93**	**AAG44839.1| Hs1pro-1-like receptor**
Tag-2452	CATGATGAATACGAGCAGCTTCGGGT	17.93	NM
Tag-1439	CATGACTGCTGTCAGACGAACTGCAC	16.14	BAD33355.1| ABC transporter
Tag-837	**CATGAATCATCCAATATGGTATGGGC**	**14.70**	**XP_002298932.1| predicted protein (UnkA)**
Tag-9719	CATGTATTCTGCTGTAAATTCAGGAA	12.77	AAG43557.1| Avr9/Cf-9 rapidly elicited protein
Tag-2978	CATGATTTTTTTCCTTCTGCTGTAT	12.55	NM
Tag-12314	**CATGTTTAGAGCAATGAGTACACGAA**	**10.81**	**EEF40825.1| hypothetical protein (UnkB)**
Tag-6199	CATGGATCGGCAAACAAAGAGATTAT	10.51	NM
Tag-7795	CATGGGTTATTCAGTGCTGTTCAGTG	5.98	AAY17949.1| ring zinc finger protein
Tag-1844	CATGAGGAAGGCTATGAAGGAGAAGA	5.82	NM
Tag-7036	CATGGCTGCTGACAACTTACCTGGAT	5.79	ACG41445.1| plastid-lipid associated protein
Tag-11559	**CATGTTATCAGTTAACTAATAAAAGC**	**5.70**	**EEF35389.1| wall-associated kinase (WAK)**
Tag-10039	**CATGTCCACCATACTAACGGAGGATT**	**5.38**	**NP_001078095.1| LPP (Lipid Phosphate Phosphatase)**
Tag-6032	CATGGAGGTCTTTCTCGTTATCTGAT	5.22	XP_002278077.1| hypothetical protein
Tag-5869	CATGGAGACTTTGCAAGTTAAGTTTT	4.26	BAC07504.2| receptor-like protein kinase
Tag-2067	CATGAGTTGGTGGATTCAAATCTTGG	4.13	EEF37528.1| wall-associated kinase (WAK)
Tag-129	CATGAAACACAGTTAGCAATTTATGA	4.03	ABD28351.1| Lissencephaly type-1-like homology
Tag-6938	CATGGCTCGGATTTGCATCTCTAAAG	3.84	NP_563839.1| transcription factor
Tag-5283	CATGCTTTGTAAAACTTAGCAACAAA	3.47	NM
Tag-2815	**CATGATTGAGTTGCAAAGCAGTGGAG**	**3.36**	**BAB16427.1|*Nicotiana* Elicited Induce Gene (NEIG)**
Tag-9434	CATGTATAGCAGATTGGTGAAATGAT	3.19	BAE44121.1| protein phosphatase 2C
Tag-2990	CATGCAAAACGTACACCGAGAAAGAA	0.09	NM

FC: fold change (FAC-elicitation vs. Wounding). NM: no match in GenBank
[1]UniTags selected for VIGS analysis are depicted in bold.

fold by 18:3-Glu elicitation (e.g., 5869, 10039; Figure 3). For transcripts corresponding to four UniTags (6032, 7036, 129, 6642), the differential regulation by 18:3-Glu elicitation could not be confirmed (Additional file 3 [Figure S1]) and they may represent false positives in the SuperSAGE analysis [25]. Finally, mRNAs for three UniTags (1439, 2452, 2990) were differentially repressed by 18:3-Glu elicitation (Additional file 3 [Figure S1]).

Functional characterization of candidate regulatory components of insect mediated responses by VIGS

To validate the use of the SuperSAGE approach for the identification of candidate regulatory components of the interaction between *N. attenuata* and *M. sexta* larvae, six genes were selected for preliminary gene function characterization by virus-induced gene silencing (VIGS). The selection of these genes was based on: 1) their kinetic of mRNA induction and 2) their fold-change compared to wounding (minimal induction by wounding -except for Tag-10039). Some of the genes encoded for putative regulatory components and two presented no similarity to any other protein of known or predicted function (Figure 3 and Table 3). The selected UniTags corresponded to a $Hs1^{pro-1}$-like protein (putative nematode resistance protein (NRP); Tag-6205), lipid phosphate phosphatase (LPP; Tag-10039), *Nicotiana* elicitor induced gene (NEIG; Tag-2815), cell wall-associated protein kinase (WAK; Tag-11559), UnkA (Tag-837) and UnkB (Tag-12314) (these last two presenting no protein annotation) (Table 4). To evaluate whether these genes participate in FAC- and insect defense-mediated responses, gene-specific silenced plants and plants transformed with the empty vector (EV; control plants) were assessed for *M. sexta* larval performance and the accumulation of JA and JA-Ile after 18:3-Glu elicitation and wounding. Gene silencing efficiency in these plants was analyzed by qPCR in 18:3-Glu-elicited leaves after 1 h of the treatment (Table 4). The morphological phenotype of the silenced-plants was indistinguishable from EV control plants (data not shown).

M. sexta larva feeding on plants silenced in the expression of LPP or UnkA showed significant increases

Gilardoni *et al. BMC Plant Biology* 2010, **10**:66
http://www.biomedcentral.com/1471-2229/10/66

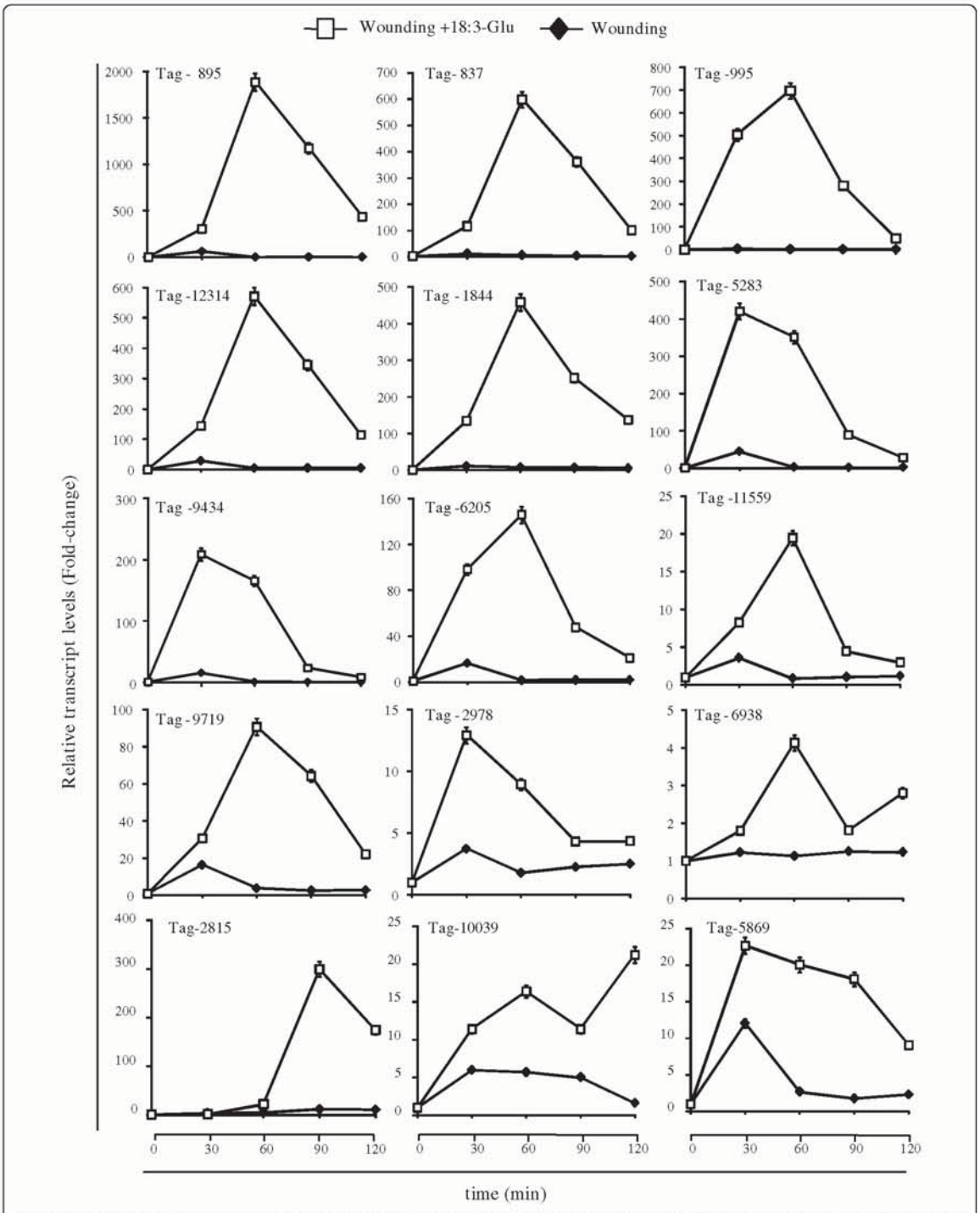

Figure 3 Analysis of mRNA accumulation corresponding to selected UniTags by qPCR. Examples of the kinetics of induction of mRNAs for 15 UniTags analyzed by qPCR after wounding and 18:3-Glu elicitation. Relative mRNA quantification was performed using the eEF1A as a reference gene for normalization and the data is expressed as fold-change relative to time 0 (unelicited leaves). Values at this time point were set arbitrary to 1. Transcripts levels were analyzed in three biological replicates (n = 3).

Gilardoni *et al. BMC Plant Biology* 2010, **10**:66
http://www.biomedcentral.com/1471-2229/10/66

Table 4 Selected genes for functional characterization by VIGS

Tag ID	Gene Name	VIGS construct	Silencing efficiency (%)[1]
Tag-6205	Nematode Resistance Protein (NRP)	pTVNRP	67 ± 1.8
Tag-10039	Lipid Phosphate Phosphatase (LPP)	pTVLPP	69 ± 2.1
Tag-11559	Wall Assocaited Kinase (WAK)	pTVWAK	83 ± 2.5
Tag-2815	*Nicotiana* Elicited Induced Gene (NEIG)	pTVNEIG	91 ± 5.2
Tag-837	UnkA	pTVUNKA	73 ± 4.7
Tag-12314	UnkB	pTVUNKB	98 ± 2.8

[1] The silencing efficiency is expressed as the reduction (%) of the mRNA levels in the VIGS-silenced plants relative to the levels of the corresponding mRNA in EV (empty vector) plants. In all cases the reductions were statistically significant ($P < 0.05$, *t*-test, EV vs VIGS).

in mass gained after 11 and/or 15 days compared to EV plants (Figure 4; see caption for statistical analysis). In contrast, larval performance was similar between EV and plants silenced in NRP, NEIG, WAK and UnkB (Additional file 3 [Figure S2]). The rate of JA and JA-Ile accumulation after wounding was similar between EV and LPP-silenced plants (Figure 5a). After 18:3-Glu elicitation, the accumulation of JA and JA-Ile was significantly slower in LPP-silenced plants however after 90 min the levels were similar to EV plants (Figure 5a, see caption for statistical analysis). Plants silenced in UnkA expression had similar rates of JA and JA-Ile accumulation to EV plants after both 18:3-Glu elicitation and wounding (Figure 5b). Likewise, induced levels of JA and JA-Ile in NRP-, WAK-, NEIG- and UnkB-silenced plants were similar to EV plants (data not shown).

Discussion

In this study we exploited the combined capacities of SuperSAGE and NGS to quantify the expression of thousands of genes in *N. attenuata* leaves elicited by one of the major elicitors (18:3-Glu) present in the OS of *M. sexta* larvae. We analyzed the expression of >335,000 SuperSAGE tags, representing 12,774 unique transcript sequences with the main objective of identifying factors with potential regulatory functions during the *M. sexta-N. attenuata* interaction. The analysis disclosed 75 annotated putative regulatory factors and from a subset of 27 selected we could confirm that the kinetic of mRNA induction for 20 of them followed the expected profile, a rapid and transient up-regulation.

Because the SuperSAGE generates 26 nt tags, DNA sequence databases are a prerequisite to warrant efficient gene annotation of the tags. Consistent with the presence of >17,000 *Nicotiana* spp nucleotide sequences publicly available in GenBank, ~88% of the *N. attenuata* UniTags matched to *Nicotiana* species (Table 2). However, only 43.5% of the 12,774 UniTags matched -with a maximum of 3 mismatches- to sequences in GenBank (Table 2). With a tolerance of 6 mismatches (20/26), 8,151 UniTags (64%) found a hit in this database (Additional file 1). Most SuperSAGE tags are derived from the 3' UTR of each mRNA molecule [20] which has been shown to be allele-specific in plants [29]. Since most of the *Nicotiana* spp nucleotide entries in GenBank correspond to *N. tabacum*, a percentage of the mismatches may be attributed to polymorphisms in the 3' UTR of mRNAs from *N. attenuata* and this tobacco species. Regarding the 547 differentially expressed UniTags, 60% could be assigned to a protein entry (Additional file 2) in GenBank and UniProtKB/TrEMBL protein databases and 25% of this fraction represented fully uncharacterized protein entries (Additional file 2), a fact that partially handicapped the functional characterization of the *N. attenuata* transcription profiles. Nevertheless, a total of 242 UniTags were reliably assigned to a GO category. However, since these 242 UniTags represented < 50% of the differentially regulated mRNAs (Additional file 2), we expect that improved gene annotation will increase (probably by factor of two) the number of putative regulators that change expression after 18:3-Glu elicitation.

Changes in the expression of mRNAs encoding for regulatory components

WRKY transcription factors (TFs) occur in large gene families in plants and orchestrate different responses including those for pathogen resistance and wound healing [30,31]. For example, WRKYs bind to W-box elements in PR1 genes and regulate their expression after salicylic acid (SA) induction and pathogen elicitation [32]. WRKY3 and 6 in *N. attenuata* have been involved in responses against insect herbivores [16]. WIZZ (wound-induced leucine zipper zinc finger) was identified as an early and transiently activated wound-responsive gene in tobacco [27] and contains a leucine-zipper motif and a WRKY domain in its structure. After wounding, WIZZ transcripts accumulate within 10 min reaching maximal levels by 30 min and decreasing thereafter to basal levels [27]. Our results suggested that several WRKY members including WIZZ may play critical roles in the coordination of *M. sexta-N. attenuata* interactions. AP2/ERF is a large family of TFs in plants, encoding transcriptional regulators with a variety of

Gilardoni *et al. BMC Plant Biology* 2010, **10**:66
http://www.biomedcentral.com/1471-2229/10/66

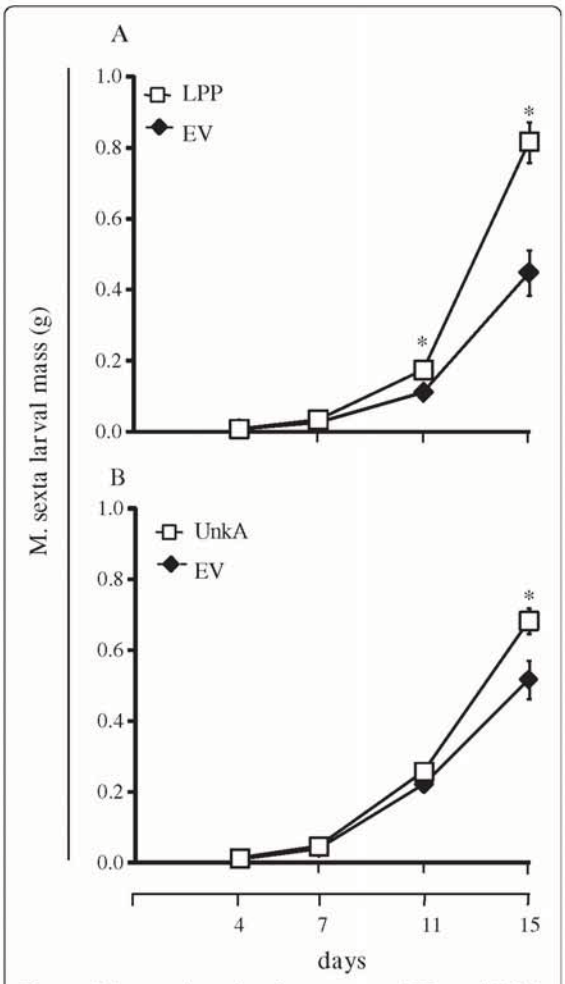

Figure 4 *M. sexta* larval performance on LPP- and UnkA-silenced plants. *N. attenuata* plants were silenced in the expression of LPP and UnkA by VIGS. Plants transformed with the empty vector (EV) were used as control. **A**, Mean (± SE) of *M. sexta* larval mass after 4, 7, 11 and 15 days of feeding on EV and LPP-silenced plants (n = 32 for each genotype). Statistical analysis was performed by repeated-measurement ANOVA ($F_{1,54}$ = 12.79, P < 0.01). **B**, Mean (± SE) of *M. sexta* larval mass after 4, 7, 11 and 15 days of feeding on EV and UnkA-silenced plants (n = 32 for each genotype). Statistical analysis was performed by repeated-measurement ANOVA ($F_{1,48}$ = 6.62, P < 0.05). In both cases asterisks represent significant differences between EV and the corresponding silenced line. Both experiments were conducted two times independently with identical results.

functions in the control of developmental and physiological processes including the integration of JA and ET signals [33]. The AP2/ERF family is classified into subfamilies containing AP2, DREB, EREBP and RAV TFs. Three AP2-like, two EREBP and two RAV TFs were rapidly up-regulated after 18:3-Glu elicitation (Additional file 2), suggesting that this family of TF may also play important roles in the orchestration of some of the plant's responses to insect feeding.

Two UniTags corresponding to the CCR4-associated factor 1 (CAF1) were up-regulated by 18:3-Glu elicitation. CAF1 is a subunit of the CCR4-NOT complex involved in mRNA degradation and Arabidopsis plants mutated in *CAF1a* and *b* genes are more susceptible to *Pseudomonas syringae* infection [34]. These authors hypothesized that the CAF1-containing complex controls the expression of a repressor of defense genes during pathogenesis. Our results suggested that the CCR4-NOT complex may also plays a role in defense responses against insects.

Several UniTags corresponding to putative cell wall-associated protein kinases (WAKs) were rapidly up-regulated after 18:3-Glu elicitation (Additional file 2). WAKs are transmembrane proteins containing a cytoplasmic Ser/Thr kinase domain and an extracellular domain in contact with components of the plant cell walls [35]. WAKs play important roles in cell expansion, pathogen resistance, and heavy-metal stress tolerance [36,37]. These protein kinases may associate changes in the cell wall structure after insect attack with downstream responses. Indirect evidence for rapid changes in cell wall structure and metabolism comes from the substantial number of genes associated with these processes that were up-regulated after 18:3-Glu elicitation (including an arabinogalactan protein (9-fold), beta-glucan-binding protein (9-fold), cellulose synthase (6-fold), α-expansin (2.5-fold), cell wall peroxidase (7-fold), raffinose synthase (7-fold), xyloglucan endotransglycosylases (3-fold), UDP-GlcUA 4-epimerase (3-fold) and xylose isomerase (4-fold; Additional file 2). Changes in the cell wall structure trigger JA- and ET-mediated defense responses in Arabidopsis as evidenced by the *cev1* mutant, carrying a genetic lesion in a cellulose synthase gene [38]. Thus, changes in cell wall structure or homeostasis after mechanical damage and FAC elicitation might influence defensive signaling in a manner analogous to the *cev1* mutant of Arabidopsis.

GSK3/SHAGGY-like kinase is a highly conserved Ser/Thr kinase involved in several signaling pathways. The Arabidopsis BRASSINOSTEROID-INSENSITIVE 2 (BIN2) gene encodes a GSK3/SHAGGY-like kinase and was identified as a negative regulator of brassinosteroid (BR) signaling [39]. Changes in the expression of transcripts for this kinase together with BRASSINOSTEROID INSENSITIVE 1-associated receptor kinase 1 (BAK1) suggested that BR play a role in the regulation of *M. sexta-N. attenuata* interaction. BR induces resistance against TMV, *P. syringae* and *Oidium* spp in tobacco plants [40]. Evidence for cytokinins also playing a role in this interaction came from the strong

Gilardoni *et al. BMC Plant Biology* 2010, **10**:66
http://www.biomedcentral.com/1471-2229/10/66

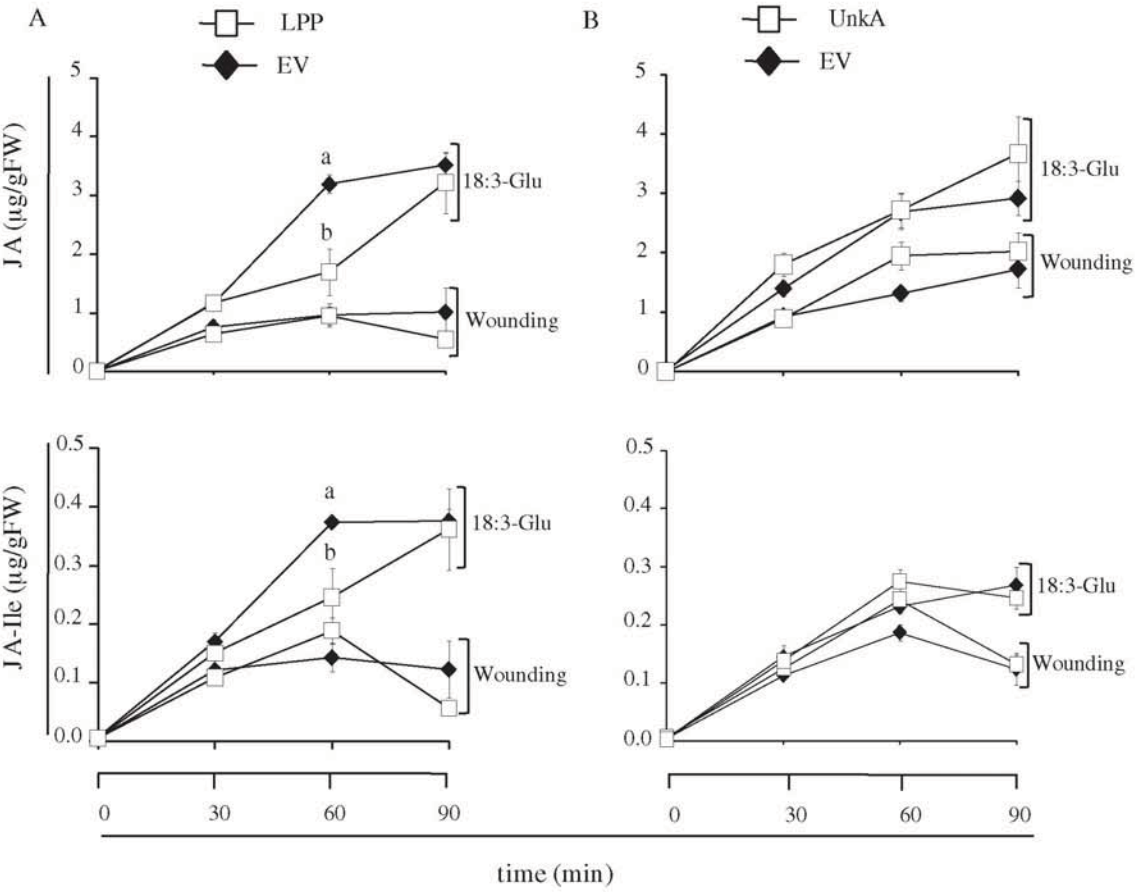

Figure 5 Quantification of JA and JA-ILE levels in LPP- and UnkA-silenced plants. Leaves from *N. attenuata* plants silenced in the expression of LPP and UnkA by VIGS were either wounded or 18:3-Glu elicited and tissue was harvested at different times. **A**, Mean (± SE) JA and JA-ILE levels in EV and LPP-silenced plants ($n = 5$). Statistical differences in JA and JA-ILE levels were analyzed by univariate ANOVA (JA, $F_{3,12} = 18.6$, $P < 0.001$; JA-ILE, $F_{3,12} = 5.6$, $P < 0.05$). Different letters denote significant differences in a Scheffé *post-hoc* test at $P < 0.05$. **B**, Mean (± SE) JA and JA-ILE levels for EV and UnkA-silenced plants ($n = 5$).

up-regulation of the *CYTOKONIN-REGULATED KINASE 1* gene (*CRK1*) [41].

UniTags corresponding to PP2A and C were up-regulated while one UniTag corresponding to a PP2C isoform was down-regulated (Additional file 2). These regulators are known to play a central role in the control of defense-associated mechanisms. For example, the Arabidopsis AP2C1 (a PP2C) inactivates MPK4 and MPK6 and the mutant *ap2c1* produces higher amounts of JA after wounding and is more resistant to phytophagous mites than WT. In contrast, plants with increased AP2C1 activity produced less ET and had compromised immunity against necrotrophic pathogens [42].

Among components associated to signal transduction processes, genes encoding for "Avr9-Cf9 rapidly elicited proteins" were the most predominant. The GO molecular function associated with these proteins was either protein kinase or receptor activity (Additional file 2) and some may correspond to R (resistance) genes in *N. attenuata*. The Avr9-Cf9 elicitor-receptor system is involved in the race-specific resistance of tomato (*S. lycopersicum*) against *Cladosporium fulvum* [43]. Interestingly, similar to wounding and OS elicitation, the Cf9 receptor induces the activation of WIPK and SIPK upon Avr9 binding and it has been proposed that these protein kinases are hubs in the integration of signals for diverse elicitors [44]. Thus, "Avr9/Cf9 rapidly elicited proteins" may be either important components in defense responses against insects or they may reflect redundancy (via activation of WIPK and SIPK and downstream gene expression) in the signal transduction pathway activated by wounding and FACs. An additional

Gilardoni et al. BMC Plant Biology 2010, 10:66
http://www.biomedcentral.com/1471-2229/10/66

regulator that shows high homology to protein kinase receptors and R genes is the putative $Hs1^{pro-1}$-like receptor (Additional file 2). The $Hs1^{pro-1}$ gene confers resistance to the beet cyst nematode *Heterodera schachtii* in sugar beet (*Beta vulgaris* L.) [45]. The transcript of $Hs1^{pro-1}$ is present at low levels in uninfected roots and it is induced specifically after nematode infection independently of SA, JA, ABA or wounding [46]. Its induction by 18:3-Glu in leaves on *N. attenuata* suggested that this gene may play a role in some plant responses against lepidopteran larvae in aboveground tissue. Up-regulation of UniTags corresponding to SGT1, a component of the Skp1-Cullin-F-box protein (SCF) ubiquitin ligases previously linked to early plant defenses responses conferred by R genes [47], also suggested that signaling pathways connected to R genes may be induced by insect elicitors in *N. attenuata*.

Early changes in gene expression after 18:3-Glu elicitation reflect a rapid reprogramming of leaf metabolism

As a validation of the SuperSAGE approach, several UniTags identified as differentially regulated by 18:3-Glu elicitation corresponded to transcripts previously identified as differentially regulated by *M. sexta* larval feeding or OS/FAC elicitation [3,6,26]. Most of these genes corresponded to proteins involved in primary metabolism (Additional file 4). Changes in the expression of these genes supported the idea of a shift in primary metabolism to supply energy, C skeletons and reducing power for the synthesis of defensive compounds and to induce tolerance mechanisms [5]. Most of the putative regulatory factors identified in the present study were not identified in previous studies except for a WRKY transcription factor [26].

Changes occurring at the level of metabolism were among the most prevalent comprising more than 60 annotated UniTags. The up-regulation of twelve UniTags corresponding to transcripts for ribosomal structural proteins, four to translation initiation factors, two to tRNA synthases and several corresponding to amino acid biosynthesis (including tryptophan synthase, threonine deaminase, prephenate dehydrataseand 2-isopropylmalate synthase (Additional files 2 and 5) suggested that, within 30 min, 18:3-Glu elicitation stimulated an increased capacity for protein biosynthesis. Additionally, several annotated UniTags corresponding to genes involved in the generation of energy and C skeletons (e.g., subunits of ATP synthases, glyceraldehyde-3-phosphate-dehydrogenase, aldose-1-epimerase, fructose-bisphosphate aldolase, phosphofructokinase, sucrose synthase) and in the generation and metabolism of reducing power (e.g., NADP-dependent malic enzyme, Fed-$NAD(P)^+$ reductase, NAD kinase, nicotinamidase) showed strong up-regulations (Additional file 2). NAD-dependent malic enzymes (MEs) catalyze the oxidative decarboxylation of malate to produce pyruvate, CO_2, and NADH in mitochondria [48] while NADP-dependent plastidic and cytosolic isoforms provide C skeletons and reducing power for defense responses, lignin biosynthesis and reactive oxygen species formation [49,50]. Changes in the expression of these genes are probably necessary to meet large requirements for NADPH to supply anabolic processes.

Interestingly, several UniTags corresponding to low abundant mRNAs for isoforms of photosynthetic proteins were found up-regulated between ~3 and 7-fold, including an oxygen-evolving protein, ribulose bisphosphate carboxylase activase, ribulose-1,5-bisphosphate carboxylase/oxygenase (RuBisCO) large subunit, chlorophyll a/b-binding protein, ferredoxin (Fed)-NADP(+) reductase and a PSI-H precursor (Additional files 2 and 5). In contrast to the up-regulation of these low abundant UniTags, high abundant UniTags corresponding to similar genes did not change significantly within 30 min after 18:3-Glu elicitation (e.g., Tags-4671, -3383, -1319 and -1133: photosystem II subunits; Tag-10791: light-harvesting chlorophyll a/b binding protein; Tags-11115, -11779, and -10899: RuBisCO subunits; Additional file 1). Why these low abundant isoforms of photosynthetic genes are up-regulated after elicitation is unknown. One possibility is that they play some specific roles during defense responses. In previous studies, it has been observed that after lepidopteran larvae feeding or OS/FAC elicitation transcripts encoding for photosynthetic enzymes (e.g., PSII, RuBisCO, RuBisCO activase) in attacked *N. attenuata* leaves tend to be down-regulated, with the lowest expression after several hours [6]. Long-term reductions in the synthesis of these proteins have been proposed as a mechanism that attacked plants use to reinvest resources into other processes such as the synthesis of secondary defense pathways or tolerance [5]. Within 30 min of FAC elicitation there were no significant reductions in the copy number of high abundance UniTags corresponding to mRNAs for photosynthetic proteins, suggesting that repressive mechanisms of major leaf isoforms act later during the FAC-induced response.

Identification of two mediators of *M. sexta-N. attenuata* interaction

The analysis of six candidate genes by VIGS identified two putative regulatory components of resistance mechanisms against lepidopteran larval feeding. Caterpillars that fed for two weeks on plants silenced in the expression of a putative lipid phosphate phosphatase (LLP) and a protein of unknown function (UnkA) gained ~2-fold and ~1.3-fold more mass, respectively, than larvae grown on EV control plants (Figure 4). Gain

Gilardoni et al. BMC Plant Biology 2010, 10:66
http://www.biomedcentral.com/1471-2229/10/66

of mass by the larvae can be achieved by increased foliar consumption by stimulatory mechanisms, increased efficiency of food intake by increased food quality, or a combination both [51]. By which mechanism *M. sexta* larvae grew larger on these plants is at present unknown and the subject of future investigations using stable transformed plants silenced in the expression of LPP and UnkA by RNA interference (RNAi). LPPs are signal transduction components that utilize a variety of lipid phosphate substrates including phosphatidic acid (PA), diacylglycerol pyrophosphate (DGPP), lyso-PA, ceramide 1-phosphate, and sphingosine 1-phosphate and it has been proposed that their function is to attenuate the signaling functions of these molecules [52,53].

Both LPP- and UnkA-silenced plants accumulated similar levels of JA and JA-Ile after wounding and FAC elicitation (Figure 5b), indicating that the effects of LLP and UnkA on *M. sexta* caterpillar performance was not the result of impaired JA biosynthesis. Together, these results suggested that mechanisms acting independently of JA biosynthesis must be affected in these plants to confer reduced resistance to *M. sexta* larval performance.

Conclusions

The analysis of FAC-elicited *N. attenuata* plants by combined SuperSAGE and NGS enabled the identification of multiple factors with potential regulatory activity during the *M. sexta-N. attenuata* interaction. Together with the use of VIGS to analyze candidate gene function we provided experimental evidence for the participation of two of these potential regulators in this interaction. The further characterization of genetically stable LLP- and UnkA-silenced plants in addition to the identification and characterization of novel regulators based on the SuperSAGE data will shed light on mechanisms used by plants to control a large reorganization of their metabolism and physiology to adjust defense and tolerance mechanisms with growth and reproduction.

Methods

Plant growth and treatments

Seeds of the 30th generation of an inbred line of *N. attenuata* plants were used as the wild-type genotype (WT) in all experiments. Plants were grown in the glasshouse at 26-30°C under 16 h of light. The second fully expanded leaf of rosette stage plants [54] were wounded by rolling a fabric pattern wheel three times on each side of the midvein and the wounds were immediately supplied with either 20 μL of 0.01% (v/v) Tween-20/water (solvent control) or 10 μL of synthetic *N*-linolenoyl-glutamic acid (18:3-Glu; 0.03 nmol/μL in 0.01% (v/v) Tween-20/water). Tissue was collected after 30 min of the treatments and frozen in liquid nitrogen for subsequent SuperSAGE analysis. For RT-qPCR experiments, leaf samples were harvested at different time points and frozen in liquid nitrogen for subsequent RNA extraction. For VIGS experiments, plants were grown in climate chambers under 20°C, 16 h light (1000 μmol $m^{-2}s^{-1}$) and 65% humidity. Wounding and FAC elicitation was performed as described above. Larvae of *M. sexta* were hatched overnight at 28°C and one neonate was placed on each VIGS-silenced plant (n = 32). The larval mass was measured using a microbalance after 4, 7, 11 and 15 days of the start of the experiment.

RNA isolation and construction of SuperSAGE libraries

Total RNA was extracted by the phenol/chloroform-LiCl method as previously described [55] and the samples were cleaned using the Plant RNA Extraction Kit (Qiagen, Hilden, Germany) following commercial instructions. poly(A)-RNA was purified from total RNA with the Oligotex mRNA mini Kit (Qiagen) according to commercial instructions. Subsequent steps for the construction of the SuperSAGE libraries and 454 sequencing were performed as previously described [21,22]. To avoid methodological artifacts and to assure the detection of true transcript variants in the libraries, double *Nla*III digestions were performed during library generation [22].

For each library, 26 bp long tags were extracted from the sequences using the GXP-Tag sorter software provided by GenXPro GmbH (Frankfurt am Main, Germany). Library comparisons were carried out using the DiscoverySpace 4.01 software [Canada's Michael Smith Genome Sciences Centre, available at http://www.bcgsc.ca/discoveryspace]. Statistical analysis of differentially expressed tags was calculated according to [25]. Briefly, the probability distribution represented by equation (2) in [25] was used considering N_1 and N_2 as the total number of Tags in libraries 1 and 2, respectively, and x as the number of copies of a given Tag in library 1 and y as the number of copies of the same Tag in library 2. For fold-change (FC) calculations the libraries were normalized to 100,000 tags (Additional file 1) and the FC for each tag was calculated by dividing the number of tags in the normalized FAC library (F) by the number of tags in the normalized wounded (W) library (F vs. W). Tags absent in one of the libraries (tag count = 0) were set to 1 for calculation.

Sequence homology alignments

BLAST searches were carried out using the BLASTN algorithm with the 12,774 UniTag sequences against plant nucleotide databases in GenBank (Additional file 1), filtering by selecting the *Nicotiana* (taxid: 4085) and Viridiplantae (taxid:33090) taxa. Low complexity regions were rejected and gap costs were set to 5-2. The

sequence annotation presented in Additional file 1 was restricted to hits that matched a minimum of 20 nt. UniTags that matched to < 20 nt were annotated as "no hit" in this Table. Multiple entries separated by "or" were included when the UniTag matched more than one hit with identical scores. UniTags that matched to the negative strand of the nucleotide sequence in the database carry the prefix "minus" in their respective gene identification (GI) column (Additional file 1). For protein and gene ontology (GO) annotations of differentially expressed UniTags (Additional file 2), their respective nucleotide sequences (Additional file 1) were used to perform BLASTX against the NCBI non-redundant protein database and hits with scores < 9.10^{-4} were used for GO determination based on the UniProtKB/TrEMBL protein databases.

Rapid amplification of cDNA ends (3'-RACE)

For cDNA synthesis, the 3'RACE System for Rapid Amplification of cDNA Ends (Invitrogen, Karlsruhe, Germany) was used following the manufacturer's instructions and using UniTag- and gene-specific primers (Additional file 5). The PCR products were cloned into the pGEM-T easy vector (Promega, Madison, WI) and sequenced using universal primers.

Real time quantitative PCR

To analyze the mRNA levels corresponding to the 27 selected UniTags (Table 3), rosette stage *N.attenuata* WT plants were either wounded or FAC elicited as described above. Leaves were harvested at 0, 30, 60, 90, and 120 min after the treatments, total RNA extracted using the TRIzol® reagent (Invitrogen) and DNase-I treated (Fermentas, St. Leon-Rot, Germany). Five μg of total RNA were reverse transcribed using oligo(dT)18 and SuperScript reverse transcriptase II (Invitrogen). Quantitative real-time PCR (qPCR) was performed with a Mx3005P Multiplex qPCR system (Stratagene, La Jolla, CA) and the qPCR Core kit for SYBR® Green I (Eurogentec, Liege, Belgium). Relative quantification of mRNA levels was performed by the comparative ΔCt method using the eukaryotic elongation factor 1A (NaeEF1A) mRNA as an internal standard. The sequences of the primers used for qPCR are listed in Additional file 5. All the reactions were performed with three biological replicates.

Virus induced gene silencing

Virus-induced gene silencing (VIGS) based on the tobacco rattle virus (TRV) was used to transiently silence the genes listed in Table 4 in *N. attenuata* as previously described [56]. The accession numbers corresponding to the sequences are listed under "Accession numbers" below. Fragments of ~300 bp were amplified by PCR with the specific primers listed in Additional file 5. PCR products were digested with BamH1 and Sal1 and inserted into plasmid pTV00 in antisense orientation. Plants transformed with the empty vector (EV) were used as control. Plants were analyzed after 15 days of leaf infiltration. Efficiency of gene silencing was evaluated by qPCR after 1 h of 18:3-Glu elicitation using the primers listed in Additional file 5.

Phytohormone extraction and quantification

For analysis of JA and JA-Ile, 0.1 g of frozen leaf material was homogenized in FastPrep® tubes containing 1 g of FastPrep® matrix (Bio101, La Jolla, CA) and 1 mL ethylacetate spiked with 0.1 μg of [9,10-$^{2}H_{2}$]-dihydro-JA and [$^{13}C_{6}$]-JA-Ile. Homogenates were centrifuged for 10 min at 4°C, the organic phase collected and plant material re-extracted with 0.5 mL ethylacetate. Organic phases were combined and the samples evaporated to dryness. The dry residue was reconstituted in 0.2 mL of 70% (v/v) methanol/water for analysis on a LC-(ESI)-MS/MS system as previously described [57].

Statistical analysis

Repeated-measurement and univariate ANOVA were calculated using SPSS v. 17.0.

Accession numbers

The SuperSAGE data was deposited in the Gene Expression Omnibus (GEO) public domain under the accession [GenBank: GSE18595]. The accession numbers for ESTs corresponding to the extended Unitag sequences are Tag-129: [GenBank: GT184388]; Tag-837: [GenBank: GT184389]; Tag-895: [GenBank: GT184390]; Tag-995: [GenBank: GT184391]; Tag-1439: [GenBank: GT184392]; Tag-1844: [GenBank: GT184393]; Tag-2067: [GenBank: GT184394]; Tag-2452: [GenBank: GT184395]; Tag-2815: [GenBank: GT184396]; Tag-2978: [GenBank: GT184397]; Tag-2990: [GenBank: GT184398]; Tag-4898: [GenBank: GT184399]; Tag-5283: [GenBank: GT184400]; Tag-5869: [GenBank: GT184401]; Tag-6032: [GenBank: GT184402]; Tag-6199: [GenBank: GT184403]; Tag-6205: [GenBank: GT184404]; Tag-6642: [GenBank: GT184405]; Tag-6938: [GenBank: GT184406]; Tag-7036: [GenBank: GT184407]; Tag-7795: [GenBank: GT184408]; Tag-9719: [GenBank: GT184409]; Tag-10039: [GenBank: GT184410]; Tag-11166: [GenBank: GT184411]; Tag-11559: [GenBank: GT184412]; Tag-12314: [GenBank: GT184413].

Additional file 1: Complete list of UniTag sequences, copy numbers, and annotations to GenBank nucleotide databases.

Additional file 2: Complete list of differentially expressed UniTags and GO categorization.

Additional file 3: Supplementary Figures. Figure S1. Analysis of mRNA accumulation corresponding to 12 UniTags by qPCR. Figure S2. *M.sexta* larval performance on VIGS silenced plants.

Additional file 4: List of differentially expressed UniTags previously identified by differential expression techniques.

Additional file 5: Supplementary Tables. Table S1. Primers for elongation of cDNAs correspondig to UniTags. Table S2. Primers for qPCR. Table S3. Primers for VIGS analysis.

Acknowledgements
PG is a fellow of the Deutscher Akademischer Austausch Dienst (DAAD). We thank Dr. E. Grosse-Wilde for his help with batch-BLAST and M. Hartl for his help with statistical analysis. This work was funded by the Deutsche Forschungsgemeinschaft (DFG; Project BO3260/3-1) and the Max Planck Society.

Author details
[1]Max Planck Institute for Chemical Ecology, Department of Molecular Ecology, Hans Knöll Str. 8, 07745 Jena, Germany. [2]GenXPro GmbH, Altenhöferallee 3, 60438 Frankfurt am Main, Germany.

Authors' contributions
PG and GB carried out the experiments, analyzed the data and drafted the manuscript. RJ and BR carried out experiments and analyzed the data. SS analyzed the data. ITB participated in the design and coordination of the study and helped to draft the manuscript. GB conceived of the study, participated in its design and coordination and helped to draft the manuscript. All authors read and approved the final manuscript.

Received: 23 December 2009 Accepted: 14 April 2010
Published: 14 April 2010

References

1. Baldwin IT, Morse L: **Up in Smoke 2. Germination of *Nicotiana attenuata* in response to smoke-derived cues and nutrients in burned and unburned soils.** *J Chem Ecol* 1994, **20**:2373-2391.
2. Baldwin IT: **Jasmonate-induced responses are costly but benefit plants under attack in native populations.** *Proc Natl Acad Sci USA* 1998, **95**:8113-8118.
3. Halitschke R, Gase K, Hui DQ, Schmidt DD, Baldwin IT: **Molecular interactions between the specialist herbivore *Manduca sexta* (Lepidoptera, Sphingidae) and its natural host *Nicotiana attenuata*. VI. Microarray analysis reveals that most herbivore-specific transcriptional changes are mediated by fatty acid-amino acid conjugates.** *Plant Physiol* 2003, **131**:1894-1902.
4. Giri AP, Wunsche H, Mitra S, Zavala JA, Muck A, Svatos A, Baldwin IT: **Molecular interactions between the specialist herbivore *Manduca sexta* (Lepidoptera, Sphingidae) and its natural host *Nicotiana attenuata*. VII. Changes in the plant's proteome.** *Plant Physiol* 2006, **142**:1621-1641.
5. Schwachtje J, Baldwin IT: **Why does herbivore attack reconfigure primary metabolism?** *Plant Physiol* 2008, **146**:845-851.
6. Hermsmeier D, Schittko U, Baldwin IT: **Molecular interactions between the specialist herbivore *Manduca sexta* (Lepidoptera, Sphingidae) and its natural host *Nicotiana attenuata*. I. Large-scale changes in the accumulation of growth- and defense-related plant mRNAs.** *Plant Physiol* 2001, **125**:683-700.
7. Kessler A, Baldwin IT: **Herbivore-induced plant vaccination. Part I. The orchestration of plant defenses in nature and their fitness consequences in the wild tobacco *Nicotiana attenuata*.** *Plant J* 2004, **38**:639-649.
8. Zavala JA, Patankar AG, Gase K, Hui DQ, Baldwin IT: **Manipulation of endogenous trypsin proteinase inhibitor production in *Nicotiana attenuata* demonstrates their function as antiherbivore defenses.** *Plant Physiol* 2004, **134**:1181-1190.
9. Schwachtje J, Minchin PEH, Jahnke S, van Dongen JT, Schittko U, Baldwin IT: **SNF1-related kinases allow plants to tolerate herbivory by allocating carbon to roots.** *Proc Natl Acad Sci USA* 2006, **103**:12935-12940.
10. Wu JQ, Hettenhausen C, Meldau S, Baldwin IT: **Herbivory rapidly activates MAPK signaling in attacked and unattacked leaf regions but not between leaves of *Nicotiana attenuata*.** *Plant Cell* 2007, **19**:1096-1122.
11. Howe GA, Jander G: **Plant Immunity to Insect Herbivores.** *Annu Rev Plant Biol* 2008, **59**:41-66.
12. Reymond P, Bodenhausen N, Van Poecke RMP, Krishnamurthy V, Dicke M, Farmer EE: **A conserved transcript pattern in response to a specialist and a generalist herbivore.** *Plant Cell* 2004, **16**:3132-3147.
13. Voelckel C, Baldwin IT: **Herbivore-induced plant vaccination. Part II. Array-studies reveal the transience of herbivore-specific transcriptional imprints and a distinct imprint from stress combinations.** *Plant J* 2004, **38**:650-663.
14. Halitschke R, Schittko U, Pohnert G, Boland W, Baldwin IT: **Molecular interactions between the specialist herbivore *Manduca sexta* (Lepidoptera, Sphingidae) and its natural host *Nicotiana attenuata*. III. Fatty acid-amino acid conjugates in herbivore oral secretions are necessary and sufficient for herbivore-specific plant responses.** *Plant Physiol* 2001, **125**:711-717.
15. Seo S, Sano H, Ohashi Y: **Jasmonate-based wound signal transduction requires activation of WIPK, a tobacco mitogen-activated protein kinase.** *Plant Cell* 1999, **11**:289-298.
16. Skibbe M, Qu N, Galis I, Baldwin IT: **Induced Plant Defenses in the Natural Environment: *Nicotiana attenuata* WRKY3 and WRKY6 Coordinate Responses to Herbivory.** *Plant Cell* 2008, **20**:1984-2000.
17. Xie DX, Feys BF, James S, Nieto-Rostro M, Turner JG: **An Arabidopsis gene required for jasmonate-regulated defense and fertility.** *Science* 1998, **280**:1091-1094.
18. Chung HS, Koo AJK, Gao X, Jayanty S, Thines B, Jones AD, Howe GA: **Regulation and function of Arabidopsis JASMONATE ZIM-domain genes in response to wounding and herbivory.** *Plant Physiol* 2008, **146**:952-964.
19. Velculescu V, Zhang L, Vogelstein B, Kinzler K: **Serial analysis of gene expression.** *Science* 1995, **270**:484-487.
20. Matsumura H, Ito A, Saitoh H, Winter P, Kahl G, Reuter M, Kruger D, Terauchi R: **SuperSAGE.** *Cell Microbiol* 2005, **7**:11-18.
21. Matsumura H, Reich S, Ito A, Saitoh H, Kamoun S, Winter P, Kahl G, Reuter M, Kruger DH, Terauchi R: **Gene expression analysis of plant host-pathogen interactions by SuperSAGE.** *Proc Natl Acad Sci USA* 2003, **100**:15718-15723.
22. Molina C, Rotter B, Horres R, Udupa SM, Besser B, Bellarmino L, Baum M, Matsumura H, Terauchi R, Kahl G: **SuperSAGE: the drought stress-responsive transcriptome of chickpea roots.** *BMC Genomics* 2008, **9**:553-581.
23. Matsumura H, Nirasawa S, Terauchi R: **Transcript profiling in rice (*Oryza sativa* L.) seedlings using serial analysis of gene expression (SAGE).** *Plant J* 1999, **20**:719-726.
24. Song SH, Qu HZ, Chen C, Hu SN, Yu J: **Differential gene expression in an elite hybrid rice cultivar (Oryza sativa, L) and its parental lines based on SAGE data.** *BMC Plant Biol* 2007, **7**:49-64.
25. Audic S, Claverie J: **The significance of digital gene expression profiles.** *Genome Research* 1997, **7**:986-995.
26. Hui D, Iqbal J, Lehmann K, Gase K, Saluz HP, Baldwin IT: **Molecular interactions between the specialist herbivore Manduca sexta (lepidoptera, sphingidae) and its natural host Nicotiana attenuata: V. microarray analysis and further characterization of large-scale changes in herbivore-induced mRNAs.** *Plant Physiol* 2003, **131**:1877-1893.
27. Hara K, Yagi M, Kusano T, Sano H: **Rapid systemic accumulation of transcripts encoding a tobacco WRKY transcription factor upon wounding.** *Mol Gen Genet* 2000, **263**:30-37.
28. Hirayama T, Oka A: **Novel protein kinase of Arabidopsis thaliana (APK1) that phosphorylates tyrosine, serine and threonine.** *Plant Mol Biol* 1992, **20**:653-662.
29. Eveland AL, McCarty DR, Koch KE: **Transcript profiling by 3'-untranslated region sequencing resolves expression of gene families.** *Plant Physiol* 2008, **146**:32-44.
30. Eulgem T, Rushton PJ, Robatzek S, Somssich IE: **The WRKY superfamily of plant transcription factors.** *Trends Plant Sci* 2000, **5**:199-205.

31. Kim CY, Zhang SQ: **Activation of a mitogen-activated protein kinase cascade induces WRKY family of transcription factors and defense genes in tobacco.** *Plant J* 2004, **38**:142-151.
32. Rushton PJ, Torres JT, Parniske M, Wernert P, Hahlbrock K, Somssich IE: **Interaction of elicitor-induced DNA-binding proteins with elicitor response elements in the promoters of parsley PR1 genes.** *EMBO J* 1996, **15**:5690-5700.
33. Pré M, Atallah M, Champion A, De Vos M, Pieterse CMJ, Memelink J: **The AP2/ERF domain transcription factor ORA59 integrates jasmonic acid and ethylene signals in plant defense.** *Plant Physiol* 2008, **147**:1347-1357.
34. Liang W, Li C, Liu F, Jiang H, Li S, Sun J, Wu X, Li C: **The Arabidopsis homologs of CCR4-associated factor 1 show mRNA deadenylation activity and play a role in plant defence responses.** *Cell Res* 2009, **19**:307-316.
35. Anderson CM, Wagner TA, Perret M, He ZH, He D, Kohorn BD: **WAKs: cell wall-associated kinases linking the cytoplasm to the extracellular matrix.** *Plant Mol Biol* 2001, **47**:197-206.
36. Wagner TA, Kohorn BD: **Wall-associated kinases are expressed throughout plant development and are required for cell expansion.** *Plant Cell* 2001, **13**:303-318.
37. Li H, Zhou SY, Zhao WS, Su SC, Peng YL: **A novel wall-associated receptor-like protein kinase gene, OsWAK1, plays important roles in rice blast disease resistance.** *Plant Mol Biol* 2009, **69**:337-346.
38. Ellis C, Karafyllidis I, Wasternack C, Turner JG: **The Arabidopsis mutant *cev1* links cell wall signaling to jasmonate and ethylene responses.** *Plant Cell* 2002, **14**:1557-1566.
39. Li J, Nam KH: **Regulation of brassinosteroid signaling by a GSK3/SHAGGY-like kinase.** *Science* 2002, **295**:1299-1301.
40. Krishna P: **Brassinosteroid-Mediated Stress Responses.** *J Plant Growth Regul* 2003, **22**:289-297.
41. Schäfer S, Schmülling T: **The CRK1 receptor-like kinase gene of tobacco is negatively regulated by cytokinin.** *Plant Mol Biol* 2002, **50**:155-166.
42. Schweighofer A, Kazanaviciute V, Scheikl E, Teige M, Doczi R, Hirt H, Schwanninger M, Kant M, Schuurink R, Mauch F: **The PP2C-type phosphatase AP2C1, which negatively regulates MPK4 and MPK6, modulates innate immunity, jasmonic acid, and ethylene levels in Arabidopsis.** *Plant Cell* 2007, **19**:2213-2224.
43. De Wit P: **Molecular characterization of gene-for-gene systems in plant-fungus interactions and the application of avirulence genes in control of plant pathogens.** *Annu Rev Phytopathol* 1992, **30**:391-418.
44. Romeis T, Piedras P, Zhang S, Klessig DF, Hirt H, Jones JDG: **Rapid Avr 9- and Cf-9-Dependent Activation of MAP Kinases in Tobacco Cell Cultures and Leaves Convergence of Resistance Gene, Elicitor, Wound, and Salicylate Responses.** *Plant Cell* 1999, **11**:273-288.
45. Cai D, Kleine M, Kifle S, Harloff HJ, Sandal NN, Marcker KA, Klein-Lankhorst RM, Salentijn EMJ, Lange W, Stiekema WJ: **Positional cloning of a gene for nematode resistance in sugar beet.** *Science* 1997, **275**:832-834.
46. Thurau T, Kifle S, Jung C, Cai D: **The promoter of the nematode resistance gene Hs1 pro 1 activates a nematode-responsive and feeding site-specific gene expression in sugar beet (Beta vulgaris L.) and Arabidopsis thaliana.** *Plant Mol Biol* 2003, **52**:643-660.
47. Tör M, Gordon P, Cuzick A, Eulgem T, Sinapidou E, Mert-Türk F, Can C, Dangl JL, Holub EB: **Arabidopsis SGT1b is required for defense signaling conferred by several downy mildew resistance genes.** *Plant Cell* 2002, **14**:993-1003.
48. Artus NN, Edwards GE: **Properties of leaf NAD-malic enzyme from the inducible crassulacean acid metabolism species *Mesembryanthemum crystallinum*.** *Plant Cell Physiol* 1985, **26**:341-350.
49. Schaaf J, Walter MH, Hess D: **Primary metabolism in plant defense (regulation of a bean malic enzyme gene promoter in transgenic tobacco by developmental and environmental cues).** *Plant Physiol* 1995, **108**:949-960.
50. Casati P, Drincovich MF, Edwards GE, Andreo CS: **Malate metabolism by NADP-malic enzyme in plant defense.** *Photosynth Res* 1999, **61**:99-105.
51. Waldbauer GP: **The consumption and utilization of food by insects.** *Advances in Insect Physiology* London, Academic Press IncBeament JWL 1965, 229-282.
52. Pierrugues O, Brutesco C, Oshiro J, Gouy M, Deveaux Y, Carman GM, Thuriaux P, Kazmaier M: **Lipid Phosphate Phosphatases in Arabidopsis: Regulation of the AtLPP1 gene in response to stress.** *J Biol Chem* 2001, **276**:20300-20308.
53. Lee S, Suh S, Kim S, Crain R, Kwak JM, Nam HG, Lee Y: **Systemic elevation of phosphatidic acid and lysophospholipid levels in wounded plants.** *Plant J* 1997, **12**:547-556.
54. Van Dam NM, Horn M, Mares M, Baldwin IT: **Ontogeny constrains systemic protease inhibitor response in *Nicotiana attenuata*.** *J Chem Ecol* 2001, **27**:547-568.
55. Bonaventure G, Ohlrogge JB: **Differential regulation of mRNA levels of acyl carrier protein isoforms in Arabidopsis.** *Plant Physiol* 2002, **128**:223-235.
56. Saedler R, Baldwin IT: **Virus-induced gene silencing of jasmonate-induced direct defences, nicotine and trypsin proteinase-inhibitors in *Nicotiana attenuata*.** *J Exp Bot* 2004, **55**:151-157.
57. Kallenbach M, Alagna F, Baldwin IT, Bonaventure G: **Nicotiana attenuata SIPK, WIPK, NPR1 and fatty acid-amino acid conjugates participate in the induction of JA biosynthesis by affecting early enzymatic steps in the pathway.** *Plant Physiol* 2010, PubMed PMID: 19897603.

doi:10.1186/1471-2229-10-66
Cite this article as: Gilardoni *et al.*: SuperSAGE analysis of the *Nicotiana attenuata* transcriptome after fatty acid-amino acid elicitation (FAC): identification of early mediators of insect responses. *BMC Plant Biology* 2010 **10**:66.

Additional files:

Additional file 1 - Complete list of UniTag sequences, copy numbers, and annotations to GenBank nucleotide databases. **(Data can be found on the attached CD-ROM).**

Additional file 2 - Complete list of differentially expressed UniTags and GO categorization. **(Data can be found on the attached CD-ROM).**

Additional file 3 – Supplementary Figures. Figure S1. Analysis of mRNA accumulation corresponding to 12 UniTags by qPCR. Figure S2. *M.sexta* larval performance on VIGS silenced plants.

Additional file 4- List of differentially expressed UniTags previously identified by differential expression techniques. **(Data can be found on the attached CD-ROM).**

Additional file 5- Supplementary Tables. Table S1. Primers for elongation of cDNAs correspondig to UniTags. Table S2. Primers for qPCR. Table S3. Primers for VIGS analysis.

Additional file 3 – Supplementary Figures

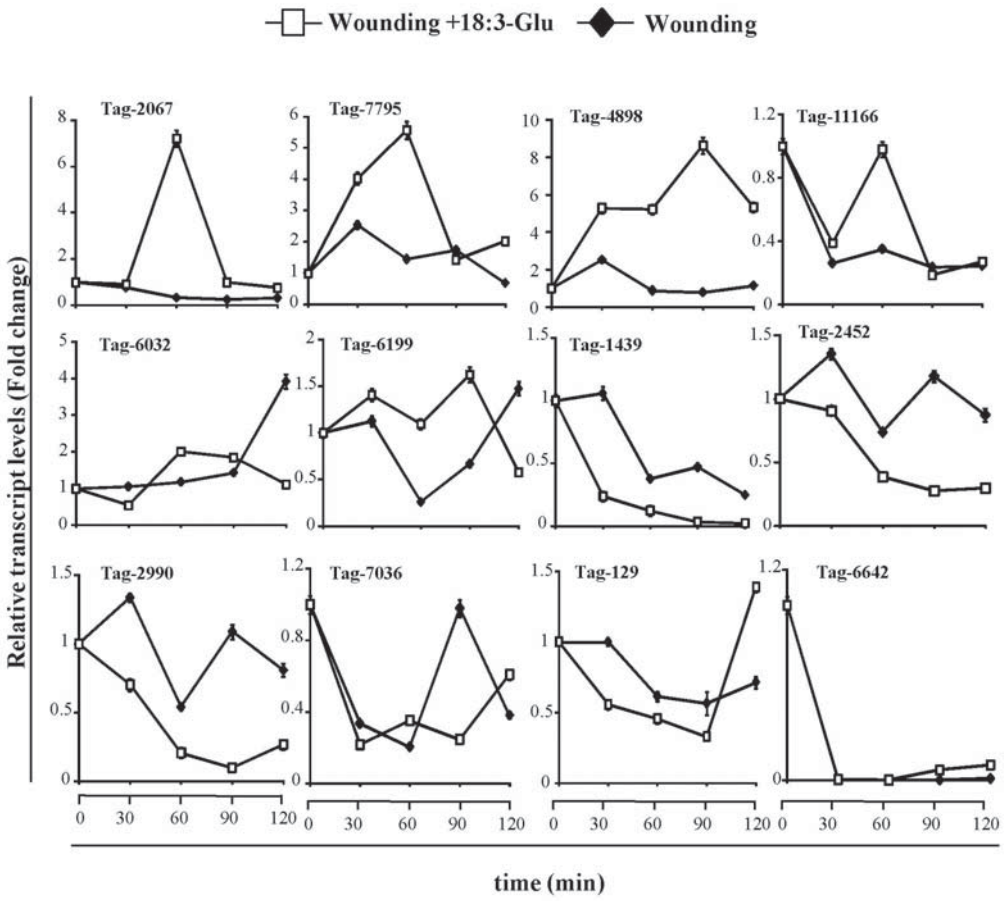

Figure S1. Analysis of mRNA accumulation corresponding to selected UniTags by qPCR. Kinetics of induction of mRNAs for 12 UniTags analyzed by qPCR after wounding and 18:3-Glu elicitation . Relative mRNA quantification was performed using the eEF1A as a reference gene for normalization and the data is expressed as fold-change relative to time 0 (unelicited leaves). Values at this time point were set arbitrary to 1. Transcripts levels were analyzed in three biological replicates (n=3).

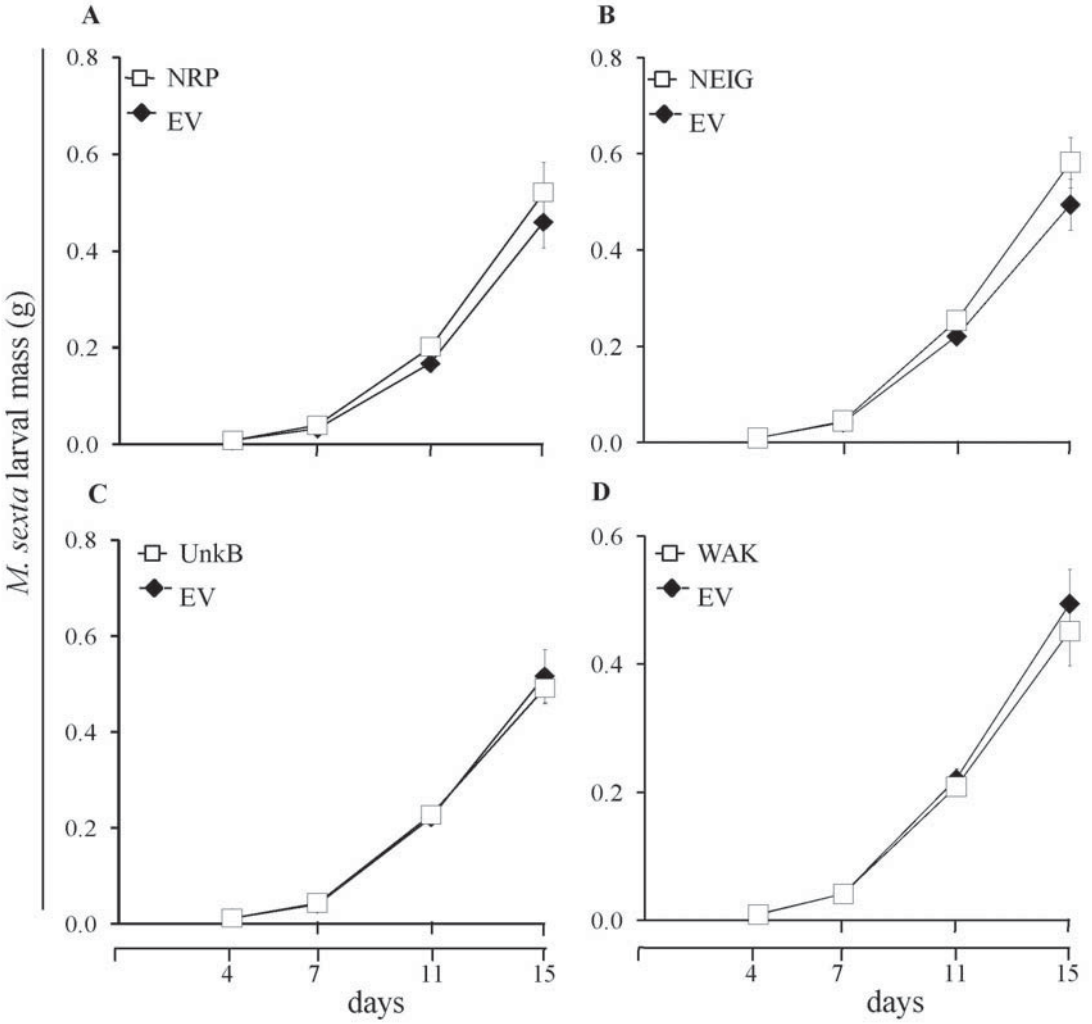

Figure S2. *M.sexta* larval performance on VIGS silenced plants.

N.attenuata plants were silenced in the expression of (A) NRP, (B) NEIG, (C) UnkB and (D) WAK by VIGS. Plants transformed with the empty vector (EV) were used as controls. Results are presented as the mean (+/- SE) of *M.sexta* larval mass after 4, 7, 11 and 15 days of feeding on EV and silenced plants (n=32 for each genotype). Statistical analysis was performed by repeated-measurement ANOVA and no significant differences were observed.

Additional file 5- Supplementary Tables.

Table S1. Primers used for elongation of cDNAs correspondig to UniTags.

Nested primers for 3'RACE		Specific primers	
Tag 837_A	CATGAATCATCCAATATGGTATG	Tag 129_Fw	TCTTAGCGTTCCATCCTCAAGA
Tag 837_B	GAATCATCCAATATGGTATGGGC	Tag 129_Rev	ACATGGTTGCTAGTGGTCGAAG
Tag 895_A	CATGAATGACACTAATGAATTCG	Tag 995 _Fw	TTGGCTTGTTTCTTGAATTCATG
Tag 895_B	GAATGACACTAATGAATTCGTCG	Tag 995_Rv	CAATTCTCAAATGGACTGATTCA
Tag 1439_A	CATGACTGCTGTCAGACGAACTG	Tag 1844_Fw	GAACATGATAAGAAGAATTTGATGA
Tag 1439_B	GACTGCTGTCAGACGAACTGCAC	Tag 1844_Rv	GAAGACGCTCATATATATGGTAC
Tag 2452_A	CATGATGAATACGAGCAGCTTCG	Tag 2067_Fw	GCAGTCAAGTAGGTCTACTAC
Tag 2452_B	GATGAATACGAGCAGCTTCGGGT	Tag 2067_Rv	CATGAGTTGGTGGATTCAAATC
Tag 2978_A	CATGATTTTTTTTCCTTCTGCTG	Tag 2815_Fw	CAAGTTGCTCTTGGGGAGATCA
Tag 2978_B	GATTTTTTTTCCTTCTGCTGTAT	Tag 2815_Rv	CAGCTCCACTGCTTTGCAACTC
Tag 2990_A	CATGCAAAACGTACACCGAGAAA	Tag 5283_Fw	CATTCGATAACCCCAGATTTTTC
Tag 2990_B	GCAAAACGTACACCGAGAAAGAA	Tag 5283_Rv	TGCTTGAATTTCACTCGCAGC
Tag 4898_A	CATGCTGCTGGGACTCTCGTA	Tag 5869_Fw	GCTGAGAAATGTAATGACTTCTG
Tag 4898_B	TGCTGGGACTCTCGTATACAG	Tag 5869_Rv	AAAACTTAACTTGCAAAGTCTCC
Tag 6199_A	CATGGATCGGCAAACAAAGAGAT	Tag 6032_Fw	CATGGAGGTCTTTCTCGTTATC
Tag 6199_B	GGATCGGCAAACAAAGAGATTAT	Tag 6032_Rv	GAACGCAAAGGTTTAAAACGTATA
Tag 6642_A	CATGGCCAAGAGTACGTTCTC	Tag 6205_Fw	CTGATCCTAGACCGTATGCG
Tag 6642_B	CCAAGAGTACGTTCTCAAAGG	Tag 6205_Rv	AAGCATTTTTGACGCGTAGATCC
Tag 11166_A	CATGTGTCAAGCTGGAAAACT	Tag 6938_Fw	TCATGGCTCGGATTTGCATCTC
Tag 11166_B	GTCAAGCTGGAAAACTTGCCA	Tag 6938_Rv	GATCAATCGAGGTGGAGAACTC
Tag 12314_A	CATGTTTAGAGCAATGAGTACAC	Tag 7036_Fw	TGAAACTCGTGCTGAGATCGT
Tag 12314_B	GTTTAGAGCAATGAGTACACGAA	Tag 7036_Rv	ATCCAGGTAAGTTGTCAGCAG
		Tag 7795_Fw	CATGGGTTATTCAGTGCTGT
		Tag 7795_Rv	AGCATAGACCAAAGCACCATTG
		Tag 9434_Fw	AGTGTGATGATAATTCAACTGCAGC
		Tag 9434_Rv	AGTTGAGAAAGAATTCATCAGGTCAC
		Tag 9719_Fw	TGATGTCTATTTTCAGTTCCTTTG
		Tag 9719_Rv	TTCCTGAATTTACAGCAGAATAC
		Tag 10039_Fw	CTTGGGTTTCTATCATTGTATTTG
		Tag 10039-Rv	CCGTTAGTATGGTGGACATG
		Tag 11559_Fw	GCTAATACTAGCTGTGGTAGAT
		Tag 11559_Rv	CATGCATGTTATCAGTTAACTAA

Table S2. Primers for qRT-PCR.

Tag 129_qFw	TAGCCATTAGCATGGAGGATTCAAC	Tag 6032_qFw	CATGGAGGTCTTTCTCGTTATCTGA
Tag 129_qRv	TCTTGTCCCATGTATCAATGCTCCA	Tag 6032_qRv	TTACAATGACAGAGAGCCAGACTCA
Tag 837_qFw	GAATCATCCAATATGGTATGGGCAA	Tag 6199_qFw	AGGAACGGACTGCACAAGATCATTC
Tag 837_qRv	TGATGACGAGAGCCATCAGCCCTT	Tag 6199_qRv	TGGATCGGCAAACAAAGAGATTATTC
Tag 895_qFw	TGAATTCGTCGTTAAGCCTTCGAGT	Tag 6205_qFw	CTGATCCTAGACCGTATGCGAACA
Tag 895_qRv	CTGTTAGTCGTAGTCGAATTCGGAT	Tag 6205_qRv	GCTGACAACCGTCGTCTCATCAGA
Tag 995_qFw	GGCTTGTTTCTTGAATTCATGTTTCT	Tag 6642_qFw	CCAAGAGTACGTTCTCAAAGGATCA
Tag 995_qRv	CAAGTCAGAGTTAGTGCAGAGAATG	Tag 6642_qRv	TTGTCCTCTGCTCAGCAGCTCCGT
Tag 1439 _qFw	ACTGCTGTCAGACGAACTGCACAGTT	Tag 6938_qFw	CAATCGAGGTGGAGAACTCAAAACG
Tag 1439_qRv	TTCCTCCCTGCTTAATGGCTTTTTG	Tag 6938_qRv	AGGCTGAGCCGACCAGTGAGAATC
Tag 1844_qFw	GTCATTACATGGTCATCCTAAGAAG	Tag 7036_qRv	GCAAAAGTCTCAGAATCGATGGTCT
Tag 1844_qRv	CGTACACAACCAGAGTGATACATAA	Tag 7036_qFw	GAAACTCGTGCTGAGATCGTTGAAC
Tag 2067_qFw	AGTCAAGTAGGTCTACTACTCTATG	Tag 7795_qFw	AGCATAGACCAAAGCACCATTGTCC
Tag 2067_qRv	GAGCACCTGCTATGTTGGTTGCCA	Tag 7795_qRv	TTGCACTATGCAGCCTATTATGGTC
Tag 2452_qFw	GATGAATACGAGCAGCTTCGGGTAA	Tag 9719_qFw	CTTGTATCAGATCACAAGACTGGTG
Tag 2452_qRv	TCGATCCAATGTCATGTGCATTGAG	Tag 9719_qRv	TAGGGAATGATAGTCTCGAAACAGT
Tag 2815_qFw	AGCTCCACTGCTTTGCAACTCAATC	Tag 10039_qFw	CACGTGTGGATGACTACTGGCATC
Tag 2815_qRv	TCTGATTCTTTGCTTGAGGCTCAGT	Tag 10039_qRv	CGTTAGTATGGTGGACATGTTGT
Tag 2978_qFw	TTCTGCTGTATAAGTTTAATTGTCCA	Tag 11166_qFw	GTCAAGCTGGAAAACTTGCCAGTG
Tag 2978_qRv	ACAAGTTATATCCGTAAATACCACCA	Tag 11166_qRv	CATTTTTCATTCGGTCTCATAGGAC
Tag 2990_qFw	CGTACACCGAGAAAGAAGGCCTCA	Tag 11559_qFw	GTCCTTGTTGAGCTGATATCATCAC
Tag 2990_qRv	AGTTTCTGTTGCCAGATGCCAAGAG	Tag 11559_qRv	AGCTAGCTCTGCAACTGAAGTAGTC
Tag 4898_qFw	ATCTGCATCGTCGAGTAGTAGACAC	Tag 12314 _qFw	CCAATCTTGGGTAAGCCAAAGTTGA
Tag 4898_qRv	CGCTCTACAATTATCACAAATCACTC	Tag 12314 _qRv	ACTGAGTAGTCGCTCGGAAATTCTC
Tag 5283_qFw	TCATGAACACAAGCTAATGCACTTG	Tag 9434_qFw	AGTGTGATGATAATTCAACTGCAGC
Tag 5283_qRv	GTTCAGTCCTTGAAATACAGTAGACT	Tag 9434_qRv	AGTTGAGAAAGAATTCATCAGGTCAC
Tag 5869_qFw	GCTTGATCTGAGTTAACATACACCT		
Tag 5869_qRv	TGCTGAGAAATGTAATGACTTCTGAG		

Table S3. Primers used for VIGS.

Primers used for construction of VIGS vectors.	
EIG_Fw	GCGGCGGTCGACTTGCATCATCTGGGAAGAGG
EIG_Rv	GCGGCGGGATCCGCATAGGTCTGGCAAGTACAC
LPP_Fw	GCGGCGGTCGACATTGTATTTGGCAGGGAAG
LPP_Rv	GCGGCGGGATCCGTTAGTATGGTGGACATG
NRP_Fw	GCGGCGGTCGACACGACGGTTGTCAGCCAGAC
NRP_Rv	GCGGCGGGATCCGTAGATCCATGTTTCGAGGATC
UNKA_Fw	GCGGCGGTCGACAAACTGTGTCACCTACAGGG
UNKA_Rv	GCGGCGGGATCCGGTCTCTACAGCTTGTATGC
UNKB_Fw	GCGGCGGTCGACAGGAGCATTCTGCTCCAATC
UNKB_Rv	GCGGCGGGATCCTGCTTCCATGTTGGATTTGG
WAK_Fw	GCGGCGGTCGACAGCGATGTGTATAGCTTCGG
WAK_Rv	GCGGCGGGATCCTCTGGTTTTCAAACTCGCCC
Primers used to evaluate gene silencing ficiency in VIGS-silenced plants	
EIG_qFw	TGCCAACAAATGTTTGTGCATTCTC
EIG_qRv	GTGTGGGTTGCTCCTCTGCTTC
LPP_qFw	CTTGGGTTTCTATCATTGTATTTGGCA
LPP_qRv	TGATGCCAGTAGTCATCCACACGTG
NRP_qFw	CTGATCCTAGACCGTATGCGAACA
NRP_qRv	ACACCTCCTCATTTCGCATTCAATG
UnkA_qFw	TATGGTATGGGCAAGTAGAGATGAC
UnkA_qRv	CCTTAGTATTCATTCATCATTACCAC
UnkB_qFw	AAGGAAGAGGAGCATTCTGCTCC
UnkB_qRw	CACCGCAGAATCAAAATCACTTTAC
WAK_qFw	CATGCATGTTTCAGTTAACTAATA
WAK_qRv	TGACATTAATCTCTTCTTTCTTCTG

Chapter 4:

The *Nicotiana attenuata* Na*LecRK1* gene suppresses the salicylic acid-mediated inhibition of induced defense responses during *Manduca sexta* herbivory.

Chapter 4

Manuscript 2

The *Nicotiana attenuata* Na*LecRK1* gene suppresses the salicylic acid-mediated inhibition of induced defense responses during *Manduca sexta* herbivory.

Running title: NaLecRK1 regulation of defense responses.

Authors: Paola Gilardoni, Christian Hettenhausen, Ian T. Baldwin and Gustavo Bonaventure.

Submited to the Plant Cell Journal, PLANTCELL/2011/088229.

Affiliations: Max Planck Institute of Chemical Ecology, Department of Molecular Ecology, Hans Knöll Str. 8, D-07745 Jena, Germany.

Corresponding author: Gustavo Bonaventure; Max Planck Institute of Chemical Ecology, Department of Molecular Ecology, Hans Knöll Str. 8, D-07745 Jena, Germany; Email: gbonaventure@ice.mpg.de; Tel: +49 3641 571118; Fax: +49 3641 571102.

Estimated length of the article: 20 pages.

"The author responsible for distribution of materials integral to the findings presented in this article in accordance with the policy described in the Instructions for Authors (www.plantcell.org) is: Ian T. Baldwin (baldwin@ice.mpg.de)."

Chapter 4

ABSTRACT

Nicotiana attenuata has the capacity to respond specifically to herbivory by its natural herbivore, *Manduca sexta,* through the perception of elicitors in larval oral secretions. We demonstrate that the induction of the G-type lectin receptor kinase 1 (NaLecRK1) during *M. sexta* herbivory suppresses the larval-mediated accumulation of salicylic acid (SA) that inhibits the elicitation of critical defense molecules. Gene function analysis performed by reducing Na*LecRK1* expression in *N. attenuata* by both virus induced gene silencing and inverted repeated RNA interference (ir-lecRK1 plants) revealed that NaLecRK1 was essential to mount a full defense response against *M. sexta* folivory; larvae growing on ir-lecRK1 plants were 40 to 100% larger than those growing on wild type plants. The induced accumulation of nicotine, diterpene-glucosides (DTGs), trypsin protease inhibitors (TPIs) and the expression of threonine deaminase (Na*TD*) were several fold reduced in ir-lecRK1 plants. The accumulation of jasmonates was unaffected during *M. sexta* herbivory in ir-lecRK1 plants however SA levels were 2-fold higher compared to wild type plants. Suppression of this enhanced SA accumulation by introgression of the *nahG* gene into ir-lecRK1 plants demonstrated that the accumulation of SA was responsible for the enhanced performance of *M. sexta* larvae and the inhibition of nicotine, DTG, TPI accumulation and Na*TD* expression.

Chapter 4

INTRODUCTION

Plant species from a wide taxonomical distribution trigger and tailor defense and tolerance responses against lepidopteran larval folivory after perception of components (HAEs: herbivore associated elicitors) in the oral secretions (OS) of the larvae (Tumlinson and Lait, 2005a; Schmelz et al., 2009b; Bonaventure et al., 2011b). These OS components function as chemical cues which convey sufficient information to the plant to initiate specific responses against the feeding insect (Howe and Jander, 2008a; Wu and Baldwin, 2009). Moreover, some HAEs can also counteract the defense response of plants, thus being in this case beneficial to the insect (Musser et al., 2002; Diezel et al., 2009a).

The HAEs that act during insect folivory are diverse in structure, ranging from enzymes (e.g., glucose oxidase; Musser *et al*., 2002) to modified forms of lipids (e.g., fatty acid-amino acid conjugates (FACs); (Alborn et al., 1997b; Halitschke et al., 2001a), sulfur-containing fatty acids (caeliferins; (Alborn et al., 2007a) and from fragments of cell walls (e.g., oligogalacturonides) to peptides released from digested plant proteins (e.g., inceptins; (Schmelz et al., 2006b).

FACs belong to a widely distributed family of HAEs present in the OS of a large number of lepidopteran species including *Manduca sexta* (Yoshinaga et al., 2010a) and they are necessary and sufficient to elicit herbivory-specific responses in several plant species including maize (*Zea mays*), soybean (*Glycine max*), eggplant (*Solanum melongena*), black nightshade (*Solanum nigrum*) and wild tobacco (*Nicotiana attenuata;* (Alborn et al., 1997b; Schmelz et al., 2009b; VanDoorn et al., 2010; Bonaventure et al., 2011b). Some of the most abundant FACs are conjugates of glutamate and glutamine with unmodified or oxidized derivatives of polyunsaturated fatty acids (Alborn et al., 1997b; Spiteller and Boland, 2003; VanDoorn et al., 2010; Yoshinaga et al., 2010a). Recently, it has been demonstrated that FACs are essential for the assimilation of nitrogen by developing larvae (Yoshinaga *et al*., 2008) making it impossible for the caterpillars to feed “stealthly” without eliciting a defense response by the plant.

Chapter 4

Nicotiana attenuata is an annual tobacco plant native to the deserts of the Southwestern USA and in its natural habitat it is frequently attacked by folivorous larvae of the specialist *M. sexta* which is frequently responsible for the majority of leaf area lost to herbivores in natural populations. In *N. attenuata*, responses to *M. sexta* herbivory and *M. sexta* OS or FAC elicitation (treatments that simulate herbivory) overlap by more than 80% and strongly differ from those induced by mechanical damage (Halitschke *et al*., 2001). These responses include among others changes in the expression of more than 500 genes, 90 proteins, 170 metabolites and the differential production of jasmonic acid (JA), ethylene (ET) and salicylic acid (SA; Hermsmeier *et al*., 2001; Giri *et al*., 2006; Gilardoni *et al*., 2010; Gaquerel *et al*., 2010; Kallenbach *et al*., 2010).

The biosynthesis of JA and jasmonyl-Isoleucine (JA-Ile) and their perception are essential for the triggering of induced defense responses to chewing arthropods in different plant species (Staswick and Tiryaki, 2004; Wang *et al*., 2007; Howe and Jander, 2008; Vandoorn *et al*., 2011). *In N. attenuata* plants, critical defense responses which are induced during *M. sexta* folivory include the accumulation of the defense metabolites 17-hydroxygeranyllinalool diterpene glycosides (HGL-DTGs), nicotine, phenylpropanoid-polyamine conjugates and protease inhibitors (PIs); when *N. attenuata* plants are engineered to produced reduced amounts of these molecules they become severely compromised in their capacity to survive *M. sexta* attack (Steppuhn *et al*., 2004; Zavala *et al*., 2004; Jassbi *et al*., 2008; Kaur *et al*., 2010). In tomato (*Solanum lycopersicum*) and *N. attenuata*, the induction of threonine deaminase (TD) is also a critical induced defense response. TD participates in the deaminaton of threonine (Thr) to form α-ketobutyrate for isoleucine (Ile) biosynthesis and in *N. attenuata* reduced Na*TD* expression compromises the levels of JA-Ile formation in leaves and thereby the induction of defense responses such as nicotine and trypsin protease inhibitor (TPI) accumulation (Kang et al., 2006b). In tomato, an active form of SlTD2 lacking its regulatory domain deaminates Thr in the gut of *M. sexta* larvae and thereby reduces the ingested levels of this essential amino acid for larval growth (Chen *et al*., 2005).

Although JA plays a prominent role in the induction of defense responses against chewing insects in plants, salicylic acid (SA) and ethylene (ET) can modulate either

positively or negatively the induction of defense responses stimulated by JA (Doherty *et al*., 1988; Doares *et al*., 1995; O'Donnell *et al*., 1996; Stotz *et al*., 2002; Zarate *et al*., 2007; Diezel *et al*., 2009) and the antagonistic and synergistic effects between JA, SA and ET signaling pathways have been extensively documented (Niki *et al*., 1998; Reymond and Farmer, 1998; Gupta *et al*., 2000; Li *et al*., 2004; Mur *et al*., 2006; Leon-Reyes *et al*., 2009; Diezel *et al*., 2009). Importantly, the stimulatory effect of JA and the modulation of the JA-mediated responses by SA and ET are the major known determinants of the final response triggered by plants during their interaction with lepidopteran larvae (Howe and Jander, 2008). Also important is the fact that the level of production of JA, SA and ET in plants depends on the attacking herbivore and thereby both plants and insects try to adjust or prevent, respectively, the induction of defense responses (Musser *et al*., 2006; Howe and Jander, 2008; Diezel *et al*., 2009).

At present, little is known about the signal transduction components operating specifically during insect herbivory and controlling the modulation of induced defense responses in plants during this biotic stress. Among the known signal components acting early upon wounding and recognition of FACs or *M. sexta* OS in *N. tabacum* and *N. attenuata* plants are two mitogen-activated protein kinases (MAPKs), WIPK (wound-induced protein kinase) and SIPK (salicylate-induced protein kinase; (Seo et al., 1999; Wu et al., 2007). In *N. attenuata,* NaSIPK and NaWIPK affect JA biosynthesis (Kallenbach *et al*., 2010) and a large number of induced defense responses (Wu *et al*., 2007) and in *N. tabacum* they affect JA and SA accumulation after wounding (Seo *et al*., 2007). In tomato, the protein kinase 1b (TPK1b) and the MAPKs LeMPK1, LeMPK2 and LeMPK3 play important roles in mediating JA- and ET-dependent defense responses against folivorous insects (Kandoth *et al*., 2007; AbuQamar *et al*., 2008).

With the aim of identifying additional signal transduction components of the pathways controlling defense and tolerance responses against lepidopteran larvae, a SuperSAGE (serial analysis of gene expression) approach combined with 454 sequencing was recently used to quantify the early transcriptional changes elicited by the FAC *N*-linolenoyl-glutamic acid (18:3-Glu) in *N. attenuata* plants (Gilardoni *et al*., 2010). The analysis targeted mRNAs encoding regulatory components: rare transcripts with very rapid

FAC-elicited kinetics. From 12,744 unique tag sequences identified (UniTags), the abundance of 430 and 117 were significantly increased and decreased, respectively, in the SuperSAGE library corresponding to 18:3-Glu-elicited leaves compared to that corresponding to wounded leaves. More than 25% of the UniTag sequences matched to putative regulatory components including 22 protein kinases (Gilardoni *et al*., 2010). Here we demonstrate that the OS/FAC-mediated induction of the *N. attenuata* G-type lectin receptor kinase 1 (NaLecRK1) is essential during *M. sexta* larval herbivory to suppress the accumulation of SA and thereby indispensable to stimulate the unfettered JA-mediated induction of critical defense metabolites in *N. attenuata*.

RESULTS

Identification of NaLecRK1 as a regulator of the interaction between *N. attenuata and M. sexta*

From the SuperSAGE analysis published recently by Gilardoni *et al* (2010), the UniTag-5358 was identified as a tag whose abundance was 11-fold enriched in the SuperSAGE library corresponding to 18:3-Glu elicited leaves compared to the library corresponding to wounded leaves. To unravel the role of the gene corresponding to UniTag-5358, we first obtained the full length cDNA of this Unitag by 5' and 3' random amplification of cDNA ends (RACE). The full length cDNA nucleotide sequence contained an open reading frame (ORF) of ~2.5 kb encoding for a predicted polypeptide of 833 amino acids (see GenBank accession number in Materials and Methods). Analysis of sequence similarity by basic local alignment (BLAST) using the complete predicted amino acid sequence of UniTag-5358 showed that the protein sequence presented on average more than 80% sequence similarity to receptor-like kinases of the lectin domain superfamily (Supplemental Figure S1 online; (Bouwmeester and Govers, 2009). The closest homologues to NaLecRK1 with known functions were the lectin receptor kinase protein NbLRK1 from *Nicotiana benthamiana* (Kanzaki *et al*., 2008), Pi-d2 from rice (*Oryza sativa;* Chen *et al*., 2006) and NgRLK1 from *Nicotiana glutinosa* (Kim *et al.*, 2010; Supplemental

Figure S1 online); the function of these genes has been associated to defense responses against microbial pathogens.

The amino acid sequence of UniTag-5358 contains a predicted N-terminal extracellular region, a single transmembrane spanning α-helix and a C-terminal cytoplasmic region (Figure 1A). The extracellular N-terminal region contains a predicted 22 amino acid signal sequence to the secretory pathway (amino acids 1 to 22), a lectin domain from amino acids 55 to 177 (e-value $4.08e^{-16}$; SMART algorithm (Letunic *et al*., 2009)), an epidermal growth factor-like domain (EGF) from amino acids 310 to 364 (e-value $6.51e^{-02}$) and a PAN_AP (plasminogen-apple-nematode motif) domain from amino acids 364 to 445 (e-value $1.47e^{-02}$; Figure 1A). The predicted transmembrane domain expands from amino acids 476 to 490 (e-value $9.9e^{-02}$) and the C-terminal cytoplasmatic region contains a predicted Ser/Thr kinase domain from amino acids 519 to 788 (e-value $9.04e^{-31}$; Figure 1A and Supplemental Figure S1 online).

In Arabidopsis, lectin receptor kinases (LecRKs) are divided in three classes based on the type of extracellular lectin domain: G-, C- and L-type LecRKs (Bouwmeester and Govers, 2009). The G-type LecRKs present a G-type lectin motif, one EGF and PAN_AP domains in the N-terminal region (Bouwmeester and Govers, 2009); domains that were present in UniTag-5358 (Figure 1A and Supplemental Figure S1 online). The gene corresponding to UniTag-5358 was therefore renamed Na*LecRK1* (*N. attenuata* G-type lectin receptor kinase 1).

SIPK and WIPK are positive regulators of NaLecRK1 expression while jasmonates have an inhibitory role

The kinetic of Na*LecRK1* mRNA induction in leaves as a response to OS elicitation (from *M. sexta*, *S. littoralis* and *Schistocera gregaria* (grasshopper)), 18:3-Glu elicitation and wounding was first evaluated in *N. attenuata* wild type (WT) plants. Consistent with the SuperSAGE data (Gilardoni *et al*., 2010), Na*LecRK1* transcript levels were strongly increased (ca. 60-fold) at 1 h after 18:3-Glu elicitation (compared to basal transcript levels in unelicited leaves; Figure 1B). Moreover, the increase was transient and Na*LecRK1*

mRNA levels decreased rapidly (within 2 h) to basal levels (Figure 1B). In wounded leaves, Na*LecRK1* mRNA levels were also increased (ca. 7-fold) at 1 h (Figure 1B) showing that mechanical damage also induces the expression of this gene however to levels lower than 18:3-Glu elicitation. Elicitation with *M. sexta* OS induced a 100-fold increase in Na*LecRK1* transcript levels and elicitation with *S. littoralis* OS induced a 50-fold increase (compared to basal levels; Figure 1B). In contrast, elicitation with *S. gregaria* OS showed an effect similar to wounding (Figure 1B), a result consistent with undetectable levels of FACs in the *S. gregaria* OS (Schafer et al., 2011).

Second, we asked whether the induction of Na*LecRK1* expression depended on NaSIPK and NaWIPK activities (these MAPKs control the earliest known molecular events that trigger defense responses against *M. sexta* herbivory; Wu *et al.*, 2007). Plants with reduced expression of these two genes (ir-sipk and ir-wipk, respectively; Wu *et al*., 2007) were elicited with 18:3-Glu and the Na*LecRK1* mRNA levels were analyzed. The induction of this transcript was delayed and reduced by approximately 2-fold in ir-sipk plants compared to WT whereas completely absent in ir-wipk plants (Figure 1C).

Third, to evaluate whether the induction of Na*LecRK1* mRNA levels was dependent on the endogenous production of JA and JA-Ile, plants with reduced expression of *LIPOXYGENASE 3* (Na*LOX3*) and *CORONATIVE INSENSITIVE 1* (Na*COI1*) genes were elicited with 18:3-Glu. These plants, ir-lox3 and ir-coi1, are deficient in JA accumulation (Allmann *et al*., 2010) and JA signaling (Paschold et al., 2008), respectively. In contrast to ir-sipk and ir-wipk plants, the induction of Na*LecRK1* transcript levels in ir-lox3 and ir-coi1 plants was accelerated and increased to levels 3 fold higher than in WT plants (Figure 1C). Together, these results indicated that, after 18:3-Glu elicitation, NaSIPK and NaWIPK are positive regulators of Na*LecRK1* gene expression whereas jasmonates have an inhibitory effect.

Finally, the tissue specific expression of Na*LecRK1* was studied and based on the accumulation of transcript levels, Na*LecRK1* was expressed ubiquitously in all tissues analyzed with higher levels of expression in roots and stems compared to rosette leaves and flower parts (Figure 1D).

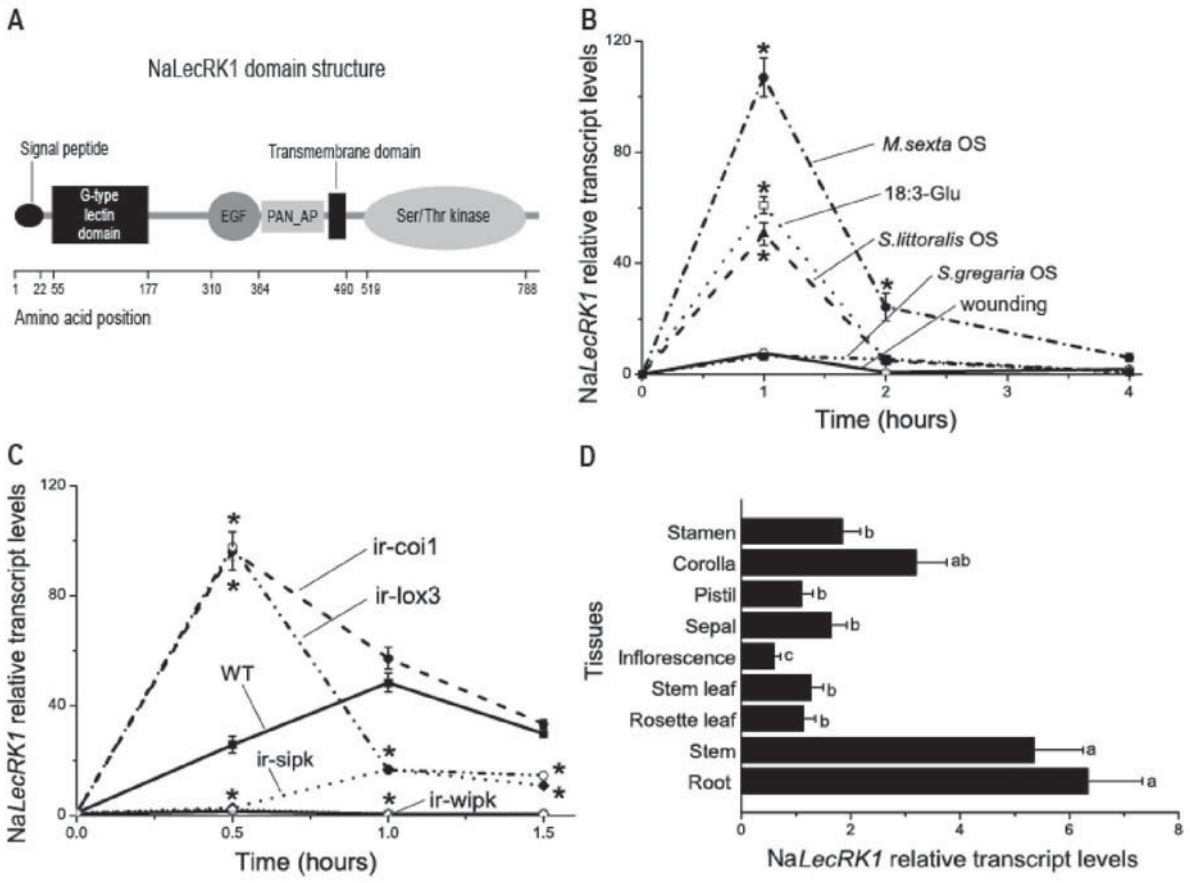

Figure 1. NaLecRK1 predicted domains and mRNA expression pattern.
(A) Schematic representation of NaLecRK1 domain composition and organization based on conserved domain analysis. PAN_AP, plasminogen-apple-nematode motif; EGF, epidermal growth factor-like motif; Ser/Thr: serine/threonine protein kinase domain.
(B) Leaves of rosette stage wild-type (WT) *N. attenuata* plants were either wounded or elicited with OS collected from different insects or synthetic FAC (18:3-Glu). The Na*LecRK1* mRNA levels were quantified by qPCR and values are expressed as the fold-change (FC) increase relative to time 0 (value set arbitrary at 1). The Na*LecRK1* mRNA levels were calculated relative to the expression level of Na*EF1A* mRNA using the ΔCT method; see Materials and Methods). *: P <0.05, Student's t-test, (wounding vs. elicitation at same time point, bars denote ±SE, n=3).
(C) Leaves of rosette stage wild-type (WT) and different ir-silenced *N. attenuata* plants were elicited with synthetic FAC (18:3-Glu). The Na*LecRK1* mRNA levels were analyzed as in (B). *: P <0.05, Student's t-test (WT vs. ir-silenced plants at same time point, bars denote ±SE, n=3).
(D) Na*LecRK1* mRNA levels were quantified by qPCR as described in (B) in different tissues of rosette stage and early flowering *N. attenuata* WT plants. Bars denote ±SE (n=3). Different letters indicate significant differences (univariate ANOVA, $F_{8, 25} = 17.38$, P <0.001, followed by a Tukey HSD post-hoc test, P <0.05).

Chapter 4

Silencing of Na*LecRK1* expression transiently by VIGS and stably by inverted-repeat RNAi reveals a critical function of this gene in *N. attenuata* defense responses against *M. sexta* folivory

The function of NaLecRK1 in the response of *N. attenuata* to *M. sexta* herbivory was first evaluated by transiently reducing the expression of the Na*lecRK1* gene by virus-induced gene silencing (VIGS). An 86 bp fragment corresponding to the 3'-UTR of the Na*LecRK1* mRNA was used to reduce its expression by the tobacco rattle virus (TRV) system (Ratcliff *et al*., 2001) and *Agrobacterium tumefasciens* leaf infiltration (Saedler and Baldwin, 2004). Fifteen days after leaf infiltration, the Na*LecRK1* mRNA levels were analyzed in newly emerged leaves of plants infected to reduce Na*LecRK1* expression (NaLecRK1-VIGS) and control plants infected with the empty vector (EV-VIGS). Na*LecRK1* transcript levels were reduced between 85% and 90% after both wounding and 18:3-Glu elicitation in NaLecRK1-VIGS plants compared to EV-VIGS plants (Supplemental Figure S2A online).

Second, freshly hatched *M. sexta* neonates were placed on these plants and the larval masses were determined at 4, 7 and 11 days after the start of the experiment. Larvae feeding on NaLecRK1-VIGS plants gained ca. 50% and 100% more mass after 7 and 11 days, respectively, compared to larvae feeding on EV-VIGS plants (Supplemental Figure S2B online). These results suggested that NaLecRK1 plays an important role in the control of the interaction between *N. attenuata* and *M. sexta*.

To examine in further detail the function of NaLecRK1, stably transformed *N. attenuata* plants with reduced expression of Na*LecRK1* were generated by inverted repeat-mediated RNA interference (IR-RNAi; see Materials and Methods for a detailed description of the generation of these plants). Two homozygous independently transformed lines (A-08-378-5-4-1 and A-08-380-6-3-8) named ir-lecRK1-378 and ir-lecRK1-380, respectively, were selected and used for all the experiments described below (Figure 2). These lines carried a single T-DNA insertion in their genomes (Figure 2A) and the levels of Na*LecRK1* mRNA were reduced on average by 95% compared to WT plants after 18:3-Glu elicitation (Figure 2B). The growth and morphology of ir-lecRK1 plants were indistinguishable from those of WT plants at all stages of development (Figure 2C).

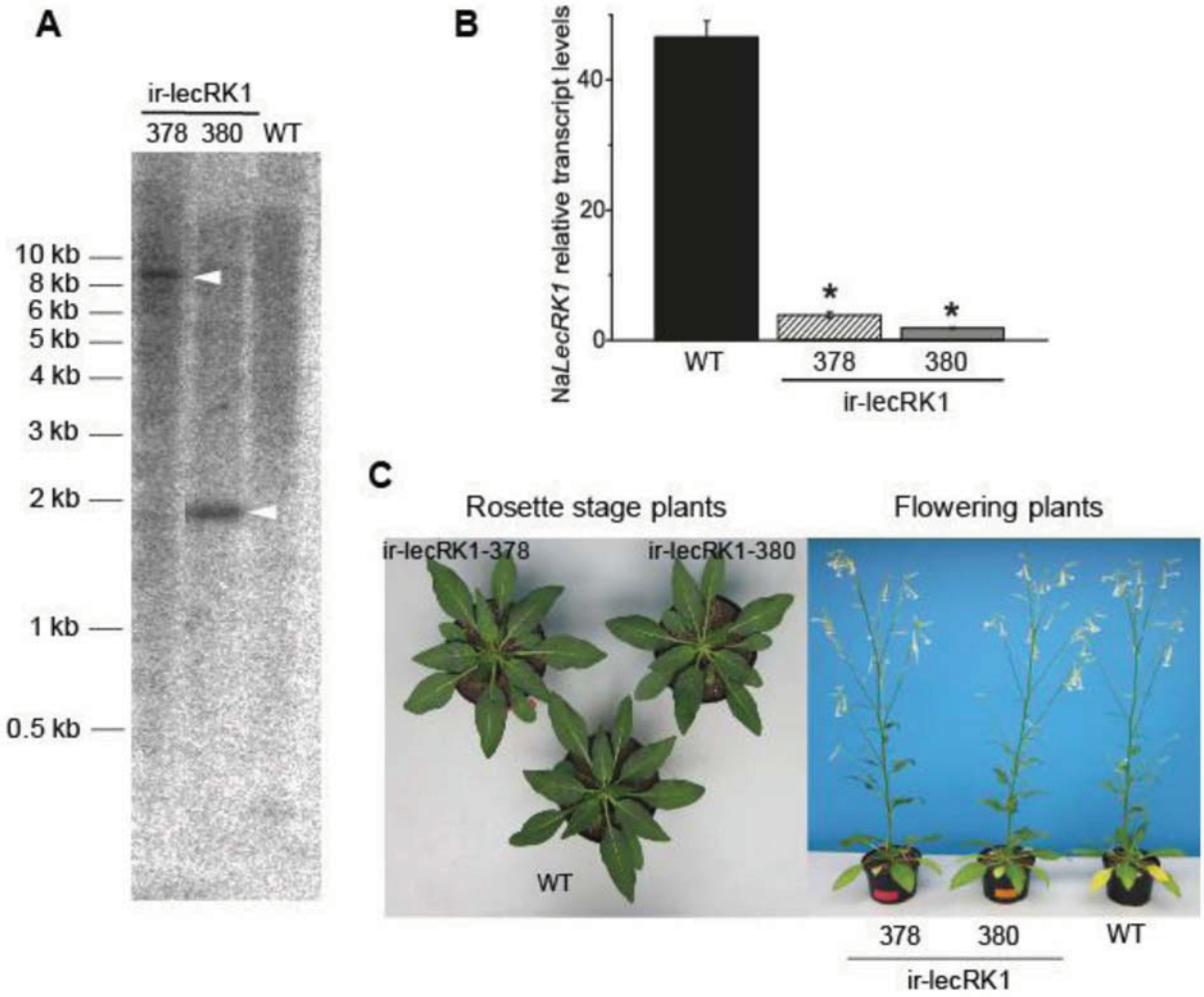

Figure 2. Silencing efficiency in ir-lecRK1 plants and growth morphology.
(A) Southern blot analysis of two independently transformed ir-lecRK1 lines (ir-lecRK1-378 and ir-lecRK1-380). Genomic DNA from ir-lecRK1-378, ir-lecRK1-380 and WT plants was digested with *EcoRV* and analyzed as described in Materials and Methods. Both ir-lecRK1 lines harbored a single T-DNA insertion (arrow head).
(B) Mean (±SE) of transcripts levels of Na*LecRK1* in leaves 1 h after *M. sexta* OS elicitation (n= 3). Na*LecRK1* mRNA levels were quantified as described in caption of Figure 1B. *: P <0.05, Student's t-test (WT vs. ir-lecRK1 plants).
(C) Morphology of WT and ir-lecRK1 plants in rosette stage (left) and mature (elongated) plants (right).

To confirm the results observed with NaLecRK1-VIGS plants, freshly hatched *M. sexta* larvae were placed on WT, ir-lecRK1-378 and ir-lecRK1-380 plants and the mass of the larvae were determined at 4, 7 and 11 days after the start of the experiment. Larvae growing on ir-lecRK1 plants gained 30% to 35% more mass after 11 days of feeding than larvae growing on WT plants (Figures 3A and 3B). Estimation of the leaf area consumed after 11 days showed that ir-lecRK1 plants lost on average 2 times the leaf area of WT plants (inset Figure 3A). The levels of total protein and starch in leaves were similar between ir-lecRK1 and WT plants (Supplemental Figure S3 online). In conclusion, the stable reduction of Na*LecRK1* expression in transgenic plants was consistent with the function of this gene in the regulation of defense responses in *N. attenuata* against *M. sexta* herbivory.

Reduction of Na*LecRK1* expression increases the accumulation of SA after simulated herbivory

To evaluate whether the reduced expression of Na*LecRK1* affected the production of JA, JA-Ile, SA and ET, the levels of these phytohormones were quantified in ir-lecRK1 and WT plants at different times after wounding and *M. sexta* OS elicitation. The accumulation of JA was similar between WT and ir-lecRK1 plants after both treatments (Figure 3C and Supplemental Figure S4A online). In contrast, 1 h after OS elicitation, JA-Ile levels were reduced by 34% and 26% in ir-lecRK1-378 and ir-lecRK1-380 plants, respectively, compared to WT plants (Figure 3D). At 1 and 3 h after wounding, the levels of JA-Ile were similar between WT and ir-lecRK1 plants (Supplemental Figure S4B online). Interestingly, 3 h after OS elicitation, the levels of SA were increased by 2- and 2.5-fold in ir-lecRK1-378 and ir-lecRK1-380 plants, respectively, remaining 1.4-fold higher at 4 h compared to WT plants (Figure 3E). After wounding, the SA levels were similar between WT plants and ir-lecRK1 plants (Supplemental Figure S4C online). Finally, the levels of ET produced by WT and ir-lecRK1 plants after OS elicitation and wounding were also similar (Supplemental Figure S5 online).

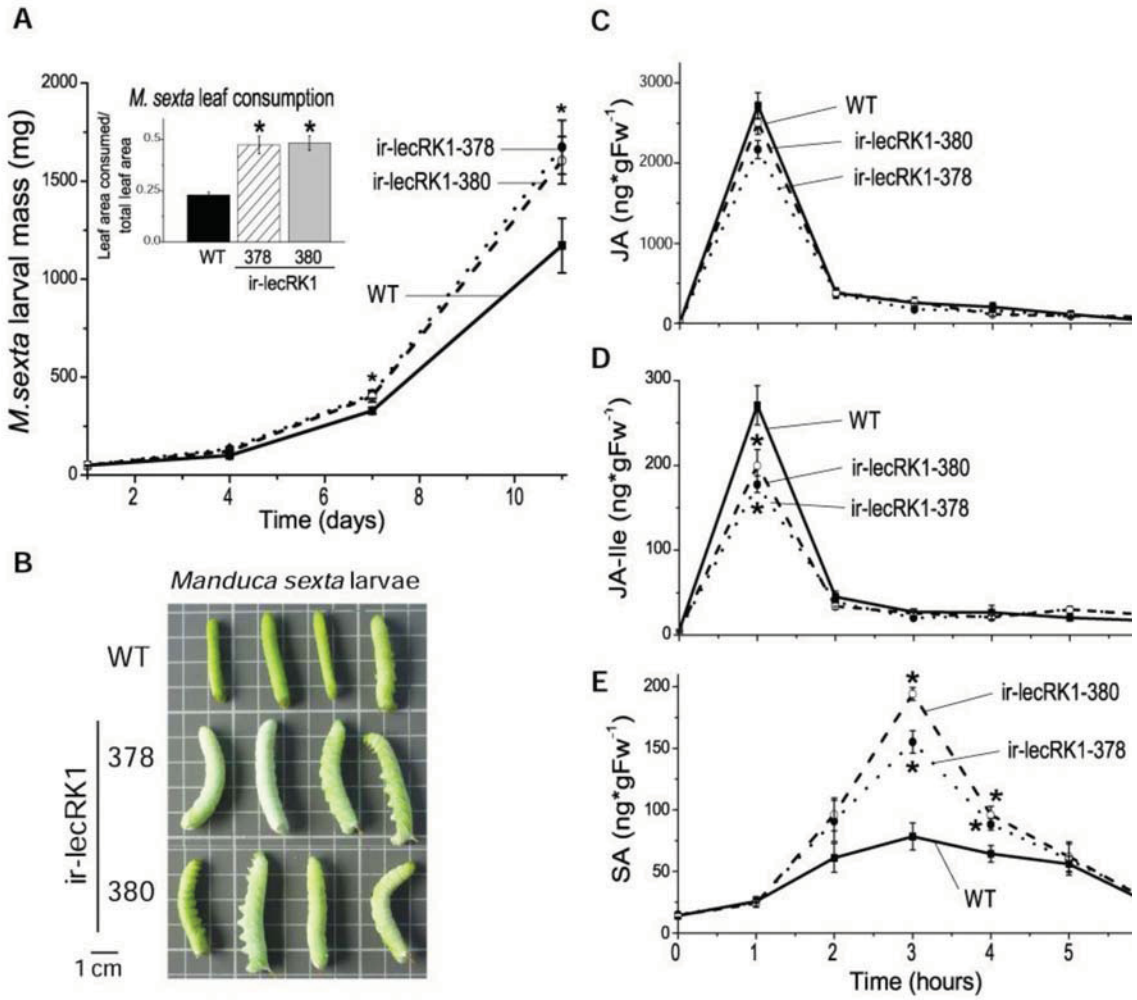

Figure 3. ir-lecRK1 plants are more susceptible to *Manduca sexta* herbivory.
(A) Mean (±SE) of *M. sexta* larval mass after 4, 7 and 11 days of feeding on WT plants and two ir-lecRK1 lines (378 and 380). Statistical analysis was performed by repeated-measurement ANOVA ($F_{1, 87} = 5.25$, $P < 0.01$, $n=30$), asterisks indicate significant differences between larvae feeding on WT plants and those feeding on ir-lecRK1 plants. The insert shows the estimation of the leaf area consumed by *M. sexta* larvae after 11 days of feeding ($n=20$ leaves obtained from 20 individual plants per genotype). *: $P<0.05$, Student's t-test (WT vs. ir-lecRK1 plants).
(B) Example of *M. sexta* larvae at 11 days after feeding on WT or on ir-lecRK1 plants.
(C) JA levels in WT and ir-lecRK1 plants. Leaves from WT and ir-lecRK1 plants were elicited with *M. sexta* OS and leaf tissue was harvested at different times after the treatments for JA quantification by LC-MS/MS.
(D) JA-Ile levels analyzed as in (C). *: $P<0.05$, Student's t-test (WT vs. genotype at the same time point), bars denote ± SE, $n=4$.
(E) SA levels analyzed as in (C). *: $P<0.05$, Student's t-test (WT vs. genotype at the same time point), bars denote ± SE, $n=4$.

Chapter 4

Metabolic profiling of ir-lecRK1 plants reveals strong changes in the accumulation of defense metabolites

Because defense responses of *N. attenuata* against *M. sexta* herbivory rely strongly on the *de novo* synthesis of defense metabolites and thereby on changes in primary and secondary metabolism, the differential accumulation of metabolites in OS-elicited leaves from ir-lecRK1 and WT plants was profiled by LC-ToF-MS (liquid chromatography time-of-flight mass spectrometry) analysis. OS-elicited leaves were harvested at 12 h and 3 and 6 days after the treatment and polar metabolites were analyzed using a modified version of a previously described LC-ToF-MS method (Gaquerel et al., 2010) see Material and Methods for a detailed description of the method used). Positively charged metabolites were selected using the ESI (electrospray ionization) interface in the positive ion mode and those metabolites eluting from the column between 125 and 550 sec and having *m/z* values ranging from 90 to 1400 were selected for analysis (see Material and Methods for a detailed description of the analysis). By using the conditions mentioned above and after data processing, a total of 2,831 ions were identified (Supplemental Table S1 online). To identify the ions that accumulated differentially in WT and ir-lecRK1-378 plants, the fold-changes in ion abundance between these two genotypes were calculated. Ion abundances that differed statistically (*P*-value ≤0.05) and had fold-changes larger than 1.5 and smaller than 0.67 (ir-lecRK1-378 vs WT) were considered as up- and down-regulated, respectively. Although this selection was arbitrary, it has proved useful for the identification of differentially regulated metabolites in *N. attenuata* plants during *M. sexta* herbivory (Gaquerel *et al*., 2010). Using these conditions, a total of 148 ions accumulated differentially after OS elicitation in ir-lecRK1-378 versus WT plants with 57 up- and 91 down-regulated (Supplemental Table S2 online). Most of these ions accumulated specifically at particular times with only 7 ions accumulating differentially after both 12 h and 3 days of the treatment and 2 ions after both 12 h and 6 d after the treatment (Figure 4A).

To facilitate the graphical interpretation of the differences among genotypes and times of treatments, the data set corresponding to the differentially accumulating ions was first analyzed by Principal Component Analysis (PCA). The first and second principal

components (PC) together explained 64.7% of the variation within this data set and PC1 and 2 clearly separated the samples based on genotype and times of the treatments (Supplemental Figure S6A online). A supervised method, PLSDA (Partial Least Squares Descriminant Analysis), was then used to help with the identification of those ions with stronger effects on the separation of samples. The first and second principal components (PCs) of the PLSDA analysis explained 62.4% of the variation in the data set and, similar to PCA analysis, these two PCs clearly separated ir-lecRK1-378 samples from WT samples at the different times of the experiment (Figure 4B). The PLSDA analysis was validated by a permutation test as previously described (Westerhuis *et al*., 2008; Supplemental Figure S6B online) and was used to calculate the VIP (variable importance in the projection) value to estimate and rank the influence of individual ions on the separation of the samples by the PLSDA model. VIP values equal to or larger than 1.0 were considered significant and the higher the VIP value was, the stronger was its influence on the separation of the samples (Xie *et al*., 2008; Qiu *et al*., 2009). A total of 42 ions presented VIP values larger or equal to 1.0 and 16 of these ions were down- and 26 up-regulated at specific times (Supplemental Table S3 online). The fold change in the abundance of these 42 ions ranged from 0.0025 to 0.67 for the down-regulated ions and from 1.5 to 146 for the up-regulated ions (ir-lecRK1 vs WT; Supplemental Table S3 online).

To define the identity of the 148 differentially accumulating ions, a search in the public metabolite database and in custom databases (Gaquerel et al., 2010; Heiling et al., 2010)) was performed using the *m/z* values (with an error of ±0.02) and the retention times. Approximately 87% of the ions did not match significantly to any of the metabolites in the databases and for some of these metabolites a theoretical elemental molecular formula could be assigned with a significant degree of confidence (Table 1 and Supplemental Tables S2 and S3 online). Importantly, among the identified metabolites, were several involved in defense responses against *M. sexta* herbivory. Different ions corresponding to nicotine and HGL-DTGs were found significantly down-regulated at different times after OS elicitation in ir-lecRK1-378 compared to WT plants (Table 1). *N. attenuata* accumulates 11 different HGL-DTG forms differing from each other in the sugar moiety they carry and in the number of malonyl ester groups in the sugar moieties (Heiling *et al*., 2010). Among the 11 HGL-DTG forms, Lyciumoside IV and Attenoside were reduced in ir-lecRK1-378 at 12 h

and 3 days after OS elicitation while the monomalonylated HGL-DTGs Nicotianoside I, Nicotianoside IV and Nicotianoside VI and the dimalonylated HGL-DTGs Nicotianoside II were reduced at 6 days after the treatment (Table 1 and Supplemental Table S2 online). Nicotine and Nicotianoside II were among the metabolites with VIPs greater or equal to 1.0 (Figure 4C and Supplemental Table S3 online), indicating that they strongly contributed to the separation of samples observed in the PLSDA analysis (Figure 4B).

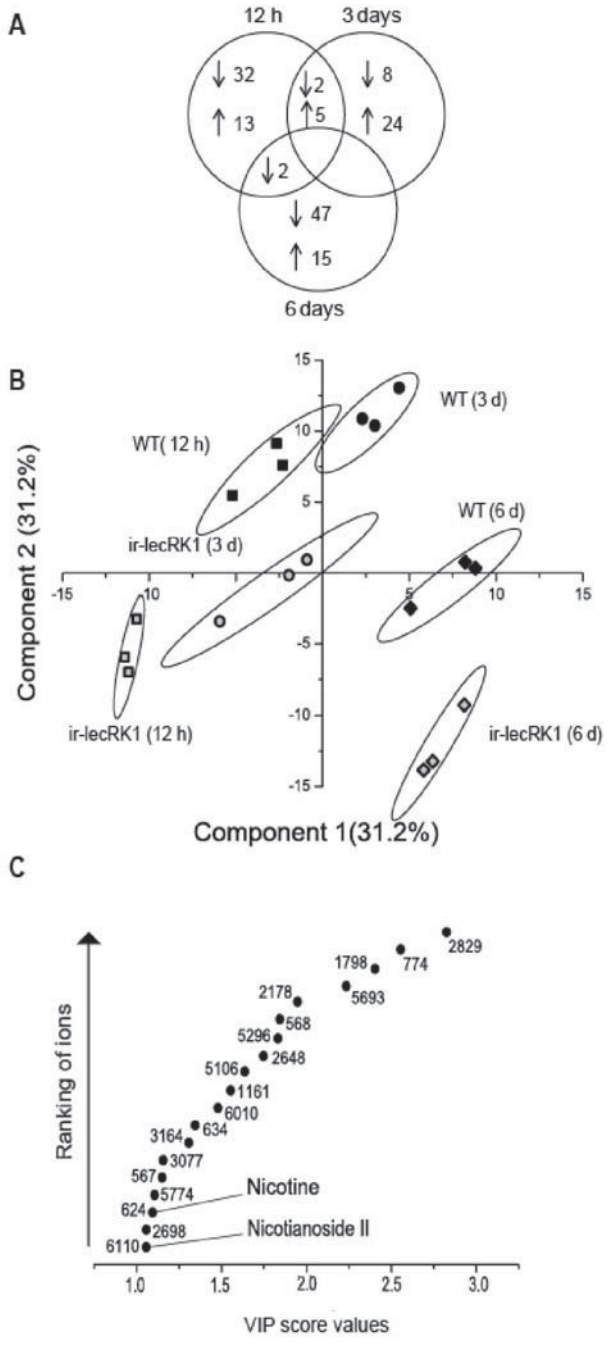

Figure 4. Leaf metabolic profiling of ir-lecRK1 and WT plants.
Leaves from rosette stage WT and ir-lecRK1-378 plants were elicited with *M. sexta* OS and leaf tissue was harvested at 0.5, 3 and 6 days after the treatment. After extraction, polar metabolites were analyzed by UPLC-ToF-MS in the positive ion mode of the ESI.
(A) Venn-diagram depicting the number of statistically up (↑) and down (↓) regulated ions in ir-lecRK1-378 vs. WT plants (*P*-values<0.05 and fold-changes (FC) ≤0.7 and ≥1.5) at different times after the treatments (see also Supplemental Table S2 online).
(B) PLSDA analysis of the down and up-regulated ions in ir-lecRK1-378 vs. WT. Principal components 1 and 2 explained together 62.4% of the variance of the samples (the explained variances per component are shown in brackets). Ellipses delimit the 95% statistical confidence areas for each biological group in the score plots.
(C) Ranking of ions presenting VIP (Variance Importance in Projection) score values bigger than 1.0 in the separation of samples by PLSDA (B). The bigger the VIP score the bigger the ranking value (*y*-axis; see Supplemental Table S3 online) and the stronger the influence of the ion. The numbers next to the dots describe the reference number for the specific ion (Supplemental Table S1 online).

Chapter 4

Na*LecRK1* expression affects the *M. sexta* OS-mediated induction of nicotine and HGL-DTG levels

Previous studies have shown that *M. sexta* larvae fed on *N. attenuata* plants with reduced levels of nicotine or HGL-DTGs gained several fold more mass than larvae fed on WT plants (Steppuhn *et al*., 2004; Jassbi *et al*., 2008). Based on the reductions in nicotine and HGL-DTGs levels detected in ir-lecRK1-378 plants by metabolic profiling, nicotine and total HGL-DTGs were quantified by HPLC in WT and the two ir-lecRK1 lines (378 and 380) at different times after wounding or *M. sexta* OS elicitation. The nicotine levels in unelicited and wounded leaves were similar between WT and ir-lecRK1 plants (Figure 5A and Supplemental Figure S7A online). In contrast, at 3 and 6 days after OS elicitation, the induced nicotine levels in ir-lecRK1-378 and ir-lecRK1-380 plants were on average 30% and 40% reduced, respectively, compared to WT plants (Figure 5A).

In unelicited and wounded leaves, total HGL-DTG levels were similar between WT and ir-lecRK1 plants (Figure 5B and Supplemental Figure S7B online) however the levels of induced HGL-DTGs were reduced on average by 60% and 40% at 3 and 6 days, respectively, after OS elicitation in ir-lecRK1 plants compared to WT plants (Figure 5B). Analysis of the different forms of HGL-DTGs revealed that the amounts of the precursor molecules Lyciumoside I and Lyciumoside II were similar between WT and ir-lecRK1-378 plants at the different times of the experiment, however, the core molecules Lyciumoside IV (the most abundant HGL-DTG form) and Nicotianoside III were reduced by 32% and 43%, respectively, at 3 days after the treatment in ir-lecRK1 plants compared to WT plants (Figures 5C and 5D). At day 6 after the treatment, the reduction in Lyciumoside IV amounts was of 60% (Figure 5D). The levels of the monomalonylated HGL-DTGs Nicotianoside and Nicotianoside IV were reduced by 70% and Nicotianoside VI by 24% in ir-lecRK1 plants compared to WT plants at 6 days after OS elicitation (Figure 5D). The levels of the dimalonylated HGL-DTGs Nicotianoside II, Nicotianoside V and Nicotianoside VII were reduced by 85%, 86% and 78%, respectively, in ir-lecRK1 plants compared to WT plants at 6 days after the treatment (Figure 5D). In summary, the accumulation of most of the core and mono and dimalonylated forms of HGL-DTG molecules was reduced in ir-lecRK1 plants after *M. sexta* OS elicitation.

The transcript levels of the plastidial geranylgeranyl pyrophosphate synthase (NaGGPPS), the enzyme involved in the biosynthesis of HGL-DTGs (Jassbi *et al*., 2008), were reduced by 2 fold in leaves of ir-lecRK1 compared to WT plants at 24 and 72 h after OS elicitation (Supplemental Figure S8A online), suggesting that NaLecRK1 affects (at least partially) the induced levels of HGL-DTGs by affecting the expression of the biosynthetic enzyme NaGGPPS.

The phenyl-propanoid-polyamine conjugates caffeoylputrescine (CP) and dicaffeoylspermidine (DCS) and the phenyl-propanoid derivatives chlorogenic acid (CGA) and rutin are metabolites whose accumulation has been associated with defense against *M. sexta* herbivory in *N. attenuata* (Kaur *et al*., 2010). The amounts of these four metabolites were quantified in ir-lecRK1 and WT plants at 3 days after both wounding and *M. sexta* OS elicitation and their levels did not differ between WT and ir-lecRK1 plants (Supplemental Figure S9 online). These results were consistent with the metabolic profiling analysis that showed no significant differences in the accumulation of these metabolites (Supplemental Table S1 online) and indicated that NaLecRK1 specifically affects the accumulation of some defense metabolites in *N. attenuata*.

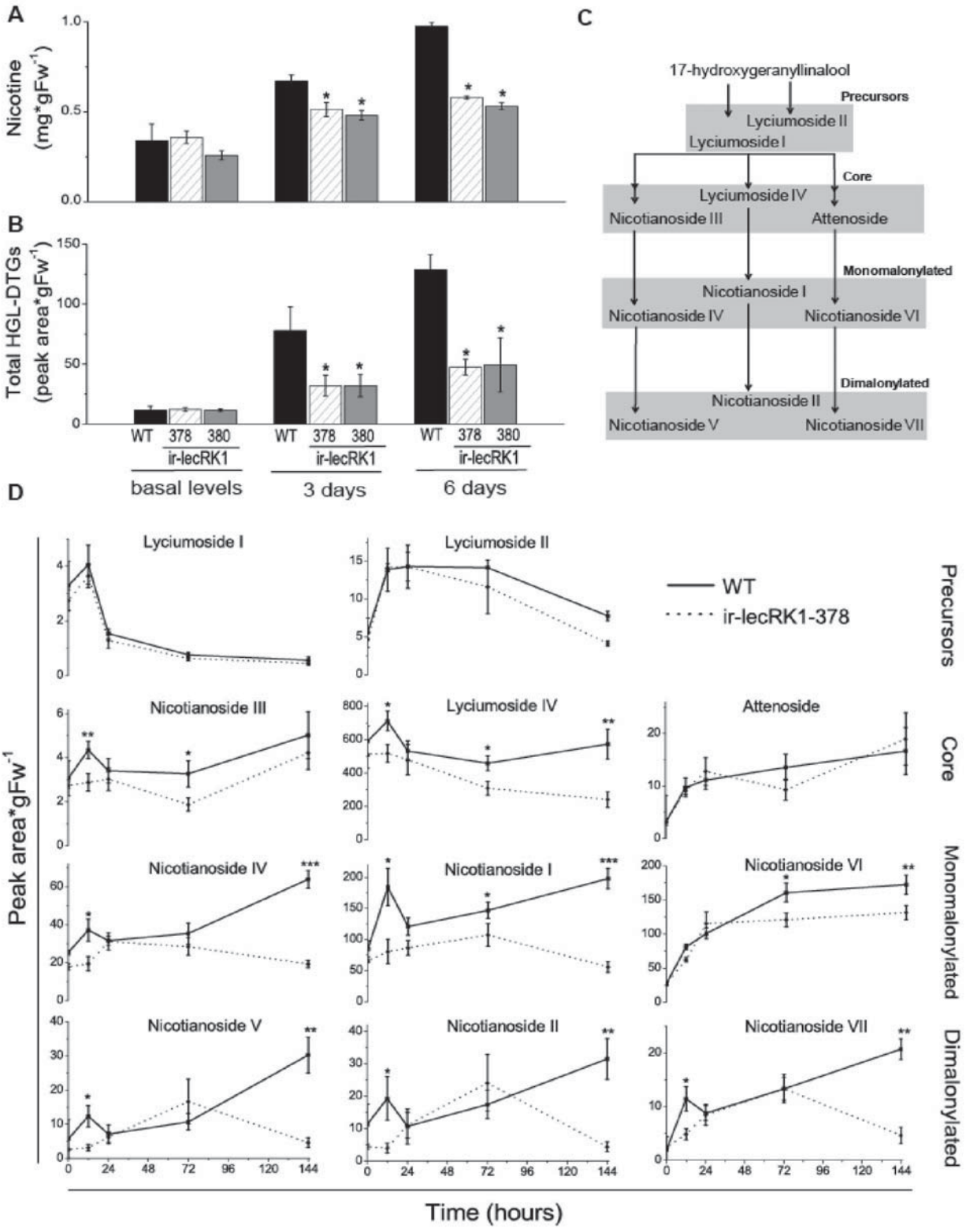
A
Nicotine (mg*gFw-1)
1.0
0.5
0.0
B
Total HGL-DTGs (peak area*gFw-1)
150
100
50
0
WT 378 380
ir-lecRK1
basal levels
3 days
6 days
C
17-hydroxygeranyllinalool
Precursors
Lyciumoside II
Lyciumoside I
Core
Lyciumoside IV
Nicotianoside III
Attenoside
Monomalonylated
Nicotianoside I
Nicotianoside IV
Nicotianoside VI
Dimalonylated
Nicotianoside II
Nicotianoside V
Nicotianoside VII
D
Lyciumoside I
Lyciumoside II
WT
ir-lecRK1-378
Nicotianoside III
Lyciumoside IV
Attenoside
Nicotianoside IV
Nicotianoside I
Nicotianoside VI
Nicotianoside V
Nicotianoside II
Nicotianoside VII
Peak area*gFw-1
Time (hours)
Precursors
Core
Monomalonylated
Dimalonylated

Figure 5. ir-lecRK1 plants induce reduced levels of nicotine and HGL-DTGs after *M. sexta* OS elicitation.
Leaves of rosette stage WT, ir-lecRK1-378 and ir-lecRK1-380 plants were elicited with *M. sexta* OS and leaf tissue was harvested at time 0 and 3 and 6 days after the treatments for analysis of nicotine and HGL-DTGs.
(A) Mean (±SE) of nicotine quantified by HPLC. *: $P < 0.05$, Student's t-test (WT vs. ir-lecRK1-378 or 380 at the same time point, $n=4$).
(B) Mean (±SE) of total HGL-DTGs quantified by HPLC. *: $P < 0.05$, Student's t-test (WT vs. ir-lecRK1-378 or 380 at the same time point, $n=4$).
(C) Scheme of the HGL-DTG biosynthesis pathway (adapted from Heiling *et al.*, 2010).
(D) Mean (±SE) of individual HGL-DTGs quantified by LC-MS/MS. In this case, leaf tissue was harvested at 0, 0.5, 1, 3 and 6 days after *M. sexta* OS elicitation. The amounts of individual HGL-DTGs were normalized by gram fresh mass and to the peak area of the internal standard glycyrrhizinic acid. *$P \leq 0.05$, **$P \leq 0.01$ and ***$P \leq 0.001$, Student's t-test (WT vs. ir-lecRK1-378 at same time point, $n=4$).

Na*LecRK1* expression affects the *M. sexta* OS-mediated induction of TPI activity

Trypsin protease inhibitors (TPIs) are induced during *M. sexta* herbivory in *N. attenuata* plants and they play a critical role as direct defenses by inhibiting the hydrolysis of ingested proteins in the digestive system of *M. sexta* larvae; *N. attenuata* plants with reduced expression of Na*TPI* are compromised in their defense against *M. sexta* herbivory (Zavala et al., 2004a). To evaluate whether NaLecRK1 affected the levels of TPI activity, leaves from WT and ir-lecRK1 plants were elicited with *M. sexta* OS and TPI activity was quantified at 2 and 3 days after the treatment. In unelicited leaves, TPI activity was similar between WT and ir-lecRK1 plants (Figure 6) and the induced levels did not differ between genotypes after wounding (Supplemental Figure S7C online). In contrast, after OS elicitation, the induced TPI activity was reduced by 40% in ir-lecRK1 plants compared to WT (Figure 6). In agreement, the induction of Na*TPI* transcript levels was reduced by ca. 50% in ir-lecRK1-378 plants compared to WT plants at 24 h after OS elicitation (Supplemental Figure S8B online). Thus, not only nicotine and HGL-DTGs were induced to lower levels than in WT in ir-lecRK1 plants but also TPI expression and activity, indicating that, although NaLecRK1 affects the specific accumulation of some defense metabolites, it may have a broader effect on the induction of defense responses against herbivores.

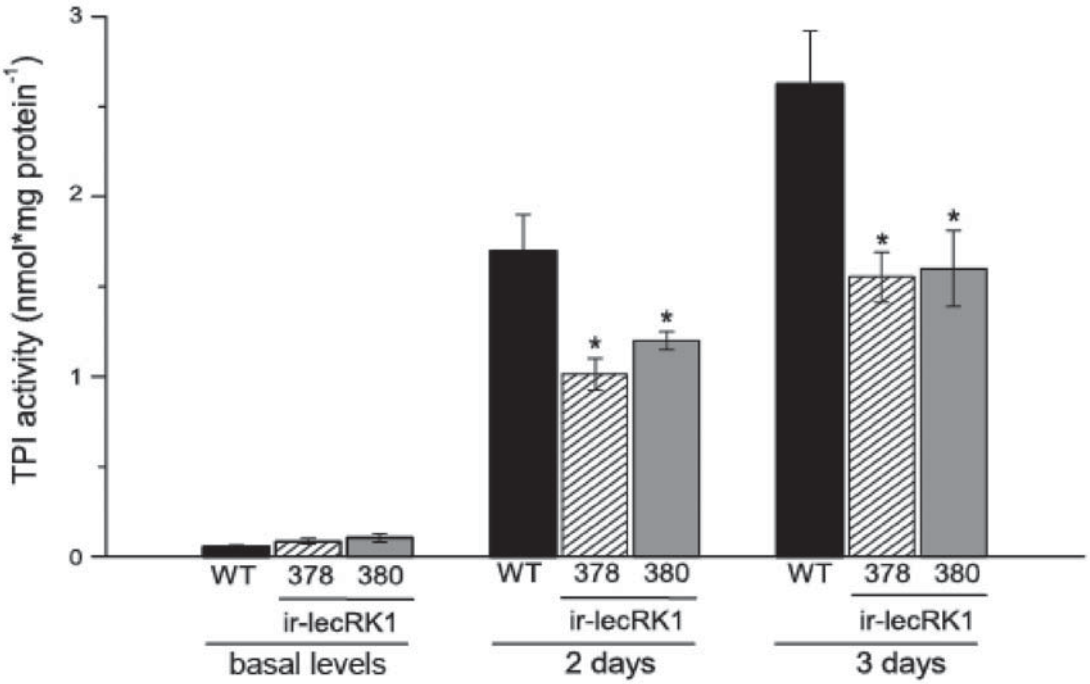

Figure 6. ir-lecRK1 plants induce reduced levels of of trypsin proteinase inhibitors (TPI). Leaves from rosette stage WT and ir-lecRK1 plants were elicited with *M. sexta* OS. After 2 and 3 days of the treatments, leaf tissue was harvested and analyzed for TPI activity by a radial diffusion assay. Basal levels are from uninduced leaves. *: $P<0.05$, Student's t-test (WT vs. ir-lecRK1 at the same time point), bars denote ± SE, $n=4$.

The expression of Na*TD* is strongly reduced in leaves of ir-lecRK1 plants after OS elicitation

To gain further insights into the mechanisms affected in ir-lecRK1 plants, changes in gene expression at 1 h after *M. sexta* OS elicitation were evaluated by microarray analysis. Differentially regulated genes were considered when $\log_2$(fold-changes; FCs) were larger or equal to 1.3 or smaller or equal to -1.3 (ir-lecRK1-378 vs. WT) and q-values were lower than 0.05 (corresponding to a 4% false discovery rate (FDR); see Materials and Methods). Using these conditions, transcripts corresponding to 78 genes were identified as differentially regulated in ir-lecRK1-378 compared to WT, with 41 down-and 37 up-regulated (Supplemental Table S4 online). Thirty of these 78 genes did not match

significantly with any of the protein entries in the non-redundant (NR) GenBank protein database and 6 matched with hypothetical proteins (Supplemental Table S4 online).

Among the most strongly down-regulated genes was, as expected, Na*LecRK1* (log_2(FC)=-3.1) and, interestingly, threonine deaminase (*TD*; log_2(FC)=-2.3; Supplemental Table S4). Additional genes down-regulated in ir-lecRK1 plants and potentially associated to defense responses were *N. attenuata* homologues of a putative protease inhibitor-I from *Nicotiana sylvestris* and of a protein from *N. tabacum* able to induce hypersensitive-response-like lesions. In the group of up-regulated genes with a predicted function in defense responses, a putative PR-10 type pathogenesis-related protein was 6-fold up-regulated in ir-lecRK1 compared to WT (Supplemental Table S4 online).

Among the remaining genes that changed expression were *N. attenuata* homologues of genes involved in the regulation of gene expression (e.g., *HTA11* (*Histone H2A variant 1*), *PAF1* (*Parafibromin 1*)), metabolic enzymes (e.g., *CK1* (*Choline kinase 1*), *CSLD2* (*cellulose synthase-like D2*), thiamine biosynthesis protein ThiC) and signal transduction components (e.g., phytochrome F and *NAP1-2* (*NUCLEOSOME ASSEMBLY PROTEIN 1;2*; Supplemental Table S4 online and see Discussion).

Theronine deaminase down-regulation in ir-lecRK1 plants affects the levels of ingested Thr by *M. sexta* larvae.

Based on the microarray results and knowing that threonine deaminase (TD) plays important roles in defense responses against lepidopteran larvae in both tomato (Chen *et al*., 2005) and *N. attenuata* (Kang et al., 2006b), we reasoned that the reduced levels of expression of this gene in ir-lecRK1 plants could contribute to the reduced defense response observed in these plants during *M. sexta* herbivory. To validate the microarray results, the transcript levels of Na*TD* were first quantified by qPCR in leaves of ir-lecRK1 and WT plants at different times after *M. sexta* OS elicitation. Na*TD* mRNA levels were reduced by 75% and 50% at 30 and 60 min after the treatment, respectively, in ir-lecRK1 compared to WT plants (Figure 7A).

Second, the levels of Thr were quantified in the midgut content and tissue of *M. sexta* larvae fed for 11 continuous days on either WT, ir-lecRK1 or *N. attenuata* plants with reduced levels of Na*TD* (as-tdm2; (Kang et al., 2006b). The larvae were dissected to isolate the midgut and to separate the midgut tissue from its contents. In parallel, the leaves of the plants were also harvested after 11 days of larval feeding and used to quantify Thr amounts. The Thr levels in the midgut tissue of *M. sexta* larvae fed on ir-lecRK1-378 and as-tdm2 plants were 34% and 50% higher, respectively, than the Thr levels in the midgut tissue of larvae fed on WT plants (Figure 7B). The Thr levels in the midgut content of the larvae fed on ir-lecRK1-378 and as-tdm2 plants were 70% and 60% higher, respectively, than the Thr levels found in the midgut content of larvae fed on WT plants (Figure 7C). Due to the high water content in the midgut content, in this case Thr levels were expressed as mol% of the levels of all amino acids (Figure 7C). In leaves, the levels of Thr and JA-Ile were similar between WT, as-tdm2 and ir-lecRK1-378 plants (Figures 7D and 7E) whereas the levels of SA were 100% higher in ir-lecRK1-378 plants compared to WT and as-tdm2 plants (Figure 7F).

Figure 7. Reduced threonine deaminase (Na*TD*) expression in ir-lecRK1 plants affect threonine accumulation in the midgut of *M. sexta* larvae.
(A) Na*TD* mRNA levels quantified by qPCR in leaves of rosette stage WT and ir-lecRK1-378 plants at different times after *M. sexta* OS elicitation. The values are expressed as the fold-change (FC) increase relative to time 0 (value set arbitrary at 1).Transcript levels were calculated relative to the expression level of Na*EF1A* mRNA using the ΔCT method; see Materials and Methods). *: P <0.05, Student's t-test (WT vs. ir-lecRK1-378 at same time point, bars denote ±SE, n=3).
(B) Mean (± SE) of threonine (Thr) levels in midgut tissue of *M. sexta* larvae fed on either WT, ir-lecRK1-378 or as-tdm2 for 11 days. The larvae were chilled on ice and dissected to separate the midgut tissue from the midgut content (one sample contains the midguts from 3 larvae) and a total of 5 samples were analyzed (n=5). *: P <0.05, Student's t-test (WT vs. genotype).
(C) Thr levels expressed in mol% as a molar percentage of all amino acids in the midgut content of *M. sexta* larvae fed on the plant genotypes described in (B). One sample contains the midgut content of 3 larvae and a total of 5 samples per plant genotype were analyzed (n=5). *: P <0.05, Student's t-test (WT vs. genotype).
(D) Mean (± SE) of Thr levels in leaf tissue from WT, ir-lecRK1-378 and as-tdm2 plants 11 days after *M. sexta* feeding (one sample consists of 3 leaves pooled from different plants, n=5).
(E) Mean (± SE) of JA-Ile levels in leaf tissue from WT, ir-lecRK1-378 and as-tdm2 plants 11 days after *M. sexta* feeding (one sample consists of 3 leaves pooled from different plants, n=5).
(F) Mean (± SE) of SA levels in leaf tissue from WT, ir-lecRK1-378 and as-tdm2 plants 11 days after *M. sexta* feeding (one sample consists of 3 leaves pooled from different plants, n=5).

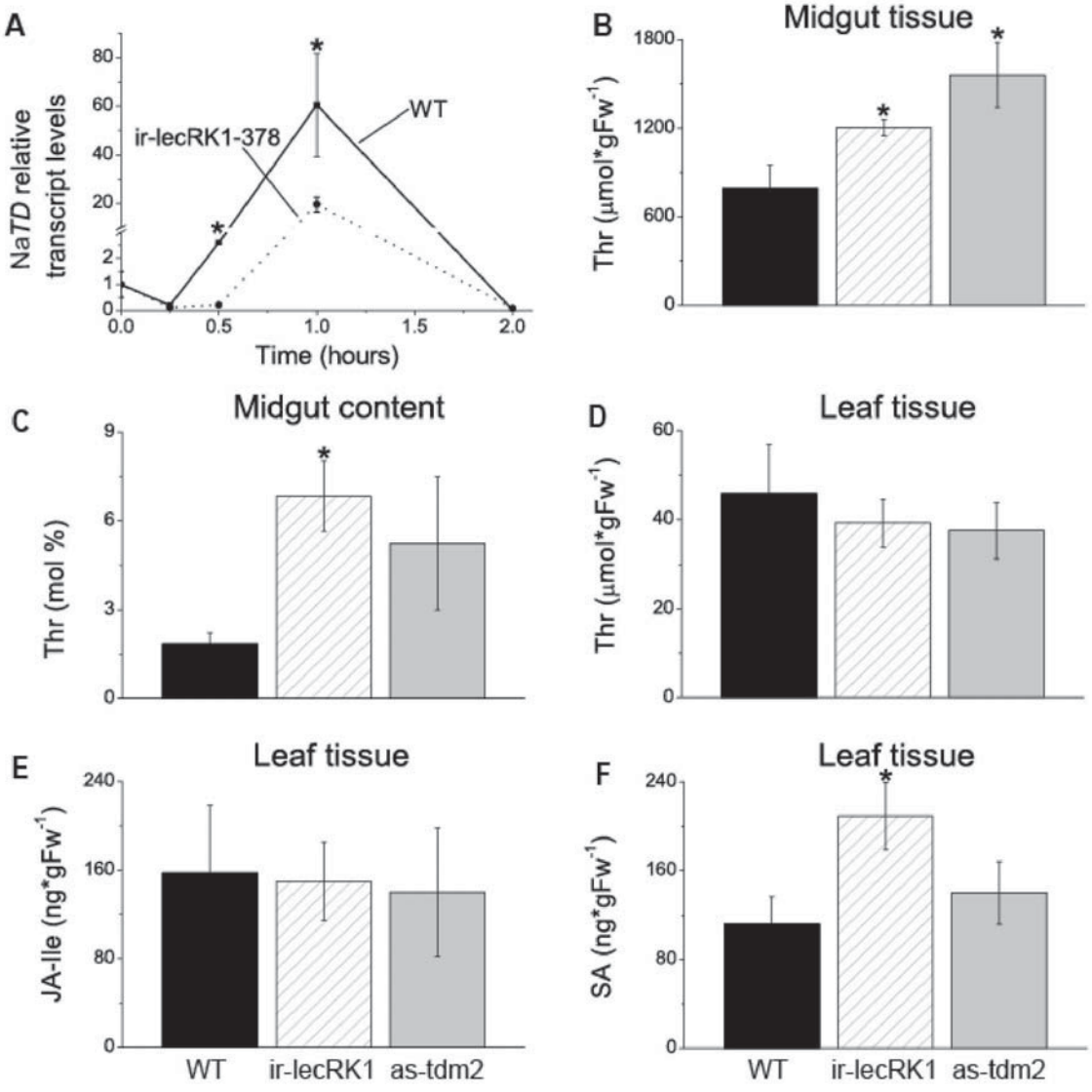

Figure 7. Reduced threonine deaminase (Na*TD*) expression in ir-lecRK1 plants affect threonine accumulation in the midgut of *M. sexta* larvae. (see figure caption in page 66)

Chapter 4

The increased *M. sexta*-elicited SA burst in ir-lecRK1 plants suppresses the induction of defense responses in *N. attenuata* leaves

The results presented in the previous section showed that, during continuous *M. sexta* larval feeding, similar levels of JA-Ile accumulate in WT and ir-lecRK1 plants but increased SA levels in the latter. Based on these results and the increased accumulation of SA in ir-lecRK1 plants upon *M. sexta* OS elicitation (Figure 3E), we reasoned that the increased performance of *M. sexta* larvae on ir-lecRK1 plants could be the result of an SA-mediated suppression of induced defense responses. To test this hypothesis, transgenic *N. attenuata* plants ectopically expressing the *Pseudomonas putida nahG* gene under the control of the CaMV35S promoter (ov-nahG; Supplemental Figure S10 online) were generated and crossed with ir-lecRK1-378 plants to generate ir-lecRK1xov-nahG plants. As a control, ir-lecRK-378 plants were also crossed with WT plants to generate ir-lecRK1xWT plants. It is important to note at this point that the basal levels of SA in ov-nahg and WT plants were similar however after a treatment that strongly induces SA levels (e.g., leaf infiltration with pathogenic bacteria), the accumulation of SA was strongly suppressed in ov-nahg plants (Supplemental Figure S10 online), indicating that the ectopic expression of *nahG* efficiently prevented the accumulation of induced levels of SA.

The levels of SA were first quantified in WT, ir-lecRK1-378, ov-nahG, ir-lecRK1xov-nahG and ir-lecRK1xWT plants at 3 h after OS elicitation (Figure 8A). SA levels were 2-fold higher in ir-lecRK1 and in ir-lecRK1xWT plants compared to WT and similar to WT levels in ov-nahG and ir-lecRK1xov-nahG plants (Figure 8A). The levels of SA were also quantified in leaves of these plants at 11 days after larval feeding and the results were similar to those observed after OS elicitation (Supplemental Figure S11A online). Thus, introgression of the *nahG* gene in ir-lecRK1 plants suppressed the OS- and *M. sexta*-elicited SA burst in these plants. The levels of JA and JA-Ile were also quantified in leaves at 11 days after *M. sexta* larval feeding and the accumulation of these two molecules was similar between the genotypes (Supplemental Figures S11B and S11C online).

Freshly hatched *M. sexta* neonates were placed on the 5 genotypes mentioned above and the larval masses were determined at 4, 7, and 11 days after the start of the experiment. Strikingly, larvae feeding on ir-lecRK1xov-nahG gained similar masses to those larvae growing on WT and ov-nahG plants (Figure 8B). In contrast, larvae performed similarly on ir-lecRK1-378 and ir-lecRK1xWT plants (*i.e.* the larvae gained on average 80% the mass of larvae feeding on WT plants (Figure 8B)).

The induced levels of total HGL-DTGs in ir-lecRK1xov-nahG plants were similar to those in ov-nagh and WT plants and 2-fold higher compared to the levels in ir-lecRK1-378 and ir-lecRK1xWT plants (Figure 8C). The levels of induced TPI activity in lecRK1xov-nahG and ov-nahG plants were statistically similar to WT plants and higher than in ir-lecRK1 and ir-lecRK1xWT plants (Figure 8D). Induced nicotine levels were increased by 15% in ir-lecRK1xov-nahG compared to ir-lecRK1 plants but remained 14% lower than in WT (Figure 8E). Finally, Na*TD* transcript levels were increased 3-fold in ir-lecRK1xov-nahG compared to ir-lecRK1 plants however the levels remained 2-fold lower than in WT plants (Figure 8F). In summary, the suppression of SA accumulation in ir-lecRK1 plants restored the induced levels of HGL-DTGs and TPI activity to WT levels while induced nicotine levels and Na*TD* expression were partially restored.

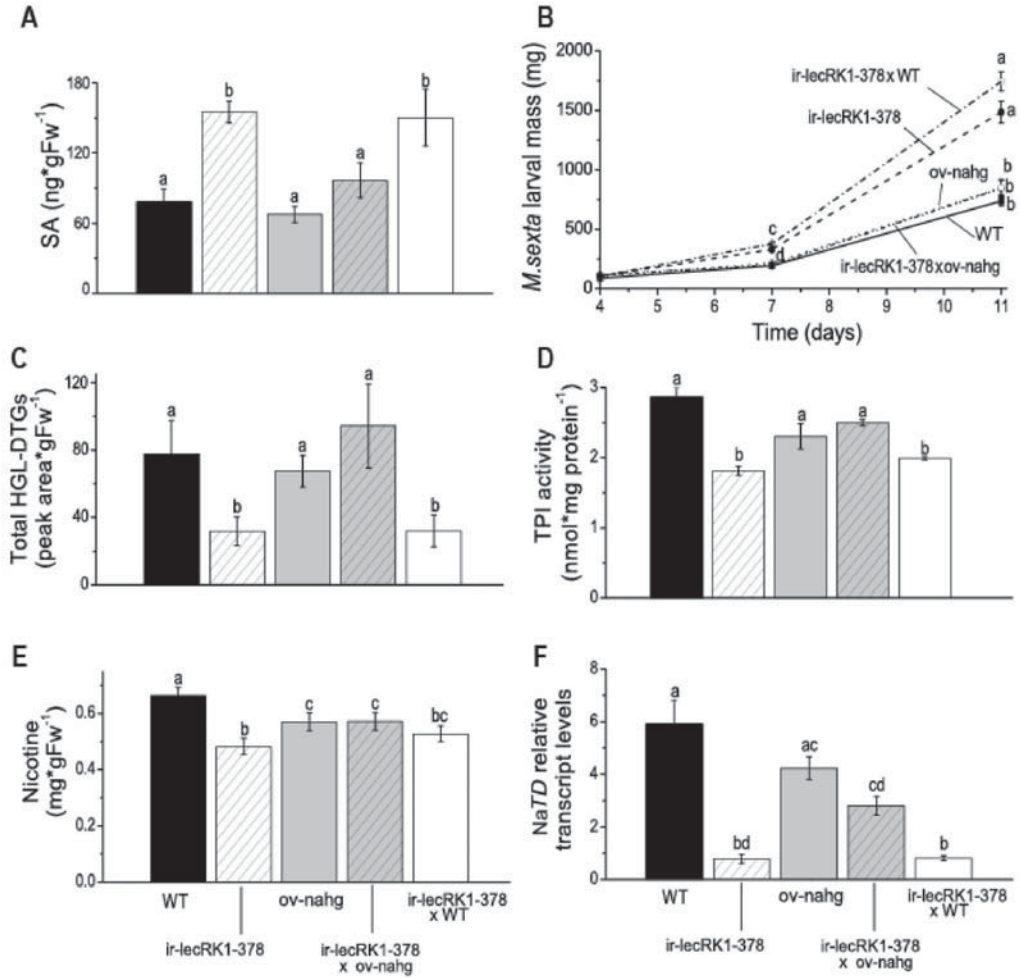

Figure 8. Suppression of SA accumulation in ir-lecRK1 plants recovers the defense response against *M. sexta* herbivory.

(A) Mean (± SE) of SA levels quantified in leaves of rosette stage WT, ir-lecRK1-378, ov-nahG, ir-lecRK1-378xov-nahG and ir-lecRK1-378xWT plants. Leaves were elicited with *M. sexta* OS and harvested 3 h after the treatment (coincident with the peak of SA accumulation, Figure 3E). Different letters indicate significant differences (univariate ANOVA; $F_{4, 13} = 18.17$, $P < 0.001$, followed by a Tukey HSD *post-hoc* test, $P < 0.05$, $n=3$).

(B) Mean (± SE) mass gain of *M. sexta* larvae fed on the 5 plant genotypes described in (A) for 4, 7 and 11 days. Different letters denote statistical significance (repeated-measurement ANOVA, $F8_{,4} = 35.06$, $P < 0.01$, $n=30$).

(C) Mean (± SE) of total HGL-DTGs quantified in leaves of the genotypes described in (A) at 3 days after elicitation with *M. sexta* OS (univariate ANOVA, $F_{4,14} = 58.78$, $P < 0.001$, followed by a Tukey HSD *post-hoc* test, $P < 0.05$, $n=3$).

(D) Mean (± SE) of nicotine quantified in leaves of the genotypes described in (A) at 3 days after elicitation with *M. sexta* OS (univariate ANOVA, $F_{4, 22} = 10.45$, $P < 0.001$, followed by a Tukey HSD *post-hoc* test, $P < 0.05$, n=4-5).

(E) Mean (± SE) of TPI activity quantified in leaves of the genotypes described in (A) at 3 days after elicitation with *M. sexta* OS (univariate ANOVA, $F_{4, 23} = 10.62$, $P < 0.001$, followed by a Tukey HSD *post-hoc* test, $P < 0.05$, $n=5$).

(F) Na*TD* mRNA levels quantified by qPCR in leaves of the genotypes described in (A) at different times after elicitation with *M. sexta* OS. The values are expressed as described in the caption for Figure 7A (univariate ANOVA, $F_{4,13} = 27.13$, $P < 0.001$, followed by a Tukey HSD *post-hoc* test, $P < 0.05$, $n=3$).

Chapter 4

DISCUSSION

NaLecRK1 encodes for a G-type lectin receptor kinase

Lectin receptor kinases (LecRKs) belong to the family of receptor kinases with approximately 86 members in Arabidopsis (Bouwmeester and Govers, 2009). Based on the type of lectin domain, 3 types of LecRKs can be distinguished: C, L and G (Bouwmeester and Govers, 2009). C-type LecRKs are calcium-dependent lectin receptor-like kinases, L-type LecRKs contain a lectin domain with sequence similarity to legume lectins and G-type LecRKs (previously categorized as B-type) contain a lectin domain with sequence similarity to mannose-specific lectins of bulbous plant species (Bouwmeester and Govers, 2009).

NaLecRK1 belongs to the G-type LecRK family and the best studied members of this subfamily are the S-locus receptor kinases that function in self-incompatibility mechanisms during pollination (Takayama and Isogai, 2005). Recently, some G-type LecRKs have also been associated to defense responses against pathogenic microorganisms. For example, the rice Pi-d2 LecRK protein participates in the resistance mechanisms against *Magnaporthe grisea* (Chen *et al*., 2006) and NgRLK1 from *N. glutinosa* participates in the resistance mechanisms against *Phytophthora capsici* (Kim *et al*., 2010). In the group of L-type LecRKs, NbLRK1 from *N. benthamiana* interacts with the *P. infestans* elicitin INF1 and triggers INF1-induced cell death (Kanzaki *et al*., 2008) and the Arabidopsis LecRK-I.9 has been identified as a putative mediator of cell wall-plasma membrane adhesion during infection with *Phytophthora* species (Bouwmeester *et al*., 2011). LecRK-I.9 binds to a *P. infestans* effector protein through an RGD (Arg-Gly-Asp) motif which is also present as a cell-attachment motif in extracellular matrix (ECM) proteins that mediate cell adhesion to the cell walls (Bouwmeester *et al*., 2011). In this study we show that lecRKs also participate in mechanisms regulating the induction of defense responses against folivorous insects.

Although the actual ligand of NalecRK1 is at present unknown and even though it is speculative at this point, one possibility is that NaLecRK1 recognizes the disruption of cell walls (either by the perception of cell wall fragments or changes in the cell wall structure)

occurring during *M. sexta* herbivory and thereby triggers changes that affect SA accumulation and the induction of defense responses. In Arabidopsis, the induction of defense responses mediated by JA and ET has been linked to changes in the cell wall structure as exemplified by the *cev1* (*constitutive expression of VSP1*) mutant which carries a genetic lesion in a cellulose synthase gene (Ellis *et al*., 2002). Moreover, folivorous insects disrupt cell walls and it has been previously shown that cell wall fragments can activate defense responses in plants (Ryan *et al*., 1993). This hypothesis requires further investigation.

The induction of Na*LecRK1* expression is tightly controlled by OS/FACs and jasmonates

Elicitation of leaves from WT *N. attenuata* plants with OS from the generalist *Spodoptera exigua* induces the accumulation of SA to levels higher than those induced by OS from the specialist *M. sexta* whereas the latter induces the accumulation of higher levels of JA and ET (Diezel *et al*., 2009). The same study showed that the lower levels of *M. sexta* OS-elicited SA are brought about by a suppression of SA accumulation mediated by enhanced ET levels however pathways independent of ET also operate (Diezel *et al*., 2009). As a final outcome, the induction of defense responses is attenuated after elicitation of leaves with *S. exigua* OS compared to *M. sexta* OS (Diezel *et al*., 2009).

In ir-lecRK1 plants, elicitation of leaves by *M. sexta* OS and larval folivory induced the accumulation of SA to levels 2-fold higher than those in WT plants, suggesting that NalecRK1 is one signal transduction component operating during *M. sexta* herbivory to suppress SA accumulation. Interestingly, the levels of ET produced by ir-lecRK1 plants were similar to those produced by WT plants, indicating that the NalecRK1-mediated signaling pathway works in a pathway independent of the ET-mediated suppression of SA accumulation (Diezel *et al*., 2009).

Analysis of Na*LecRK1* mRNA expression in plants deficient in JA biosynthesis or perception suggested that jasmonates inhibit the induction of this gene (Figure 1C). Moreover, plants with reduced expression of Na*SIPK* and Na*WIPK* showed that these two

regulatory components effect positively the expression of the Na*LecRK1* gene, consistent with their central role in the activation of defense responses against *M. sexta* herbivory (Wu *et al*., 2007; Figure 9). These results revealed that the induction of Na*LecRK1* expression is under tight control; it is induced by OS/FAC elicitation but the levels of induction are checked by jasmonates (in a COI1-dependent manner) which are also produced after OS/FAC elicitation. Thus, in this case, jasmonate levels would tune Na*LecRK1* expression and thereby the accumulation of SA levels during insect herbivory (Figure 9).

The induced accumulation of central defense metabolites is affected by reducing expression of Na*LecRK1* in *N. attenuata* plants

When *N. attenuata* plants are reduced either in the accumulation of HGL-DTGs or nicotine or in the expression of TPI or Na*TD, M. sexta* larvae feeding on these plants can gain from 50 to 300% more mass than larvae feeding on WT plants (Jassbi et al., 2008b)). Consistent with these previous studies, an increased performance of *M. sexta* larvae on ir-lecRK1 plants was accompanied with reductions in the induced accumulation of these defense metabolites or proteins (Figures 5, 6 and 7).

In agreement with the role of TD in the deamination of Thr in the insect gut (Chen *et al*., 2005), the levels of Thr in the midgut tissue and content of *M. sexta* larvae fed on ir-lecRK1 were 34% and 70 % higher, respectively, than the level of Thr in the midgut tissue and content of larvae fed on WT plants (Figure 7B and C). Also in agreement with the role of NaTD in the supplying of Ile for JA-Ile biosynthesis in leaves after *M. sexta* OS elicitation (Kang *et al*., 2006), the accumulation of JA-Ile was reduced on average by 30% at 1 h after this treatment (Figure 3D). However, after 11 days of continuous *M. sexta* larval feeding, the levels of JA-Ile were similar between WT and ir-lecRK1 plants (Figures 7E), indicating that the reduced levels of Na*TD* expression in the latter did not affect the accumulation of JA-Ile after several days of larval feeding. This effect could be brought about, for example, by changes in the metabolism of JA-Ile in ir-lecRK1 plants. It has been shown that not only the biosynthesis but also the metabolism of JA-Ile is tightly regulated in plants, as exemplified by the miss-regulated accumulation of JA-Ile in plants with reduced expression

of COI1 (Paschold *et al*., 2008; VanDoorn *et al*., 2011). Importantly, together with the 2-fold increased levels of SA observed after 11 days of *M. sexta* larvae continuous feeding (Figure 7F), the results suggested that the reduced induction of nicotine, HGL-DTGs, TPI and NaTD levels was not the results of reduced JA-Ile accumulation whereas of a suppressive effect of SA.

NaLecRK1 suppresses SA accumulation during *M. sexta* herbivory allowing the unfettered induction of defense responses

Although the levels of OS- and *M. sexta*-elicited SA were only moderately increased (2-fold) in ir-lecRK1 plants (Figures 3E, 7F, 8A and Supplemental Figure S11A online), the reduction of SA levels in ir-lecRK1xov-nahG plants (Figure 8A) was sufficient to recover the defense response as determined by *M. sexta* larval performance (Figure 8B). Moreover total HGL-DTG levels and TPI activity were fully recovered in ir-lecRK1xov-nahG plants (Figures 8C and D), suggesting that the accumulation of these compounds was fully inhibited by SA in ir-lecRK1 plants. In contrast, nicotine levels were only partially recovered in lecRK1xov-nahG plants compared to WT plants (Figure 8E). This partial recovery was probably due to the fact that nicotine levels were significantly reduced by 15% in ov-nahG plants compared to WT, indicating that the ectopic expression of *nahG* has a slight negative effect on nicotine accumulation (Figure 8E). However, *M. sexta* larvae performed similarly on WT and ov-nahG plants (Figure 8A), indicating that defense responses were not impaired in the latter. Consistently, the levels of HGL-DTGs, TPI activity, and NaTD expression were not significantly different between WT and ov-nahG plants (Figure 8C, D and F).

Similar to induced nicotine accumulation, Na*TD* expression was also partially recovered in ir-lecRK1xov-nahG plants compared WT and since Na*TD* expression levels were statistically similar between WT and ov-nahG plants, this partial recovery was probably the result of a partial involvement of the OS-elicited SA burst in the suppression of Na*TD* expression in ir-lecRK1 plants (Figure 8F).

In summary, these results showed that the suppression of the OS/*M. sexta*-elicited SA burst in ir-lecRK1 plants decreased the performance of *M. sexta* larvae and that this suppression was sufficient to fully restore the induced accumulation of HGL-DTGs and TPI activity and to partially restore the induced accumulation of nicotine and NaTD expression in ir-lecRK1 plants to levels in WT plants.

Additional changes in the metabolome and transcriptome affected by reduced expression of Na*LecRK1*

Even though the work was primarily focused on the effect of NaLecRK1 on known defense responses in *N. attenuata*, the accumulation of 148 ions were affected in ir-lecRK1 plants compared to WT (Supplemental Table S2 online). The identity of most of the corresponding metabolites could not be unambiguously determined and remains the focus of future work. Some of these metabolites may also be critical for the interaction between *M. sexta* and *N. attenuata* and their accumulation may also be affected by increased OS-elicited SA levels (in a manner similar to the defense metabolites analyzed in detail in this study). Consistent with the number of ions detected as differentially regulated in ir-LecRK1 versus WT plants, a previous study has identified 173 metabolites as differentially regulated in *N. attenuata* WT plants at 1 h and 5 days after *M. sexta* elicitation (Gaquerel *et al*., 2010). Thus, from these numbers it can be preliminary concluded that NaLecRK1 has a prominent effect on the accumulation of metabolites induced by *M. sexta* OS elicitation in leaves of *N. attenuata* plants. This effect is however specific to some degree since the induction of defense metabolites derived from the phenyl-propanoid pathway were not affected in ir-lecRK1 plants (Supplemental Figure S9 online).

Gene expression analysis of leaf tissue from ir-lecRK1 and WT plants at 1 h after *M. sexta* OS elicitation showed that the reduced expression of Na*LecRK1* affects the accumulation of 77 transcripts (using the conditions described in the Results section) and, based on gene ontology annotation (Supplemental Table S4 online), the functions of these genes were distributed among diverse cellular processes (e.g., defense, metabolism, transcriptional regulation, transport and oxidative-reduction processes). What is the role of

these genes in the response of *N. attenuata* plants to *M. sexta* herbivory is at present unknown and the focus of future work.

The unraveling of the complexity of the changes occurring in the metabolome and transcriptome of ir-lecRK1 plants during *M. sexta* herbivory will provide further insights into additional mechanisms controlled by NaLecRK1 and affecting the response of *N. attenuata* to *M. sexta* herbivory.

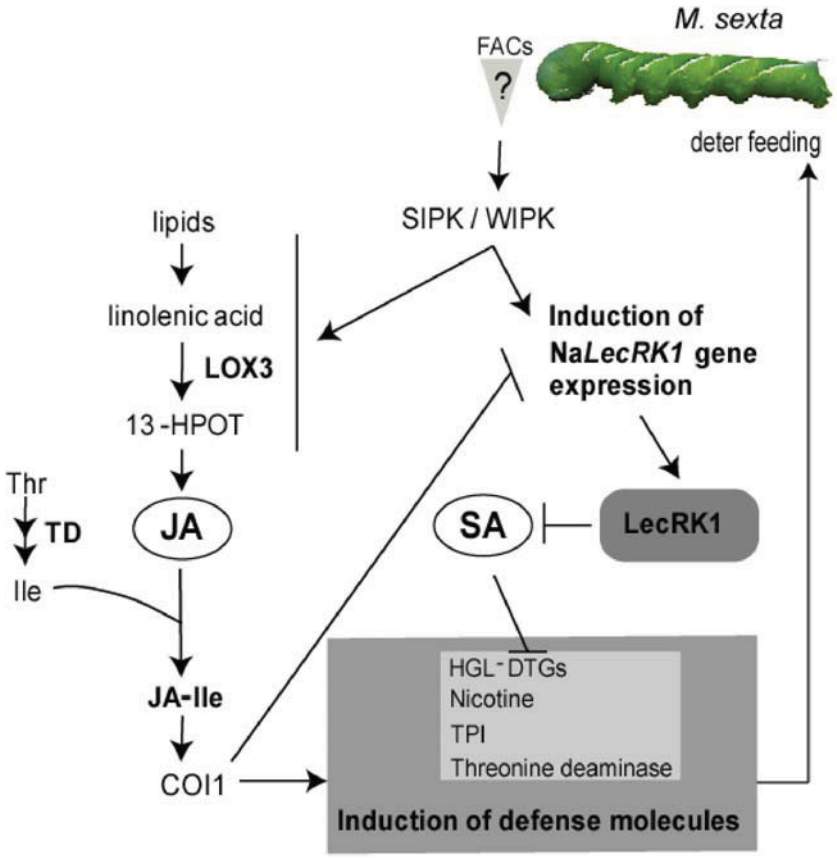

Figure 9. Proposed model for the role of NaLecRK1 in the *N. attenuata* defense response against *M. sexta*.
During herbivory by *M. sexta* larvae, the FACs present in the larval OS induced the expression of the Na*LecRK1* gene. This induction depends on the activity of SIPK and WIPK which in parallel activate the biosynthesis of JA (Kallenbach *et al*., 2010). JA is conjugated to Ile to form JA-Ile and TD supplies Ile for this biosynthetic process (Kang *et al*., 2006). JA-Ile induces the accumulation of defense metabolites or proteins (including nicotine, TPIs, HGL-DTGs and TD) via COI1-dependent mechanisms (Paschhold *et al*., 2007; Heiling *et al*., 2010) and inhibits the expression of Na*LecRK1*. NaLecRK1 suppresses the SA burst induced by *M. sexta* herbivory which in turn allows for an unfettered induction of the defense metabolites nicotine, TPIs, HGL-DTGs and TD. LOX3: lipoxygenase 3; 13-HPOT: 13*S*-hydroperoxy-octadecatrienoic acid; SIPK, salycilate-induced protein kinase; WIPK, wound-induced protein kinase, threonine deaminase (TD).

Chapter 4

MATERIALS AND METHODS

Plant growth and treatments

Seeds of the 31st generation of an inbred line of *N. attenuata* plants were used as the wild-type (WT) genotype in all experiments. Seeds from WT and genetically transformed plants were germinated as previously described (Krügel *et al*., 2002). Plants were grown in the glasshouse under high-pressure sodium lamps (200-300 µmol s^{-1} m^{-2} light) with a day/night cycle of 16 h(26-28°C)/8 h(22-24°C) and 45 to 55% humidity. Crosses between *N. attenuata* lines were performed by removing anthers from flowers of homozygous ir-lecRK1-378 plants before pollen maturation and by brushing the stigma with pollen from homozygous plants ectopically expressing the *nahG* gene (ov-nahG) or WT. For wounding and elicitation treatments, leaves were wounded by rolling a fabric-pattern wheel three times on each side of the midvein and the wounds were supplemented either with 20 µL of water (wounding treatment), 20 µL of 18:3-Glu (0.03 nmol/µL; FAC elicitation) or 20 µL of *M. sexta, S. littoralis* or *S. gregaria* OS diluted 1:5 (v/v) in water (OS elicitation). Tissue expression profile of Na*LecRK1* was evaluated by collecting different plant tissues from WT *N. attenuata* plants; rosette leaves and roots were collected from 30 day-old (rosette stage; Figure 2C) plants whereas stems, systemic leaves, sepals, pistils, corolla, inflorescence and stamens were collected from 50 day-old (early flowering) plants.

Insect rearing, feeding experiments and OS collection

Larvae of the tobacco hornworm (*Manduca sexta* L., Lepidoptera, Sphingidae) were obtained from in-house colonies. One freshly hatched larva of *M. sexta* was placed on the leaf of early rosette stage (Figure 2C) *N. attenuata* plants (*n*=30). Larval mass was determined using a microbalance after 4, 7 and 11 days of the start of the experiment. OS from *M. sexta* and *S. littoralis* reared on *N. attenuata* WT plants were collected as described by Roda *et al* (2004) and OS from *S. gregaria* were collected as described by Schäfer *et al* (2011). For the estimation of the leaf area consumed after 11 days of *M.*

sexta larval feeding, 20 leaves in which larvae has fed were excised (one leaf per plant per genotype was used) and scanned (CanoScanLide20 scanner, Cannon). The area consumed was calculated by subtracting the total leaf area (estimated by reconstruction of the leaf contour) to the remaining leaf area.

Virus induced gene silencing

Virus-induced gene silencing (VIGS) based on the tobacco rattle virus (TRV; Ratcliff *et al*., 2001) was used to transiently silenced Na*LecRK1* as previously described (Saedler and Baldwin, 2004). An 86 bp fragment corresponding to the 3'-UTR of Na*LecRK1* (see accession number below) was amplified by PCR with the primers LecRK1-33 and LecRK1-30 (Supplemental Table S5 online). The PCR product was digested with *BamH1* and *Sal1* and inserted into plasmid pTV00 in antisense orientation to generate the VIGS-lecRK1 vector. Plants transformed with the empty vector (EV) were used as control. Efficiency of gene silencing was evaluated by real-time qPCR (see below) using the primers 5358 Fw and 5358 Rv (Supplemental Table S5 online) 1 h after wounding and 18:3-Glu elicitation.

Generation of stable silenced lines

The same 86 pb fragment used for generating the VIGS-lecRK1 vector was subcloned into the pSOL8 transformation vector (Bubner *et al*., 2006) as an inverted-repeat construct. This construct was used to transform *N. attenuata* WT plants using *Agrobacterium*-mediated transformation and plant regeneration as previously described (Krügel *et al*., 2002). T_1 transformed plants were analyzed for T-DNA insertion number by Southern blot hybridization (see below). Segregation analysis for hygromycin resistance in T_2 seedlings was performed on agar plates supplemented with hygromycin (0.025 mg ml^{-1}). Two lines, A-08-378-5-4-1 (ir-lecRK1-378) and A-08-380-6-3-8 (ir-lecRK1-380) had a single T-DNA insertion in the genome and they were used for all experiments. For Southern blot analysis, genomic DNA from WT and ir-lecRK1 plants was isolated by the cetyltrimethylammonium bromide (CTAB) method. DNA samples (10 µg) were digested

with EcoRV (New England Biolabs, Frankfurt, Germany) overnight at 37°C according to commercial instructions and separated on a 1% (w/v) agarose gel using standard conditions. DNA was blotted onto Gene Screen Plus Hybridisation Transfer membranes (Perkin Elmer Life and Analytical Sciences, Boston, MA) using the capillary transfer method. A gene-specific probe for the hygromycin resistance gene *hptII* was generated by PCR using the primers HYG1-18 and HYG3-20 (Supplemental Table S5 online). The probe was labeled with [α-^{32}P]dCTP (Perkin Elmer) using the Rediprime II kit (Amersham Pharmacia, Freiburg, Germany) according to commercial instruction. Efficiency of gene silencing was evaluated by qPCR (see below) after 1 h of wounding and 18:3-Glu treatment using the primers 5358 Fw and 5358 Rv (Supplemental Table S5 online).

For the generation of *N. attenuata* plants ectopically expressing the bacterial salicylate hydroxylase gene (*nahG*) from *Pseudomonas putida*, a 690 bp fragment corresponding to this gene was amplified with primers NahG1-33 and NahG1-34 (Supplemental Table S5 online) using *P. putida* genomic DNA as template and subcloned into the pSOL1 vector (Bubner *et al*., 2006) to generate pSOL1-nahg1 and this vector was used to transform *N. attenuata* WT plants using *Agrobacterium*-mediated transformation as previously described (Krügel *et al*., 2002). Segregation analysis for hygromycin resistance in T_2 seedlings was performed on agar plates supplemented with hygromycin (0.025 mg mL^{-1}) and homozygous T_2 transformed plants were analyzed for expression of the *nahG* gene by RT-PCR using the primers NahG1-Fw and NahG1-Rv (Supplemental Table S5 online). For Southern blot analysis, genomic DNA was isolated as described above. DNA samples (10 µg) were digested with *EcoRV* and *DraI* (New England Biolabs) overnight at 37°C according to commercial instructions and separated on a 1% (w/v) agarose gel using standard conditions. DNA was blotted onto nylon membranes as described above. Membranes were hybridized with a nahG-specific radio-labeled probe that was generated by PCR using the primer pairs NahG1 Fw and NahG1 Rv (Supplemental Table S5 online) and [α- ^{32}P]dCTP (Perkin Elmer) using the Rediprime II kit (Amersham Pharmacia) according to commercial instruction. *Pseudomonas syringe* DC3000 (Pst DC3000) grown at O.D. = 0.001 or water (control) was syringe-infiltrated into leaves of WT and ov-nahG plants and infiltrated leaf tissue was harvested 2 days after the treatment for analysis of SA levels (see below).

Rapid amplification of cDNA ends and sequence analysis

For cloning of the full length Na*LecRK1* cDNA sequence, 5 µg of total RNA were isolated from leaves of *N. attenuata* plants. The 3´RACE and 5'RACE Systems for Rapid Amplification of cDNA Ends (Invitrogen, Karlsruhe, Germany) were used following the manufacturer's instructions and the primers listed in Supplemental Table S5 online. The PCR products were cloned into the pGEM-T easy vector (Promega, Madison, WI) and sequenced using universal primers. Sequence alignments were performed using BLAST (http://blast.ncbi.nlm.nih.gov) and ExPASy (http://expasy.org). Structural domain prediction was performed using SMART (http://smart.embl-heidelberg.de; Letunic *et al*., 2009) and Pfam (http://pfam.sanger.ac.uk) databases. Prediction of trasmembrane domains was performed using TMHMM (http://www.cbs.dtu.dk/services/TMHMM) and SOSUI (http://bp.nuap.nagoya-u.ac.jp/sosui) web servers. Prediction of signal peptides was performed using SignalP 3.0 (http://www.cbs.dtu.dk/services/SignalP).

Quantitative real-time PCR

For all treatments, *N. attenuata* rosette leaves were harvested and immediately frozen in liquid nitrogen. Total RNA was extracted using the TRIzol® reagent (Invitrogen) and 5 µg of total RNA were reverse transcribed using oligo$(dT)_{18}$ and SuperScript reverse transcriptase II (Invitrogen). Quantitative real-time PCR (qPCR) was performed with a Mx3005P Multiplex qPCR system (Stratagene, La Jolla, CA) and the qPCR Core kit for SYBR® Green I (Eurogentec, Liege, Belgium). Relative quantification of mRNA levels was performed by the comparative ΔCt method using the eukaryotic elongation factor 1A (Na*EF1A*) mRNA as an internal standard (Gilardoni *et al*., 2010). The sequences of the primers used for qPCR are listed in Supplemental Table S5 online. All the reactions were performed with three biological replicates using the following qPCR conditions: initial denaturation step of 95°C for 30 s, followed by 40 cycles each of 95°C for 30 s and 60°C for 1 min, with a final extension step of 95°C for 30 s and 60°C for 1 min.

Phytohormone extraction and quantification

For analysis of JA, JA-Ile and SA, 0.1 g of frozen leaf tissue was homogenized to a fine powder with a Geno/Grinder 2000 (BTC and OPS Diagnostics, Bridgewater, USA) in the presence of liquid nitrogen. One mL of ethylacetate spiked with 200 ng [$^2H_2$]JA and [$^2H_4$]SA and 40 ng JA-[$^{13}C_6$]Ile was added to the samples and after vortexing the samples were centrifuged for 15 min at 12,000xg (4°C). The upper organic phase was transferred into a fresh tube and the leaf material was re-extracted with 0.5 mL ethylacetate without internal standards. The organic phases were pooled and evaporated to dryness under reduced pressure. The dry residue was reconstituted in 0.4 mL of 70/30 (v/v) methanol/water for analysis with an LC-ESI-MS/MS instrument (Varian 1200 Triple-Quadrupole-LC-MS system; Varian, Palo Alto, CA). Ten µL of the sample were injected in a ProntoSIL® column (C18-ace-EPS, 50 x 2 mm, 5 µm, 120 Å, Bischoff, Leonberg, Germany) connected to a pre-column (C18, 4 x 2mm, Phenomenex, Torrance, CA). As mobile phases 0.05% formic acid in water (solvent A) and methanol (solvent B) were used in a gradient mode with the following conditions: time/concentration (min/%) for B: 0.0/15; 2.5/15; 4.5/98; 10.5/98; 12.0/15; 15.0/15; time/flow (min/mL min^{-1}): 0.0/0.4; 1.5/0.2; 1.5/0.2; 10.5/0.4; 15.0/0.4. Compounds were detected in the ESI negative mode and multiple reaction monitoring (MRM) according to the parameters previously published (Bonaventure *et al*., 2011b).

For the analysis of ET, the youngest fully expanded leaf of rosette stage *N.attenuata* plants was either wounded or OS elicited and it was immediately excised, weighed and transferred into a 250-mL glass vessel. Five leaves per treatment and genotype were used (*n*=5). After a 5 h incubation period (glass vessels were kept in the glasshouse under the same conditions as the plants), the headspace of the vessels was flushed into a laser photo-acoustic spectrometer (PAS; INVIVO, Adelzhausen, Germany) for determination of ET levels as previously described (Körner *et al*., 2009). Ethylene emissions are expressed as nL $h^{-1}g^{-1}$ fresh weight. Untreated leaves were used to determine basal ET levels.

Metabolic profiling of leaves by UPLC-ToF-MS

One hundred milligrams of leaf tissue were ground with a Geno/Grinder 2000 (BTC and OPS Diagnostics) in the presence of liquid nitrogen and thoroughly extracted with 1 mL of extraction buffer (40% (v/v) methanol/water; 50 mM acetate buffer (pH 4.8)). Homogenized samples were centrifuged at 12,000*x*g for 20 min at 4°C, the supernatant was transferred into a fresh 1.5 mL microcentrifuge tube and the samples were centrifuged again using the same conditions. 100 µL of the supernatant were transferred into HPLC vials.

Four µL of the leaf extract were injected into a C18 Acclaim column (2.2 µm particle size, 150 mm x 2.1 mm inner diameter; Dionex Corp., Sunnyvale, USA) and separated using a RSLC system (Dionex). Solvent A was de-ionized water containing 0.1 % (v/v) acetonitrile (Baker, HPLC grade) and 0.05 % (v/v) formic acid. Solvent B was acetonitrile and 0.05 % (v/v) formic acid. The gradient condition was applied as follows: 0 – 0.5 min 10 % B, 0.5 – 6.5 min linear gradient 80 % B, 6.5 – 10 min 80 % B, and re-equilibration at 10 % B for 3 min. The flow rate was 300 µL min^{-1}. Eluted compounds were detected with a MicroToF mass spectrometer (Bruker Daltonik, Bremen, Germany) equipped with an electrospray ionization source in positive ion mode. Instrument settings were as follows: capillary voltage, 4500 V; capillary exit, 130 V; dry gas temperature, 200 ºC; dry gas flow, 8 L min^{-1}. Mass calibration was performed using sodium formate clusters (10 mM solution of NaOH in 50/50% (v/v) isopropanol/water containing 0.2% formic acid). Data sets were evaluated from 125 to 550 sec in the mass range *m/z* 90 to 1400. The raw data files were converted to netCDF format using the export function of the Data Analysis version 4.0 software (Bruker Daltonics, Bremen, Germany) and processed using the XCMS package (Tautenhahn *et al*., 2008) and the R-package CAMERA (http://www.bioconductor.org/biocLite.R) as previously described (Gaquerel *et al*., 2010). Peak detection was performed using the centWave method (Tautenhahn *et al*., 2008) and the parameter settings ppm=20, snthresh=10, peakwidth=5 to 20 s. Retention time (RT) correction was achieved using the parameter settings minfrac=1, bw=60 s, mzwid=0.1D, span=1, and missing=extra=0 (Gaquerel *et al*., 2010).

The Metaboanalyst software ((Xia et al., 2009) was used to perform multivariate analysis (PCA and PLSDA). The data was filtered using the coefficient of variation (CV) and it was normalized using Pareto scaling ((Xia et al., 2009)Gaquerel *et al*., 2010). PLSDA ((Eriksson L, 2006; Xie et al., 2008) was validated using a permutation test as previously described (Westerhuis *et al*., 2008). An important output of the PLSDA analysis is that it estimates and ranks the influence of individual features (ions) on the model by assigning to each variable a VIP (variable importance in the projection) value, VIP values bigger than or equal to 1.0 are considered statistical significant for group discrimination (Xie *et al*., 2008; Mazzara *et al*., 2011). For elemental molecular formula calculation, the SmartFormula algorithm (Data-Analysis 4.0 software, Bruker Daltonik) was used following maximum elemental composition $C_aH_bN_cO_dNa_eK_f$ and the restrictions $1 \leq b/a \leq 3$; e=0 or 1; f=0 or 1; a, b, c, and d not limited. Rings plus double bonds values from -0.5 to 40, the nitrogen rule, and ions of even electron configuration were also considered (Gaquerel *et al*., 2010). The public metabolite databases used for analysis were Prime (http://prime.psc.riken.jp/), Metlin (http://metlin.scripps.edu/), MetDAT2 (http://www.sdwa.nus.edu.sg/METDAT2/), KEEG (http://www.genome.jp/kegg/), PubChem (http://pubchem.ncbi.nlm.nih.gov/) and Knapsack (http://kanaya.naist.jp/KNApSAcK/).

Analysis of TPI activity

Leaf tissue from 40-day-old ir-lecRK1-378, ir-lecRK-380 and WT plants was harvested 2 and 3 days after wounding and *M. sexta* OS elicitation. Unelicited tissue was used as control for basal TPI activity. 100 mg of leaf tissue were ground using a Geno/Grinder 2000 (BTC and OPS Diagnostics) in 2 mL microcentrifuge tubes and extracted with 0.3 mL of ice-cold extraction buffer (0.1 M Tris-Cl (pH 7.6), 5% (w/w) polyvinylpolypyrrolidone (Sigma), 2 mg/mL phenylthiourea (Sigma), 5 mg/mL diethyldithiocarbamate (Sigma), 0.05 M Na_2EDTA). The samples were thoroughly vortexed and centrifuged at 4ºC for 20 min at 12,000x*g.* The supernatant was transferred into a fresh tube and kept on ice for protein quantification and TPI analysis. Protein concentration was determined with the Protein Assay kit (Bio-Rad, München, Germany) using bovine

serum albumina (BSA; Sigma) as a standard. TPI activity was analyzed by a radial diffusion assay as previously described (Van Dam *et al*., 2001).

Analysis of HGL-DTGs, nicotine and phenyl-propanoid derivatives.

For quantification of total HGL-DTGs and nicotine levels, leaf samples were harvested after the treatments and times indicated in the figure captions and homogenized to a fine powder with a Geno/Grinder 2000 (BTC and OPS Diagnostics). Samples were extracted with 40% (v/v) methanol/water containing 0.5% (v/v) acetic acid and analyzed by HPLC as previously described (Keinänen *et al*., 2001; Jassbi *et al*., 2008). An external calibration curve was generated with a dilution series of nicotine and glycyrrhizinic acid and samples were normalized by gram fresh weight (gFW^{-1}). Individual HGL-DTG species were quantified by reverse-phase LC-MS/MS as previously described (Heiling *et al*., 2010). Derivatives of the phenyl-propanoid pathway were analyzed as previously described (Kaur *et al*., 2010).

Amino acid determination in *M. sexta* midgut and leaf tissue

M. sexta larvae reared on *N. attenuata* plants for 11 days were placed on ice and their midguts were dissected with forceps under a stereomicroscope. The midgut tissue and content were separated and immediately transferred into screw cap 10 mL glass tubes placed on ice. Midgut tissue and content were homogenized separately in the presence of 1 mL 1/1 (v/v) chloroform/methanol containing 0.01% (v/v) formic acid. After centrifugation for 15 min at 700*x*g (4°C), the supernatant was transferred into a fresh 10 mL glass tube and the aqueous phase/tissue was re-extracted with 1 mL chloroform. After centrifugation for 15 min at 700*x*g (4°C), the supernatants were pooled and transferred into 4 mL HPLC vials. Midgut and midgut content were diluted 1/40 (v/v) in water before analysis. Leaves were extracted using the same protocol but diluted 1/1 (v/v) in water before analysis. Chromatography was performed on an Agilent 1200 HPLC system (Agilent Technologies, Boeblingen, Germany) using a Zorbax Eclipse XDB-C18 column (50 x 4.6 mm, 1.8 µm,

Agilent Technologies). Formic acid (0.05%) in water and acetonitrile were employed as mobile phases A and B, respectively. The elution profile was: 0-1 min, 100% A; 1-3 min, 0-100% B in A; 3-4 min 100% B and 4.1-7 min 100% A. The mobile phase flow rate was 0.8 mL min^{-1}. The column temperature was maintained at 25°C. An API 3200 tandem mass spectrometer (Applied Biosystems, Darmstadt, Germany) equipped with a Turbospray ion source was operated in positive ionization mode. The instrument parameters were optimized by infusion experiments with pure threonine standard (Sigma). The ionspray voltage was maintained at 5500 eV. The turbo gas temperature was set at 700 °C. Nebulizing gas was set at 70 psi, curtain gas at 35 psi, heating gas at 70 psi and collision gas at 2 psi. Multiple reaction monitoring (MRM) was used to monitor analyte parent ion → product ion as described by Jander *et al* (2004). External calibration curves for amino acids were created by linear regression in the range from 0.2 to 5 µM.

Starch quantification

Leaf samples were harvested at different times after *M. sexta* OS elicitation and homogenized to a fine powder with a Geno/Grinder 2000. Samples were extracted with 1 mL 80% (v/v) ethanol/water and centrifuged at 12,000x*g* for 15 min at 4°C. The pellet was washed with 1 mL 80% (v/v) ethanol/water and centrifuged at 12,000x*g* for 15 min. 500 µL of water were added to the pellet and the samples were vortexed for 5 min. 650 µL of perchloric acid (Carl-Roth, Karlsruhe, Germany) was added and the samples were completely homogenized by pipetting several times up and down with a micropipette. The homogenates were incubated on ice for 20 min and then centrifuged at 12,000x*g* for 15 min at 4°C. The starch-containing supernatant was transferred to a new 1.5 mL microcentrifuge tube and 10 µL were diluted with 90 µL of water. 400 µL of anthrone reagent (100 mg anthrone (Sigma-Aldrich) in 100 mL 95% (v/v) H_2SO_4/water (Carl-Roth)) were added and the reactions were kept for 8 min in a boiling water bath (Viles and Silverman, 1949). After samples cooled down, absorbance was measured at 630 nm with the Ultrospec® 3000 (Pharmacia Biotech, Cambridge, England) spectrophotometer. Standard curves were generated with D-glucose (Sigma-Aldrich) from 0.05 to 1 mg/mL.

Microarray analysis

Total RNA was extracted based on the method of Kistner and Matamoros (2005) and its quality checked by spectrophotometry (NanoDrop, Wilmington, DE). Genomic DNA was removed by DNAse treatment following commercial instructions (Turbo DNase; Ambion, Europe), RNA was cleaned up with RNeasy MinElute columns (Qiagen, Hilden, Germany) and the RNA quality was checked with the RNA 6000 Nano kit (Agilent, Santa Clara, CA) using an Agilent 2100 Bioanalyzer. Total RNA was used to generate labeled cRNA with the Quick Amp labeling kit (Agilent) following commercial specifications and the yield of cRNA was determined spectrophotometrically (NanoDrop). Labeled cRNA was hybridized using the Gene Expression Hybridization kit (Agilent) following commercial instructions onto a 44K custom designed 60mer *N. attenuata* Agilent microarrays (Kallenbach *et al*., 2011) containing 43,533 sequences (see Accession numbers). Microarrays were hybridized overnight at 65°C and slides were washed with the Gene Expression Wash Buffer kit (Agilent) as outlined in the One-Color Microarray-Based Gene Expression Analysis manual (Agilent). Three biological replicates were used per treatment with a total of six arrays (see Accession numbers). Arrays were scanned with an Agilent G2565BA scanner and image data was acquired with the Agilent Scan Control software (version A.7.0.1 for the B scanner). Data was extracted using the Agilent Feature Extraction software (version 9.5) and analyzed with the SAM (Significance Analysis of Microarrays) software (Tusher *et al*., 2001). The q-values for each gene corresponded to a computed false discovery rate (FDR) of 4%. Significant changes in gene expression were considered when the $\log_2$(fold change; treatment versus control) were greater than 1.3 or smaller than -1.3 and q-values lower than 0.05 (according to the FDR value calculated by SAM).

Statistical analysis

Statistics were calculated using the SPSS software version 17.0.

Accession numbers

Na*LecRK1* (JF919621), Agilent Chip platform (GPL13527; NCBI GEO database), microarray data (GSE29905; NCBI GEO database).

ACKNOWLEDGMENTS

PG is a fellow of the Deutscher Akademischer Austausch Dienst (DAAD). We thank E. Gaquerel for his help with the analysis of the metabolic profiling data and M. Reichelt for his assistance with amino acid analysis. This work was funded by the Deutsche Forschungsgemeinschaft (DFG; Project BO3260/3-1) and the Max Planck Society.

AUTHOR CONTRIBUTIONS

P.G. carried out the experiments, analyzed the data and wrote the manuscript. C.H. characterized and provided the ov-nahg plants. I.T.B. participated in the design and coordination of the study and wrote the manuscript. G.B. conceived of the study, participated in its design and coordination and wrote the manuscript.

TABLES

Table I. List of ions corresponding to defense metabolites differentially accumulating in leaves of ir-lecRK1 plants after *M. sexta* OS elicitation.

Ref no.	*m/z*	RT	Metabolite	*P*-value	FC	days after treatment
607	163.125	180.94	Nicotine, $[M+H]^+$	0.04	0.34	6
128	106.066	178.94	Nicotine, $[M+H]^+$, fragment	0.02	0.66	6
4847	613.354	310.89	Attenoside, $[M+H]^+$, fragment	0.03	0.41	3
1639	289.251	358.51	Lyciumoside IV, $[M+H]^+$, fragment	0.01	0.56	6
4325	543.331	332.26	Lyciumoside IV, $[M+H]^+$,fragment	0.01	0.50	0.5
1182	237.078	335.26	Nicotianoside III, $[M+H]^+$, fragment	0.03	0.36	6
3128	433.269	344.98	Nicotianoside IV, $[M+H]^+$, fragment	<0.01	0.33	6
5920	829.421	338.35	Nicotianoside IV, $[M+H]^+$, fragment	0.03	0.52	6
6199	991.481	335.21	Nicotianoside IV, $[M+H-H_20]^+$, fragment	<0.01	0.01	6
5977	863.432	335.59	Nicotianoside I, $[M+H]^+$	0.02	0.52	6
6229	1025.483	314.39	Nicotianoside VI, $[M+H]^+$	0.02	0.45	6
5911	827.403	317.87	Nicotianoside VI, $[M+H\text{-glucose-}H_20]^+$, fragment	0.04	0.63	0.5
6110	931.425	343.64	Nicotianoside II, $[M+H-H_20]^+$, fragment	<0.01	<0.01	6
6164	971.414	341.82	Nicotianoside II, $[M+Na]^+$	0.03	0.15	6

Ref no.: Reference number for the specific ion (Supplemental Table S1 online)

RT: Retention time (in seconds)

P-value: TTEST-based probability value calculated by the XCMS software (Tautenhahn *et al*., 2008)

FC: fold change in ion intensity (ir-lecRK1-378 vs WT)

Chapter 4

Supplemental data

Table S1. List of ions identified by UPLC-ToF-MS analysis (positive ion mode) in WT and ir-NalecRK1 plants. **(Data can be found on the attached CD-ROM).**

Table S2. List of ions differentially accumulating in leaves of ir-lecRK1 plants at different times after *M. sexta* OS elicitation. **(Data can be found on the attached CD-ROM).**

Table S3. List of ions with VIP values bigger or equal to 1. **(Data can be found on the attached CD-ROM).**

Table S4. List of genes differentially regulated in ir-lecRK1 plants at 1 h after *M. sexta* OS elicitation. **(Data can be found on the attached CD-ROM).**

Table S5. List of primers.

Figure S1. Protein alignment of NaLecRK1 with LecRKs from different plants species.

Figure S2. Analysis of plants reduced in Na*LecRK1* expression by VIGS.

Figure S3. Starch and protein levels in ir-lecRK1 plants after OS elicitation.

Figure S4. Quantification of JA, JA-Ile and SA levels in ir-lecRK1 plants after wounding.

Figure S5. Ethylene analysis in leaves of WT and ir-lecRK1 plants after wounding and OS elicitation.

Figure S6. PCA and validation of PLSDA analysis of ions accumulating differentially in ir-lecRK1 plants.

Figure S7. Analysis of nicotine, HGL-DTGs and TPI activity in ir-lecRK1 plants after wounding.

Figure S8. Kinetic of Na*GGPPs* and Na*TPI* transcript accumulation in ir-lecRK1 plants.

Figure S9. Analysis of derivatives of the phenyl-propanoid pathway.

Figure S10. Analysis of *N. attenuata* plants ectopically expressing the *nahG* gene (ov-nahg).

Supplemental Table

Supplemental Table S5. List of primers

LecRK1-33	GCGGCGGTCGACGCTAAATTCTAGTTTTGCTAG
LecRK1-30	GCGGCGGGATCCCAATTTACACAGCAGTATC
HYG1-18	CCGGATCGGACGATTGCG
HYG3-20	CGTCTGTCGAGAAGTTTCTG
NahG1-33	GCGGCGCTCGAGATGAAAAACAATAAACTTGGC
NahG1-34	GCGGCGGGTCACCTCACCCTTGACGTAGCGCACC
LecRK_5'_1	TACACAGCAGTATCCATTATC
LecRK_5'_2	CAGCAGTAAGCAAGCTGCACTTC
LecRK_5'_3	CTTCTCATCTAGGAGTATG
LecRK_5'_4	GTAAGCTAATCCTTTGGCTATGTC
LecRK_5'_5	GGATGGTAGGTAGCAGTC
LecRK_5'_6	GCATCTTTACAGGCATTCATATCAG
LecRK_5'_7	TGGCAAGTCCTATGACAG
LecRK_5'_8	GCAGCTGGTTCAGCTTCAACCTG
LecRK_5'_9	CAACCTCGGCTAGGAATG
LecRK_5'_10	CTTGGTGAAGTTCTCTGTTGCAG
LecRK_5'_11	TGAGCTGAGGATGCTG
LecRK_5'_12	TGGAGCCTCCACTAGTATTCAATC
LecRK_3'_1	CATGGAAAATTTTGCTAAATTCT
LecRK_3'_2	GGAAAATTTTGCTAAATTCTAGT
5358 Fw	GGAAAATTTTGCTAAATTCTAGTTTTG
5358 Rv	CAATTTACACAGCAGTATCCATTATC
EF1a F	ACACTTCCCACATTGCTGTCA
EF1a R	AAACGACCCAATGGAGGGTAC
NaTPI Fw	TCAGGAGATAGTAAATATGGCTGTTCA
NaTPI Rv	ATCTGCATGTTCCACATTGCTTA
NaGGPPS Fw	CCAAAACTGCTGGGATTGGA
NaGGPPS Rv	CAGCTGTTGTTTAGCATCTCG
NaTD Fw	TAAGGCATTTGATGGGAGGC
NaTD Rv	TCTCCCTGTTCACGATAATGGAA
NahG1 Fw	CGTTGCCTTAGCACTGGAAC
NahG1 Rv	GTCGGAGATGAAAGCCACCA

Supplemental figures

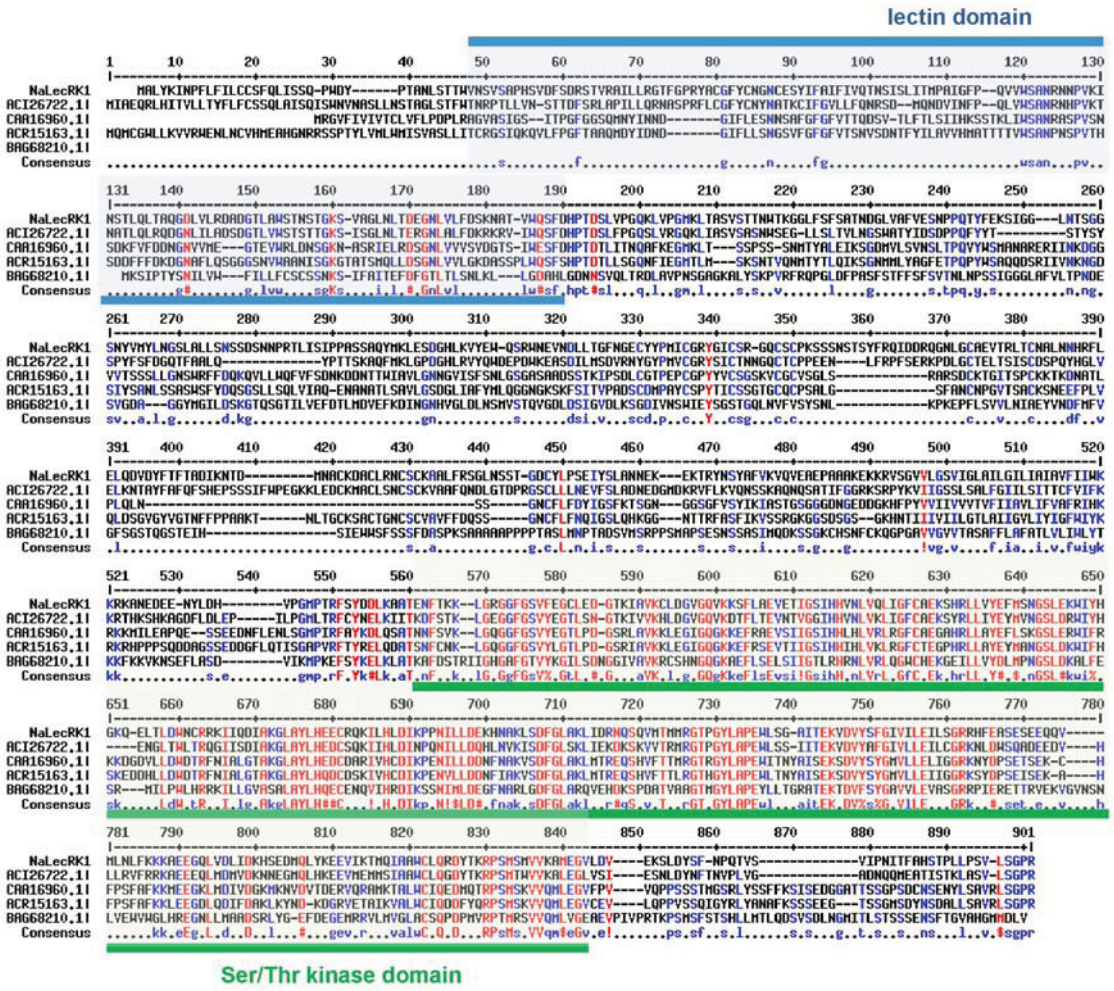

Supplemental Figure S1. Protein alignment of NaLecRK1 with lecRKs from different plants species.

The amino acid sequence of NaLecRK1 was aligned using ClustalW with homologous sequences of lecRKs from different plant species: S-receptor kinase from *Arabidopsis thaliana* (GenBank Accession CAA16960.1); NbLRK1 from *Nicotiana benthamiana* (GenBank Accession BAG68210.1); Pi-d2 from *Oryza sativa* (GenBank Accession ACR15163.1); and NgRLK1 from *Nicotiana glutinosa* (GenBank Accession ACI26722.1). The blue line marks the position of the conserved lectin domain and the green line marks the position of the conserved Ser/Thr kinase domain.

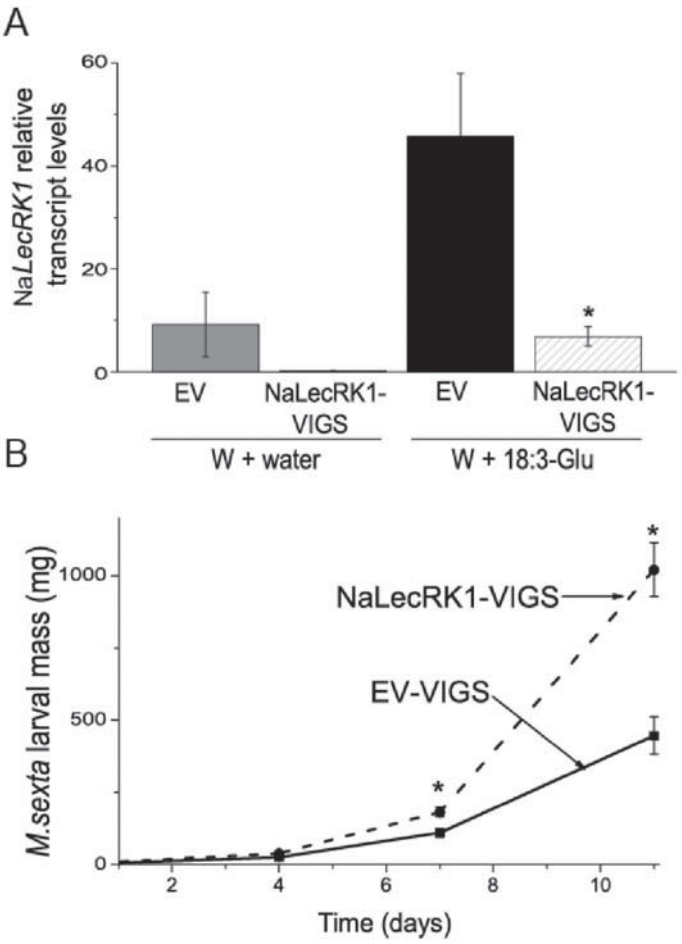

Supplemental Figure S2. Analysis of plants reduced in NaLecRK1 expression by VIGS.

N. attenuata plants with reduced levels of *NaLecRK1* expression were generated by virus induced gene silencing (VIGS; NaLecRK1-VIGS). EV-VIGS were plants transformed with the empty vector (EV).

(A) Leaves from EV-VIGS and NaLecRK1-VIGS plants were wounded and supplemented with water or 18:3-Glu and leaf tissue was harvested 1 h after the treatments. *NaLecRK1* mRNA levels were quantified by qPCR. The values are expressed as the fold-change (FC) increase relative to time 0 (value set arbitrary at 1).Transcript levels were calculated relative to the expression level of NaEF1A mRNA using the ΔCT method; see Materials and Methods). *: P <0.05, Student's t-test, (EV-VIGS vs. NaLecRK1-VIGS same treatment, bars denote ±SE, n=5).

(B) Mean (±SE) of *M. sexta* larval mass after 4, 7 and 11 of feeding on EV-VIGS or NaLecRK1-VIGS plants. Statistical analysis was performed by repeated-measurement ANOVA ($F_{1, 56}$ = 34.242, P <0.01; n=32), asterisks indicate significant differences between larvae feeding on EV-VIGS and those feeding on NaLecRK1-VIGS plants.

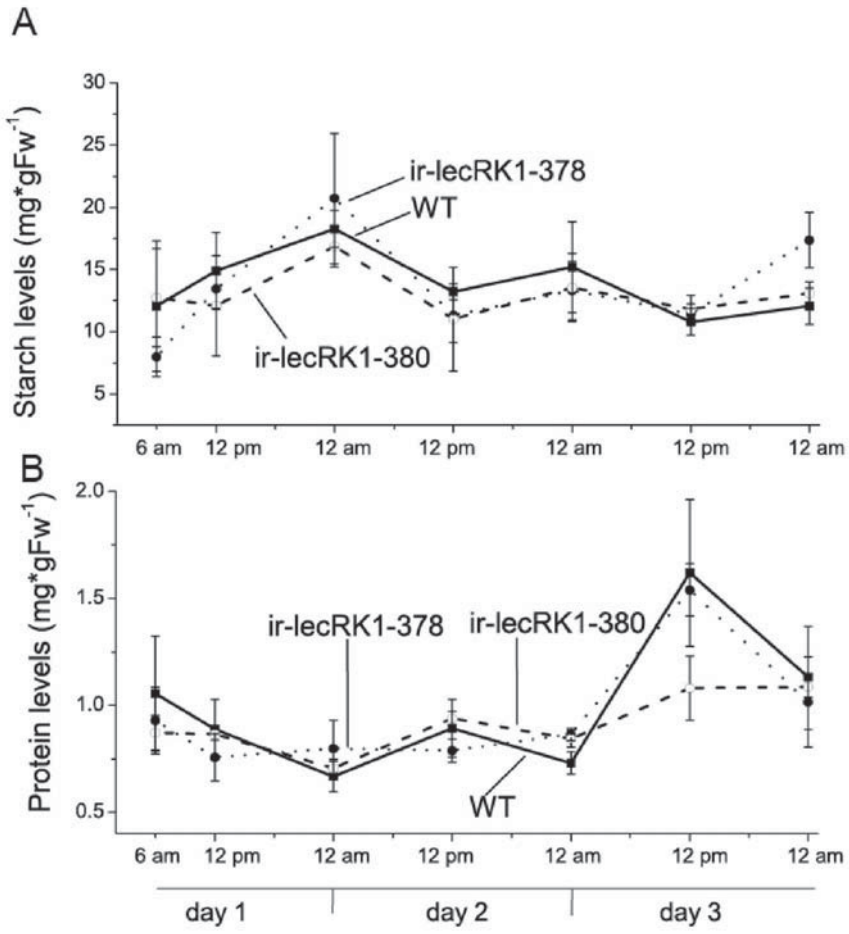

Supplemental Figure S3. Starch and protein levels in ir-lecRK1 plants after OS elicitation.

Leaves from WT and ir-lecRK1 plants were elicited with *M. sexta* OS at 6 pm of the day before tissue harvesting started (6 am). Leaf tissue was harvested at the times indicated in the x-axis during a period of 3 days.

(A) Mean (±SE) of starch levels in WT and ir-lecRK1 plants (*n*=5).

(B) Mean (±SE) of total protein levels in WT and ir-lecRK1 plants (*n*=5).

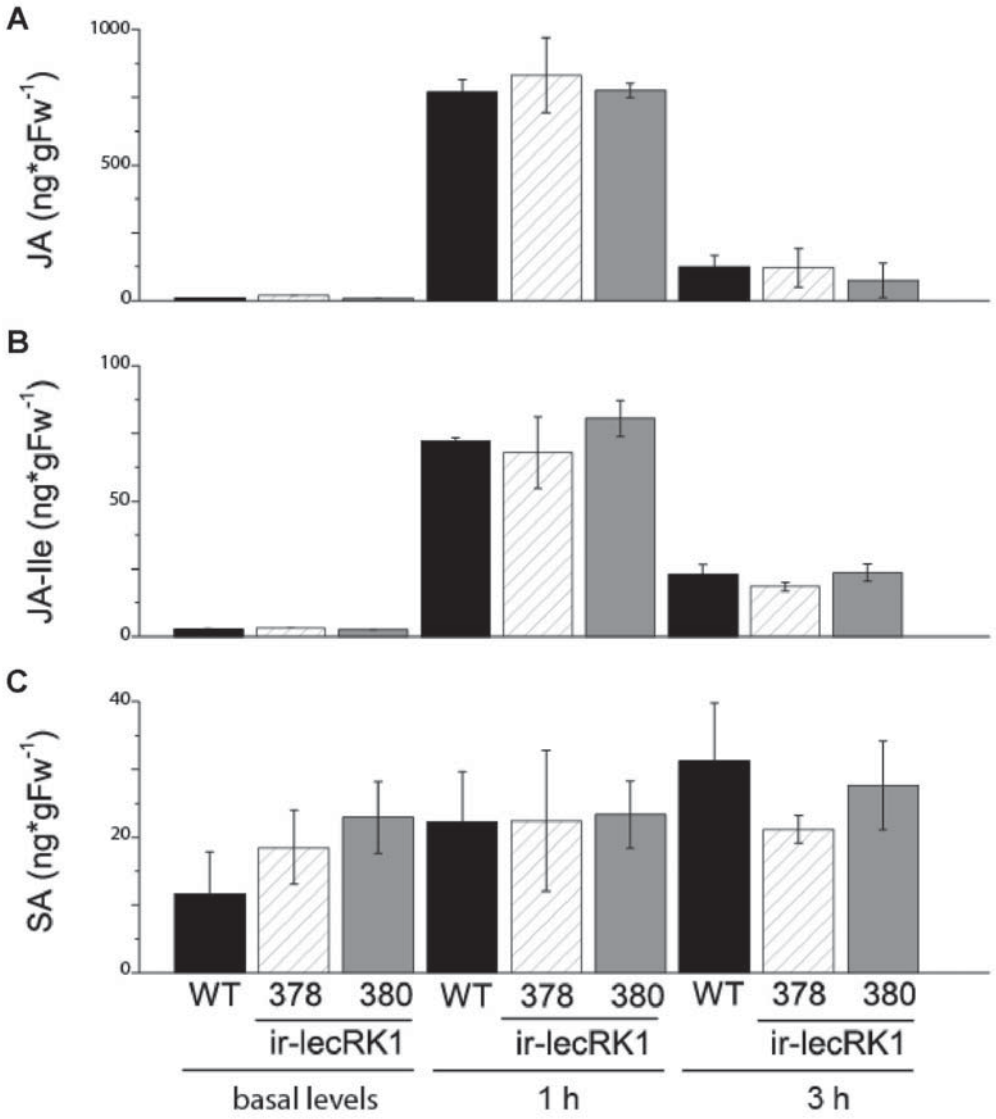

Supplemental Figure S4. Quantification of JA, JA-Ile and SA levels in ir-lecRK1 plants after wounding.

Leaves from WT and ir-lecRK1 plants were wounded and leaf tissue was harvested at different times after the treatment for phytohormone analysis by LC-MS/MS.

(A) Mean (±SE) of JA levels in WT and ir-lecRK1 plants (*n*=4).

(B) Mean (±SE) of JA-Ile levels in WT and ir-lecRK1 plants (*n*=4).

(C) Mean (±SE) of SA levels in WT and ir-lecRK1 plants (*n*=4).

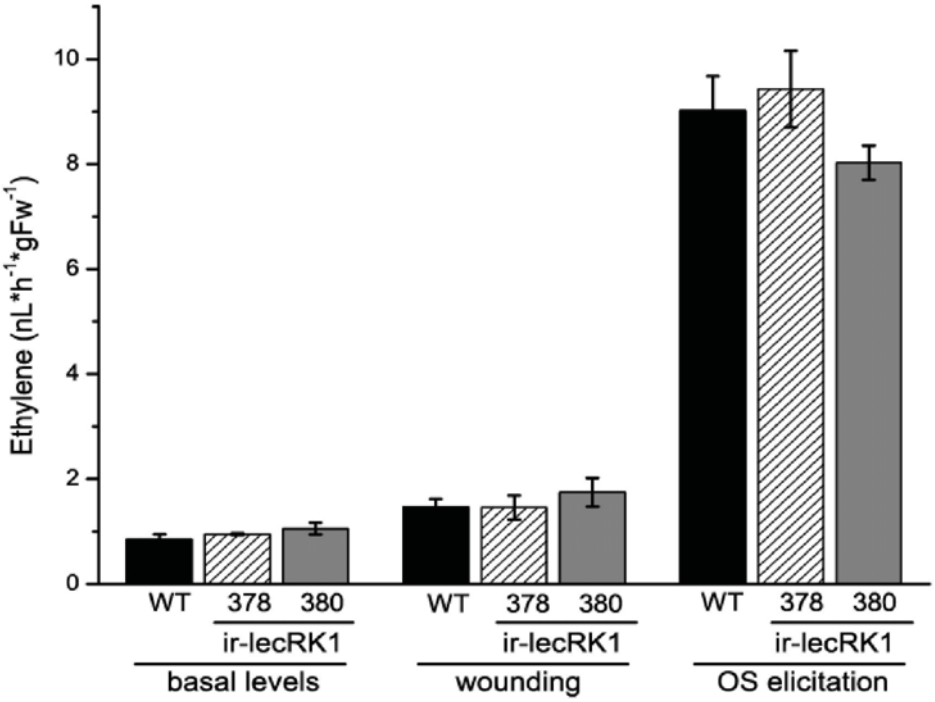

Supplemental Figure S5. Ethylene analysis in leaves of WT and ir-lecRK1 plants after wounding and OS elicitation.
Leaves of rosette stage WT and ir-lecRK1 (378 and 380) plants were either wounded or elicited with *M. sexta* OS and the levels of ethylene produced by excised leaves during a 5 h period were determined by photo-acoustic spectrometer (PAS). Bars denote ±SE. (*n*=5). Untreated leaves were used to determine basal ET levels.

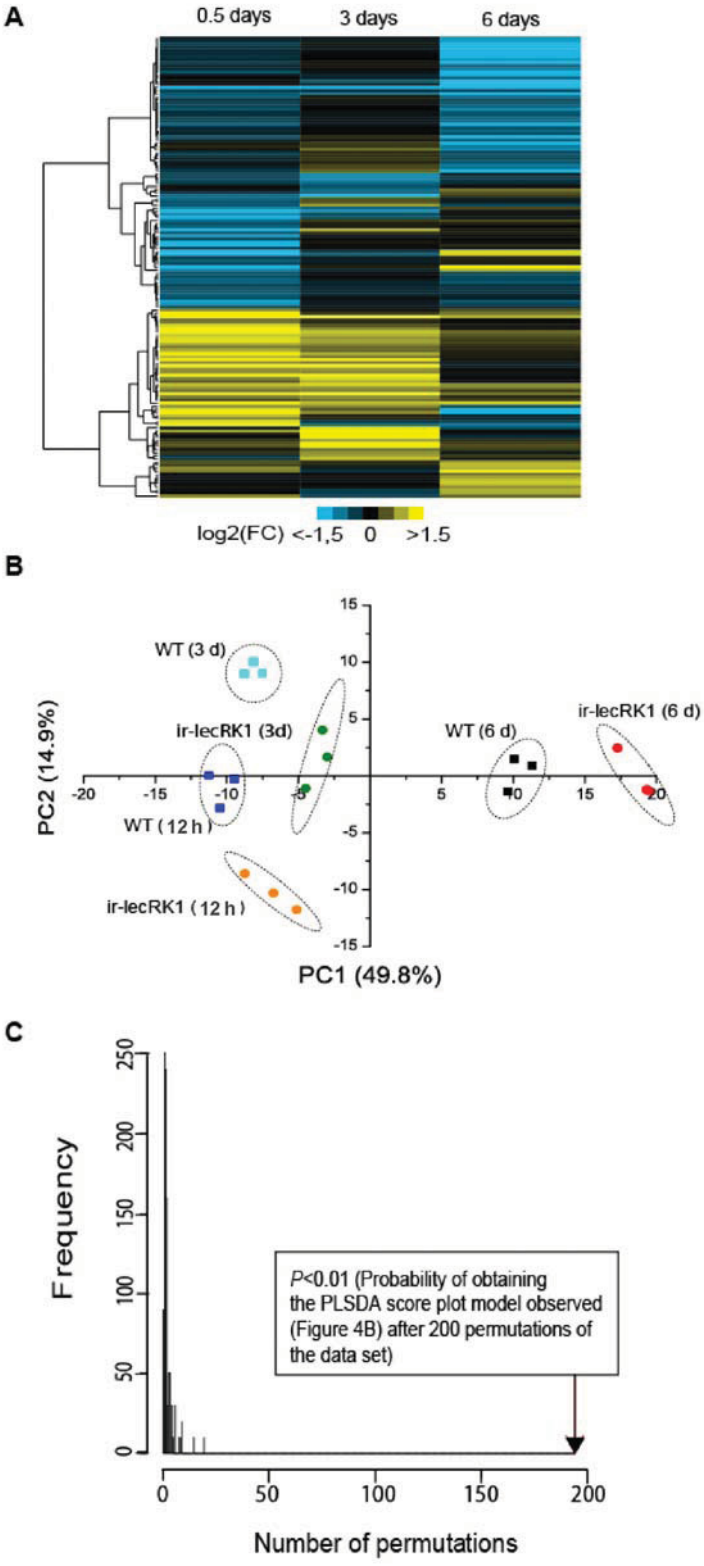

Supplemental Figure S6. PCA and validation of PLSDA analysis of ions accumulating differentially in ir-lecRK1 plants.

Leaves from rosette stage *N. attenuata* WT and ir-lecRK1-378 plants were elicited with *M. sexta* OS and leaf tissue was harvested at 12 h and 3 and 6 days after the treatments. After extraction, polar metabolites were analyzed by UPLC-ToF-MS in the positive ion detection mode as described in Materials and Methods.

(A) Hierarchical clustering analysis of 148 ions differentially accumulating in ir-lecRK1 plants compared to WT plants (fold change data was log(2) transformed before analysis; correlation (uncentered) as similarity metrics).

(B) PCA analysis of the 148 ions differentially accumulating in ir-lecRK1 plants. Components 1 and 2 explained together 64.7% of the variance of the samples (the explained variances per component are shown in brackets). Ellipses delimit the 95% statistical confidence areas for each biological group in the score plots.

(C) Validation of the PLSDA analysis (see Figure 4B) by the permutation test described by Westerhuis *et al.* (2008). *y*-axis, Probability distribution (Frequency).

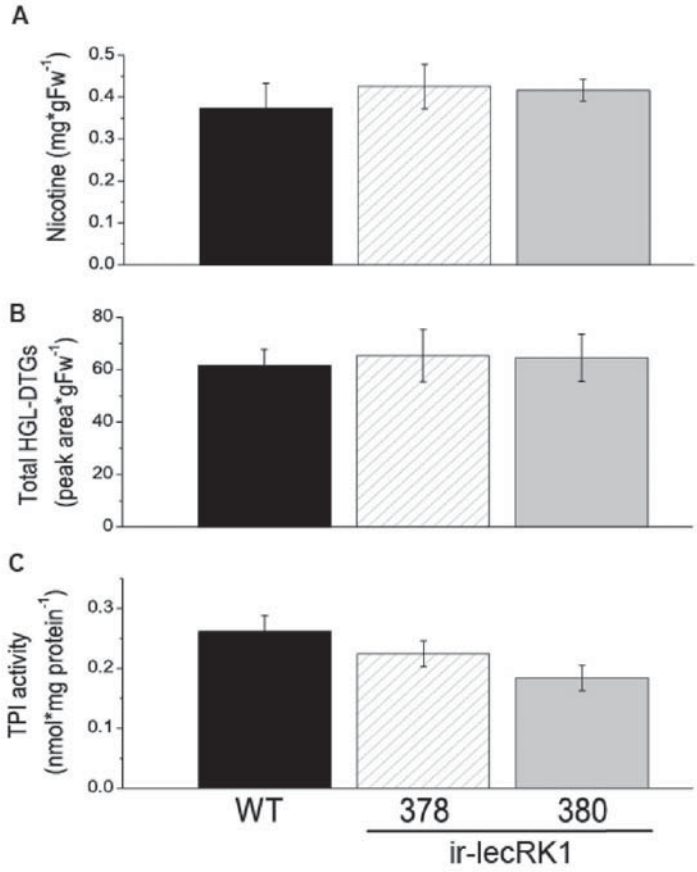

Supplemental Figure S7. Analysis of nicotine, HGL-DTGs and TPI activity in ir-lecRK1 plants after wounding.
Leaves of rosette stage WT, ir-lecRK1-378 and ir-lecRK1-380 plants were wounded and leaf tissue was harvested 3 days after the treatment for analysis of nicotine and HGL-DTG accumulation and TPI activity.
(A) Mean (±SE) of nicotine quantified by HPLC (*n*=4).
(B) Mean (±SE) of total HGL-DTGs quantified by HPLC (*n*=4).
(C) Mean (±SE) of TPI activity analyzed by a radial diffusion assay (*n*=4).

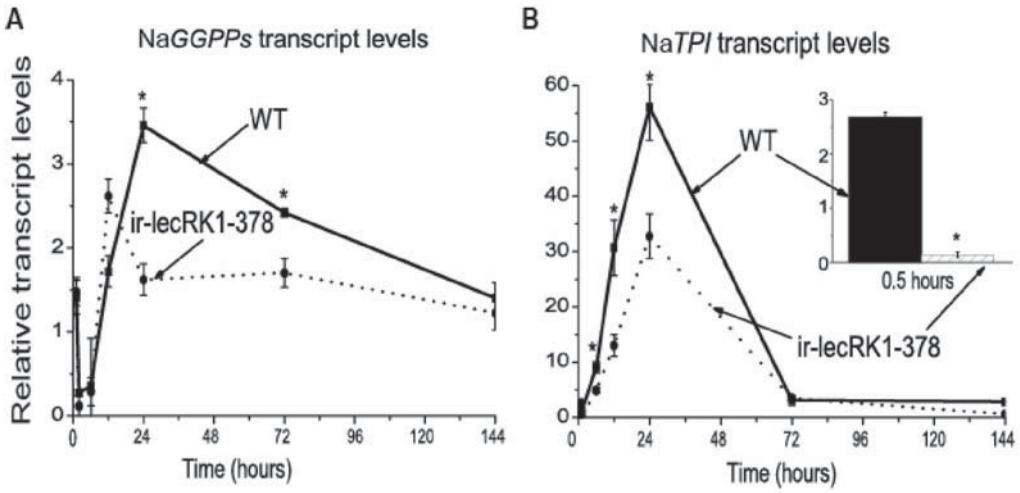

Supplemental Figure S8. Kinetic of Na*GGPPs* and Na*TPI* transcript accumulation in ir-lecRK1 plants.

(A) Leaves from rosette stage WT and ir-lecRK1-378 plants were elicited with *M. sexta* OS. Na*GGPPs* mRNA levels were quantified by qPCR. The values are expressed as the fold-change (FC) increase relative to time 0 (value set arbitrary at 1). The Na*GGPPs* mRNA levels were calculated relative to the expression level of Na*EF1A* mRNA using the ΔCT method; see Materials and Methods). *: P <0.05, Student's t-test, (WT vs. ir-lecRK1-378 plants at same time point, bars denote ±SE, n=3).

(B) Leaves from rosette stage WT and ir-lecRK1-378 plants were elicited with *M. sexta* OS. Na*TPI* mRNA levels were quantified by qPCR an expressed as described in (A). *: P <0.05, Student's t-test (WT vs. ir-lecRK1-378 plants at same time point, bars denote ±SE, n=3).

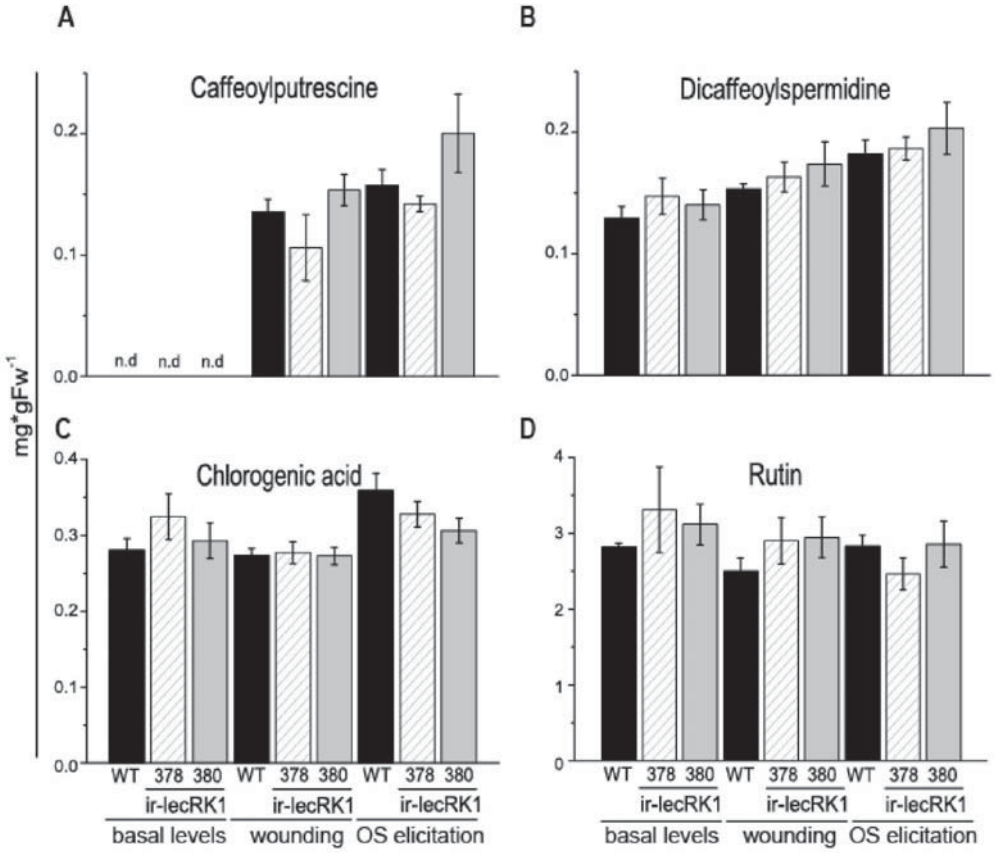

Supplemental Figure S9. Analysis of derivatives of the phenyl-propanoid pathway.
Leaves of rosette stage WT, ir-lecRK1-378 and ir-lecRK1-380 plants were either wounded or elicited with *M. sexta* OS (W+OS). Leaf tissue was harvested 3 days after the treatments and the samples were analyzed by HPLC. Untreated plants served as controls for basal levels of the metabolites analyzed.
(A) Mean (±SE) of caffeoylputrescine (*n*=4).
(B) Mean (±SE) of dicaffeoylspermidine (*n*=4).
(C) Mean (±SE) of chlorogenic acid (*n*=4).
(D) Mean (±SE) of rutin (*n*=4).

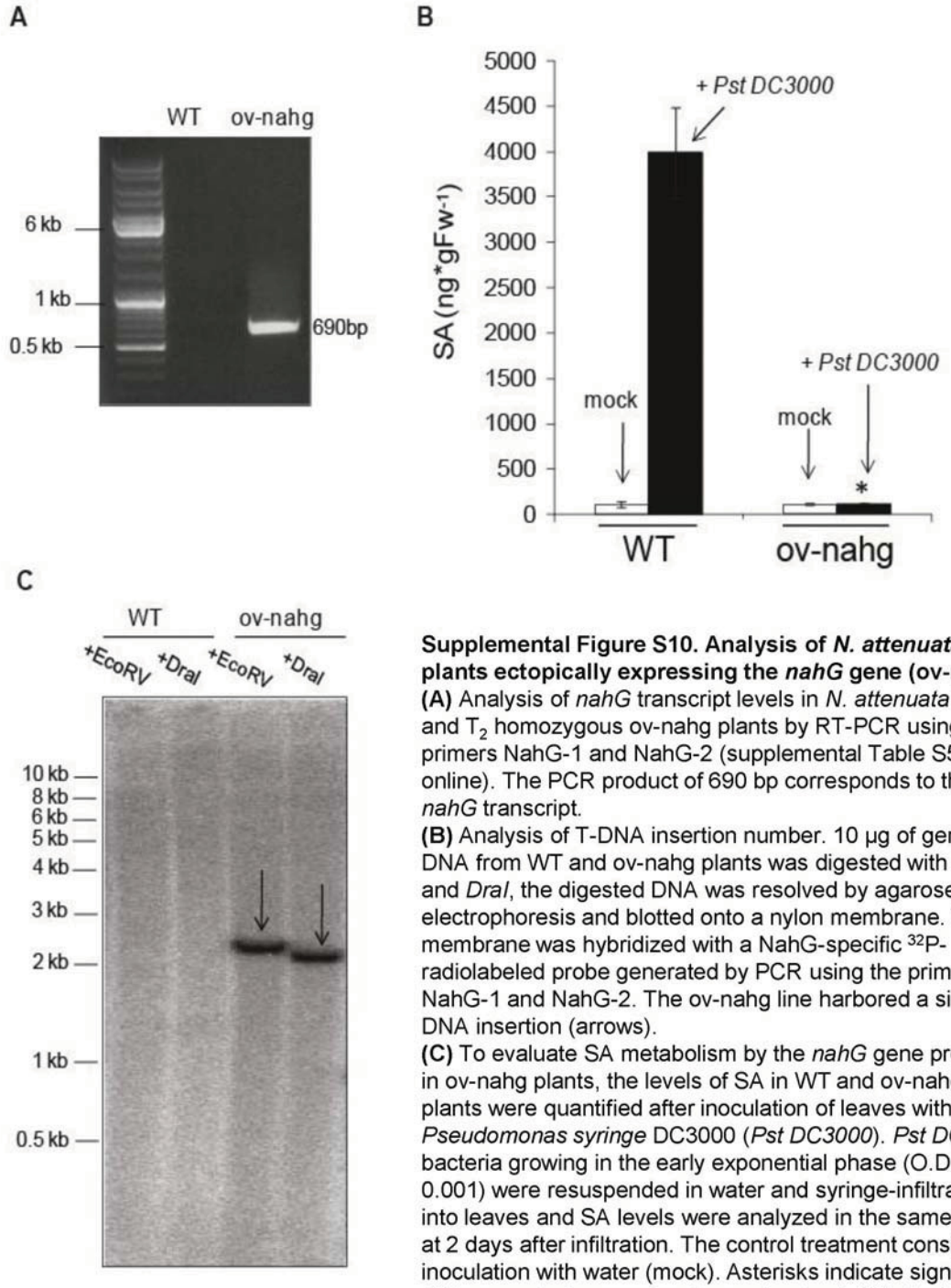

Supplemental Figure S10. Analysis of *N. attenuata* plants ectopically expressing the *nahG* gene (ov-nahg).
(A) Analysis of *nahG* transcript levels in *N. attenuata* WT and T_2 homozygous ov-nahg plants by RT-PCR using primers NahG-1 and NahG-2 (supplemental Table S5 online). The PCR product of 690 bp corresponds to the *nahG* transcript.
(B) Analysis of T-DNA insertion number. 10 µg of genomic DNA from WT and ov-nahg plants was digested with *EcoRV* and *DraI*, the digested DNA was resolved by agarose gel electrophoresis and blotted onto a nylon membrane. The membrane was hybridized with a NahG-specific ^{32}P-radiolabeled probe generated by PCR using the primer pairs NahG-1 and NahG-2. The ov-nahg line harbored a single T-DNA insertion (arrows).
(C) To evaluate SA metabolism by the *nahG* gene product in ov-nahg plants, the levels of SA in WT and ov-nahg plants were quantified after inoculation of leaves with *Pseudomonas syringe* DC3000 (*Pst DC3000*). *Pst DC3000* bacteria growing in the early exponential phase (O.D. = 0.001) were resuspended in water and syringe-infiltrated into leaves and SA levels were analyzed in the same leaves at 2 days after infiltration. The control treatment consisted of inoculation with water (mock). Asterisks indicate significant differences between wt and ov-nahg plants (Student's t-test; *: $P < 0.001$ (WT vs ov-nahg); $n = 10$). The morphology of ov-nahg plants was indistinguishable from that of WT plants at all developmental stages (not shown).

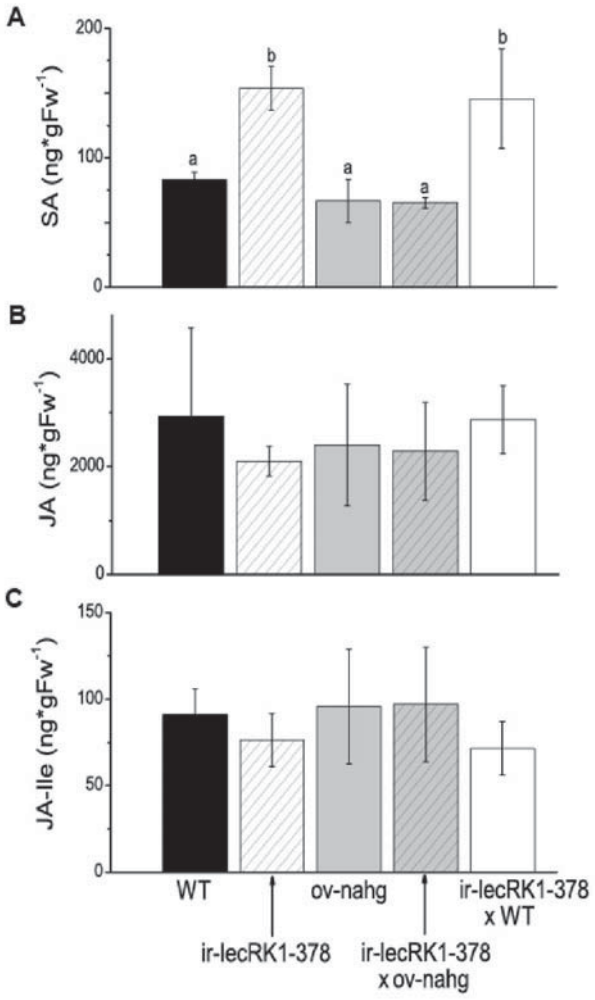

Supplemental Figure S11. Levels of SA, JA and JA-Ile in 5 different genotypes after *M. sexta* herbivory.

Freshly hatched *M. sexta* neonates were allowed to feed on WT *N. attenuata* plants and ir-lecRK1-378, ov-nahg, ir-lecRK1-378 x ov-nahg and ir-lecRK1-378 x WT plants for 11 days. Leaf tissue was harvested from these plants at this time point and used to quantify SA, JA and JA-Ile levels by LC-MS/MS.

(A) Mean (±SE) of SA levels (univariate ANOVA, $F_{4,13} = 10{,}57$ $P < 0.002$, followed by a Tukey HSD post-hoc test, $P < 0.05$, $n=3$).

(B) Mean (±SE) of JA levels ($n=3$).

(C) Mean (±SE) of JA-Ile levels ($n=3$).

References:

AbuQamar, S., Chai, M.-F., Luo, H., Song, F., and Mengiste, T. (2008). Tomato protein kinase 1b mediates signaling of plant responses to necrotrophic fungi and insect herbivory. Plant Cell **20,** 1964-1983.

Alborn, H.T., Turlings, T.C., Jones, T.H., Stenhagen, G., Loughrin, J.H., and Tumlinson, J.H. (1997). An elicitor of plant volatiles from beet armyworm oral secretion. Science **276,** 945-949.

Alborn, H.T., Hansen, T.V., Jones, T.H., Bennett, D.C., Tumlinson, J.H., Schmelz, E.A., and Teal, P.E. (2007). Disulfooxy fatty acids from the American bird grasshopper *Schistocerca americana*, elicitors of plant volatiles. Proc Natl Acad Sci USA **104,** 12976-12981.

Allmann, S., Halitschke, R., Schuurink, R.C., and Baldwin, I.T. (2010). Oxylipin channelling in *Nicotiana attenuata*: lipoxygenase 2 supplies substrates for green leaf volatile production. Plant Cell Environ **33,** 2028-2040.

Bonaventure, G., Vandoorn, A., and Baldwin, I.T. (2011a). Herbivore-associated elicitors: FAC signaling and metabolism. Trends Plant Sci. PMID: 21354852.

Bonaventure, G., Schuck, S., and Baldwin, I.T. (2011b) Revealing complexity and specificity in the activation of lipase-mediated oxylipin biosynthesis: A specific role of the *Nicotiana attenuata* GLA1 lipase in the activation of JA biosynthesis in leaves and roots. Plant Cell Environ PMID: 21554327.

Bouwmeester, K., and Govers, F. (2009). Arabidopsis L-type lectin receptor kinases: phylogeny, classification, and expression profiles. J Exp Bot **60,** 4383-4396.

Bubner, B., Gase, K., Berger, B., Link, D., and Baldwin, I.T. (2006). Occurrence of tetraploidy in *Nicotiana attenuata* plants after Agrobacterium-mediated transformation is genotype specific but independent of polysomaty of explant tissue. Plant Cell Reports **25,** 668-675.

Chen, H., Wilkerson, C.G., Kuchar, J.A., Phinney, B.S., and Howe, G.A. (2005). Jasmonate-inducible plant enzymes degrade essential amino acids in the herbivore midgut. Proc Natl Acad Sci USA **102,** 19237-19242.

Chen, X., Shang, J., Chen, D., Lei, C., Zou, Y., Zhai, W., Liu, G., Xu, J., Ling, Z., Cao, G., Ma, B., Wang, Y., Zhao, X., Li, S., and Zhu, L. (2006). A B-lectin receptor kinase gene conferring rice blast resistance. Plant J **46,** 794-804.

Diezel, C., von Dahl, C.C., Gaquerel, E., and Baldwin, I.T. (2009). Different lepidopteran elicitors account for cross-talk in herbivory-induced phytohormone signaling. Plant Physiol **150,** 1576-1586.

Doares, S.H., Narvaez-Vasquez, J., Conconi, A., and Ryan, C.A. (1995). Salicylic acid inhibits synthesis of protease inhibitors in tomato leaves induced by systemin and jasmonic acid. Plant Physiol **108,** 1741-1746.

Doherty, H.M., Selvendran, R.R., and Bowles, D.J. (1988). The wound response of tomato plants can be inhibited by aspirin and related hydroxy-benzoic acids. Physiol Mol Plant Pathol **33,** 377-384.

Ellis, C., Karafyllidis, I., Wasternack, C., and Turner, J.G. (2002). The Arabidopsis mutant cev1 links cell wall signaling to jasmonate and ethylene responses. Plant Cell **14,** 1557-1566.

Eriksson L., Johansson E., Kettaneh-Wold N., Trygg J., Wikström C., and Wold S. (2006) Multi- and megavariate data analysis. Part I. Basic principles and applications. Umetrics Academy, Umea, Sweden, ISBN-10: 91-973730-2-8

Gaquerel, E., Heiling, S., Schoettner, M., Zurek, G., and Baldwin, I.T. (2010). Development and validation of a liquid chromatography−electrospray ionization−time-of-flight mass spectrometry method for induced changes in *Nicotiana attenuata* leaves during simulated herbivory. J Agric Food Chem **58,** 9418-9427.

Gilardoni, P.A., Schuck, S., Jungling, R., Rotter, B., Baldwin, I.T., and Bonaventure, G. (2010). SuperSAGE analysis of the *Nicotiana attenuata* transcriptome after fatty acid-amino acid elicitation (FAC): identification of early mediators of insect responses. BMC Plant Biol **10,** 66.

Giri, A.P., Wünsche, H., Mitra, S., Zavala, J.A., Muck, A., Svatos, A., and Baldwin, I.T. (2006). Molecular interactions between the specialist herbivore *Manduca sexta* (Lepidoptera, Sphingidae) and its natural host *Nicotiana attenuata*. VII. Changes in the plant's proteome. Plant Physiol **142,** 1621-1641.

Gupta, V., Willits, M.G., and Glazebrook, J. (2000). Arabidopsis thaliana EDS4 contributes to salicylic acid (SA)-dependent expression of defense responses: evidence for inhibition of jasmonic acid signaling by SA. Mol Plant Microbe Interact **13,** 503-511.

Halitschke, R., Schittko, U., Pohnert, G., Boland, W., and Baldwin, I.T. (2001). Molecular interactions between the specialist herbivore Manduca sexta (Lepidoptera, Sphingidae) and its natural host *Nicotiana attenuata*. III. Fatty acid-

amino acid conjugates in herbivore oral secretions are necessary and sufficient for herbivore-specific plant responses. Plant Physiol **125,** 711-717.

Halitschke, R., Gase, K., Hui, D.Q., Schmidt, D.D., and Baldwin, I.T. (2003). Molecular interactions between the specialist herbivore Manduca sexta (Lepidoptera, Sphingidae) and its natural host *Nicotiana attenuata*. VI. Microarray analysis reveals that most herbivore-specific transcriptional changes are mediated by fatty acid-amino acid conjugates. Plant Physiol **131,** 1894-1902.

Heiling, S., Schuman, M.C., Schoettner, M., Mukerjee, P., Berger, B., Schneider, B., Jassbi, A.R., and Baldwin, I.T. (2010). Jasmonate and ppHsystemin regulate key malonylation steps in the biosynthesis of 17-hydroxygeranyllinalool diterpene glycosides, an abundant and effective direct defense against herbivores in *Nicotiana attenuata*. Plant Cell **22,** 273-292.

Hermsmeier, D., Schittko, U., and Baldwin, I.T. (2001). Molecular interactions between the specialist herbivore *Manduca sexta* (Lepidoptera, Sphingidae) and its natural host *Nicotiana attenuata*. I. Large-scale changes in the accumulation of growth- and defense-related plant mRNAs. Plant Physiol **125,** 683-700.

Howe, G.A., and Jander, G. (2008). Plant immunity to insect herbivores. Ann Rev Plant Biol **59,** 41-66.

Jain, A.K., Duin, R.P.W., and Jianchang, M. (2000). Statistical pattern recognition: a review. Pattern analysis and machine intelligence, IEEE Transactions **22,** 4-37.

Jander, G., Norris, S.R., Joshi, V., Fraga, M., Rugg, A., Yu, S., Li, L., and Last, R.L. (2004). Application of a high-throughput HPLC-MS/MS assay to Arabidopsis mutant screening; evidence that threonine aldolase plays a role in seed nutritional quality. Plant J **39,** 465-475.

Jassbi, A.R., Gase, K., Hettenhausen, C., Schmidt, A., and Baldwin, I.T. (2008). Silencing geranylgeranyl diphosphate synthase in *Nicotiana attenuata* dramatically impairs resistance to tobacco hornworm. Plant Physiol **146,** 974-986.

Kandoth, P.K., Ranf, S., Pancholi, S.S., Jayanty, S., Walla, M.D., Miller, W., Howe, G.A., Lincoln, D.E., and Stratmann, J.W. (2007). Tomato MAPKs LeMPK1, LeMPK2, and LeMPK3 function in the systemi n-mediated defense response against herbivorous insects. Proc Natl Acad Sci USA **104,** 12205-12210.

Kang, J.H., Wang, L., Giri, A., and Baldwin, I.T. (2006). Silencing threonine deaminase and JAR4 in *Nicotiana attenuata* impairs jasmonic acid-isoleucine-mediated defenses against Manduca sexta. Plant Cell **18,** 3303-3320.

Kanzaki, H., Saitoh, H., Takahashi, Y., Berberich, T., Ito, A., Kamoun, S., and Terauchi, R. (2008). NbLRK1, a lectin-like receptor kinase protein of *Nicotiana benthamiana* , interacts with *Phytophthora infestans* INF1 elicitin and mediates INF1-induced cell death. Planta **228,** 977-987.

Kaur, H., Heinzel, N., Schöttner, M., Baldwin, I.T., and Gális, I. (2010). R2R3-NaMYB8 regulates the accumulation of phenylpropanoid-polyamine conjugates, which are essential for local and systemic defense against insect herbivores in *Nicotiana attenuata*. Plant Physiol **152,** 1731-1747.

Keinänen, M., Oldham, N.J., and Baldwin, I.T. (2001). Rapid HPLC screening of jasmonate-induced increases in tobacco alkaloids, phenolics, and diterpene glycosides in *Nicotiana attenuata*. J Agric Food Chem **49,** 3553-3558.

Kim, Y.T., Oh, J., Kim, K.H., Uhm, J.Y., and Lee, B.M. (2010). Isolation and characterization of NgRLK1, a receptor-like kinase of *Nicotiana glutinosa* that interacts with the elicitin of *Phytophthora capsici*. Mol Biol Rep **37,** 717-727.

Kistner C., and Matamoros M. (2005) RNA isolation using phase extraction and LiCl precipitation. In A Márquez, ed, Lotus japonicus Handbook. Springer Netherlands, pp 123-124.

Körner, E., Von Dahl, C., Bonaventure, G., and Baldwin, I. T. (2009). Pectin methylesterase NaPME1 contributes to the emission of methanol during insect herbivory and to the elicitation of defence responses in *Nicotiana attenuata*. J Exp Bot **60,** 2631-2640.

Krügel, T., Lim, M., Gase, K., Halitschke, R., and Baldwin, I.T. (2002). Agrobacterium-mediated transformation of *Nicotiana attenuata*, a model ecological expression system. Chemoecology **12,** 177-183.

Leon-Reyes, A., Spoel, S.H., De Lange, E.S., Abe, H., Kobayashi, M., Tsuda, S., Millenaar, F.F., Welschen, R.A.M., Ritsema, T., and Pieterse, C.M.J. (2009). Ethylene modulates the role of NONEXPRESSOR OF PATHOGENESIS-RELATED GENES1 in cross talk between salicylate and jasmonate Signaling. Plant Physiol **149,** 1797-1809.

Letunic, I., Doerks, T., and Bork, P. (2009). SMART 6: recent updates and new developments. Nucl Acids Res **37,** 229-232.

Li, J., Brader, G., and Palva, E.T. (2004). The WRKY70 transcription factor: a node of convergence for jasmonate-mediated and salicylate-mediated signals in plant defense. Plant Cell **16,** 319-331.

Mazzara, S., Cerutti, S., Iannaccone, S., Conti, A., Olivieri, S., Alessio, M., and Pattini L. (2011) Application of multivariate data analysis for the classification of two dimensional gel images in neuroproteomics. J Proteomics Bioinform **4,** 16-21.

Mitaku, S., Hirokawa, T., and Tsuji, T. (2002). Amphiphilicity index of polar amino acids as an aid in the characterization of amino acid preference at membrane-water interfaces. Bioinformatics **18,** 608-616.

Mur, L.A.J., Kenton, P., Atzorn, R., Miersch, O., and Wasternack, C. (2006). The outcomes of concentration-specific interactions between salicylate and jasmonate signaling include synergy, antagonism, and oxidative stress leading to cell death. Plant Physiol **140,** 249-262.

Musser, R.O., Hum-Musser, S.M., Eichenseer, H., Peiffer, M., Ervin, G., Murphy, J.B., and Felton, G.W. (2002). Herbivory: caterpillar saliva beats plant defences. Nature **416,** 599-600.

Niki, T., Mitsuhara, I., Seo, S., Ohtsubo, N., and Ohashi, Y. (1998). Antagonistic effect of salicylic acid and jasmonic acid on the expression of pathogenesis-related (PR) protein genes in wounded mature tobacco leaves. Plant Cell Physiol **39,** 500-507.

O'Donnell, P.J., Calvert, C., Atzorn, R., Wasternack, C., Leyser, H.M.O., and Bowles, D.J. (1996). Ethylene as a signal mediating the wound response of tomato plants. Science **274,** 1914-1917.

Paschold A., Halitschke R., and Baldwin I.T. (2007) Co(i)-ordinating defenses: NaCOI1 mediates herbivore- induced resistance in *Nicotiana attenuata* and reveals the role of herbivore movement in avoiding defenses. Plant J **51,** 79-91.

Paschold A., Bonaventure G., Kant M., and Baldwin I. T. (2008) Jasmonate perception regulates jasmonate biosynthesis and JA-Ile metabolism: the case of COI1 in *Nicotiana attenuata*. Plant Cell Physiol **49,** 1165-1175.

Qiu, Y., Cai, G., Su, M., Chen, T., Zheng, X., Xu, Y., Ni, Y., Zhao, A., Xu, L.X., Cai, S., and Jia, W. (2009). Serum metabolite profiling of human colorectal cancer using GC−TOFMS and UPLC−QTOFMS. J Prot Res **8,** 4844-4850.

Ratcliff F., Martin-Hernandez A.M., and Baulcombe D.C. (2001). Technical Advance. Tobacco rattle virus as a vector for analysis of gene function by silencing. Plant J **25,** 237-245.

Rayapuram, C., and Baldwin, I.T. (2007). Increased SA in NPR1-silenced plants antagonizes JA and JA-dependent direct and indirect defenses in herbivore-attacked *Nicotiana attenuata* in nature. Plant J **52,** 700-715.

Reymond, P., and Farmer, E.E. (1998). Jasmonate and salicylate as global signals for defense gene expression. Curr Opin Plant Biol **1,** 404-411.

Ryan, C.A., Farmer, E.E., McGurl, B., Pearce, G., and Johnson, S. (1993). Oligouronides, systemin and jasmonates as signals for plant defensive genes. J Cell Biochem**,** 13-13.

Saedler, R., and Baldwin, I.T. (2004). Virus-induced gene silencing of jasmonate-induced direct defences, nicotine and trypsin protease-inhibitors in *Nicotiana attenuata*. J Exp Bot **55,** 151-157.

Schafer, M., Fischer, C., Meldau, S., Seebald, E., Oelmuller, R., and Baldwin, I.T. (2011). Lipase activity in insect oral secretions mediates defense responses in Arabidopsis thaliana. Plant Physiol PMID: 21546453

Schmelz, E.A., Engelberth, J., Alborn, H.T., Tumlinson, J.H., and Teal, P.E.A. (2009). Phytohormone-based activity mapping of insect herbivore-produced elicitors. Proc Natl Acad Sci USA **106,** 653-657.

Schmelz, E.A., Carroll, M.J., LeClere, S., Phipps, S.M., Meredith, J., Chourey, P.S., Alborn, H.T., and Teal, P.E. (2006). Fragments of ATP synthase mediate plant perception of insect attack. Proc Natl Acad Sci USA **103,** 8894-8899.

Seo, S., Sano, H., and Ohashi, Y. (1999). Jasmonate-based wound signal transduction requires activation of WIPK, a tobacco mitogen-activated protein kinase. Plant Cell **11,** 289-298.

Seo, S., Katou, S., Seto, H., Gomi, K., and Ohashi, Y. (2007). The mitogen-activated protein kinases WIPK and SIPK regulate the levels of jasmonic and salicylic acids in wounded tobacco plants. Plant J **49,** 899-909.

Spiteller, D., and Boland, W. (2003). N-(15,16-Dihydroxylinoleoyl)-glutamine and N-(15,16-epoxylinoleoyl)-glutamine isolated from oral secretions of lepidopteran larvae. Tetrahedron **59,** 135-139.

Staswick, P., and Tiryaki, I. (2004). The oxylipin signal jasmonic acid is activated by an enzyme that conjugates it to Isoleucine in Arabidopsis. Plant Cell **16,** 2117-2127.

Steppuhn, A., Gase, K., Krock, B., Halitschke, R., and Baldwin, I.T. (2004). Nicotine's defensive function in nature. PLoS Biol **2,** e217.

Stotz, H., Koch, T., Biedermann, A., Weniger, K., Boland, W., and Mitchell-Olds, T. (2002). Evidence for regulation of resistance in Arabidopsis to Egyptian cotton worm by salicylic and jasmonic acid signaling pathways. Planta **214,** 648-652.

Takayama, S., and Isogai, A. (2005). Self-incompatibility in plants. Ann Rev Plant Biol **56,** 467-489.

Tautenhahn, R., Bottcher, C., and Neumann, S. (2008). Highly sensitive feature detection for high resolution LC/MS. BMC Bioinformatics **9,** 504.

Tumlinson, J., and Lait, C. (2005). Biosynthesis of fatty acid amide elicitors of plant volatiles by insect herbivores. Arch Insect Biochem Physiol **58,** 54-68.

Tusher V.G., Tibshirani R., and Chu G. (2001) Significance analysis of microarrays applied to the ionizing radiation response. Proc Natl Acad Sci U S A **98,** 5116-5121.

Van Dam, N.M., Horn, M., Mareš, M., and Baldwin, I.T. (2001). Ontogeny constrains systemic protease inhibitor response in *Nicotiana attenuata*. J Chem Ecol **27,** 547-568.

VanDoorn, A., Kallenbach, M., Borquez, A.A., Baldwin, I.T., and Bonaventure, G. (2010). Rapid modification of the insect elicitor N-linolenoyl-glutamate via a lipoxygenase-mediated mechanism on *Nicotiana attenuata* leaves. BMC Plant Biol **10,** 164.

VanDoorn A., Bonaventure G., Schmidt D.D., Baldwin I.T. (2011) Regulation of jasmonate metabolism and activation of systemic signaling in *Solanum nigrum*: COI1 and JAR4 play overlapping yet distinct roles. New Phytol **190,** 640-652.

Viles, F.J., and Silverman, L. (1949) Determination of starch and cellulose with anthrone. Anal Chem **21,** 950-953.

Wang, L., Halitschke, R., Kang, J.H., Berg, A., Harnisch, F., and Baldwin, I.T. (2007). Independently silencing two JAR family members impairs levels of trypsin protease inhibitors but not nicotine. Planta **226,** 159-167.

Westerhuis, J., Hoefsloot, H., Smit, S., Vis, D., Smilde, A., van Velzen, E., van Duijnhoven, J., and van Dorsten, F. (2008). Assessment of PLSDA cross validation. Metabolomics **4,** 81-89.

Wu, J., Hettenhausen, C., Meldau, S., and Baldwin, I.T. (2007). Herbivory rapidly activates MAPK signaling in attacked and unattacked leaf regions but not between leaves of *Nicotiana attenuata*. Plant Cell **19,** 1096-1122.

Wu, J., and Baldwin, I.T. (2009). Herbivory-induced signalling in plants: perception and action. Plant Cell Environ **32,** 1161-1174.

Xia, J., Psychogios, N., Young, N., and Wishart, D.S. (2009). MetaboAnalyst: a web server for metabolomic data analysis and interpretation. Nucl Acids Res **37,** 652-660.

Xia, J., and Wishart, D.S. (2011). Web-based inference of biological patterns, functions and pathways from metabolomic data using MetaboAnalyst. Nat Protocols **6,** 743-760.

Xie, G., Ni, Y., Su, M., Zhang, Y., Zhao, A., Gao, X., Liu, Z., Xiao, P., and Jia, W. (2008). Application of ultra-performance LC-TOF MS metabolite profiling techniques to the analysis of medicinal Panax herbs. Metabolomics **4,** 248-260.

Yoshinaga, N., Alborn, H., Nakanishi, T., Suckling, D., Nishida, R., Tumlinson, J., and Mori, N. (2010). Fatty acid-amino acid conjugates diversification in lepidopteran caterpillars. J Chem Ecol **36,** 319-325.

Zarate, S.I., Kempema, L.A., and Walling, L.L. (2007) Silverleaf whitefly induces salicylic acid defenses and suppresses effectual jasmonic acid defenses. Plant Physiol **143,** 866-875.

Zavala, J.A., Patankar, A.G., Gase, K., Hui, D.Q., and Baldwin, I.T. (2004). Manipulation of endogenous trypsin protease inhibitor production in *Nicotiana attenuata* demonstrates their function as antiherbivore defenses. Plant Physiol **134,** 1181-1190.

Chapter 5:

C_{12} derivatives of the hydroperoxide lyase pathway are produced by product recycling through lipoxygenase-2 in *Nicotiana attenuata* leaves.

Manuscript 3

New Phytologist

Research

C_{12} derivatives of the hydroperoxide lyase pathway are produced by product recycling through lipoxygenase-2 in *Nicotiana attenuata* leaves

Mario Kallenbach, Paola A. Gilardoni, Silke Allmann, Ian T. Baldwin and Gustavo Bonaventure

Department of Molecular Ecology, Max Planck Institute of Chemical Ecology, Hans Knöll Str. 8, D-07745 Jena, Germany

Author for correspondence:
Gustavo Bonaventure
Tel: +49 3641 571118
Email: gbonaventure@ice.mpg.de

Received: *7 March 2011*
Accepted: *13 April 2011*

New Phytologist (2011)
doi: 10.1111/j.1469-8137.2011.03767.x

Key words: herbivory, hydroperoxide lyase (HPL), lipoxygenase (LOX), oxylipin, tobacco (*Nicotiana attenuata*), traumatic acid, traumatin.

Summary

- In response to diverse stresses, the hydroperoxide lyase (HPL) pathway produces C_6 aldehydes and 12-oxo-(9*Z*)-dodecenoic acid ((9*Z*)-traumatin). Since the original characterization of (10*E*)-traumatin and traumatic acid, little has been added to our knowledge of the metabolism and fluxes associated with the conversion of (9*Z*)-traumatin into diverse products in response to wounding and herbivory.
- A liquid chromatography–mass spectrometry/mass spectrometry (LC-MS/MS) method was developed to quantify C_{12} derivatives of the HPL pathway and to determine their metabolism after wounding and simulated herbivory in *Nicotiana attenuata* leaves.
- Ninety-eight per cent of the (9*Z*)-traumatin produced was converted to 9-hydroxy-(10*E*)-traumatin (9-OH-traumatin); two-thirds by product recycling through lipoxygenase-2 (NaLOX2) activity and one-third by nonenzymatic oxidation. Thirty-eight per cent of the *de novo* produced 9-OH-traumatin was conjugated to glutathione, consistent with this oxylipin being a reactive electrophile species. 12-OH-(9*Z*)-dodecenoic and dodecenedioic acids also showed rapid increases after wounding and simulated herbivory and a role for C_{12} derivatives as signals in these processes was consistent with their ability to elicit substantial changes in gene expression.
- These results underscore the importance of metabolite reflux through LOX2, an insight which creates new opportunities for a functional understanding of C_{12} derivatives of the HPL pathway in the regulation of stress responses.

Abbreviations: (10*E*)-traumatin, 12-oxo-(10*E*)-dodecenoic acid; (9*Z*)-traumatin, 12-oxo-(9*Z*)-dodecenoic acid; 13S-HPODE, 13S-hydroperoxy-(9*Z*,11*E*)-octadecadienoic acid; 13S-HPOTE, 13S-hydroperoxy-(9*Z*,11*E*)-octadecatrienoic acid; 4-OH-traumatic acid, 4-hydroxy-(2*E*)-dodecenedioic acid; 9,12-hydroxy-(10*E*)-dodecenoic acid, 9,12-OH-(10*E*)-dodecenoic acid; 9,12-OH-(10*E*)-dodecanoic acid, 9,12-hydroxy-(10*E*)-dodecanoic acid; 9-OH-traumatin, 9-hydroxy-12-oxo-(10*E*)-dodecenoic acid; traumatic acid, (2*E*)-dodecenedioic acid.

Introduction

In plants, the production of oxylipins from polyunsaturated fatty acids (PUFAs) is immediately induced in response to diverse stresses including wounding, and insect and pathogen attacks (Turner *et al.*, 2002; Farmer *et al.*, 2003; Mueller, 2004; Taki *et al.*, 2005; Matsui, 2006; Browse, 2009; Mosblech *et al.*, 2009). Oxylipins are diverse in structure and they play essential roles as signaling molecules during the plant's responses to these environmental stresses. For example, jasmonic acid is essential for the induction of defense responses against pathogens and insect herbivores (Farmer *et al.*, 2003; Kessler *et al.*, 2004; Browse, 2005), C_6 aldehydes are important signals acting during pathogenesis and plant–insect communication (Croft *et al.*, 1993; Matsui, 2006; Baldwin, 2010), C_{12} diacids and ω-oxo-acids were originally described as wound-associated hormones (Bonner & English, 1937; Zimmerman & Coudron, 1979), divinyl ethers inhibit mycelial growth and spore germination of some oomycete species (Prost *et al.*,

2005) and phytoprostanes play diverse roles in biotic stress responses (Loeffler *et al.*, 2005).

13-lipoxygenases (13-LOXs) initiate the enzymatic biosynthesis of oxylipins by di-oxygenating PUFAs such as linoleic ($18{:}2^{\Delta 9,12}$; 18:2) and α-linolenic ($18{:}3^{\Delta 9,12,15}$; 18:3) acids to generate 13*S*-hydroperoxy dienoic (13S-HPODE) and trienoic (13S-HPOTE) acids, respectively. Hydroperoxide lyase (HPL) cleaves 13S-HPODE and -HPOTE to generate the green leaf volatiles (GLVs) hexanal and (3*Z*)-hexenal, respectively, and 12-oxo-(9*Z*)-dodecenoic acid ((9*Z*)-traumatin; compound 1a in Fig. 1) (Vick & Zimmerman, 1976). In *Nicotiana attenuata* leaves, the supply of 13S-HPODE and 13S-HPOTE for the biosynthesis of hexanal and (3*Z*)-hexenal requires the activity of the lipoxygenase-2 gene (*NaLOX2*); plants with reduced expression of this gene have a greatly reduced production of GLVs (Allmann *et al.*, 2010). *Nicotiana attenuata* plants with reduced expression of *NaHPL* have similarly reduced production of GLVs (Halitschke *et al.*, 2004 and this study).

Hexanal, (3*Z*)-hexenal and (9*Z*)-traumatin undergo rapid modifications by diverse enzymatic and nonenzymatic reactions, generating multiple potential chemical signals. These modifications involve, among others, the isomerization of double bonds (*Z* to *E*), the oxidation of the aldehyde groups to carboxyl groups, their reduction to alcohols and their esterification (Grechkin, 2002). These modifications change the physicochemical properties of the molecules, and in some cases their importance in biological processes has been demonstrated (Zimmerman & Coudron, 1979; Ivanova *et al.*, 2001; Allmann & Baldwin, 2010). In the case of (9*Z*)-traumatin, the *Z* double bond isomerizes to *E* to form 12-oxo-(10*E*)-dodecenoic acid ((10*E*)-traumatin; compound 1b in Fig. 1), and the aldehyde group can auto-oxidize to form (3*Z*)- or (2*E*)-dodecenedioic acid ((3*Z*)- or (2*E*)-traumatic acid; compounds 2a and 2b in Fig. 1) (Zimmerman & Coudron, 1979) or be reduced to form (9*Z*)- or (10*E*)-12-hydroxy-dodecenoic acid (12-OH-dodecenoic acid; compounds 3a and 3b in Fig. 1) (Grechkin, 2002). (9*Z*)-traumatin can be oxidized to 9-hydroxy-12-oxo-(10*E*)-dodecenoic acid (9-OH-traumatin; compound 4 in Fig. 1) either enzymatically by a LOX-mediated mechanism (Gardner, 1998) or nonenzymatically (Noordermeer *et al.*, 2000). A recent study showed that 9-OH-traumatin can be subsequently converted into 4-hydroxy-(2*E*)-dodecenedioic acid (4-OH-traumatic acid; compound 5 in Fig. 1), 9,12-hydroxy-(10*E*)-dodecenoic acid (9,12-OH-(10*E*)-dodecenoic acid; compound 6 in Fig. 1) and 9,12-hydroxy-(10*E*)-dodecanoic acid (9,12-OH-(10*E*)-dodecanoic acid; compound 7 in Fig. 1) in pea (*Pisum sativum*) seedlings (Mukhtarova *et al.*, 2011). 9-OH-traumatin belongs to a class of oxylipins defined as oxylipin-reactive electrophile species (RES) based on their chemical reactivity, which in turn results from an α-β unsaturated carbonyl group (Gardner, 1998; Farmer & Davoine, 2007; Mueller & Berger, 2009) (Fig. 1). Moreover, the presence of the hydroxyl group at C-4 of the α-β unsaturated carbonyl group increases the reactivity of C-3 to nucleophiles such as thiols and amines (Esterbauer *et al.*, 1976; Uchida, 2003).

In the case of C_{12} derivatives of the HPL pathway, early experiments have shown that (10*E*)-traumatin and (2*E*)-traumatic acid have growth-stimulating and wound-healing activities in plants (Bonner & English, 1937, 1938; English & Bonner, 1937; Zimmerman & Coudron, 1979) and, more recently, 12-OH-(9*Z*)-dodecenoic acid has been shown to act as a potent stimulator of the mitotic cycle (Ivanova *et al.*, 2001). In recent years, research has been focused primarily on the biochemical and functional characterization of GLVs during herbivore and pathogen attacks, and less attention has been paid to the metabolism and signal capacities of the C_{12} derivatives of the HPL pathway. As a result, the metabolic fluxes and fates of these molecules under these stress conditions are largely unknown in plants. These shortcomings hamper the development of new hypotheses concerning the potential roles of these molecules as signals. Hence, in this study we present a detailed analysis of the fluxes and metabolism of C_{12} derivatives of the HPL pathway in *N. attenuata* plants induced by wounding and simulated herbivory. Part of this analysis is based on a new liquid chromatography–mass spectrometry/mass spectrometry (LC-MS/MS) method developed for the quantification of these metabolites. We reveal new aspects of the biogenesis of C_{12} derivatives of the HPL pathway and open new perspectives for possible roles of these metabolites in the regulation of stress responses.

Materials and Methods

Plant growth and treatments

Seeds of *Nicotiana attenuata* Torr. ex S. Watson wild-type (WT), ir-lox2 (line 52-2) (Allmann *et al.*, 2010), ir-lox2/ir-lox3 (Kallenbach *et al.*, 2010) and ir-hpl (line 428-8; Supporting Information Methods S1) plants were germinated on agar plates containing Gamborg's B5 medium as previously described (Krügel *et al.*, 2002). Plates were maintained in a growth chamber (Snijders Scientific, Tilburg, the Netherlands) at 26°C : 16 h (155 μmol s^{-1} m^{-2} light), 24°C : 8 h dark for 10 d. Ten-day-old seedlings were transferred to TEKU pots (Pöppelmann GmbH & Co. KG, Lohne, Germany) with Klasmann plug soil (Klasmann-Deilmann GmbH, Geesten, Germany). After 10 d, seedlings were transferred to soil in 1-l pots and grown in the glasshouse under high-pressure sodium lamps (200–300 μmol s^{-1} m^{-2}) with a day : night ratio of 16 h (26–28°C) : 8 h (22–24°C) and 45–55% humidity.

Leaf wounding was performed by rolling a fabric pattern wheel three times on each side of the midvein of the leaves

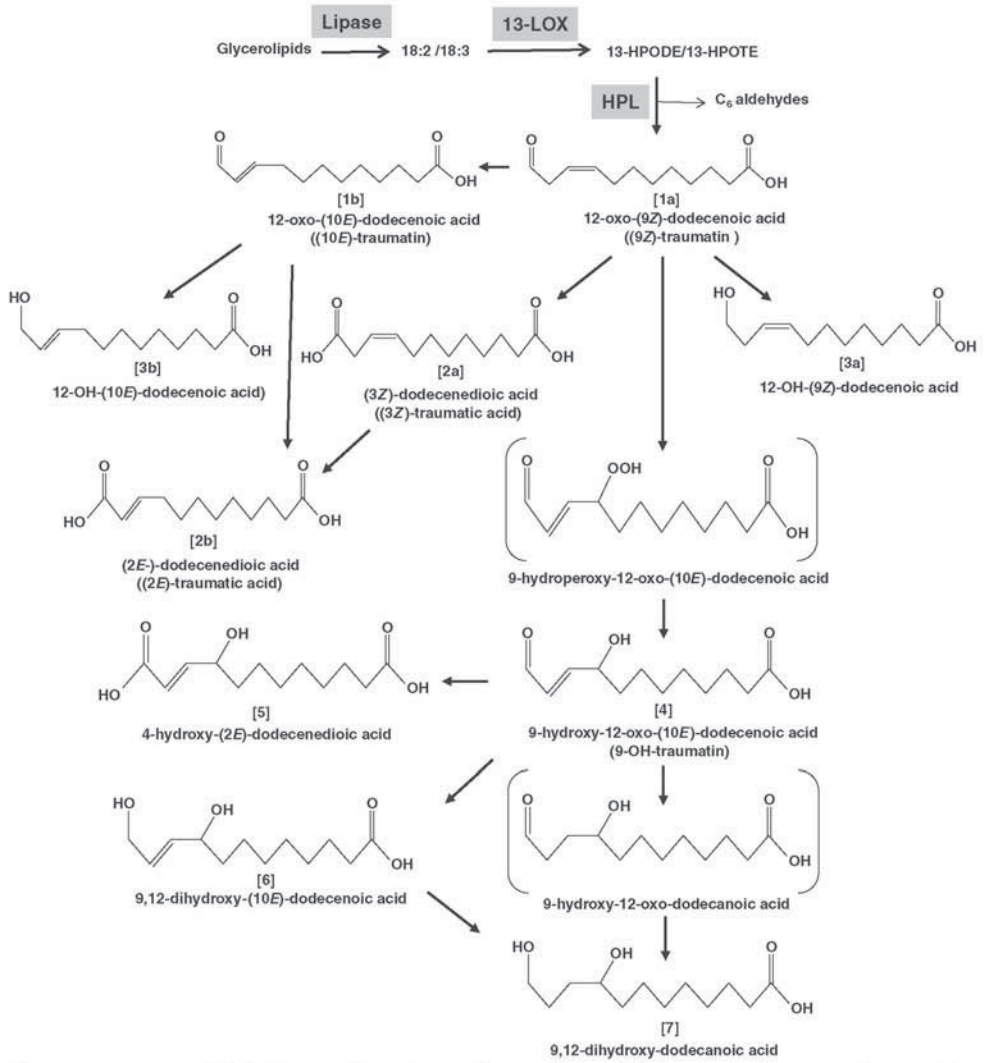

Fig. 1 Schematic representation of the hydroperoxide lyase (HPL) pathway in plants and the generation of derivatives of 12-oxo-(9*Z*)-dodecenoic acid ((9*Z*)-traumatin). In leaves, 18:2 and 18:3 fatty acids are released from membranes and dioxygenated by 13-lipoxygenases (13-LOXs) to generate 13*S*-hydroperoxides (13-HPODE and 13-HPOTE, respectively). These molecules are substrates of HPL and are cleaved to produce C_6 aldehydes and (9*Z*)-traumatin (compound 1a). This molecule can undergo several enzymatic and nonenzymatic modifications to be converted into the products (10*E*)-traumatin (compound 1b), (3*Z*)-traumatic acid (compound 2a), (2*E*)-traumatic acid (compound 2b), 12-OH-(9*Z*)-dodecenoic acid (compound 3a), 12-OH-(10*E*)-dodecenoic acid (compound 3b) and 9-OH-traumatin (compound 4). The latter compound can be converted into 4-OH-traumatic acid (compound 6), 9,12-OH-(10*E*)-dodecenoic acid (compound 5) and 9,12-OH-(10*E*)-dodecanoic acid (compound 4) according to Mukhtarova *et al.* (2011). The formation of 9-OH-traumatin by LOX-mediated activity has been proposed by Gardner (1998), whereas its nonenzymatic formation has been proposed by Noordermeer *et al.* (2000).

of 40-d-old rosette-stage plants, and the wounds were immediately supplemented with water. For fatty acid–amino acid conjugate (FAC) elicitation, the wounds were immediately supplemented with 20 µl of synthetic *N*-linolenoyl-glutamic acid (18:3-Glu; 0.03 nmol μl^{-1}). Leaf tissue was collected at different times after the treatments and was frozen immediately in liquid nitrogen (N) for subsequent analysis. For C_{12} treatments, leaves from ir-lox2/ir-lox3 plants were wounded as described above and a 1 : 1 mixture of (9Z)-traumatin:9-OH-traumatin (1 µg each per leaf dissolved in 0.02% aqueous Tween-20) or solvent (control treatment) was immediately applied to the wounds.

Purchased chemicals and synthesis of C_{12} derivatives of the HPL pathway

(9*Z*)-traumatin and (10*E*)-traumatin were purchased from Larodan (Malmö, Sweden); (2*E*)-traumatic acid was purchased from Sigma (Taufkirchen, Germany). 12-OH-(9*Z*)-dodecenoic acid and 12-OH-(10*E*)-dodecenoic acid were synthesized by reduction of 25 μg of (9*Z*)-traumatin or (10*E*)-traumatin, respectively, with excess $NaBH_4$ in 1 ml of ethanol for 4 h at 0°C. After acidification with HCl to pH 4, the products were purified by reverse solid-phase extraction (SPE) on a C18 column (Vac C18 3cc; Waters, Eschborn, Germany) by washing with water and eluting with methanol. 9-OH-traumatin was generated *in vitro* by two different methods: nonenzymatic oxidation (Noordermeer *et al.*, 2000); and processing of *N. attenuata* leaf extracts using the protocol described in the section '*In vitro* assays with leaf extracts'. 9-OH-traumatin was fractionated by reverse-phase HPLC on a Gemini-NX® column (C18; 3 μm, 150 × 2 mm; Phenomenex, Aschaffenburg, Germany) using methanol and water as running solvents in a gradient mode in a Dionex UPLC system (Dionex, Germering, Germany) equipped with a fraction collector (WPS3000-FC; Dionex). The structures of the synthetic 12-OH-dodecenoic acids and 9-OH-traumatin were confirmed by gas chromatography–mass spectrometry (GC-MS) analysis: the carboxyl group of 12-OH-dodecenoic acids was transmethylated with diazomethane and the terminal hydroxyl group was silylated (trimethylsilyloxy ether (OTMSi)) by N-methy-N-(trimethylsilyl) trifluoroacetamide (MSTFA) (Machery-Nagel, Düren, Germany); the aldehyde group in 9-OH-traumatin was reduced with excess $NaBH_4$, the carboxyl group transmethylated with diazomethane and the hydroxyl groups finally silylated (OTMSi) with MSTFA. GC-MS analyses were performed on a Varian CP-4000 GC coupled to a Varian Saturn 4000 ion trap MS in electron ionization (EI; 70 eV) mode (Varian, Palo Alto, CA, USA). One microliter of the sample was injected using a 1 to 10 split ratio on a DB-5 column (30 m × 0.25 mm i.d.; 0.25-μm film thickness; Agilent, Boeblingen, Germany) with helium at a constant flow of 1 ml min^{-1} as the carrier gas. The injector was at 260°C. The oven temperature program was: 140°C for 2 min, 180°C at 6.0°C min^{-1}, 20°C min^{-1} ramp to 240°C and hold for 1 min. Electron impact (EI) spectra were recorded in scan mode from 40 to 400 *m/z*.

The glutathione (GSH) adduct of 9-OH-traumatin was synthesized by mixing 10 μg of HPLC-purified 9-OH-traumatin with 13 μg of GSH in 1 ml of buffer (10 mM MOPS and 0.02% (v/v) Tween-20; pH 7.0) for 4 h at room temperature. The solution was reduced to *c.* 50 μl in an Eppendorf SpeedVac® (Eppendorf, Wesseling-Berzdorf, Germany) connected to a high-vacuum membrane pump (Varian SH100; Varian). Then 200 μl of methanol was added to the sample and the 9-OH-traumatin–GSH conjugate was purified by reverse-phase HPLC using a Dionex UPLC system as described for the purification of 9-OH-traumatin.

Analysis of synthetic standards, and detection and isomeric separation of C_{12} derivatives of the HPL pathway in leaves

Optimization of the multiple reaction monitoring (MRM) parameters for LC-(electrospray ionization (ESI))-MS/MS analysis was carried out by direct injection of single analytes (1 ng μl^{-1} in 70% (v/v) methanol/water) into the ESI–MS interface. Ionization was performed in the negative mode and the first quadrupole was set on their corresponding $[M\text{-}H]^-$ masses (Table S1). The third mass analyzer was set in the scan mode, ranging from 50 to 350 *m/z*. The MS/MS fragmentation patterns of the analytes were obtained by collision-induced dissociation (CID) with argon gas in the second quadrupole with increasing collision energies. The parent > daughter (*m/z*) ion transitions that gave the highest intensities were used to optimize the separation and detection of the analytes, and the final parameters used are listed in Table S1.

For the chromatographic separation of the C_{12} analytes and their *Z*/*E* isomers, 10 μl of standard solutions (1 ng μl^{-1}) was injected onto a Gemini-NX® column (C18; 3 μm, 50 × 2 mm; Phenomenex) connected to a pre-column (Gemini-NX; C18, 4 × 2 mm; Phenomenex). As mobile phases, 0.05% : 1% (v/v/v) formic acid : acetonitrile : water (solvent A) and methanol (solvent B) were used. The solvent gradient of the mobile phases was 5% of B for 2 min (prerun), followed by a linear gradient to 45% of B to 6 min, 45% of solvent B to 22 min, a linear gradient to 98% of solvent B to 24 min, 98% of B to 27 min, a linear gradient to 5% of B to 28 min, and 5% of solvent B to 32 min. The total flow rates were 0.4 ml min^{-1} for 0.5 min, 0.2 ml min^{-1} from 0.5 to 26 min and 0.4 ml min^{-1} to 32 min.

Extraction and quantification of C_{12} derivatives of the HPL pathway in leaf extracts

For extraction, 0.3 g of frozen leaf material was homogenized in 2-ml tubes containing two steel beads (ASK, Korntal-Muenchingen, Germany) by shaking the tubes in a Genogrinder (SPEX Certi Prep, Metuchen, NJ, USA) for 30 s at 1300 strokes min^{-1}. One milliliter 2 : 1 (v/v) methanol : chloroform spiked with 200 ng of 10-hydroxy-(2*E*)-decenoic acid (internal standard (IS)) and containing 1% (w/v) butylhydroxytoluene (BHT) as a radical scavenger was added and the samples were vortexed for 10 min. After centrifugation for 10 min at 4°C (16 100 *g*), the organic phase was collected and the residual plant material was re-extracted with 0.5 ml of 2 : 1 (v/v) methanol : chloroform. The organic phases were combined and the solvent

New Phytologist

was evaporated under reduced pressure avoiding complete dryness. The samples were reconstituted in 0.2 ml of 70% (v/v) methanol : water for analysis.

Analysis was performed on an LC-(ESI)-MS/MS system (Varian 1200 Triple-Quadrupole-LC-MS system; Varian). Ten microliters of the sample was injected onto a ProntoSIL® column (C18; 5 μm, 50 × 2 mm; Bischoff, Leonberg, Germany) connected to a precolumn (C18; 4 × 2 mm; Phenomenex). As mobile phases, 0.05% : 1% (v/v/v) formic acid : acetonitrile : water (solvent A) and methanol (solvent B) were used in a gradient mode with the following conditions: time : concentration (min:%) for B: 0.0 : 5; 1.0 : 5; 8.0 : 98; 16.0 : 98; 17.0 : 5; 20.0 : 5; time : flow (min:ml min^{-1}): 0.0 : 0.4; 0.5 : 0.2; 15.5 : 0.2; 16.0 : 0.4; 20.0 : 0.4. Compounds were detected in the ESI negative mode and MRM (Table S2).

The response curves of the synthetic or purified C_{12} analytes vs the IS (10-hydroxy-(2*E*)-decenoic acid) were determined and used to calculate the response factors (Fig. S4). For quantification of endogenous C_{12} derivatives, the corresponding peak areas obtained in the LC chromatogram were integrated and divided by the peak area of the IS, and the values were corrected by the respective response factor. For determination of the linearity and the sensitivity of the method, the standards of all C_{12} analytes were dissolved at different concentrations in a leaf matrix derived from unelicited ir-lox2 plants. Linearity (as expressed by the correlation coefficient (r)) was calculated by the method of least squares and sensitivity was calculated by determining the limit of detection according to the calibration curve method (Fig. S2).

In vitro assays with leaf extracts

Per assay, one 50-mm^2 leaf disc was cut from rosette-stage *N. attenuata* plants with a cork borer and was gently and thoroughly crushed with a pestle in a 1.5-ml tube containing 0.2 ml of reaction buffer (10 mM MOPS and 15% (w/v) glycerol; pH 6.8). The sample was centrifuged at 4°C for 5 min at 2300 ***g*** to pull down tissue debris and the supernatant was kept on ice. The amount of protein in the extract was quantified using the Bio-Rad Protein Assay kit (Bio-Rad, München, Germany) and BSA as a standard. One microgram of either (9*Z*)-traumatin or (10*E*)-traumatin (dissolved in 10 μl of 0.02% (v/v) Tween-20 : water) was added to 200 μl of reaction buffer containing 100 μg of total protein and the reaction was carried out at room temperature for different times. The reaction was stopped by the addition of 1 ml of 2 : 1 (v/v) chloroform : methanol containing 1 μg of 10-hydroxy-(2*E*)-decenoic acid (IS) and 1% (w/v) BHT. After centrifugation (1 min at 16 100 ***g***), the supernatant was collected and concentrated under a stream of N, avoiding complete dryness, and the samples were reconstituted in 1 ml of 70% (v/v) methanol : water for LC-MS/MS analysis as described previously in the section 'Extraction and quantification of C_{12} derivatives of the HPL pathway in leaf extracts'.

For LOX activity inhibition, a final concentration of 10 mM 3,4-dihydroxy-phenylethanol (DHPE; Sigma) was used in the reaction. Leaf extracts were heat-inactivated by incubation at 95°C for 5 min.

Analysis of surface-deposited C_{12} derivatives of the HPL pathway

Unelicited and elicited leaves from rosette-stage *N. attenuata* plants were cut at the base of the petiole, weighed, and washed for 1 min in 8 ml of methanol. Then 500 ng of 10-hydroxy-(2*E*)-decenoic acid (IS) and 1% (w/v) BHT were added to the 8-ml wash. The remaining leaf material was extracted with 2 : 1 (v/v) methanol : chloroform containing 500 ng of 10-hydroxy-(2*E*)-decenoic acid (IS) and 1% (w/v) BHT. The solvent was evaporated under a stream of N, avoiding complete dryness, and both leaf wash and leaf samples were reconstituted in 0.5 ml of 70% (v/v) methanol : water for analysis by LC-MS/MS as described above in Extraction and quantification of C_{12} derivatives of the HPL pathway in leaf extracts.

Microarray analysis

Total RNA was extracted based on the method of Kistner & Matamoros (2005) and its quality checked by spectrophotometry (NanoDrop, Wilmington, DE, USA). Genomic DNA was removed by DNAse treatment following commercial instructions (Turbo DNase; Ambion), RNA was cleaned up using RNeasy MinElute columns (Qiagen, Hilden, Germany) and the RNA quality was checked with the RNA 6000 Nano kit (Agilent, Santa Clara, CA, USA) using an Agilent 2100 Bioanalyzer. Total RNA was used to generate labeled cRNA with the Quick Amp labeling kit (Agilent) and the yield was determined spectrophotometrically (NanoDrop). Labeled cRNA was hybridized using the Gene Expression Hybridization kit (Agilent) onto 44 K custom-designed 60-mer *N. attenuata* Agilent microarrays (sequences available upon request) containing 43 533 sequences. Microarrays were hybridized overnight at 65°C and slides were washed with the Gene Expression Wash Buffer kit (Agilent) as outlined in the One-Color Microarray-Based Gene Expression Analysis manual (Agilent). Three biological replicates were used per treatment with a total of six arrays. Arrays were scanned with an Agilent G2565BA scanner and image data were acquired with the Agilent SCAN CONTROL software (version A.7.0.1 for the B scanner). Data were extracted using the Agilent FEATURE EXTRACTION software (version 9.5) and analyzed with the SIGNIFICANCE ANALYSIS OF MICROARRAYS (SAM) software (Tusher *et al.*, 2001). The *q*-values for each gene corresponded to a computed false discovery rate (FDR) of

3.3%. Significant changes in gene expression were considered when the $\log_2$(fold change; treatment vs control) was > 1 or < −1 and q-values < 0.035 (according to the FDR value calculated by SAM).

Statistical analysis

Statistics were calculated using the SPSS software version 17.0 (SPSS, Chicago, IL, USA).

Results

Development of a method for the analysis of C_{12} derivatives of the HPL pathway by LC-MS/MS

The standards (9*Z*)-traumatin, (10*E*)-traumatin, 12-hydroxy-(9*Z*)-dodecenoic acid, 12-hydroxy-(10*E*)-dodecenoic acid, 9-OH-traumatin, (2*E*)-traumatic acid, (3*Z*)-traumatic acid and 10-hydroxy-(2*E*)-decenoic acid (used as internal standard) were either purchased or synthesized (see the Materials and Methods section). These standards were first directly injected into the ESI–MS interface to determine their $[M\text{-}H]^-$ parent ion and their parent > daughter (m/z) ion transitions by collision-induced dissociation (CID) using increasing voltage energies. The parent > daughter (m/z) ion transitions giving the strongest intensity at fixed collision energies were selected (Tables S1,S2) for MRM during the chromatographic separation of the standards by LC. This separation was performed by reverse-phase LC and the method was first established for the separation of the *E* and *Z* stereoisomers of the standards (Fig. 2a).

Next, to determine the C_{12} derivatives of the HPL pathway that accumulated endogenously in leaves of *N. attenuata* plants, the method was applied to the analysis of leaf extracts from unelicited and wounded WT plants. (9*Z*)-traumatin, 9-OH-traumatin, (2*E*)-traumatic acid, (3*Z*)-traumatic acid, and 12-OH-(9*Z*)-dodecenoic acid were detected while (10*E*)-traumatin, 12-OH-(10*E*)-dodecenoic acid, 4-OH-traumatic acid, 9,12-OH-(10*E*)-dodecenoic acid and 9,12-OH-(10*E*)-dodecanoic acid were either absent or below the limit of detection (LoD; Table S2).

Based on these results, a shorter method that did not discriminate between the dodecenedioic acid isomers ((2*E*)- and (3*Z*)-traumatic acids) was developed for the quantification of C_{12} derivatives in a large number of samples. When this method was used, all C_{12} analytes eluted from the column within 13 min (Fig. 2b). The C_{12} analytes presented a linear response, with an r value of 0.99 and LoD values of *c.* 1 ng in the column (Fig. S2). The extraction method was validated by performing 10 biological replicates of *N. attenuata* unelicited and wounded leaves after 60 min of the treatment. For each replicate, 0.3 g of leaf tissue was extracted and analyzed by LC-MS/MS. The standard deviations of the calculated amounts were below 10% of the average values for all detectable compounds. To determine the extraction recovery rate, the residual leaf material obtained after the extraction protocol was re-extracted and analyzed for the presence of C_{12} derivatives. The recovery rates were > 98% for all the molecules tested.

To corroborate the endogenous production of 9-OH-traumatin, leaf extracts from *N. attenuata* plants were supplied with (9*Z*)-traumatin and the products of the reaction were analyzed by GC-MS. Fig. 2(c) shows a chromatogram and the MS spectrum corresponding to 9-OH-traumatin. Formation of 11-OH-traumatin could not be detected in leaf extracts; however, it was detected when (9*Z*)-traumatin was subjected to auto-oxidation *in vitro* (Fig. S1), as previously described (Noordermeer *et al.*, 2000).

9-OH-traumatin is the most abundant C_{12} derivative accumulating after wounding and FAC elicitation in *N. attenuata* leaves

The endogenous accumulation of C_{12} molecules was first quantified in leaves of WT *N. attenuata* after wounding and simulated herbivory. For the latter treatment, wounds were supplemented with the fatty acid–amino acid conjugate (FAC) *N*-linoleyl-glutamic acid (18:3-Glu), a major elicitor of herbivore responses in this plant species (Halitschke *et al.*, 2001). The accumulation of C_{12} molecules was quantified in both treated (local) and distal (systemic) leaves.

In unelicited leaf tissue of early rosette-stage *N. attenuata* plants (40 d old), 9-OH traumatin accumulated to *c.* 2 nmol g^{-1} FW while (9*Z*)-traumatin, 12-OH-(9*Z*)-dodecenoic acid and dodecenedioic acids accumulated to < 0.1 nmol g^{-1} FW (Fig. 3). Fifteen minutes after wounding and FAC elicitation, 9-OH-traumatin concentrations increased on average to 8 and 10 nmol g^{-1} FW, respectively, and then decreased to reach on average 3 nmol g^{-1} FW after 8 h (Fig. 3). The concentrations of dodecenedioic acids and 12-OH-(9*Z*)-dodecenoic acid also increased several-fold rapidly after wounding and FAC elicitation; however, the absolute amounts remained below 0.25 nmol g^{-1} FW (Fig. 3). Analysis of earlier time-points (within 5 min) failed to show a rapid burst of (9*Z*)-traumatin after induction by wounding and FAC elicitation (data not shown), suggesting that this HPL product is rapidly utilized after production. In systemic leaves, no significant changes in the concentrations of these molecules were detected (data not shown).

NaLOX2 and NaHPL supply the substrates for the biosynthesis of (9Z)-traumatin

To validate the analysis of the C_{12} derivatives of the HPL pathway in *N. attenuata* leaves, ir-lox2 plants with reduced expression of *NaLOX2* (Allmann *et al.*, 2010) and ir-hpl plants with reduced expression of *NaHPL* (Methods S1,

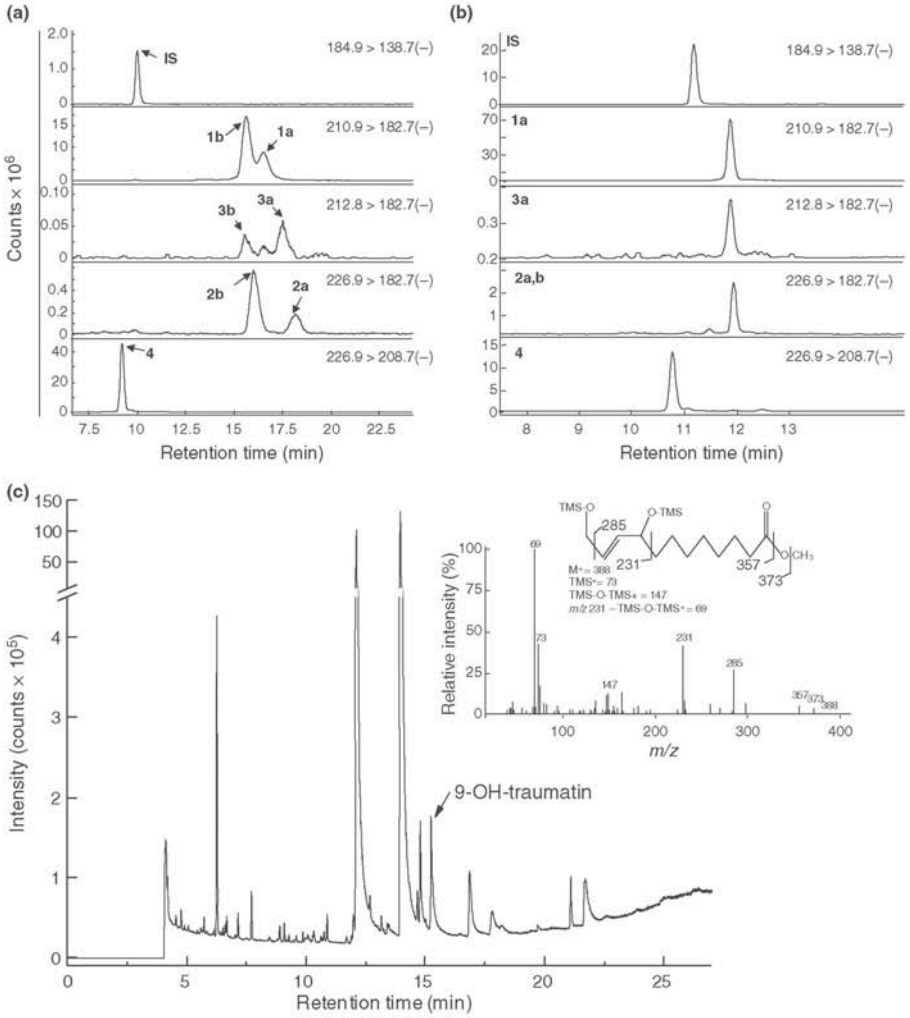

Fig. 2 Chromatographic profiles of C_{12} derivatives of the hydroperoxide lyase (HPL) pathway. (a) Example of the chromatographic separation of *Z*/*E* isomers of C_{12} standards. Compounds were separated by reverse phase on a Gemini-NX column, ionized by electrospray ionization (ESI) and detected in the multiple reaction monitoring (MRM) negative mode. (b) Example of the chromatographic separation of C_{12} molecules obtained from leaf samples of wounded *Nicotiana attenuata* plants. Compounds were separated by reverse phase on a ProntoSIL column, ionized by ESI and detected in the MRM negative mode. Compounds: internal standard (IS), 10-OH-(2*E*)-decenoic acid; 1a, (9*Z*)-traumatin; 1b, (10*E*)-traumatin; 2a, (3*Z*)-traumatic acid; 2b, (2*E*)-traumatic acid; 3a, 12-OH-(9*Z*)-dodecenoic acid; 3b, 12-OH-(10*E*)-dodecenoic acid; 4, 9-OH-traumatin. (c) Leaf extracts from wild-type (WT) *N. attenuata* plants were supplied with 1 μg of (9*Z*)-traumatin for 1 h and subjected to reduction with $NaBH_4$, diazomethane derivatization and silylation (OTMSi) for gas chromatography–mass spectrometry (GC-MS) analysis. The mass spectrum shown in the insert corresponds to derivatized 9-OH-traumatin.

Figs S5, S6 and Table S4) were also analyzed. In unelicited leaves of ir-lox2 plants, 9-OH-traumatin accumulated to < 0.2 nmol g^{-1} FW (Fig. 4). Moreover, after wounding and FAC elicitation, the concentrations of this C_{12} metabolite remained largely unchanged and the absolute concentrations were below 0.2 nmol g^{-1} FW (Fig. 4). (9*Z*)-traumatin, 12-OH-(9*Z*)-dodecenoic acid and dodecenedioic acids were either not detected or accumulated to very low concentrations in leaves of ir-lox2 plants (Fig. S3).

Analysis of ir-hpl plants showed that the concentrations of 9-OH-traumatin were reduced to *c.* 50% of WT concentrations in unelicited leaves and that they were increased twofold after wounding (Fig. 4a). After FAC elicitation, the concentrations of this metabolite increased but at lower

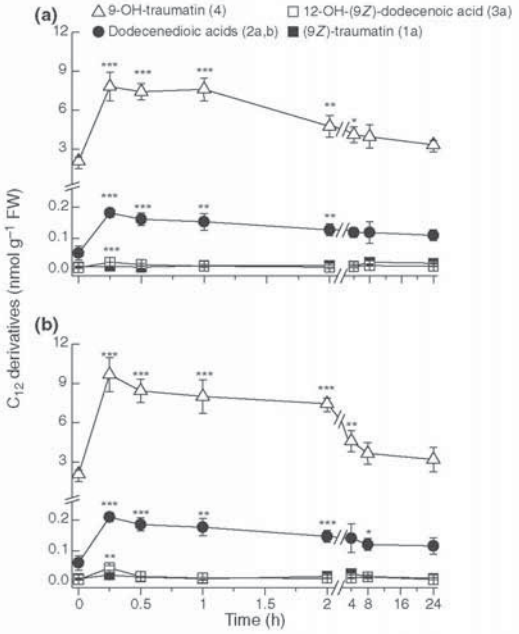

Fig. 3 Accumulation of C_{12} metabolites in leaves of wild-type (WT) *Nicotiana attenuata* plants after wounding and fatty acid–amino acid conjugate (FAC) elicitation. Leaves from WT plants were either wounded with a fabric pattern wheel (a) or subjected to wounding plus the addition of 18:3-Glu (b; FAC elicitation). Leaf samples were harvested at different times, extracted and the amounts of C_{12} derivatives of the hydroperoxide lyase (HPL) pathway (Fig. 1) were quantified by liquid chromatography–mass spectrometry/mass spectrometry (LC-MS/MS) (*, $P < 0.05$; **, $P < 0.01$; ***, $P < 0.001$; Student's *t*-test (T0 vs different times); $n = 3$; bars indicate ± SE).

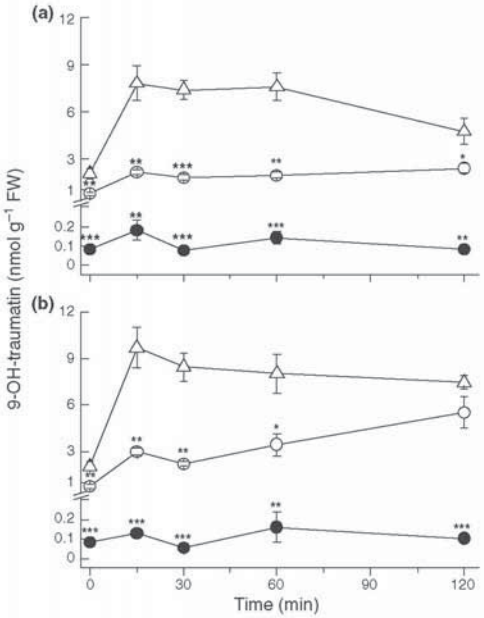

Fig. 4 Accumulation of 9-OH-traumatin in leaves of *Nicotiana attenuata* wild-type (WT; triangles), ir-lox2 (closed circles) and ir-hpl (open circles) plants after wounding and fatty acid–amino acid conjugate (FAC) elicitation. Leaves from WT, ir-lox2 and ir-hpl plants were either wounded with a fabric pattern wheel (a) or subjected to wounding plus the addition of 18:3-Glu (b; FAC elicitation). Leaf samples were harvested at different times, extracted and the amounts of 9-OH-traumatin were quantified by liquid chromatography–mass spectrometry/mass spectrometry (LC-MS/MS) (*, $P < 0.05$; **, $P < 0.01$; ***, $P < 0.001$; Student's *t*-test (WT vs transgenic line at the same time-point); $n = 3$; bars indicate ± SE).

rates than in WT, and attained WT concentrations after 2 h of treatment (Fig. 4b). These results were consistent with a 50% reduction in green leaf volatile production in ir-hpl plants (Table S4) and therefore with residual HPL activity in these plants. The concentrations of the remaining C_{12} derivatives were also reduced in leaves of ir-hpl plants compared with the WT (Fig. S3).

The majority of 9-OH-traumatin is formed from (9Z)-traumatin via NaLOX2 activity

The mechanism of 9-OH-traumatin formation from (9*Z*)-traumatin in plants has been a matter of controversy, with some results supporting the enzymatic (Gardner, 1998) and others the nonenzymatic biogenesis of this metabolite (Noordermeer *et al.*, 2000). To investigate the mechanism of 9-OH-traumatin formation in *N. attenuata*, equal amounts of proteins from leaf extracts of WT and ir-lox2 plants were incubated with either (9*Z*)-traumatin or (10*E*)-traumatin and the reaction products were analyzed by LC-MS/MS.

Consistent with the nonenzymatic formation of 9-OH-traumatin from (9*Z*)-traumatin (Noordermeer *et al.*, 2000), approximately one-third of *de novo* produced 9-OH-traumatin in WT leaf extracts was generated immediately (first phase: T0) after supplying the substrate; however, the remaining two-thirds required an incubation period of at least 15 min (second phase; Fig. 5a). When leaf extracts of ir-lox2 plants were supplied with (9*Z*)-traumatin, the amount of 9-OH-traumatin produced immediately was similar to that in WT leaf extracts; however, the second phase of accumulation was suppressed (Fig. 5a). Consistent with the formation of the major fraction of 9-OH-traumatin by enzymatic mechanisms, the heat inactivation of WT leaf extracts suppressed the accumulation of 9-OH-traumatin (Fig. 5b) and co-incubation of WT leaf extracts with the LOX inhibitor 3,4-dihydroxy-phenylethanol (DHPE) also suppressed its accumulation during the second phase of the reaction (Fig. 5b). When (10*E*)-traumatin was used as the substrate, *de novo* formation of 9-OH-traumatin in WT

New Phytologist

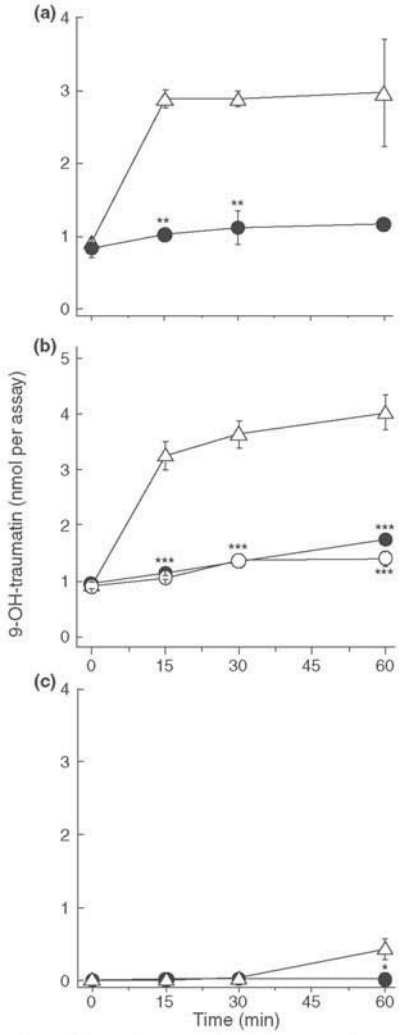

Fig. 5 Analysis of the mechanisms of 9-OH-traumatin formation in leaves of *Nicotiana attenuata* plants. (a) 100 μg of total protein from wild-type (WT; triangles) and ir-lox2 (circles) leaf extracts was incubated in 0.2 ml of reaction buffer supplied with 1 μg of (9*Z*)-traumatin. (b) 100 μg of total protein from WT leaf extracts were incubated in 0.2 ml of reaction buffer supplied with 1 μg of (9*Z*)-traumatin. Heat inactivation was achieved by incubating the leaf extracts for 5 min at 95°C before the addition of the substrate. The lipoxygenase inhibitor dihydroxyphenylethanol (DHPE) was added to obtain a final concentration of 10 mM. Triangles, control; closed circles, heat-inactivated; open circles, 10 mM DHPE. (c) 100 μg of total protein from WT (triangles) and ir-lox2 (circles) leaf extracts was incubated in 0.2 ml of reaction buffer supplied with 1 μg of (10*E*)-traumatin. In all cases the reactions were carried out at room temperature and stopped by the addition of chloroform : methanol. After extraction, 9-OH-traumatin was quantified by liquid chromatography–mass spectrometry/mass spectrometry (LC-MS/MS) (*, $P < 0.05$; **, $P < 0.01$; ***, $P < 0.001$; Student's *t*-test (WT vs genotype or treatment at same time point); $n = 3$; bars indicate ± SE).

and ir-lox2 leaf extracts was 10 times lower compared with its formation from (9*Z*)-traumatin (Fig. 5c).

It has been previously shown that the co-incubation of soybean (*Glycine max*) LOX-1 *in vitro* with (3*Z*)-nonenal and C_{18} hydroperoxides stimulated the activity of this enzyme toward formation of 4-OH-(2*E*)-nonenal (4HNE) (Gardner & Grove, 1998). To evaluate whether the oxidation of (9*Z*)-traumatin by NaLOX2 was indirect and depended on the accumulation of C_{18}-hydroperoxides, equimolar amounts of (9*Z*)-traumatin and C_{18}-hydroperoxides were added to leaf extracts of WT and ir-lox2 plants. The accumulation of 9-OH-traumatin was not affected by the added C_{18}-hydroperoxides (data not shown).

9-OH-traumatin forms conjugates with GSH during the wound and FAC elicitation response

9-OH-traumatin is an oxylipin-RES (Gardner, 1998) and as a soft electrophile it is liable to form Michael-type adducts with, for example, the sulfhydryl groups of abundant nucleophilic targets, such as reduced glutathione (GSH) (Farmer & Davoine, 2007; Mueller & Berger, 2009). GSH is an important intracellular redox buffer that accumulates at 1–5 mM in leaves and controls the concentrations of reactive molecules (Mueller & Berger, 2009). To first evaluate whether 9-OH-traumatin forms adducts with GSH, purified 9-OH-traumatin was incubated *in vitro* with commercial GSH and the reaction products were analyzed by LC-MS/MS. Formation of the 9-OH-traumatin–GSH conjugate occurred *in vitro* and, after 4 h of reaction at room temperature, > 50% of the initial amount of 9-OH-traumatin reacted with GSH (data not shown). To analyze the endogenous formation of this adduct, leaves of WT and ir-lox2 *N. attenuata* plants were wounded and the levels of 9-OH-traumatin-GSH accumulation were quantified (Fig. 6a). In WT plants, 9-OH-traumatin-GSH adducts were < 0.05 nmol g^{-1} FW in unelicited leaves; however, their concentrations increased rapidly after the treatments to reach *c.* 9 nmol g^{-1} FW within 1 h (Fig. 6a). In ir-lox2 plants, 9-OH-traumatin-GSH was undetected in unelicited leaves and accumulated at < 0.3 nmol g^{-1} FW after wounding (Fig. 6a).

9-OH-traumatin is not deposited on the leaf surfaces of *N. attenuata* plants

In addition to conjugation, cells can control the effects of reactive molecules by depositing them outside cells; for example, on the leaf surface. To investigate whether this was the case for 9-OH-traumatin, the surfaces from unelicited and wounded leaves were washed with methanol and both the washes and the surface-washed leaves were analyzed (Fig. 6b). In unelicited leaves, 9-OH-traumatin and 9-OH-traumatin-GSH accumulated primarily in the surface-

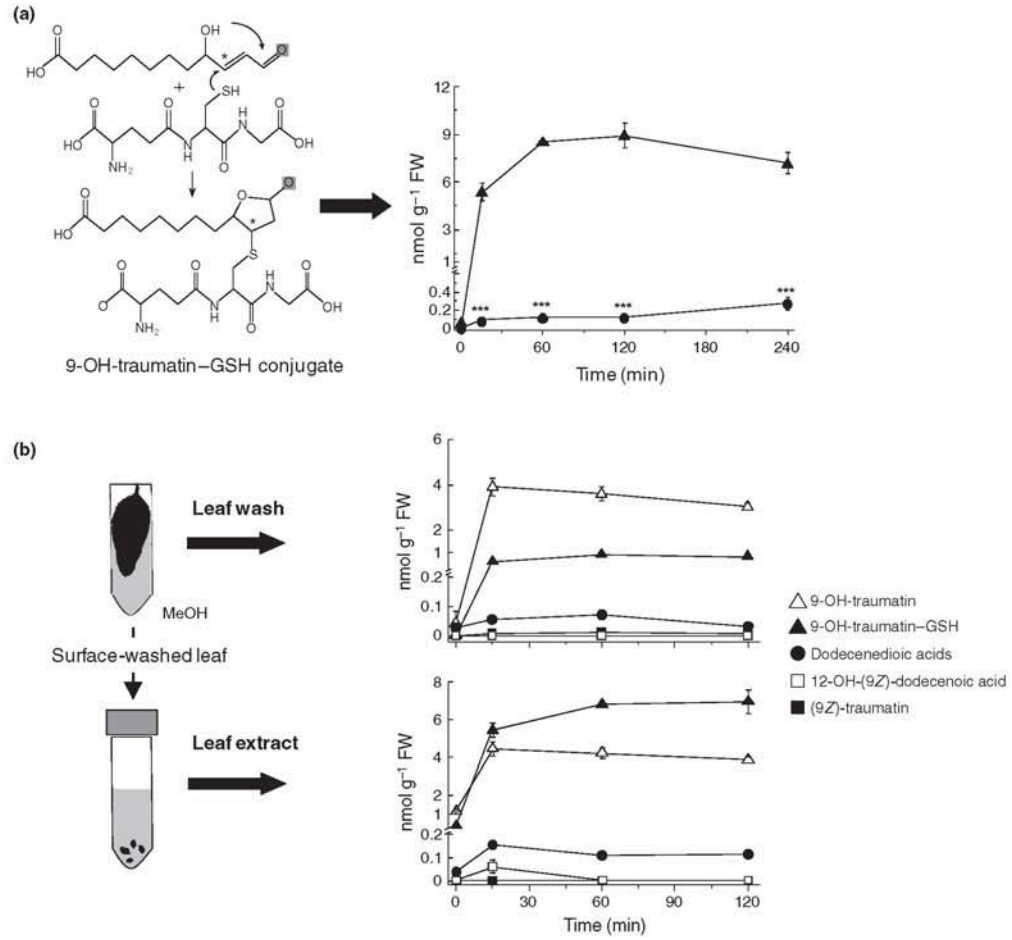

Fig. 6 Analysis of the formation of 9-OH-traumatin-glutathione (GSH) adducts and localization of 9-OH-traumatin. (a) Leaves from *Nicotiana attenuata* wild-type (WT; triangles) and ir-lox2 (circles) plants were wounded with a fabric pattern wheel and leaf samples were harvested at different times, extracted and the amounts of 9-OH-traumatin–GSH adducts were quantified by liquid chromatography–mass spectrometry/mass spectrometry (LC-MS/MS) (***, $P < 0.001$; Student's *t*-test (WT vs ir-lox2 at the same time-point); $n = 3$; bars indicate ± SE). (b) Intact and wounded leaves from WT *N. attenuata* plants were washed for 1 min with methanol to extract methanol-soluble surface compounds and both the wash and the remaining surface-washed leaf were used for quantification of C_{12} molecules (Fig. 1) and 9-OH-traumatin–GSH adducts by LC-MS/MS ($n = 3$; bars indicate ± SE).

washed leaf, with lower amounts in the wash (time 0; Fig. 6b), while the remaining C_{12} derivatives were detected at very low levels (< 0.1 nmol g^{-1} FW) in both fractions (Fig. 6b). At 15 min after wounding, 9-OH-traumatin was recovered from the wash and the surface-washed leaf extract in comparable amounts (*c.* 4 nmol g^{-1} FW) whereas 9-OH-traumatin-GSH was detected in higher amounts (6 vs 1 nmol g^{-1} FW) in the surface-washed leaf (Fig. 6b). The remaining C_{12} derivatives were *c.* 2 times more abundant in the leaf extract than in the wash (Fig. 6b). These results suggested that 9-OH-traumatin was retained in the cells and that after wounding it probably became accessible to methanol through the damaged tissue during the leaf wash.

Formation of 9-OH-traumatin by NaLOX2 activity establishes a major flux for the production of reactive C_{12} derivatives of the HPL pathway

Calculation of the rates of accumulation of the C_{12} derivatives of the HPL pathway within 15 min of the wound response showed that on average 1 g of leaf converted 850 pmol min^{-1} of (9*Z*)-traumatin to 9-OH-traumatin, with approximately two-thirds of this conversion being

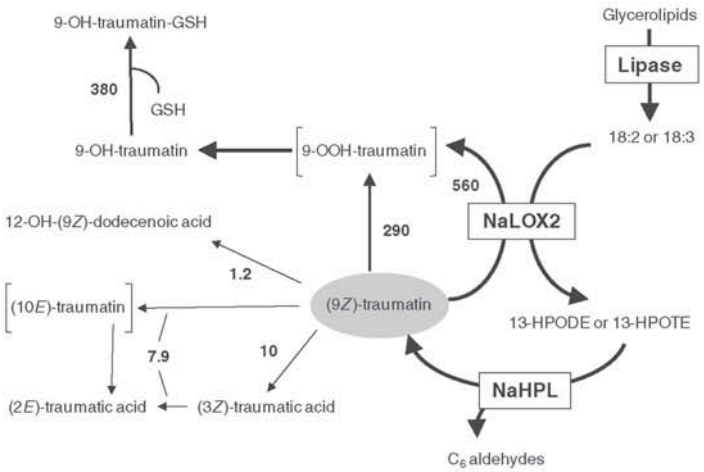

Fig. 7 Proposed model for the biosynthesis and metabolism of C_{12} derivatives of the hydroperoxide lyase (HPL) pathway in *Nicotiana attenuata* leaves. Upon wounding and fatty acid–amino acid conjugate (FAC) elicitation, 18:2 and 18:3 are released from membrane glycerolipids and dioxygenated by lipoxygenase-2 (NaLOX2) to generate 13-hydroperoxides (13-HPODE and 13-HPOTE, respectively). These molecules are substrates for NaHPL which produces C_6 aldehydes and (9*Z*)-traumatin. Formation of 9-OH-traumatin determines the major flux of C_{12} derivatives in leaves (850 pmol min^{-1} g^{-1} FW) and recycling NaLOX2 activity determines two-thirds of this flux (560 pmol min^{-1} g^{-1} FW) while the remaining third is determined by the nonenzymatic oxidation of (9*Z*)-traumatin (290 pmol min^{-1} g^{-1} FW). Formation of (2*E*)-traumatic acid may occur via (10*E*)-traumatin (not detected) auto-oxidation or isomerization of (3*Z*)-traumatic acid. The rates of accumulation were calculated based on the amounts of C_{12} molecules generated *de novo* within 15 min of the wound response.

catalyzed by NaLOX2 activity and the remaining one-third nonenzymatically (Fig. 7). It was found that 380 pmol min^{-1} of the 9-OH-traumatin was conjugated to GSH and the remaining (9*Z*)-traumatin was converted to (2*E*)-traumatic acid (7.9 pmol min^{-1}), (3*Z*)-traumatic acid (2.1 pmol min^{-1}) and 12-OH-(9*Z*)-dodecenoic acid (1.2 pmol min^{-1}; Fig. 7).

C_{12} derivatives of the HPL pathway induce changes in gene expression

To evaluate the signaling capacity of the C_{12} derivatives of the HPL pathway during the wound response, leaves of plants with reduced expression of *NaLOX2* and *NaLOX3* (ir-lox2/ir-lox3; Kallenbach *et al.*, 2010) were used. In this case, doubly silenced lines were chosen to minimize the effects of endogenously produced C_{12} derivatives and jasmonates after wounding. Thus, ir-lox2/ir-lox3 plants were wounded with a fabric pattern wheel, and either a 1 : 1 mixture of (9Z)-traumatin : 9-OH-traumatin or solvent (control treatment) was immediately applied to the wounds. In this case, 1 μg of each component was applied per leaf; amounts that corresponded to the endogenous amounts produced by leaves after wounding (Fig. 3). Total RNA was extracted from leaves at 120 min after the treatments and used for analysis of gene expression by microarray hybridization (see the Materials and Methods section).

The results of the analysis showed that, after the treatment with C_{12} derivatives, 320 genes showed significant changes in expression ($-1 > \log_2$(fold change) > 1; q-value < 0.035; FDR 3.3%) compared with the control treatment, with five genes down-regulated and the remainder up-regulated. A subset of these genes is presented in Table 1 and the complete list of genes in Table S3. Among the genes with known function that were most strongly up-regulated were *N. attenuata* homologs of glutathione *S*-transferase (GST), serine incorporator 1 (SERC1), monodehydroascorbate reductase (MDAR), protein disulfide isomerase (PDI) and a thioredoxin domain-containing protein; genes associated with oxidative stress responses in plants and animals (Table 1; see the Discussion section). Among the up-regulated genes were also four homologs of basic-helix-loop-helix (bHLH)-containing domain transcription factors and homologs of the defense-associated genes *PATHOGENESIS-RELATED PROTEIN 5* (*PR5*), proteinase inhibitor (*PI*) and a disease resistance response gene (Table 1). Among the signaling components, homologs of *ETHYLENE RECEPTOR 1* (*ETR1*), receptor-like protein kinase BRASSINOSTEROID INSENSITIVE 1 (BRI1)-like 3 (*BRL3*) and *MITOGEN-ACTIVATED KKK3* (*MKKK3*) were also up-regulated (Table 1). Among the down-regulated genes was BAK1 (BRASSINOSTEROID INSENSITIVE 1-associated receptor kinase 1; Table S3).

Discussion

Understanding the biosynthesis and function of the C_{12} derivatives of the HPL pathway has been a challenge in

Table 1 Example of genes up-regulated by C_{12} treatment of wounded leaves from ir-lox2/ir-lox3 *Nicotiana attenuata* plants

Gene ID	log_2(FC)	SD	*q*-value	Gene annotation
Na_30516	3.3	0.92	< 0.001	Unknown function
Na_24874	3.1	0.84	< 0.001	lQ7REH6lGST Glutathione *S*-transferase (*Plasmodium yoelii*)
Na_11850	2.8	0.61	0.013	Unknown function
Na_26610	2.8	0.43	0.009	Unknown function
Na_21166	2.6	0.52	< 0.001	lQ8WW36.1lZCH13 Zinc finger CCHC domain-containing protein 13 (*Homo sapiens*)
Na_11915	2.5	0.19	< 0.001	lP40561.1lSGN1 RNA-binding protein Salivary gland transcription factor 1 (SGN1) (*Saccharomyces cerevisiae*)
Na_28441	2.5	0.60	0.017	lQ3MHV9lSERC1 Serine incorporator 1 (*Bos taurus*)
Na_22608	2.3	0.48	0.005	lBAB13708.1l Elicitor inducible protein (*Nicotiana tabacum*)
Na_17639	2.2	0.30	< 0.001	lQ9FFT9.1lRH32 DEAD-box ATP-dependent RNA helicase 32 (*Arabidopsis thaliana*)
Na_09481	2.1	0.18	0.004	lQ9LK94lMDAR2 Monodehydroascorbate reductase (*Arabidopsis thaliana*)
Na_29882	2.1	0.41	0.017	lQ9FF55.1lPDI14 Protein disulfide isomerase-like 1-4 (*Arabidopsis thaliana*)
Na_11459	2.0	0.30	0.017	lQ9CQ79.1lTXND9 Thioredoxin domain-containing protein 9 (*Mus musculus*)
Na_15649	1.9	0.21	0.006	splQ9SEL7.3lDEGP5 Protease Do-like 5 (*Arabidopsis thaliana*)
Na_20636	1.9	0.16	0.004	lQ6J163.1l5NG4 Auxin-induced protein 5NG4 (*Pinus taeda*)
Na_05174	1.8	0.23	< 0.001	lQ9LJF3lBRL3 Receptor-like protein kinase BRASSINOSTEROID INSENSITIVE 1 (BRI1)-like 3 (*Arabidopsis thaliana*)
Na_01467	1.5	0.15	0.013	lQ9C5M8.2lPEL18 Pectate lyase 18 (*Arabidopsis thaliana*)
Na_21450	1.4	0.04	0.017	lQ9C670l Transcription factor basic-helix-loop-helix (bHLH) 76 (*Arabidopsis thaliana*)
Na_09136	1.4	0.14	0.021	lP28493lPR5 Pathogenesis-related protein 5 (*Arabidopsis thaliana*)
Na_15178	1.4	0.09	< 0.001	lP83241llP23 Proteinase inhibitor PSI-1.2 (*Capsicum annuum*)
Na_30583	1.4	0.04	0.006	lQ08080lHSP7S Stromal 70-kDa heat shock-related protein (*Spinacia oleracea*)
Na_09273	1.4	0.11	0.021	lQ9ZWL6lETR1 Ethylene receptor (*Pinus edulis*)
Na_18991	1.3	0.13	< 0.001	lQ9FLI1l Transcription factor bHLH36 (*Arabidopsis thaliana*)
Na_09028	1.3	0.12	0.017	lP13240lDR206 Disease resistance response protein 206 (*Pisum sativum*)
Na_32575	1.3	0.05	0.006	lO81893.3llTPK3 Inositol-tetrakisphosphate 1-kinase 3 (*Arabidopsis thaliana*)
Na_17734	1.3	0.03	0.013	lO22042lMKKK3 Mitogen-activated protein kinase kinase kinase 3 (*Arabidopsis thaliana*)
Na_13278	1.2	0.07	0.006	lQ9XEF0l Transcription factor bHLH51 (*Arabidopsis thaliana*)
Na_39624	1.1	0.05	0.031	lQ8S3D5lBH069 Transcription factor bHLH69 (*Arabidopsis thaliana*)

FC, fold change (treatment vs control); SD, standard deviation.

plant biology, and efforts initiated to this end a few decades ago have not been pursued with the same impetus as those associated with the C_6 derivatives of this pathway. With the opportunity to use reverse genetic approaches in the unraveling of the biosynthesis and signaling capacities of these molecules, the requirement for a suitable method for their analysis is self-evident. Here, we have described an LC-MS/MS-based approach to quantify C_{12} derivatives of the HPL pathway and have shown its application in the detection of changes induced by wounding and FAC elicitation in WT plants and by genetic deficiencies of biosynthetic enzymes (i.e. NaLOX2 and NaHPL).

Generation of 9-OH-traumatin in *N. attenuata* leaves

9-OH-traumatin was initially isolated as a product of 13-HPODE in extracts of soybean and alfalfa (*Medicago sativa*) seedlings, and it has been suggested that (9*Z*)-traumatin is converted to 9-OH-traumatin by LOX activity (Gardner, 1998). A subsequent study showed, however, that 9-OH-traumatin is formed preferentially nonenzymatically and perhaps indirectly via 13-HPODE formation and not directly by LOX activity towards (9*Z*)-traumatin (Noordermeer *et al.*, 2000). We observed that approximately one-third of the *de novo* synthesized 9-OH-traumatin was formed nonenzymatically. However, consistent with the proposed LOX-mediated biogenesis of this oxylipin, the production of the remaining two-thirds depended either directly or indirectly on NaLOX2 activity. The reduced capacity of ir-lox2 leaf extracts to produce 9-OH-traumatin after exogenous addition of (9Z)-traumatin, the sensitivity of its production to heat inactivation and to the LOX inhibitor DHPE, and the independence of its accumulation to the presence of C_{18} hydroperoxides strongly suggested that NaLOX2 directly acts on (9*Z*)-traumatin to form 9-OH-traumatin. Although it is unlikely, we cannot completely rule out the possibility that the formation of 9-OH-traumatin by this enzyme is indirect via the generation of an oxidative metabolite other than C_{18} hydroperoxides. We have previously shown that NaLOX2 also oxidizes the fatty acid moiety of the FAC 18:3-Glu to form 13-OOH-18:3-Glu and its derivatives (Vandoorn

et al., 2010). Thus, the range of substrates that this enzyme can use is not restricted to free 18:2 and 18:3 and may include (9*Z*)-traumatin to generate 9-OH-traumatin, as previously proposed in other systems (Gardner, 1998).

Generation of other low-abundance C_{12} derivatives of the NaHPL pathway and systemic accumulation

Alcohol dehydrogenase activity reduces the aldehyde groups of (9*Z*)-traumatin to form 12-OH-(9*Z*)-dodecenoic acid (Grechkin *et al.*, 1990). The low amounts of this derivative accumulating in wounded and FAC-elicited *N. attenuata* leaves suggest that either this enzymatic activity is very low in this tissue or the rapid oxidation of (9*Z*)-traumatin to 9-OH-traumatin outcompetes its reduction. The low levels of accumulation of dodecenedioic acids in wounded and FAC-elicited leaves were consistent with the rapid exchange of (9*Z*)-traumatin from NaHPL to NaLOX2, as the accumulation of dodecenedioic acids remained below 0.02 nmol g^{-1} FW (Fig. S3).

Even though the concentrations of dodecenedioic acids and 12-OH-(9*Z*)-dodecenoic acid were much lower than those of 9-OH-traumatin, their accumulation increased rapidly and transiently upon wounding and FAC elicitation (Fig. 3b). Thus, a possible scenario is that, as previously demonstrated for different plant responses (English & Bonner, 1937; Bonner & English, 1938; Ivanova *et al.*, 2001), these molecules may work as signals during the responses of *N. attenuata* to wounding and herbivory.

In distal leaves, the concentrations of the C_{12} metabolites did not change significantly within 2 h after wounding and FAC elicitation; however, we cannot exclude the possibility that some of these derivatives are vascularly transported in small amounts to distal leaves. It has been recently shown that azelaic acid, a saturated C_9 dicarboxylic acid, accumulates in the sap of *Arabidopsis thaliana* and confers local and systemic resistance against *Pseudomonas syringae* (Jung *et al.*, 2009).

The role of C_{12} derivatives as potential signaling molecules acting during the response to wounding and herbivory

9-OH-traumatin accumulated to *c.* 2 nmol g^{-1} FW in unelicited WT leaves, probably reflecting a basal flux of 18:2 and 18:3 through NaLOX2 and NaHPL in this tissue and the cellular tolerance to small amounts of this oxylipin RES. This basal flux was also reflected in the basal production of C_6 volatiles in WT plants (Table S4). The effect of oxylipin RES in cellular processes has been well documented in both plants and animals. For example, they can negatively affect cellular metabolism by the chemical modification of enzymes or by reducing photosynthetic rates (Almeras *et al.*, 2003; Mueller & Berger, 2009). At the level of gene expression, oxylipin RES can induce the transcription of genes related to detoxification, stress responses and secondary metabolism (Bate & Rothstein, 1998; Vollenweider *et al.*, 2000; Almeras *et al.*, 2003; Weber *et al.*, 2004; Mueller *et al.*, 2008). Thus, one possibility is that 9-OH-traumatin plays a role in the wound and herbivore responses through its RES properties; for example, by the activation of cell protection genes (Farmer & Davoine, 2007). After wounding, 38% of *de novo* synthesized 9-OH-traumatin conjugated to GSH, indicative of a strict control of its accumulation above certain levels, probably to prevent cytotoxic effects. The formation of oxylipin RES conjugates with GSH has been observed during the hypersensitive response (HR) induced by cryptogein elicitation in tobacco leaves (Davoine *et al.*, 2006) and it has been proposed that the generation of these conjugates may play a direct role in signaling; for example, by the alteration of the cellular redox balance (Meyer & Hell, 2005; Mullineaux & Rausch, 2005; Ogawa, 2005; Davoine *et al.*, 2006). Thus, an additional possibility is that the conjugation of 9-OH-traumatin to GSH plays a signaling role during the responses of *N. attenuata* to wounding and herbivory.

Consistent with the potential signaling roles of C_{12} derivatives of the HPL pathway during the wound response, gene expression analysis by microarrays showed that these derivatives have the capacity to exert changes in the expression of 320 genes. Among the top 12 most up-regulated transcripts (> 4-fold at 120 min) were several involved in responses to oxidative stress and protein chemical modification; a result consistent with 9-OH-traumatin being sensed as an RES by cells. These transcripts corresponded to GST (an enzyme that conjugates GSH to electrophilic centers on a wide variety of substrates, including peroxidized lipids and RES), MDAR (a component of the GSH-ascorbate antioxidant system; Dinakar *et al.*, 2010), PDI (an enzyme involved in the formation of disulfide bonds in chloroplasts; Wittenberg & Danon, 2008) and SERC1 (an enzyme involved in the protein mis-folding response in the ER-Golgi system; Aoki *et al.*, 2002). Interestingly, the expression of four transcription factors (TFs) corresponding to the bHLH family were induced by C_{12} derivatives (Table 1). This family of TFs contains the well-characterized Myelocytomatosis transcription factor (MYC)2, 3 and 4 which are involved in the regulation of defense responses in plants (Niu *et al.*, 2011). These results suggested that these TFs could also participate in the mediation of responses induced by C_{12} derivatives. In summary, the effect of these derivatives on the expression of 320 genes encoding proteins involved in diverse cellular processes including defense (e.g. PR5 and PI), signaling (e.g. ETR1, MKKK3 and BRLK3) and redox homeostasis (e.g. GST, MDAR and PDI; Tables 1,S3) provided strong evidence for the contribution of C_{12} derivatives of the HPL pathway to the control of plant responses to wounding and probably herbivory in *N. attenuata*. Future work will focus on

disentangling the potential specific roles of 9-OH-traumatin, 9-OH-traumatin-GSH, 12-OH-(9*Z*)-dodecenoic acid and dodecenedioic acids in the regulation of responses to wounding and herbivory and on the mechanisms underlying the formation of 9-OH-traumatin from (9Z)-traumatin by NaLOX2.

Acknowledgements

We acknowledge the Max Planck Society for financial support. We thank Anja Paschold for performing the Southern blot for ir-hpl plants and Wibke Kröber and Ivan Galis for assistance with microarray experiments and data analysis.

References

Allmann S, Baldwin IT. 2010. Insects betray themselves in nature to predators by rapid isomerization of green leaf volatiles. *Science* **329**: 1075–1078.

Allmann S, Halitschke R, Schuurink RC, Baldwin IT. 2010. Oxylipin channelling in *Nicotiana attenuata*: lipoxygenase 2 supplies substrates for green leaf volatile production. *Plant, Cell & Environment* **33**: 2028–2040.

Almeras E, Stolz S, Vollenweider S, Reymond P, Mene-Saffrane L, Farmer EE. 2003. Reactive electrophile species activate defense gene expression in Arabidopsis. *Plant Journal* **34**: 202–216.

Aoki S, Su Q, Li H, Nishikawa K, Ayukawa K, Hara Y, Namikawa K, Kiryu-Seo S, Kiyama H, Wada K. 2002. Identification of an axotomy-induced glycosylated protein, AIGP1, possibly involved in cell death triggered by endoplasmic reticulum–Golgi stress. *Journal of Neuroscience* **22**: 10751–10760.

Baldwin IT. 2010. Plant volatiles. *Current Biology* **20**: 392–397.

Bate NJ, Rothstein SJ. 1998. C_6-volatiles derived from the lipoxygenase pathway induce a subset of defense-related genes. *Plant Journal* **16**: 561–569.

Bonner J, English J. 1937. Purification of traumatin, a plant wound hormone. *Science* **86**: 352–353.

Bonner J, English J. 1938. A chemical and physiological study of traumatin, a plant wound hormone. *Plant Physiology* **13**: 331–348.

Browse J. 2005. Jasmonate: an oxylipin signal with many roles in plants. *Vitamins and Hormones* **72**: 431–456.

Browse J. 2009. Jasmonate passes muster: a receptor and targets for the defense hormone. *Annual Review of Plant Biology* **60**: 183–205.

Croft K, Juttner F, Slusarenko AJ. 1993. Volatile products of the lipoxygenase pathway evolved from *Phaseolus vulgaris* (L.) leaves inoculated with *Pseudomonas syringae* pv *phaseolicola*. *Plant Physiology* **101**: 13–24.

Davoine C, Falletti O, Douki T, Iacazio G, Ennar N, Montillet JL, Triantaphylides C. 2006. Adducts of oxylipin electrophiles to glutathione reflect a 13 specificity of the downstream lipoxygenase pathway in the tobacco hypersensitive response. *Plant Physiology* **140**: 1484–1493.

Dinakar C, Abhaypratap V, Yearla SR, Raghavendra AS, Padmasree K. 2010. Importance of ROS and antioxidant system during the beneficial interactions of mitochondrial metabolism with photosynthetic carbon assimilation. *Planta* **231**: 461–474.

English J, Bonner J. 1937. The wound hormones of plants I. Traumatin, the active principle of the bean test. *Journal of Biological Chemistry* **121**: 791–799.

Esterbauer H, Ertl A, Scholz N. 1976. The reaction of cysteine with α,β-unsaturated aldehydes. *Journal of Chemical Ecology* **32**: 285–289.

Farmer EE, Almeras E, Krishnamurthy V. 2003. Jasmonates and related oxylipins in plant responses to pathogenesis and herbivory. *Current Opinion in Plant Biology* **6**: 372–378.

Farmer EE, Davoine C. 2007. Reactive electrophile species. *Current Opinion in Plant Biology* **10**: 380–386.

Gardner HW. 1998. 9-Hydroxy-traumatin, a new metabolite of the lipoxygenase pathway. *Lipids* **33**: 745–749.

Gardner HW, Grove MJ. 1998. Soybean lipoxygenase-1 oxidizes 3*Z*-nonenal. A route to 4*S*-hydroperoxy-2*E*-nonenal and related products. *Plant Physiology* **116**: 1359–1366.

Grechkin AN. 2002. Hydroperoxide lyase and divinyl ether synthase. *Prostaglandins & Other Lipid Mediators* **68-69**: 457–470.

Grechkin AN, Kuchtina NV, Gafarova TE, Kuramshin RA. 1990. Oxidation of [1-^{14}C]linoleic acid in isolated microsomes from pea leaves. *Plant Science* **70**: 175–180.

Halitschke R, Schittko U, Pohnert G, Boland W, Baldwin IT. 2001. Molecular interactions between the specialist herbivore *Manduca sexta* (Lepidoptera, Sphingidae) and its natural host *Nicotiana attenuata*. III. Fatty acid-amino acid conjugates in herbivore oral secretions are necessary and sufficient for herbivore-specific plant responses. *Plant Physiology* **125**: 711–717.

Halitschke R, Ziegler J, Keinanen M, Baldwin IT. 2004. Silencing of hydroperoxide lyase and allene oxide synthase reveals substrate and defense signaling crosstalk in *Nicotiana attenuata*. *Plant Journal* **40**: 35–46.

Ivanova AB, Yarin AY, Antsygina LL, Gordon LK, Grechkin AN. 2001. (9Z)-12-Hydroxy-9-dodecenoic acid is an inducer of oxygen consumption and extracellular pH changes by cut wheat roots. *Doklady Biochemistry and Biophysics* **379**: 302–303.

Jung HW, Tschaplinski TJ, Wang L, Glazebrook J, Greenberg JT. 2009. Priming in systemic plant immunity. *Science* **324**: 89–91.

Kallenbach M, Alagna F, Baldwin IT, Bonaventure G. 2010. *Nicotiana attenuata* SIPK, WIPK, NPR1 and fatty acid-amino acid conjugates participate in the induction of JA biosynthesis by affecting early enzymatic steps in the pathway. *Plant Physiology* **152**: 96–106.

Kessler A, Halitschke R, Baldwin IT. 2004. Silencing the jasmonate cascade: induced plant defenses and insect populations. *Science* **305**: 665–668.

Kistner C, Matamoros M. 2005. RNA isolation using phase extraction and LiCl precipitation. In: Márquez A, ed. Lotus japonicus *handbook*. Dordrecht, the Netherlands: Springer, 123–124.

Krügel T, Lim M, Gase K, Halitschke R, Baldwin IT. 2002. *Agrobacterium*-mediated transformation of *Nicotiana attenuata*, a model ecological expression system. *Chemoecology* **12**: 177–183.

Loeffler C, Berger S, Guy A, Durand T, Bringmann G, Dreyer M, von Rad U, Durner J, Mueller MJ. 2005. B1-phytoprostanes trigger plant defense and detoxification responses. *Plant Physiology* **137**: 328–340.

Matsui K. 2006. Green leaf volatiles: hydroperoxide lyase pathway of oxylipin metabolism. *Current Opinion in Plant Biology* **9**: 274–280.

Meyer AJ, Hell R. 2005. Glutathione homeostasis and redox-regulation by sulfhydryl groups. *Photosynthesis Research* **86**: 435–457.

Mosblech A, Feussner I, Heilmann I. 2009. Oxylipins: structurally diverse metabolites from fatty acid oxidation. *Plant Physiology and Biochemistry* **47**: 511–517.

Mueller MJ. 2004. Archetype signals in plants: the phytoprostanes. *Current Opinion in Plant Biology* **7**: 441–448.

Mueller MJ, Berger S. 2009. Reactive electrophilic oxylipins: pattern recognition and signalling. *Phytochemistry* **70**: 1511–1521.

Mueller S, Hilbert B, Dueckershoff K, Roitsch T, Krischke M, Mueller MJ, Berger S. 2008. General detoxification and stress responses are

mediated by oxidized lipids through TGA transcription factors in Arabidopsis. *Plant Cell* **20**: 768–785.

Mukhtarova LS, Mukhitova FK, Gogolev YV, Grechkin AN. 2011. Hydroperoxide lyase cascade in pea seedlings: non-volatile oxylipins and their age and stress dependent alterations. *Phytochemistry* **72**: 356–364.

Mullineaux PM, Rausch T. 2005. Glutathione, photosynthesis and the redox regulation of stress-responsive gene expression. *Photosynthesis Research* **86**: 459–474.

Niu Y, Figueroa P, Browse J. 2011. Characterization of JAZ-interacting bHLH transcription factors that regulate jasmonate responses in Arabidopsis. *Journal of Experimental Botany* **62**: 2143–2154.

Noordermeer MA, Feussner I, Kolbe A, Veldink GA, Vliegenthart JFG. 2000. Oxygenation of (3*Z*)-alkenals to 4-hydroxy-(2*E*)-alkenals in plant extracts: a nonenzymatic process. *Biochemical and Biophysical Research Communications* **277**: 112–116.

Ogawa K. 2005. Glutathione-associated regulation of plant growth and stress responses. *Antioxidants & Redox Signaling* **7**: 973–981.

Prost I, Dhondt S, Rothe G, Vicente J, Rodriguez MJ, Kift N, Carbonne F, Griffiths G, Esquerre-Tugaye MT, Rosahl S *et al.* 2005. Evaluation of the antimicrobial activities of plant oxylipins supports their involvement in defense against pathogens. *Plant Physiology* **139**: 1902–1913.

Taki N, Sasaki-Sekimoto Y, Obayashi T, Kikuta A, Kobayashi K, Ainai T, Yagi K, Sakurai N, Suzuki H, Masuda T *et al.* 2005. 12-oxo-phytodienoic acid triggers expression of a distinct set of genes and plays a role in wound-induced gene expression in Arabidopsis. *Plant Physiology* **139**: 1268–1283.

Turner JG, Ellis C, Devoto A. 2002. The jasmonate signal pathway. *Plant Cell* **14**: S153–S164.

Tusher VG, Tibshirani R, Chu G. 2001. Significance analysis of microarrays applied to the ionizing radiation response. *Proceedings of the National Academy of Sciences, USA* **98**: 5116–5121.

Uchida K. 2003. 4-Hydroxy-2-nonenal: a product and mediator of oxidative stress. *Journal of Chemical Ecology* **42**: 318–343.

Vandoorn A, Kallenbach M, Borquez AA, Baldwin IT, Bonaventure G. 2010. Rapid modification of the insect elicitor N-linolenoyl-glutamate via a lipoxygenase-mediated mechanism on *Nicotiana attenuata* leaves. *BMC Plant Biology* **10**: 164.

Vick BA, Zimmerman DC. 1976. Lipoxygenase and hydroperoxide lyase in germinating watermelon seedlings. *Plant Physiology* **57**: 780–788.

Vollenweider S, Weber H, Stolz S, Chetelat A, Farmer EE. 2000. Fatty acid ketodienes and fatty acid ketotrienes: Michael addition acceptors that accumulate in wounded and diseased Arabidopsis leaves. *Plant Journal* **24**: 467–476.

Weber H, Chetelat A, Reymond P, Farmer EE. 2004. Selective and powerful stress gene expression in Arabidopsis in response to malondialdehyde. *Plant Journal* **37**: 877–888.

Wittenberg G, Danon A. 2008. Disulfide bond formation in chloroplasts. *Plant Science* **175**: 459–466.

Zimmerman DC, Coudron CA. 1979. Identification of traumatin, a wound hormone, as 12-oxo-trans-10-dodecenoic acid. *Plant Physiology* **63**: 536–541.

Supporting Information

Additional supporting information may be found in the online version of this article.

Fig. S1 Auto-oxidation of (9*Z*)-traumatin *in vitro*.

Fig. S2 Determination of the linearity and limit of detection of C_{12} metabolites.

Fig. S3 Accumulation of C_{12} derivatives in leaves of wild-type (WT), ir-lox2 and ir-hpl plants after wounding and fatty acid–amino acid conjugate (FAC) elicitation.

Fig. S4 Calibration curves for C_{12} standards.

Fig. S5 Quantification of *Nicotiana attenuata* hydroperoxide lyase (*NaHPL*) mRNA levels in wild-type (WT) and ir-hpl plants.

Fig. S6 Southern blot analysis of ir-hpl plants.

Table S1 Parameters used for detection of C_{12} molecules by liquid chromatography–mass spectrometry/mass spectrometry (LC-MS/MS)

Table S2 Parameters used for quantification of C_{12} molecules by liquid chromatography–mass spectrometry/mass spectrometry (LC-MS/MS)

Table S3 Complete list of genes changing expression in wounded leaves of ir-lox2/ir-lox3 plants after treatment with 9Z-traumatin : 9-OH-traumatin (1 : 1)

Table S4 Analysis of C_6 volatiles emitted by wild-type (WT) and ir-hpl plants

Methods S1 Characterization of ir-hpl plants.

Please note: Wiley-Blackwell are not responsible for the content or functionality of any supporting information supplied by the authors. Any queries (other than missing material) should be directed to the *New Phytologist* Central Office.

Supporting information

Fig. S1. Auto-oxidation of (9*Z*)-traumatin in vitro.

Fig. S2. Determination of the linearity and limit of detection of C_{12} metabolites.

Fig. S3. Accumulation of C_{12} derivatives in leaves of wild-type (WT), ir-lox2 and ir-hpl plants after wounding and fatty acid–amino acid conjugate (FAC) elicitation.

Fig. S4. Calibration curves for C_{12} standards.

Fig. S5. Quantification of Nicotiana attenuata hydroperoxide lyase (Na*HPL*) mRNA levels in wild-type (WT) and ir-hpl plants.

Fig. S6 .Southern blot analysis of ir-hpl plants.

Table S1. Parameters used for detection of C_{12} molecules by liquid chromatography–mass spectrometry／mass spectrometry (LC-MS／MS)

Table S2. Parameters used for quantification of C_{12} molecules by liquid chromatography–mass spectrometry／mass spectrometry (LC-MS／MS)

Table S3. Complete list of genes changing expression in wounded leaves of ir-lox2／ir-lox3 plants after treatment with 9*Z*-traumatin : 9-OH-traumatin (1 : 1). **(Data can be found on the attached CD-ROM).**

Table S4. Analysis of C_6 volatiles emitted by wild-type (WT) and ir-hpl plants

Appendix S1. Characterization of ir-hpl plants.

Supporting figures

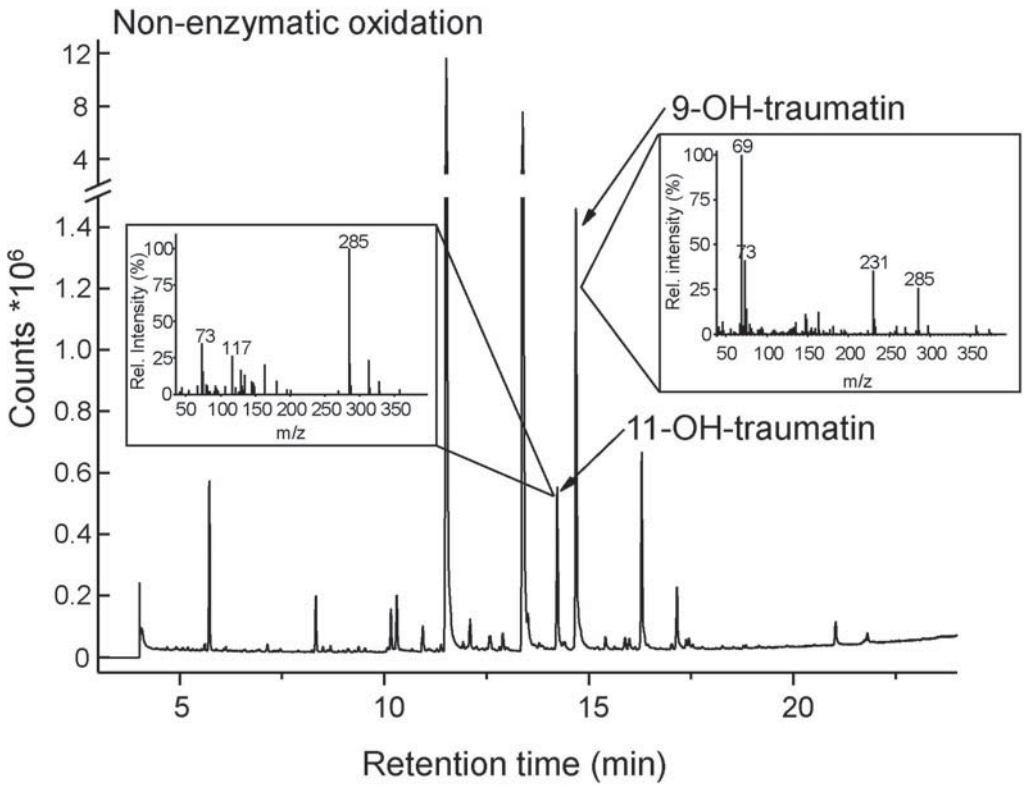

Figure S1. Auto-oxidation of (9*Z*)-traumatin *in vitro*
A solution of (9*Z*)-traumatin in methanol was air-dried at room temperature for 2 hours. After reconstituting the sample in methanol, the products were reduced with excess $NaBH_4$ and derivatized with diazomethane and MSTFA. The derivatized products were analyzed by GC-MS. Formation of 9-OH-traumatin and 11-OH-traumatin as auto-oxidation products was detected, consistently with Noordermeer *et al* (2000).

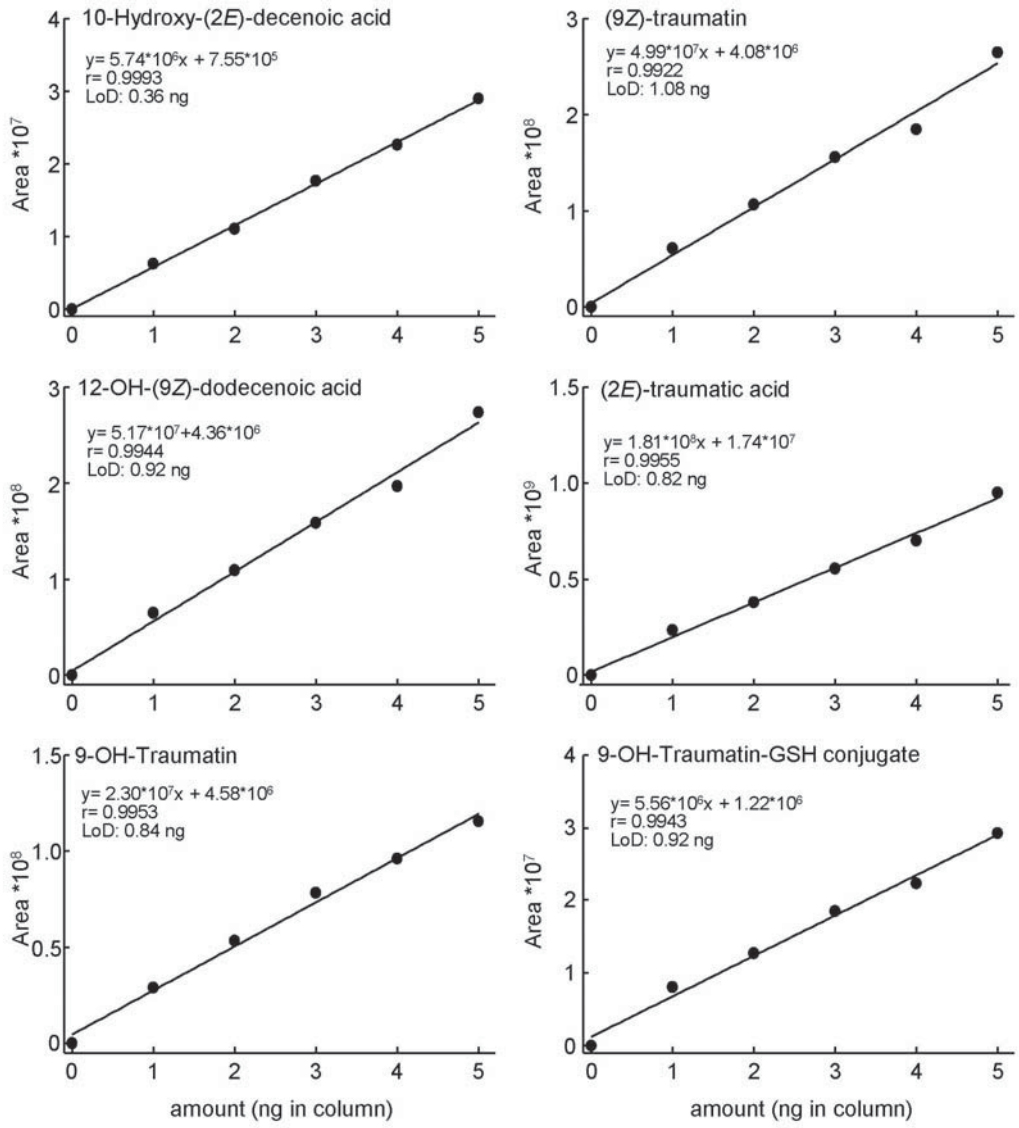

Figure S2. Determination of the linearity and limit of detection (LoD) for C_{12} metabolites. Commercial standards and synthetic compounds were spiked at different concentrations in leaf-derived matrix obtained from ir-lox2 plants. Samples were analyzed by LC-MS/MS in the negative MRM mode and the peak areas corresponding to each analyte were integrated and plotted against the amount of analyte injected in the column (ng in column).

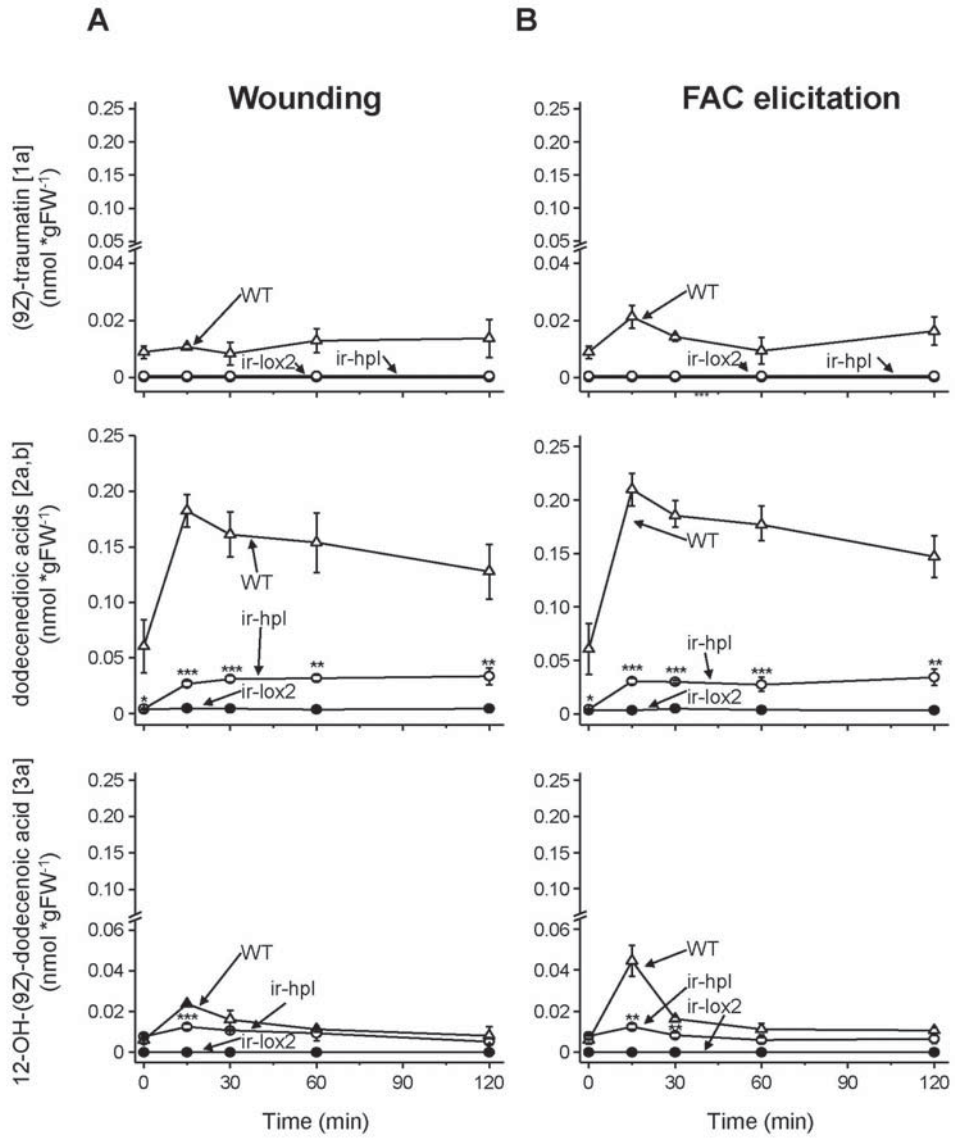

Figure S3. Accumulation of C_{12} derivatives in leaves of WT, ir-lox2 and ir-hpl plants after wounding and FAC elicitation

Leaves from WT, ir-lox2 and ir-hpl plants were either wounded with a fabric pattern wheel **(a)** or wounded plus the addition of 18:3-Glu (**b**; FAC elicitation). Leaf samples were harvested at different times, extracted and the amounts of C_{12} derivatives were quantified by LC-MS/MS (*: $P < 0.05$, **: $P < 0.01$, ***: $P < 0.001$, Student's t-test (WT vs transgenic line at same time point), $n=3$, bars indicate SE).

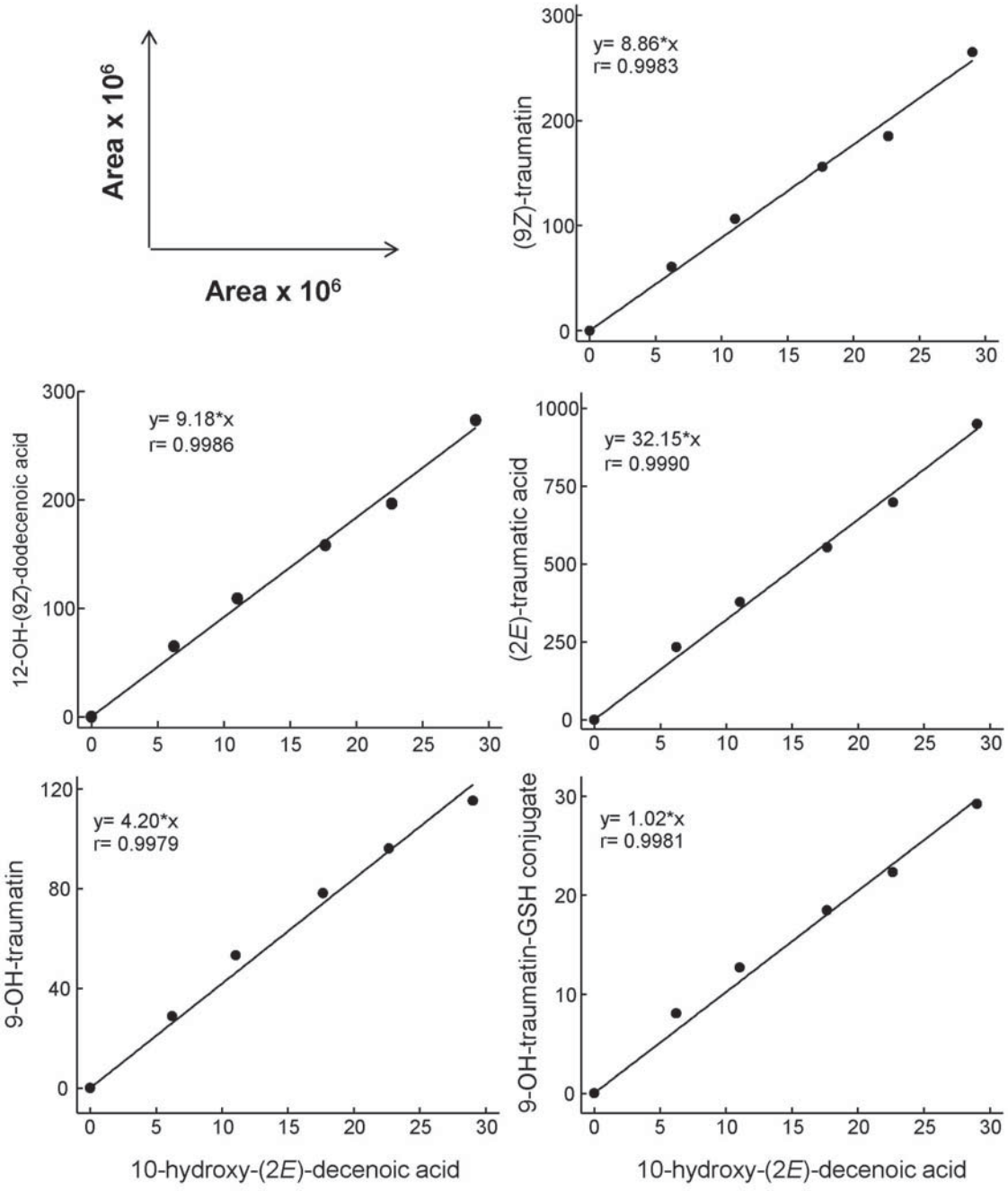

Figure S4. Calibration curves for C_{12} standards.
Different amounts of C_{12} standards were spiked in leaf extracts (matrix) from ir-lox2 plants and analyzed by LC-MS/MS using the parameters described in Material and Methods. Units in the Y and X axis are peak areas (x 10^6).

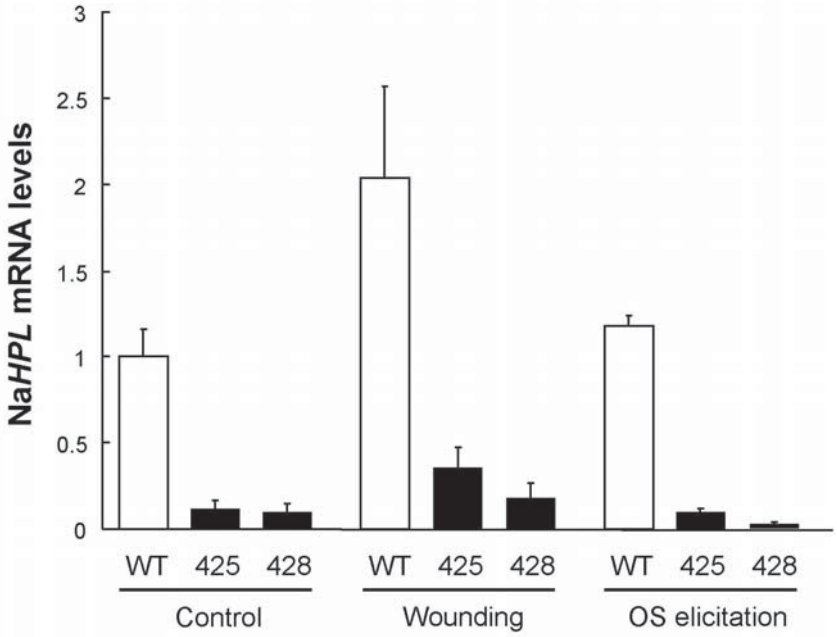

Figure S5. Quantification of Na*HPL* mRNA levels in WT and ir-hpl plants.
Total RNA was extracted from leaves of either WT or ir-hpl (lines 425 and 428) plants before (control) and 45 min after wounding and OS elicitation. The abundance of Na*HPL* transcripts was analyzed by qPCR using Na*Actin* mRNA as a reference. Na*HPL* mRNA levels represent the relative levels to the reference gene (Bars represent ±SE, *n*=5).

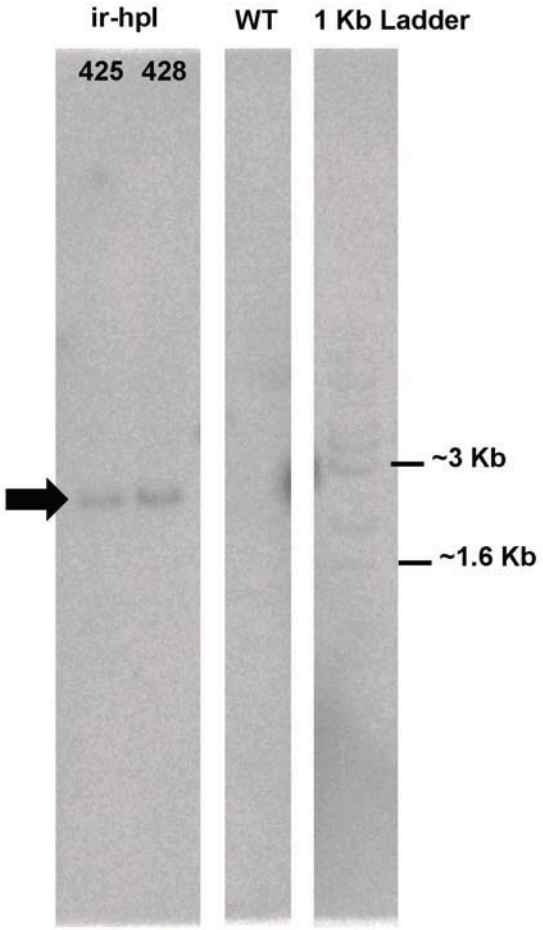

Figure S6. Southern blot analysis of ir-hpl plants.
Genomic DNA was isolated from WT and ir-hpl (lines 425 and 428) plants, digested with EcoRV and separated by agarose-gel electrophoresis using standard conditions (see Appendix S1 for methodological details). A gene-specific probe corresponding to the hygromycin resistance gene (*hptII*) was labeled with [α-32P] dCTP and used for hybriditazion. The arrow points to the single T-DNA insertions in ir-hpl lines.

Supporting tables

Table S1. Parameters used for detection of C_{12} molecules by LC-MS/MS

Reference	Compound	Capillary CID (V)	Transition [M-H]-		[M-X]-	Collison energy (V)	Retention time (min)
IS	10-OH-(2E)-decenoic acid (IS)	-35	185	>	139	15	9.9
1a	12-oxo-(9Z)-dodecenoic acid	-35	211	>	183	13.5	16.5
1b	12-oxo-(10E)-dodecenoic acid	-35	211	>	183	13.5	15.5
2a	12-OH-(9Z)-dodecenoic acid	-35	213	>	183	15.5	17.4
2b	12-OH-(10E)-dodecenoic acid	-35	213	>	183	15.5	15.5
3a	(3Z)-dodecenedioic acid	-35	227	>	183	13	18.1
3b	(2E)-dodecenedioic acid	-35	227	>	183	13	15.9
4	9-OH-12-oxo-(11E)-dodecenoic acid	-35	227	>	209	9.5	9.2

Table S2. Parameters used for quantification of C_{12} molecules by LC-MS/MS

Reference	Compound	Capillary CID (V)	Transitions [M-H]-		[M-X]-	Collison energy (V)	Retention time (min)	LoD (ng on column)
IS	10-OH-(2E)-decenoic acid (IS)	-35	185	>	139	15	11.05	0.36
1a	12-oxo-(9Z)-dodecenoic acid	-35	211	>	183	13.5	11.73	1.08
2a	12-OH-(9Z)-dodecenoic acid	-35	213	>	183	15.5	11.73	1.08
3a,b	(2E)- and (3Z)-dodecenedioic acids	-35	227	>	183	13	11.95	0.82
4	9-OH-12-oxo-(11E)-dodecenoic acid	-35	227	>	209	9.5	10.82	0.84
5	4-OH-(2E)-dodecenedioic acid	-35	243	>	225	9.5	n.d.	
6	9,12-OH-(10E)-dodecenoic acid	-35	229	>	211	9.5	n.d.	
7	9,12-OH-(10E)-dodecanoic acid	-35	231	>	213	9.5	n.d.	
8	9-OH-traumatin-GSH adduct	-35	534	>	306	16.5	10.16	0.92

n.d., not detected

Table S4. Analysis of C_6 volatiles emitted by wild-type (WT) and ir-hpl plants (n=6, ±SE).

Treatment	class	Volatile	RT (s)		Relative VOC released	
			RT1	RT2	WT	irhpl (428)
Control	aldehyde	(3Z)-hexenal	174	1.93	**0.01** ± 0.005	**0.01** ± 0.002
		(2E)-hexenal	246	2.90	**0.02** ± 0.013	**n.d.**
	alcohole	(3Z)-hexenol	246	2.58	**0.24** ± 0.189	**0.02** ± 0.003
		(2E)-hexenol	270	2.73	**0.10** ± 0.091	**n.d.**
	hexenyl-ester	(3Z)-hexenyl acetate	570	2.89	**0.04** ± 0.034	**n.d.**
		(2E)-hexenyl acetate	594	2.95	**n.d.**	**n.d.**
		(3Z)-hexenyl propionate	756	2.78	**0.01** ± 0.005	**n.d.**
		(2E)-hexenyl propionate	774	2.82	**n.d.**	**n.d.**
		(3Z)-hexenyl butyrate	912	2.64	**0.03** ± 0.025	**n.d.**
		(2E)-hexenyl butyrate	930	2.70	**n.d.**	**n.d.**
	Total				**0.44 ± 0.368**	**0.03 ± 0.005**
Wounding	aldehyde	(3Z)-hexenal	174	1.93	**4.40** ± 0.592	**2.05** ± 0.371
		(2E)-hexenal	246	2.90	**1.39** ± 0.338	**0.51** ± 0.090
	alcohole	(3Z)-hexenol	246	2.58	**6.77** ± 0.495	**4.52** ± 0.729
		(2E)-hexenol	270	2.73	**3.82** ± 0.538	**1.38** ± 0.283
	hexenyl-ester	(3Z)-hexenyl acetate	570	2.89	**0.36** ± 0.034	**0.23** ± 0.042
		(2E)-hexenyl acetate	594	2.95	**0.03** ± 0.005	**0.01** ± 0.002
		(3Z)-hexenyl propionate	756	2.78	**0.03** ± 0.006	**0.03** ± 0.005
		(2E)-hexenyl propionate	774	2.82	**n.d.**	**n.d.**
		(3Z)-hexenyl butyrate	912	2.64	**0.16** ± 0.012	**0.09** ± 0.013
		(2E)-hexenyl butyrate	930	2.70	**0.02** ± 0.003	**0.01** ± 0.003
	Total				**16.99 ± 2.023**	**8.84 ± 1.539**
OS-elicitation	aldehyde	(3Z)-hexenal	174	1.93	**1.67** ± 0.417	**0.58** ± 0.089
		(2E)-hexenal	246	2.90	**2.65** ± 0.356	**1.18** ± 0.133
	alcohole	(3Z)-hexenol	246	2.58	**4.04** ± 0.629	**2.49** ± 0.207
		(2E)-hexenol	270	2.73	**5.24** ± 0.714	**2.78** ± 0.172
	hexenyl-ester	(3Z)-hexenyl acetate	570	2.89	**0.19** ± 0.031	**0.13** ± 0.022
		(2E)-hexenyl acetate	594	2.95	**0.05** ± 0.006	**0.03** ± 0.002
		(3Z)-hexenyl propionate	756	2.78	**0.03** ± 0.006	**0.03** ± 0.009
		(2E)-hexenyl propionate	774	2.82	**0.01** ± 0.001	**n.d.**
		(3Z)-hexenyl butyrate	912	2.64	**0.08** ± 0.012	**0.08** ± 0.034
		(2E)-hexenyl butyrate	930	2.70	**0.04** ± 0.005	**0.02** ± 0.006
	Total				**14.00 ± 2.179**	**7.32 ± 0.675**

Appendix S1. Characterization of ir-hpl plants

Materials and Methods

Generation of transgenic ir-hpl lines

Transgenic *N. attenuata* (ir-hpl) plants reduced in the expression of NaHPL were generated via leaf disc *Agrobacterium*-mediated transformation and seedling regeneration as previously described (Krügel *et al*., 2002). The binary vector used for plant transformation was pSOL3 (Bubner et al., 2006) engineered to carry a fragment of the NaHPL cDNA (GenBank accession: AJ414400) subcloned in inverted repeat orientation (vector pSOL3HPL). T_1 transformed plants were analyzed by quantification of Na*HPL* mRNA levels by real-time quantitaive PCR in unelicited leaves and in leaves elicited with *Manduca sexta* oral secretions (OS) and for T-DNA single insertion by Southern blot hybridization (see below). Segregation analysis of hygromycin resistance in T_2 seedlings was performed on agar plates supplemented with hygromycin (0.025 mg mL^{-1}). Two lines, ir-hpl 425-4 (425) and 428-8 (428) showed the lowest levels of Na*HPL* mRNA accumulation (Figure AS1) and had a single T-DNA insertion in their genomes (Figure AS2).

For Southern blot analysis, genomic DNA of the WT and ir-hpl lines was isolated by the cetyltrimethylammonium bromide (CTAB) method. DNA samples (10 µg) were digested with EcoRV overnight at 37 C according to commercial instructions and separated on a 0.8% (w/v) agarose gel using standard conditions. DNA was blotted onto Gene Screen Plus Hybridisation Transfer membranes (Perkin Elmer Life and Analytical Sciences, Boston, MA, USA) using the capillary transfer method. A gene-specific probe for the hygromycin resistance gene *hptII* was generated by PCR using the primer pairs HYG1-18 (5′-CCGGATCGGACGATTGCG-3′) and HYG3-20 (5′-CGTCTGTCGAGAAGTTTCTG-3′). The probe was labeled with [α-^{32}P]dCTP (Perkin Elmer) using the Rediprime II kit (Amersham Pharmacia) according to commercial instruction.

Plant treatments

Leaf wounding was performed by rolling three times a fabric pattern wheel on each side of the midvein of 40-day-old rosette stage plants. For a wounding + water (w+w) treatment, 20 µL of deionized water were immediately pipetted onto the wounded leaf. For a wounding + oral secretions (w+OS) treatment, 20 µL of *Manduca sexta* oral secretion (diluted 1:3 in water, v/v) was applied to the wounds. Samples from untreated plants were used as controls.

Volatile collection and analysis

Single leaves (+1 position) of wild type and ir-hpl plants (n=6 per genotype and treatment) were enclosed immediately after treatment between two 50 mL food-quality plastic containers (Huhtamaki, Bad Bertricher, Germany) secured with miniature claw-style hair clips. Ambient air was pulled through the collection chamber and a glass tube (ARS, Inc., Gainsville, FL, USA) packed with glass wool and 20 mg of Super Q (Alltech, Düsseldorf, Germany). Airflow was created by a vacuum pump (model DAA-V114-GB; Gast Mfg; Benton Harbour, MI, USA) at ~200 mL min^{-1}. SuperQ traps were eluted with 250 µL dichloromethane into a GC vial containing a glass insert after spiking each trap with 400 ng tetralin (Sigma-Aldrich, Germany) as an internal standard. Samples were analyzed on an Agilent 6890N gas chromatograph equipped with an Agilent 7683 autoinjector (Agilent Technologies, Böblingen, Germany) and coupled with a LECO Pegasus III time-of-flight mass spectrometer with a 4D thermal modulator upgrade (LECO, Mönchengladbach, Germany) as described by Gaquerel et al. (2009). GLVs were identified and quantified using standard solutions of (3Z)-hexenal, (2E)-hexenal, (3Z)-hexenol, (2E)-hexenol, (3Z)-hexenyl-acetate, (2E)-hexenyl-acetate, (3Z)-hexenyl-propanoate, (3Z)-hexenyl-butanoate, (2E)-hexenyl-butanoate (Sigma-Aldrich , Germany) and (2E)-hexenyl -propanoate (Bedoukian Research Inc, Danbury, USA).

Quantitative real-time PCR assay

Total RNA was extracted from single leaves (+2 position) of WT and ir-hpl plants with TRI Reagent (Sigma-Aldrich, Germany) according to the manufacturer's instruction. Reverse transcription of 1µg of total RNA was performed using SuperScript II Reverse Transcriptase (Invitrogen, Germany) and a poly-T primer. Quantitative real-time PCR (ABI PRISM™7000, Applied Biosystems, Foster City, CA, USA) was conducted with 40 ng cDNA using the qPCR™ core reagent kit (Eurogentec, Köln, Germany) and NaHPL-specific primer pairs (FP: 5' CACTTAGACTTAGTCCACCTGTGC 3', RP: 5' AACACAAACTTTTCAGGATCATCA 3'). The PCR products were detected by gene-specific double fluorescent dye-labeled TaqMan® probes (Probe: 5' TCAGCCATTGGTAATGAGAGATCCAAAGG 3'). For calibration we used a duplicated dilution series of cDNAs which had been transcribed from induced RNA samples of the same experiment and calculated the relative transcript abundance by efficiency-correcting for each primer pair and normalizing to the *N. attenuata* actin gene (FP: 5' GGTCGTACCACCGGTATTGTG 3', RP: 5' GTCAAGACGGAGAATGGCATG 3', Probe: 5' TCAGCCACACCGTCCCAATTTATGAGG 3').

Supplemental References

Krügel T, Lim M, Gase K, Halitschke R, Baldwin IT (2002) Agrobacterium-mediated transformation of Nicotiana attenuata, a model ecological expression system. Chemoecology 12: 177-18:3

Gaquerel E, Weinhold A, Baldwin IT (2009) Molecular interactions between the specialist herbivore Manduca sexta (Lepidoptera, Sphigidae) and its natural host Nicotiana attenuata. VIII. An unbiased GCxGC-ToFMS analysis of the plant's elicited volatile emissions. Plant Physiol 149:1408-1423

Chapter 6: Discussion

Identification of the early mediators of the FAC signal transduction pathway

Recent years have brought progress in the elucidation of early signaling events triggered after herbivore perception; however, the molecular mechanisms through which plants decode insect feeding are still largely unknown. Recently, the advent of new quantitative techniques for gene expression profiling and high throughput sequencing capacity has made it possible to explore the genome-wide changes occurring in the transcriptome of plants for which little nucleotide sequence information is currently available in public databases. I used the SuperSAGE technique to identify the molecular components triggering insect-specific responses in *Nicotiana attenuata* after perception of the main elicitors present in *Manduca sexta* OS: fatty acid-amino acid conjugates (FACs). I analyzed the changes in the expression of thousands of genes in *N. attenuata* leaves after perception of the FAC 18:3-Glu.

Two SuperSAGE libraries were generated from FAC-induced leaf samples (F library) and wounded leaf samples (W library) with the goal of identifying transcripts that were rapidly and differentially regulated by FACs. A total of 354,930 tags were sequenced from which 12,774 unique transcripts (UniTags) were identified. I analyzed the statistically significant changes in tag copy number between the F and W libraries and identified 547 differentially regulated UniTags (*P*-value < 0.05; FC ≥ 2.5 for up-regulated UniTags and FC ≤ 0.4 for down-regulated UniTags). Among these UniTags, 430 were up-regulated and 117 down-regulated after 18:3-Glu elicitation compared to wounding. Sixty percent of the differentially expressed UniTags could be assigned to a protein entry in GenBank and UniProtKB/TrEMBL protein databases. The remaining UniTags could not be annotated, most likely because the SuperSAGE tags are derived from the 3' UTR of each mRNA molecule: since most of the *Nicotiana* spp nucleotide entries in GenBank correspond to *N. tabacum*, some mismatches may be attributed to polymorphisms in the 3' UTR of mRNAs from *N. attenuata* and this tobacco species.

Gene Ontology (GO) was used to assign gene function categories and the analysis disclosed a total of 75 UniTags with potential regulatory function. Among these were 22 protein kinases and 30 transcription factors. The remaining UniTags with putative regulatory function belonged to the GO classes protein phosphatase, signal transduction and nucleic acid binding. As a validation method, I quantified the mRNA levels corresponding to 27 UniTags by qPCR and validated the data obtained by SuperSAGE for 20 UniTags.

The biological relevance of seven selected putative regulatory components was analyzed by virus induce gene silencing (VIGS). Three putative regulatory components of resistance mechanisms against lepidopteran larval feeding were identified: a lipid phosphate phosphatase (LLP), a protein of unknown function (Unk-A) and a lectin receptor-like kinase (LecRK1). Interestingly, the mass gain observed in *M.sexta* larvae feeding on NaUnk-A, NaLPP and NaLecRK1-silenced plants was more than 2-fold the mass gain by larvae fed on control EV plants. Since a large number of defense-related genes are regulated by JA and JA-Ile, the levels of these phytohormones were quantified after wounding and wounding plus 18:3-Glu elicitation. Compared to EV control plants, NaLPP-silenced plants displayed significantly reduced JA and JA-Ile accumulation after 18:3-Glu elicitation. This reduction in JA and JA-Ile could result in impaired defense responses against *M. sexta* herbivory in NaLPP-silenced plants. Plants silenced in NaUnkA expression had similar levels of JA and JA-Ile accumulation compared to EV control plants after 18:3-Glu elicitation. These results indicated that *M. sexta* larval performance was not the result of impaired JA biosynthesis in NaUnkA-silenced plants and thus suggested that another mechanism acting independently of JA and JA-Ile regulates defense responses in *N. attenuata*. The exact molecular mechanisms regulated by NaLPP and NaUnkA are still unknown.

NaLecRK1*: a novel lectin receptor-like kinase involved in the regulation of *Nicotiana attenuata*'s defense responses against *Manduca sexta

In the SuperSAGE analysis, I identified a receptor-like kinase (NaLecRK1), which is rapidly induced after wounding and OS of *M. sexta* or FAC treatment and, when silenced

by virus induced gene silencing (VIGS) or inverted repeated RNA interference in *N. attenuata* plants (ir-lecRK1 plants), substantially increased *M. sexta* larval performance. These results encouraged me to fully characterize the role of NaLecRK1 in the FAC signal transduction pathway and defense responses against insects. Based on sequence similarity and according to the current classification of lectin receptor-like kinases (LRKs; Bouwmeester and Govers, 2009), NaLecRK1 belongs to the G-type LRK class. Previous studies have associated some G-type LRKs with defense responses against pathogens. For example, NgRLK1 from *N. glutinosa* and NbLRK1 from *N. benthamiana* interact with the extracellular proteins (elicitins) from *Phytophthora capsici* fungi (Kim et al., 2010) and *P. infestans* (Kanzaki et al., 2008), respectively. Also, in rice the LRK Pi-d2 confers resistance to *Magnaporthe grisea* fungi (Chen et al., 2006). NaLecRK1 displayed amino acid sequence to NgRLK1, NbLRK1 and Pi-d2, which suggest that NaLecRK1 may also participate in the pathogen response.

In *N. attenuata,* one of the earliest events differentially induced by OS and FACs compared to wounding is the activation of the protein kinases WIPK and SIPK (Wu et al., 2007). Activation of these protein kinases takes place immediately after wounding and is augmented several-fold by additional supply of *M. sexta* OS (Wu et al., 2007). In this study, I evaluated the dependence of Na*LecRK1* mRNA regulation on WIPK and SIPK. I found that silencing of SIPK and WIPK (ir-sipk and ir-wipk) largely abolished the transcriptional activation of Na*LecRK1* after 18:3-Glu elicitation, suggesting a positive regulation of SIPK and WIPK in Na*LecRK1* transcriptional regulation. A JA burst also occurrs upon *M. sexta* herbivory in *N. attenuata* (Halitschke et al., 2001), thus I also evaluated the transcriptional regulation of Na*LecRK1* in plants deficient in JA biosynthesis or perception and found that jasmonates inhibit the induction of this gene. These results revealed that the induction of Na*LecRK1* expression is under tight temporal control; it is induced by OS/FAC elicitation but the levels of induction are checked by JA, which is produced following OS/FAC elicitation.

In *N. attenuata*, responses to *M. sexta* herbivory and OS or FAC elicitation overlap by 80% (Halitschke et al., 2001) and include changes in the expression of more than 500 genes, 90 proteins, 170 primary and secondary metabolites and the differential production

of JA, ET and SA (Hermsmeier et al., 2001; Giri et al., 2006; Gaquerel et al., 2010; Kallenbach et al., 2010). JA and JA-Ile play essential roles in mediating plant responses to chewing arthropods (Wang et al., 2007; Howe and Jander, 2008), whereas SA coordinates the elicitation of defense responses against biotrophic pathogens (Ryals et al., 1996; Rivas-San Vicente and Plasencia, 2011) and in herbivore defense responses, SA antagonizes JA induced defenses (Diezel et al., 2009). When Na*LecRK1* expression is silenced (ir-lecRK1 plants), elicitation of ir-lecRK1 leaves by *M. sexta* OS and larval folivory induced the accumulation of SA to levels 2-fold higher than those in WT plants. This suggests that Na*LecRK1* expression negatively controls the amount of SA produced by *N. attenuata* upon herbivory and thereby the differential induction of defense responses (see below).

As introduced in chapter 1, *N. attenuata* plants posses a broad arsenal of defense metabolites known to interfere with larval growth and fitness, including 17-hydroxygeranyllinalool diterpene glycosides (HGL-DTGs), nicotine, phenylpropanoid-polyamine conjugates and protease inhibitors (PIs). In tomato (*Solanum lycopersicum*) and *N. attenuata*, the induction of threonine deaminase (TD) is also a critical induced defense response (Chen et al., 2005; Kang et al., 2006). Threonine deaminase (TD) catalyzes the formation of Threonine (Thr) to α-ketobutyrate in the isoleucine (Ile) biosynthetic pathway. In *N. attenuata* reduced Na*TD* expression compromises the levels of JA-Ile formation in leaves and thereby the induction of defense responses (Kang et al., 2006). In tomato, loss of the regulatory domain of TD deaminates Thr in the gut of *M. sexta* larvae and thereby reduces the ingested levels of this essential amino acid (Chen et al., 2005). When *N. attenuata* plants are compromised in the accumulation of HGL-DTGs (Jassbi et al., 2008) or nicotine (Steppuhn et al., 2004), or in the expression of TPI (Zavala et al., 2004) or Na*TD* (Kang et al., 2006), *M. sexta* larvae feeding on these plants gain more mass than larvae feeding on WT plants. Consistent with these previous studies, an increased performance of *M. sexta* larvae on ir-lecRK1 plants was accompanied by reductions in the induced accumulation of HGL-DTGS, TPIs, nicotine, and Na*TD* expression.

The specificity of a defense response to a particular attacker is the result of fine-tuned interplay among signal transduction pathways. In *N.attenuata*, the production of

defense secondary metabolites against *M. sexta* is mainly regulated by JA and JA-Ile and modulated by the action of SA and ET (Diezel et al., 2009; Leon-Reyes et al., 2009; Pieterse et al., 2009). Previous studies have pointed to a dose-dependent antagonism of SA on JA-mediated herbivore defenses (Doares et al., 1995; Diezel et al., 2009; Pieterse et al., 2009; Smith et al., 2009). In this study, I quantified the levels of JA, JA-Ile, SA and ethylene accumulation in order to evaluate whether silencing Na*LecRK1* expression affects the biosynthesis of these phytohormones and consequently influences the accumulation of secondary metabolites. The results showed reduced levels of JA-Ile after OS elicitation which, in line with previous studies (Kang et al., 2006; Steppuhn et al., 2004; Zavala et al., 2004; Heiling, Schuman et al., 2010) could lead to lower accumulation of HGL-DTGs, nicotine, or TPI, or Na*TD* expression. However, the 2-fold increase in SA levels as compared to WT levels of JA-Ile after *M. sexta* herbivory on ir-lecRK1 plants, led to the hypothesis that reduced levels of nicotine, HGL-DTGs, TPI, and Na*TD* expression were the result of SA-mediated suppression of JA and JA-Ile induced defense responses. To test this hypothesis, we generated *N. attenuata* plants ectopically expressing a bacterial *nahG* gene (ov-nahg) that were able to deplete endogenous SA levels. To reduce the SA levels in ir-lecRK1 plants, the ov-nahg plants were crossed with ir-lecRK1 plants to generate ir-lecRK1xov-nahG plants. The reduction of SA levels in ir-lecRK1xov-nahG plants was sufficient to recover the defense response as shown by *M. sexta* larval performance assays in which larvae performed similar in WT, ov-nahg and ir-lecRK1xov-nahG. Upon quantification of the accumulation of defense secondary metabolites, I found that the total HGL-DTG levels and TPI activity were fully recovered in ir-lecRK1xov-nahG plants, suggesting that the accumulation of these compounds was suppressed by SA in ir-lecRK1 plants. In contrast, nicotine levels were only partially recovered in lecRK1xov-nahG plants compared to WT plants. This partial recovery could be explained by the fact that nicotine levels were significantly reduced by 15% in ov-nahG plants compared to WT, indicating that the ectopic expression of *nahG* negatively affects nicotine accumulation. Na*TD* expression was also partially recovered in ir-lecRK1xov-nahG plants compared WT. As Na*TD* expression levels were similar between WT and ov-nahG plants, this partial recovery was probably the result of a partial involvement of the OS-elicited SA burst in the suppression of Na*TD* expression in ir-lecRK1 plants.

In summary, these results demonstrated that the suppression of the OS/*M. sexta*-elicited SA burst in ir-lecRK1 plants decreased the performance of *M. sexta* larvae. This suppression was sufficient to fully restore the induced accumulation of HGL-DTGs and TPI activity and to partially restore the induced accumulation of nicotine and Na*TD* expression in ir-lecRK1 plants to WT levels. We concluded that NaLecRK1 negatively regulates the SA burst, allowing the unfettered elicitation of JA-mediated defenses.

Analysis of C_{12} derivatives of the HPL pathway.

The hydroperoxide lyase (HPL) pathway in plants uses 13-hydroperoxy derivatives of polyunsaturated C_{18} fatty acids to produced C_6 aldehyde volatiles and unsaturated C_{12} ω-oxo-acids (12-oxo-9*Z*-dodecenoic acid or (9*Z*)-traumatin). In recent years, research has been extensively exploring the metabolism and function of C_6 volatiles with relatively less attention placed on the metabolism and function of C_{12} acids. One of the first products of the HPL pathway is the formation of (9*Z*)-traumatin which is then oxidized to yield 9-OH-traumatin. The mechanism of formation of 9-OH-traumatin has been controversial, with some results pointing to a enzymatic conversion (Gardner, 1998) and others supporting an non-enzymatic biogenesis (Noordermeer et al., 2000). Our results were in agreement with both mechanims: one-third of *de novo* produced 9-OH-traumatin originated non-ezymatically and the remaining two-thirds originated enzymatically in a mechanism dependent indirectly or directly on NaLOX2 activity. 9-OH-traumatin is a reactive electrophile species (RES) which forms Michael-type adducts with the sulfhydryl group of reduced glutathione (GSH; Farmer and Davoine, 2007; Mueller and Berger, 2009). The formation of oxylipin RES conjugates with GSH has been observed during the hypersensitive response (HR) induced by the fungal elicitor cryptogein in tobacco leaves (Davoine et al., 2006), and it has been proposed that the generation of these conjugates may play a direct role in signaling. One possibility is that 9-OH-traumatin conjugated to GSH plays signaling roles in *N. attenuata'*s responses to wounding and herbivory. The precursor (9*Z*)-traumatin is additionally converted to (2*E*)-traumatic acid, and then into (3*Z*)-traumatic acid and 12-OH-(9*Z*)-dodecenoic acid.

Chapter 6

The signaling role of the C_{12} derivatives was assessed by gene expression analysis using microarrays. A total of 320 genes were differentially regulated by C_{12} derivatives, among them several involved in oxidative stress and protein chemical modification. Additionally, transcription factors involved in plant defense responses (MYC transcription factors) and signaling genes have been identified. These results strongly suggested that the C_{12} derivatives of the HPL pathway play a role in *N. attenuata*'s response to wounding and probably to herbivory as well.

Summary

Plants have evolved sophisticated mechanisms to specifically recognize attacker-derived molecules and respond consequently. *Nicotiana attenuata* is an annual fire-chasing plant native to the Great Basin desert of the southwestern USA which has evolved a plethora of induced responses against a large number of generalist and specialist herbivore species. *N. attenuata* identifies the nature of the attacker by recognizing elicitors present in the herbivore oral secretions (OS). The hornworm *Manduca sexta* is often the main insect defoliator of *N.attenuata* plants, and the most potent elicitors present in its OS are fatty acid-amino acid conjugates (FACs). The presence of FACs is necessary and sufficient for the elicitation of jasmonic acid (JA) and ethylene (ET) production, triggering the accumulation of secondary metabolites, and for most of the herbivore-induced transcriptional changes and metabolic responses. The mechanism by which plants perceive FACs and activate signal transduction mechanisms to induce these specific defense responses remain at present largely unknown.

In order to unravel these mechanisms, in this thesis I investigated the early cellular events triggered by FACs in *N. attenuatta* leaves. For this purpose, SuperSAGE was used to find early transcriptional targets of the FAC signal transduction pathway with the goal of identifying regulatory components of insect mediated responses. I generated two SuperSAGE libraries from FAC-elicited and wounded (control) leaf samples for the identification of transcripts rapidly and differentially regulated by FACs. From 12,744 unique transcript sequences identified (UniTags), 429 and 117 were significantly up- and down-regulated ≥2.5-≤0.4 fold, respectively, after 18:3-Glu elicitation compared to wounding. Based on gene ontology classification, more than 25% of the annotated Unitags corresponded to putative regulatory components. qPCR analysis confirmed the FAC regulation of 70% of a subset of 27 UniTags selected. Seven FAC-regulated genes were functionally characterized by VIGS and three, a G-type lectin receptor-like kinase (LecRK1), a putative lipid phosphate phosphatase (LPP) and a protein of unknown function (UnkA), were identified as important mediators of the *M. sexta-N. attenuata* interaction.

Summary

I characterized the G-type lectin receptor-like kinase (Na*LecRK1*) gene in more detail. Silencing the expression of Na*LecRK1* by VIGS or RNAi (ir-lecRK1 plants) highlighted its importancein the regulation of the defense response to *M. sexta* herbivory. *M. sexta* larvae fed on ir-lecRK1 plants were 40 to 100% larger than those fed on WT plants, and this corresponded to a several-fold reduction in the accumulation of jasmonate-mediated defense metabolites such as nicotine, 17-hydroxygeranyllinalool diterpene glycosides (HGL-DTGs) and tripsin protease inhibitos (TPI) or Na*TD* expression. The production of jasmonic acid (JA) and jasmonyl-isoleucine (JA-Ile) was unaffected during *M. sexta* herbivory in ir-lecRK1 plants; however, the production of salicylic acid (SA) was twice that in WT plants. Suppression of the SA burst by introgression of the *nahG* gene into ir-lecRK1 plants demonstrated that the increased OS-elicited SA formation was responsible for the inhibition of nicotine, HGL-DTG and TPIs accumulation and Na*TD* expression, as well as for the enhanced performance of *M. sexta* larvae on these plants.

I also contributed to the understanding of the biogenesis and function of the C_{12} derivatives of the HPL pathway in *N. attenuata* plants after wounding and herbivory, as well as a functional understanding of the role of these C_{12} derivatives in plant responses to wounding and herbivory.

Zusammenfassung

Pflanzen haben ausgeklügelte Mechanismen entwickelt um herbivoren-spezifische Substanzen zu erkennen und dementsprechend auf eine Attacke zu reagieren. *Nicotiana attenuata*, eine einjährige Pflanze beheimatet im Südwesten der USA, muss sich gegen eine Vielzahl verschiedener Pflanzenfresser verteidigen und hat deshalb vielfältige induzierbare Vertedigungsmechanismen entwickelt. Die Identität des jeweiligen Angreifers indentifiziert *N. attenuata* indem die Pflanze spezielle Moleküle aus dem Oralsekret (OS) wahrnimmt. Einer der wichtigsten Frassfeinde von *N. attenuata* ist die Raupe des Tabakschwärmers *Manduca sexta*. Das Oralsekret von *M. sexta* enthält verschiedene Fettsäure-Aminosäure-Konjugate (FACs) und diese FACs sind in der Lage, die Biosynthese und Akkumulation von Jasmonsäure (JA) und Ethylen (ET) in der Pflanze auszulösen. JA und ET steuern ihrerseits die Akkumulation von Sekundärmetaboliten. Desweiteren wird durch FACs eine herbvioren-spezifische Expression von Verteidungsgenen ausgelöst sowie weitere metabolische Veränderungen. Allerdings ist es zum jetzigen Zeitpunkt größtenteils unbekannt, wie Pflanzen FACs erkennen und dadurch Signal-transduktionsmechanismen aktivieren um die spezifischen Verteidigungsreaktionen zu induzieren.

Um die oben genannte Abläufe in der Pflanze besser zu verstehen, habe ich in dieser Arbeit die früheren, durch FACs ausgelösten zellulären Ereignisse in *N. attenuata* Blättern untersucht. Zu diesem Zweck wurde die SuperSAGE Technologie verwendet, die es ermöglicht, frühe transkriptionelle Ziele des FAC Signaltransduktionsweges zu identifizieren. Ziel dieser Technik ist die Identifizierung von regulatorischen Komponenten der durch Insekten ausgelösten Reaktionen. Ich habe hierzu zwei SuperSAGE Bibliotheken, von entweder nur verwundeten oder zusätzlich FAC induzierten Blattproben erstellt, um Transkripte zu identifizieren, die unverzüglich und spezifisch von FACs reguliert werden. Von 12.744 identifizierten Transkriptsequenzen (UniTags) zeigten in FAC induzierten Proben 429 signifikant erhöhte Transkription (≥ 2,5-fach) und 117 signifikant verminderte Transkription (≤ 0.4-fach) im Vergleich zu ausschliesslich verwundeten Blattproben. Mehr als 25% der annotierten Unitags entsprachen, basierend auf Genontology, putativen regulatorischen Komponenten. Eine qPCR Analyse bestätigte die

FAC basierte Regulation von 70% der 27 ausgewählten UniTags. Sieben FAC-regulierte Gene wurden in *N. attenuata* mithilfe von „virus-induced-gene-silencing“ (VIGS) untersucht und drei dieser Gene, eine G-Typ Lectin rezeptor-ähnliche Kinase (LecRK1), eine mutmassliche Lipid Phosphat Phosphatase (LPP) und ein Protein mit inbekannter Funktion (UnkA), wurden als wichtige Mediatoren der *M. sexta*-*N. attenuata* Interaktion identifiziert.

Anschließend habe ich die G-Typ Lectin rezeptor-ähnliche Kinase (LecRK1) detailierter charakterisiert. Die Verminderung der Transkription von LecRK1 in *N. attenuata* (NaLecRK1), entweder mithilfe von VIGS oder „inverted-repeat-RNA-interference“ (ir-*lecrRK1* Pflanzen), hob die Wichtigkeit von NaLecRK1 in der Regulierung von Abwehrmechanismen gegen *M. sexta* Attacken hervor. *M. sexta* Raupen, die auf ir-*lecRK1* Pflanzen fraßen, wurden 40% - 100% größer als Raupen die zur gleichen Zeit auf Wildtyp (WT) Pflanzen fraßen. Dies resultierte aus der in ir-*LecRK1* verminderten Akkumulierung von Verteidigungssubstanzen, wie beispielsweise Nikotin, glykosidische Diterpene (HGL-DTGs), Trypsin-proteinase-inhibitoren (TPI), oder verminderte Expression von NaTD. Die Synthese von JA und JA-isoleucin (JA-Ile) wurde während *M. sexta* Fraß in ir-*lecRK1* Pflanzen nicht beeinflusst, jedoch zeigte sich in Vergleich zu WT Pflanzen eine 2-fach erhöhte Salizylsäure (SA)-synthese. Durch die Unterdrückung der SA Akkumulierung durch Introgression des *nahG* Gens in ir-*lecRK1* Pflanzen konnte ich zeigen, dass die durch *M. sexta* OS induzierte SA-produktion die Ursache für die oben genannten Unterschiede zu WT Pflanzen war.

Desweiteren habe ich geholfen, die Biogenese und Funktion der nach Pflanzenverwundung und –herbivorie durch HPL produzierten C_{12}-Derviate in *N. attenuata* zu untersuchen. Wir untersuchten die Funktion dieser C_{12} Derivate während der Reaktion der Pflanze auf Verwundung und Herbivorie.

References

Alborn, H.T., Turlings, T.C., Jones, T.H., Stenhagen, G., Loughrin, J.H., and Tumlinson, J.H. (1997). An elicitor of plant volatiles from beet armyworm oral secretion. Science **276,** 945-949.

Alborn, H.T., Hansen, T.V., Jones, T.H., Bennett, D.C., Tumlinson, J.H., Schmelz, E.A., and Teal, P.E. (2007). Disulfooxy fatty acids from the American bird grasshopper *Schistocerca americana*, elicitors of plant volatiles. Proc Natl Acad Sci USA **104,** 12976-12981.

Allmann, S., and Baldwin, I.T. (2010). Insects Betray Themselves in Nature to Predators by Rapid Isomerization of Green Leaf Volatiles. Science **329,** 1075-1078.

Arimura, G.-i., Kost, C., and Boland, W. (2005). Herbivore-induced, indirect plant defences. Biochimica et Biophysica Acta (BBA) - Molecular and Cell Biology of Lipids 1734, 91-111.

Baldwin, I.T. (1988). Damage-induced alkaloids in tobacco: Pot-bound plants are not inducible. Journal of Chemical Ecology **14,** 1113-1120.

Baldwin, I.T., and Morse, L. (1994). Up in smoke: II. Germination of *Nicotiana attenuata* in response to smoke-derived cues and nutrients in burned and unburned soils. Journal of Chemical Ecology **20,** 2373-2391.

Baldwin, I.T., Zhang, Z.-P., Diab, N., Ohnmeiss, T.E., McCloud, E.S., Lynds, G.Y., and Schmelz, E.A. (1997). Quantification, correlations and manipulations of wound-induced changes in jasmonic acid and nicotine in *Nicotiana sylvestris*. Planta 201, 397-404.

Baldwin, I.T. (1998). Jasmonate-induced responses are costly but benefit plants under attack in native populations. Proc Natl Acad Sci USA **95,** 8113-8118.

Baldwin, I.T. (2001). An Ecologically Motivated Analysis of Plant-Herbivore Interactions in Native Tobacco. Plant Physiology **127,** 1449-1458.

Baldwin, I.T. (2010). Plant volatiles. Current biology : CB **20,** R392-R397.

Bari, R., and Jones, J. (2009). Role of plant hormones in plant defence responses. Plant Molecular Biology **69,** 473-488.

Block, A., Schmelz, E., Jones, J.B., and Klee, H.J. (2005). Coronatine and salicylic acid: the battle between Arabidopsis and Pseudomonas for phytohormone control. Molecular Plant Pathology **6,** 79-83.

Bodenhausen, N., and Reymond, P. (2007). Signaling Pathways Controlling Induced Resistance to Insect Herbivores in Arabidopsis. Molecular Plant-Microbe Interactions **20,** 1406-1420.

Bonaventure, G., Vandoorn, A., and Baldwin, I.T. (2011). Herbivore-associated elicitors: FAC signaling and metabolism. Trends Plant Sci.

References

Bouwmeester, K., and Govers, F. (2009). Arabidopsis L-type lectin receptor kinases: phylogeny, classification, and expression profiles. Journal of Experimental Botany **60,** 4383-4396.

Chen, H., Wilkerson, C.G., Kuchar, J.A., Phinney, B.S., and Howe, G.A. (2005). Jasmonate-inducible plant enzymes degrade essential amino acids in the herbivore midgut. Proc Natl Acad Sci USA **102,** 19237-19242.

Chen, M.-S. (2008). Inducible direct plant defense against insect herbivores: A review. Insect Science **15,** 101-114.

Chen, X., Shang, J., Chen, D., Lei, C., Zou, Y., Zhai, W., Liu, G., Xu, J., Ling, Z., Cao, G., Ma, B., Wang, Y., Zhao, X., Li, S., and Zhu, L. (2006). A B-lectin receptor kinase gene conferring rice blast resistance. The Plant Journal **46,** 794-804.

Collatz, K.-G., and Mommsen, T. (1974). Die Struktur der emulgierenden Substanzen verschiedener Invertebraten. Journal of Comparative Physiology B: Biochemical, Systemic, and Environmental Physiology **94,** 339-352.

Croft, K., Juttner, F., and Slusarenko, A.J. (1993). Volatile Products of the Lipoxygenase Pathway Evolved from *Phaseolus vulgaris* (L.) Leaves Inoculated with *Pseudomonas syringae pv phaseolicola*. Plant Physiol **101,** 13-24.

Croteau, R., Kutchan, T. M., and Lewis, N. G. . (2000). Natural products (secondary metabolites). In Biochemistry and Molecular Biology of Plants. , W.G. In B. Buchanan, and R. Joneas, eds., ed American Society of Plant Biologists, Rockville, MD., pp. 1250–1268

Davies, P. (1995). The Plant Hormones: Their Nature, Occurrence and Functions. In Plant Hormones, P.J. Davies, ed (Springer Netherlands), pp. 1-15.

Davoine, C., Falletti, O., Douki, T., Iacazio, G., Ennar, N., Montillet, J.-L., and Triantaphylidès, C. (2006). Adducts of Oxylipin Electrophiles to Glutathione Reflect a 13 Specificity of the Downstream Lipoxygenase Pathway in the Tobacco Hypersensitive Response. Plant Physiol **140,** 1484-1493.

Diezel, C., von Dahl, C.C., Gaquerel, E., and Baldwin, I.T. (2009). Different lepidopteran elicitors account for cross-talk in herbivory-induced phytohormone signaling. Plant Physiol **150,** 1576-1586.

Doares, S.H., Narvaez-Vasquez, J., Conconi, A., and Ryan, C.A. (1995). Salicylic Acid Inhibits Synthesis of Protease Inhibitors in Tomato Leaves Induced by Systemin and Jasmonic Acid. Plant Physiol **108,** 1741-1746.

Doherty, H.M., Selvendran, R.R., and Bowles, D.J. (1988). The wound response of tomato plants can be inhibited by aspirin and related hydroxy-benzoic acids. Physiological and Molecular Plant Pathology **33,** 377-384.

Farmer, E.E., and Davoine, C. (2007). Reactive electrophile species. Current Opinion in Plant Biology **10,** 380-386.

Farmer, E.E., Alméras, E., and Krishnamurthy, V. (2003). Jasmonates and related oxylipins in plant responses to pathogenesis and herbivory. Current Opinion in Plant Biology **6,** 372-378.

References

Fonseca, S., Chico, J.M., and Solano, R. (2009). The jasmonate pathway: the ligand, the receptor and the core signalling module. Current Opinion in Plant Biology **12,** 539-547.

Gao, L.-L., Anderson, J.P., Klingler, J.P., Nair, R.M., Edwards, O.R., and Singh, K.B. (2007). Involvement of the Octadecanoid Pathway in Bluegreen Aphid Resistance in *Medicago truncatula*. Molecular Plant-Microbe Interactions **20,** 82-93.

Gaquerel, E., Heiling, S., Schoettner, M., Zurek, G., and Baldwin, I.T. (2010). Development and Validation of a Liquid Chromatography−Electrospray Ionization−Time-of-Flight Mass Spectrometry Method for Induced Changes in *Nicotiana attenuata* Leaves during Simulated Herbivory. Journal of Agricultural and Food Chemistry **58,** 9418-9427.

Gardner, H. (1998). 9-Hydroxy-traumatin, a new metabolite of the lipoxygenase pathway. Lipids **33,** 745-749.

Giri, A.P., Wünsche, H., Mitra, S., Zavala, J.A., Muck, A., Svatos, A., and Baldwin, I.T. (2006). Molecular Interactions between the Specialist Herbivore *Manduca sexta* (Lepidoptera, Sphingidae) and Its Natural Host *Nicotiana attenuata.* VII. Changes in the Plant's Proteome. Plant Physiol **142,** 1621-1641.

Grechkin, A.N. (2002). Hydroperoxide lyase and divinyl ether synthase. Prostaglandins & Other Lipid Mediators **68-69,** 457-470.

Gupta, V., Willits, M.G., and Glazebrook, J. (2000). *Arabidopsis thaliana* EDS4 Contributes to Salicylic Acid (SA)-Dependent Expression of Defense Responses: Evidence for Inhibition of Jasmonic Acid Signaling by SA. Molecular Plant-Microbe Interactions **13,** 503-511.

Halitschke, R., Schittko, U., Pohnert, G., Boland, W., and Baldwin, I.T. (2001). Molecular Interactions between the Specialist Herbivore *Manduca sexta* (Lepidoptera, Sphingidae) and Its Natural Host *Nicotiana attenuata.* III. Fatty Acid-Amino Acid Conjugates in Herbivore Oral Secretions Are Necessary and Sufficient for Herbivore-Specific Plant Responses. Plant Physiol **125,** 711-717.

Halitschke, R., Gase, K., Hui, D., Schmidt, D.D., and Baldwin, I.T. (2003). Molecular Interactions between the Specialist Herbivore *Manduca sexta* (Lepidoptera, Sphingidae) and Its Natural Host *Nicotiana attenuata*. VI. Microarray Analysis Reveals That Most Herbivore-Specific Transcriptional Changes Are Mediated by Fatty Acid-Amino Acid Conjugates. Plant Physiol **131,** 1894-1902.

Harborne, J.B. (1999). Classes and functions of secondary products from plants, in Walton N.J. and Brown D.E. (eds), Chemicals from plants-perspectives on plant secondary products:. London, Imperial College Press**,** p. 1-25.

Heil, M., Koch, T., Hilpert, A., Fiala, B., Boland, W., and Linsenmair, K.E. (2001). Extrafloral nectar production of the ant-associated plant, *Macaranga tanarius*, is an induced, indirect, defensive response elicited by jasmonic acid. Proc Natl Acad Sci USA **98,** 1083-1088.

References

Heiling, S., Schuman, M.C., Schoettner, M., Mukerjee, P., Berger, B., Schneider, B., Jassbi, A.R., and Baldwin, I.T. (2010). Jasmonate and ppHsystemin Regulate Key Malonylation Steps in the Biosynthesis of 17-Hydroxygeranyllinalool Diterpene Glycosides, an Abundant and Effective Direct Defense against Herbivores in *Nicotiana attenuata*. Plant Cell **22,** 273-292.

Hermsmeier, D., Schittko, U., and Baldwin, I.T. (2001). Molecular Interactions between the Specialist Herbivore *Manduca sexta* (Lepidoptera, Sphingidae) and Its Natural Host *Nicotiana attenuata*. I. Large-Scale Changes in the Accumulation of Growth- and Defense-Related Plant mRNAs. Plant Physiol **125,** 683-700.

Howe, G.A., and Schilmiller, A.L. (2002). Oxylipin metabolism in response to stress. Current Opinion in Plant Biology **5,** 230-236.

Howe, G.A., and Jander, G. (2008). Plant Immunity to Insect Herbivores. Annual review of plant biology **59,** 41-66.

Jassbi, A.R., Gase, K., Hettenhausen, C., Schmidt, A., and Baldwin, I.T. (2008). Silencing geranylgeranyl diphosphate synthase in Nicotiana attenuata dramatically impairs resistance to tobacco hornworm. Plant Physiol **146,** 974-986.

Kallenbach, M., Alagna, F., Baldwin, I.T., and Bonaventure, G. (2010). *Nicotiana attenuata* SIPK, WIPK, NPR1, and Fatty Acid-Amino Acid Conjugates Participate in the Induction of Jasmonic Acid Biosynthesis by Affecting Early Enzymatic Steps in the Pathway. Plant Physiol **152,** 96-106.

Kang, J.H., Wang, L., Giri, A., and Baldwin, I.T. (2006). Silencing threonine deaminase and JAR4 in *Nicotiana attenuata* impairs jasmonic acid-isoleucine-mediated defenses against *Manduca sexta*. Plant Cell **18,** 3303-3320.

Kanzaki, H., Saitoh, H., Takahashi, Y., Berberich, T., Ito, A., Kamoun, S., and Terauchi, R. (2008). NbLRK1, a lectin-like receptor kinase protein of *Nicotiana benthamiana*, interacts with *Phytophthora infestans* INF1 elicitin and mediates INF1-induced cell death. Planta **228,** 977-987.

Kaur, H., Heinzel, N., Schöttner, M., Baldwin, I.T., and Gális, I. (2010). R2R3-NaMYB8 Regulates the Accumulation of Phenylpropanoid-Polyamine Conjugates, Which Are Essential for Local and Systemic Defense against Insect Herbivores in *Nicotiana attenuata*. Plant Physiol **152,** 1731-1747.

Kessler, A., and Baldwin, I.T. (2002). PLANT RESPONSES TO INSECT HERBIVORY: The Emerging Molecular Analysis. Annual Review of Plant Biology **53,** 299-328.

Kessler, A., Halitschke, R., and Baldwin, I.T. (2004). Silencing the Jasmonate Cascade: Induced Plant Defenses and Insect Populations. Science **305,** 665-668.

Kim, Y.-T., Oh, J., Kim, K.-H., Uhm, J.-Y., and Lee, B.-M. (2010). Isolation and characterization of a receptor-like kinase of *Nicotiana glutinosa* that interacts with the elicitin of *Phytophthora capsici*. Molecular Biology Reports **37,** 717-727.

Lawrence, P.K., and Koundal, K.R. (2002). Plant protease inhibitors in control of phytophagous insects. Electronic Journal of Biotechnology **5,** 5-6.

References

Lee, H.I., León, J., and Raskin, I. (1995). Biosynthesis and metabolism of salicylic acid. Proc Natl Acad Sci USA **92,** 4076-4079.

Leon-Reyes, A., Spoel, S.H., De Lange, E.S., Abe, H., Kobayashi, M., Tsuda, S., Millenaar, F.F., Welschen, R.A.M., Ritsema, T., and Pieterse, C.M.J. (2009). Ethylene Modulates the Role of NONEXPRESSOR OF PATHOGENESIS-RELATED GENES1 in Cross Talk between Salicylate and Jasmonate Signaling. Plant Physiol **149,** 1797-1809.

Li, C., Williams, M.M., Loh, Y.-T., Lee, G.I., and Howe, G.A. (2002). Resistance of Cultivated Tomato to Cell Content-Feeding Herbivores Is Regulated by the Octadecanoid-Signaling Pathway. Plant Physiol **130,** 494-503.

Li, J., Brader, G., and Palva, E.T. (2004). The WRKY70 Transcription Factor: A Node of Convergence for Jasmonate-Mediated and Salicylate-Mediated Signals in Plant Defense. The Plant Cell Online **16,** 319-331.

Loake, G., and Grant, M. (2007). Salicylic acid in plant defence--the players and protagonists. Current Opinion in Plant Biology **10,** 466-472.

Lou, Y., and Baldwin, I.T. (2006). Silencing of a Germin-Like Gene in *Nicotiana attenuata* Improves Performance of Native Herbivores. Plant Physiol **140,** 1126-1136.

Maffei, M., Bossi, S., Spiteller, D., Mithöfer, A., and Boland, W. (2004). Effects of Feeding *Spodoptera littoralis* on Lima Bean Leaves. I. Membrane Potentials, Intracellular Calcium Variations, Oral Secretions, and Regurgitate Components. Plant Physiol **134,** 1752-1762.

Matsumura, H., Ito, A., Saitoh, H., Winter, P., Kahl, G., Reuter, M., Krüger, D.H., and Terauchi, R. (2005). SuperSAGE. Cellular Microbiology **7,** 11-18.

Matsumura, H., Reich, S., Ito, A., Saitoh, H., Kamoun, S., Winter, P., Kahl, G., Reuter, M., Krüger, D.H., and Terauchi, R. (2003). Gene expression analysis of plant host–pathogen interactions by SuperSAGE. Proc Natl Acad Sci USA **100,** 15718-15723.

Millar, N., and Denholm, I. (2007). Nicotinic acetylcholine receptors: targets for commercially important insecticides. Invertebrate Neuroscience **7,** 53-66.

Mueller, M.J., and Berger, S. (2009). Reactive electrophilic oxylipins: Pattern recognition and signalling. Phytochemistry **70,** 1511-1521.

Musser, R.O., Hum-Musser, S.M., Eichenseer, H., Peiffer, M., Ervin, G., Murphy, J.B., and Felton, G.W. (2002). Herbivory: caterpillar saliva beats plant defences. Nature **416,** 599-600.

Nemhauser, J.L., Hong, F., and Chory, J. (2006). Different Plant Hormones Regulate Similar Processes through Largely Nonoverlapping Transcriptional Responses. Cell **126,** 467-475.

Noordermeer, M.A., Feussner, I., Kolbe, A., Veldink, G.A., and Vliegenthart, J.F.G. (2000). Oxygenation of (3Z)-Alkenals to 4-Hydroxy-(2E)-Alkenals in Plant Extracts: A Nonenzymatic Process. Biochemical and Biophysical Research Communications **277,** 112-116.

References

O'Donnell, P.J., Calvert, C., Atzorn, R., Wasternack, C., Leyser, H.M.O., and Bowles, D.J. (1996). Ethylene as a Signal Mediating the Wound Response of Tomato Plants. Science **274,** 1914-1917.

Pieterse, C.M.J., Leon-Reyes, A., Van Der Ent, S., and Van Wees, S.C.M. (2009). Networking by small-molecule hormones in plant immunity. Nature Chemical Biology **5,** 308-316.

Rayapuram, C., and Baldwin, I.T. (2007). Increased SA in NPR1-silenced plants antagonizes JA and JA-dependent direct and indirect defenses in herbivore-attacked *Nicotiana attenuata* in nature. The Plant Journal **52,** 700-715.

Reymond, P., and Farmer, E.E. (1998). Jasmonate and salicylate as global signals for defense gene expression. Current Opinion in Plant Biology **1,** 404-411.

Rivas-San Vicente, M., and Plasencia, J. (2011). Salicylic acid beyond defence: its role in plant growth and development. Journal of Experimental Botany.

Ryals, J.N., UH; Willits, MG; Molina, A; Steiner, HY; and Hunt, MD (1996). Systemic Acquired Resistance. Plant Cell **8,** 1809–1819.

Schaller, F., Schaller, A., and Stintzi, A. (2004). Biosynthesis and Metabolism of Jasmonates. Journal of Plant Growth Regulation **23,** 179-199.

Schittko, U., Hermsmeier, D., and Baldwin, I.T. (2001). Molecular Interactions between the Specialist Herbivore *Manduca sexta* (Lepidoptera, Sphingidae) and Its Natural Host *Nicotiana attenuata.* II. Accumulation of Plant mRNAs in Response to Insect-Derived Cues. Plant Physiol **125,** 701-710.

Schmelz, E.A., Engelberth, J., Alborn, H.T., Tumlinson, J.H., and Teal, P.E.A. (2009). Phytohormone-based activity mapping of insect herbivore-produced elicitors. Proc Natl Acad Sci USA **106,** 653-657.

Schmelz, E.A., Carroll, M.J., LeClere, S., Phipps, S.M., Meredith, J., Chourey, P.S., Alborn, H.T., and Teal, P.E. (2006). Fragments of ATP synthase mediate plant perception of insect attack. Proc Natl Acad Sci USA **103,** 8894-8899.

Schwachtje, J., Minchin, P.E.H., Jahnke, S., van Dongen, J.T., Schittko, U., and Baldwin, I.T. (2006). SNF1-related kinases allow plants to tolerate herbivory by allocating carbon to roots. Proc Natl Acad Sci USA **103,** 12935-12940.

Schwachtje, J., and Baldwin, I.T. (2008). Why Does Herbivore Attack Reconfigure Primary Metabolism? Plant Physiol 146, 845-851.

Skibbe, M., Qu, N., Galis, I., and Baldwin, I.T. (2008). Induced Plant Defenses in the Natural Environment: *Nicotiana attenuata* WRKY3 and WRKY6 Coordinate Responses to Herbivory. The Plant Cell Online **20,** 1984-2000.

Smith, J.L., De Moraes, C.M., and Mescher, M.C. (2009). Jasmonate- and salicylate-mediated plant defense responses to insect herbivores, pathogens and parasitic plants. Pest Management Science **65,** 497-503.

Staswick, P.E., and Tiryaki, I. (2004). The Oxylipin Signal Jasmonic Acid Is Activated by an Enzyme That Conjugates It to Isoleucine in Arabidopsis. The Plant Cell Online **16,** 2117-2127.

References

Steppuhn, A., Gase, K., Krock, B., Halitschke, R., and Baldwin, I.T. (2004). Nicotine's Defensive Function in Nature. PLoS Biol **2,** e217.

Stotz, H., Koch, T., Biedermann, A., Weniger, K., Boland, W., and Mitchell-Olds, T. (2002). Evidence for regulation of resistance in Arabidopsis to Egyptian cotton worm by salicylic and jasmonic acid signaling pathways. Planta **214,** 648-652.

Truitt, C.L., Wei, H.-X., and Paré, P.W. (2004). A Plasma Membrane Protein from *Zea mays* Binds with the Herbivore Elicitor Volicitin. The Plant Cell Online **16,** 523-532.

Tumlinson, J.H., and Lait, C.G. (2005). Biosynthesis of fatty acid amide elicitors of plant volatiles by insect herbivores. Archives of Insect Biochemistry and Physiology **58,** 54-68.

Velculescu, V.E., Zhang, L., Vogelstein, B., and Kinzler, K.W. (1995). Serial Analysis of Gene Expression. Science **270,** 484-487.

Vick, B. A., and Zimmerman, D. C. (1976). Lipoxygenase and hydroperoxide lyase in germinating watermelon seedlings. Plant Physiology 57: 780–788.

Vlot, A.C., Dempsey, D.M.A., and Klessig, D.F. (2009). Salicylic Acid, a Multifaceted Hormone to Combat Disease. Annual Review of Phytopathology **47,** 177-206.

von Dahl, C., and Baldwin, I. (2007). Deciphering the Role of Ethylene in Plant–Herbivore Interactions. Journal of Plant Growth Regulation **26,** 201-209.

Wang, K.L.-C., Li, H., and Ecker, J.R. (2002). Ethylene Biosynthesis and Signaling Networks. The Plant Cell Online **14,** S131-S151.

Wang, L., Halitschke, R., Kang, J.-H., Berg, A., Harnisch, F., and Baldwin, I. (2007). Independently silencing two JAR family members impairs levels of trypsin protease inhibitors but not nicotine. Planta **226,** 159-167.

Winz, A. R., and Baldwin, I. T. (2001). Molecular interactions between the specialist herbivore *Manduca sexta* (Lepidoptera, Sphingidae) and its natural host *Nicotiana attenuata*. IV. Insect-induced ethylene reduces jasmonate-induced nicotine accumulation by regulating putrescine N-methyltransferase transcripts. Plant Physiol **125,** 2189-2202.

Wittstock, U., and Gershenzon, J. (2002). Constitutive plant toxins and their role in defense against herbivores and pathogens. Current Opinion in Plant Biology **5,** 300-307.

Wu, J., Hettenhausen, C., Meldau, S., and Baldwin, I.T. (2007). Herbivory Rapidly Activates MAPK Signaling in Attacked and Unattacked Leaf Regions but Not between Leaves of *Nicotiana attenuata*. Plant Cell **19,** 1096-1122.

Yan, J., Zhang, C., Gu, M., Bai, Z., Zhang, W., Qi, T., Cheng, Z., Peng, W., Luo, H., Nan, F., Wang, Z., and Xie, D. (2009). The Arabidopsis CORONATINE INSENSITIVE1 Protein Is a Jasmonate Receptor. The Plant Cell Online **21,** 2220-2236.

Yang, T.F., Gonzalez-Carranza, Z.H., Maunders, M.J., and Roberts, J.A. (2008). Ethylene and the Regulation of Senescence Processes in Transgenic Nicotiana sylvestris Plants. Annals of Botany **101,** 301-310.

References

Yoshinaga, N., Alborn, H., Nakanishi, T., Suckling, D., Nishida, R., Tumlinson, J., and Mori, N. (2010). Fatty Acid-amino Acid Conjugates Diversification in Lepidopteran Caterpillars. Journal of Chemical Ecology **36,** 319-325.

Zarate, S.I., Kempema, L.A., and Walling, L.L. (2007). Silverleaf Whitefly Induces Salicylic Acid Defenses and Suppresses Effectual Jasmonic Acid Defenses. Plant Physiol **143,** 866-875.

Zavala, J.A., Giri, A.P., Jongsma, M.A., and Baldwin, I.T. (2008). Digestive Duet: Midgut Digestive Proteases of *Manduca sexta* Ingesting *Nicotiana attenuata* with Manipulated Trypsin Protease Inhibitor Expression. PLoS ONE **3**, 2008.

Zavala, J.A., Patankar, A.G., Gase, K., Hui, D.Q., and Baldwin, I.T. (2004). Manipulation of endogenous trypsin protease inhibitor production in *Nicotiana attenuata* demonstrates their function as antiherbivore defenses. Plant Physiol **134,** 1181-1190.

Acknowledgements

I would like to express my gratitude to all those who gave me the possibility to complete this thesis, especially to:

- Prof Ian T. Baldwin for his guidance and support during my entire PhD.
- Dr. Gustavo Bonaventure for his kind supervision, guidance and constant support throughout my PhD.
- DAAD for founding.
- All other lab members of department of Molecular ecology, who have helped in one way or the other. Especially to all Lab 17 members for the nice working atmosphere and for eating my stony-cakes.
- GUBO group members for the fruitfuil discussions.
- Our Molecular and Analytical Team. Especially to Antje Wissgott for teaching me how to transform *N. attenuata*.
- Danny and Celi for their help in the field season.
- Dr. Tamara Krügel, Andreas Schünzel and all the gardeners for providing me with a lot of plants. Tamara I will really miss your green hands.
- Dr. Karin Groten for her invaluable help and huge patience.
- Martin Niebergall for fixing my computer even when was a matter of turning it on and off.
- Dr. Emmanuel Gaquerel for introducing me in the world of Metabolomics
- My proofreading team and counseling team: Merry, Rohit, Vari and Mari. And Mario for writing the Zusammenfassung.

But my last 4 years would have been empty if weren't for:

- The Schnapps Leute and the Movie night people.
- Ich danke meinen lieben Nachbarn, den Gallas, die mich wie ein Familienmitglied behandelt haben.
- My friends who were always right there and tolerate my Argentinean explosive temperament. Lady Marian por haberme contenido al principio, por las aventuras en la super city y por haber hecho de tu casa la mia. SuperMerry for trying and really hard to understand the logic of my thoughts, for the loooong walks that exhausted my tongued y

porque sos una gran amiga mia!. Mari e Vari as primeiras brasileiras que gostaram de uma argentina, exceto em jogos de futebol!!. E Vari, não consigo escrever quanto a sua amizade é importante para mim porque sería mais comprida que a minha tese. Mario, you only knows what working with me in Utah means, thanks for share that unique atmosphere. Michi for the lalalas and tralalas. Las hermanas Peru: Yaque y Giova por las chelas compartidas. Arjen for always being next door and for the nice scientific discussions. Markus for tolerating my since the very begging in the lab. Sandy por ser simplemente una tedesca diferente. Arne sharing the office with you was really nice and I think you will miss my sweet voice. Alex for giving always a smile as an answer. Delfi, Kwan, Maaaarten, Martin, Katha, Cori, Daniel and Young Joo for the nice moments.

- A Sofia quien estuvo desde el primer día hasta hoy. Porque compartimos más de un crudo invierno y nos bancamos mutuamente en situaciones buenas y malas. Cuando hay un océano que nos separa de nuestra gente, encontrar a alguien como vos hace todo más fácil. Gracias totales.
- A mis amigos de allá, esos que conozco desde que empecé a caminar hasta el día de hoy: Iva, Floren, Eri, Vale, Bren, Celi, Juli, Nati, Lore, Andre, Rodri, Isa y Lau. Con ustedes me traje los recuerdos más divertidos de mi vida. Las risas compartidas no se erosionaron con el paso del tiempo y fueron mi droga cuando tuve que afrontar el frio alemán.
- A toda la familia que por llamadas, mails y skypeadas siempre estuvo presente. A Valen y mis “sobrinas” (Jose, Malen, Tomi, So, Ju y Marti) por las hermosas obras de arte que decoraron mi cuarto y llenaron mi corazón.
- A mis padres y hermanos por haberme apoyado en la decisión. Y haber estado presente en mis momentos más difíciles: cuando era más fácil hacer las valijas estuvieron ahí para recordarme que mi cuarto había sido usurpado. Especialmente a vos Ma que no me dejaste caer.
- Rohit ko dhanyawad phir se mere dil ko dhadkane ko. Gracias por haberme aguantado las locuras y no haber salido corriendo.
- Sobre todo a mis NONOS que no son doctores ni profesores pero que indudablemente son sabios en temas de familia y amor. Porque son las dos personitas que alimentaron mi corazón constantemente y me dieron fuerzas para seguir.

Curriculum vitae

Personal Information

Name: Paola Alejandra Gilardoni

Date of birth: 30. 07. 1981

Place of birth: Rosario, Argentina

Nationality: Argentinian

Current address: Katharinenstrasse 25, 07743-Jena, Germany

E-mail: pgilardoni@ice.mpg.de

Research experience

- Molecular Biology: DNA and RNA extraction and quantification. Gel electrophoresis. DNA restriction, cloning methods, DNA sequencing. Diverse PCR methods including quantitative real time PCR. Microarray data analysis. Plant transformation. Mammalian cell culture and mouse dissection.
- Biochemistry: Protein extraction and quantification. SDS-PAGE. Western blot.
- Microbiology: Microorganism isolation and identification. Pathogen inoculation in plants.
- Analytical Chemistry: LC-MS/MS and HPLC instrument operation and data analysis. UPLC/ESI-TOF-MS: general data processing and analysis.
- Ecology: identification of insects and insect damage on plants. Herbivore bioassays

Education

2007-present. Ph.D. student at Department of Molecular Ecology, Max Planck Institute for Chemical Ecology and Friedrich Schiller University, Jena, Germany.

2000-2007. School of Biochemical and Pharmaceutical Sciences, Rosario National University, Rosario, Argentina.

Graduation thesis: **"Regulatory mechanism of the expression of the enzyme CTP:phosphocholine cytidylyltransferase isoform β (CTβ)"**.

Curriculum vitae

2004. Postgraduate course: "Introduction to Oncology. Cellular and Tumoral Biology". School of Medical Sciences. Rosario National University, Rosario, Argentina.

Publications

- Kallenbach, M., **Gilardoni, P.A**., Bonaventure, G., Wissgott, A. and Baldwin, I.T. "Eavesdropping on jasmonic acid biosynthesis as criteria for host choice". (Manuscript in preparation)
- **Gilardoni, P.A**., Hettenhausen, C., Baldwin, I.T. and Bonaventure, G. "The *Nicotiana attenuata* Na*LecRK1* gene suppresses the salicylic acid-mediated inhibition of induced defense responses during *Manduca sexta* herbivory". (Submitted to The Plant Cell, PLANTCELL/2011/088229).
- Kallenbach, M., **Gilardoni, P.A**., Allmann, S., Baldwin, I.T. and Bonaventure, G. "C_{12} derivatives of the HPL pathway are produced by product-recycling through LOX2 1 in *Nicotiana attenuata* leaves". Accepted for publication in New Phytologist..
- **Gilardoni, P.A**., Schuck, S., Jüngling, R., Rotter, R., Baldwin, I.T. and Bonaventure, G. "SuperSAGE analysis of the *Nicotiana attenuata* transcriptome after fatty acid-amino acid elicitation (FAC): Identification of early mediators of insect responses". BMC Plant Biol. 10: p.66.
- Marcucci, H., Elena, C., **Gilardoni, P.A**. and Banchio, C. "Characterization of the murine CTP:phosphocholine cytidylyltransferase beta gene promoter". Biochim Biophys Acta, 2008. 1781(5): p.254.
- Astronomical Report observation of the "Leonidas meteor shower". MeteorObs. 17.11.96. http://www.meteorobs.org/maillist/msg02379.html

Oral presentations

- "LecRK: a novel receptor-like kinase involved in Nicotiana attenuata's defense against Manduca sexta". **Gilardoni, P.A.**, Baldwin, I.T., and Bonaventure, G. 15.02.10. 9th IMPRS Symposium, Jena, Germany.

- "Elucidating the role of PNRP, AEP150 and AEP65 in plant defense against herbivores and pathogens. Schuck, S., **Gilardoni, P.A.**, Baldwin, I.T., and Bonaventure, G. 15.02.10. 9 Th IMPRS Symposium, Jena, Germany.
- "Characterization of a receptor-like kinase of Nicotiana attenuata". **Gilardoni, P.A**., Baldwin, I.T., and Bonaventure, G. 08-11.11.09. Ringberg Symposium. Kreuth, Germany.
- "Identification of components of the FAC signal transduction pathway in Nicotiana attenuata". **Gilardoni, P.A.**, Baldwin, I.T., and Bonaventure, G. 22.06.09. Institute Symposium 2009. Max Planck Institute for Chemical Ecology. Jena, Germany.
- Marcucci, H., **Gilardoni, P.A.**, Banchio, C. *"Biosynthesis of phosphatidylcholine during neuronal differentiation".* XLII Annual Meeting of the Argentine Society for Biochemistry and Molecular Biology (SAIB). Rosario, Argentina. 12-15 November 2006.

Poster presentations

- "LecRK: a novel receptor-like kinase involved in *Nicotiana attenuata's* defense against *Manduca sexta".* **Gilardoni, P.A.**, Baldwin, I.T., and Bonaventure, G. 07.02.11. 10th IMPRS Symposium, Jena, Germany.
- "Jasmonic acid as a direct defense against herbivores: Empoasca spp. choose their host plants by eavesdropping on aposmatic JA". Kallenbach, M., **Gilardoni, P.A**., Bonaventure, G., and Baldwin, I.T. *07.02.11. 10th IMPRS Symposium, Jena, Germany.*
- "The transcriptome platform: Next generation sequencing and quantification of mRNA and smRNA". Gase, K., Gaquerel,E., **Gilardoni, P.A**., Galis,I., Kroeber, W., Bonaventure, G., Pandey, S., Hahn, T., Gulati, J. and Baldwin, I.T. SAB 2010, Jena, Germany.
- "Signaling in the real world: aposomatic JA signaling, evil lollipops and what the neighbors think about alarm calling". Kallenbach, M., **Gilardoni, P.A.**, Weinhold, A., Schuman, M., Bonaventure, G., Gaquerel, E., Wissgott, A. and Baldwin, I.T. SAB 2010, Jena, Germany.
- "Profiling the derivatives of the HPL pathway in *N. attenuata*: Hydroxylated C12 alkenal as major product of NaLOX2". Kallenbach, M., **Gilardoni, P.A.**, Baldwin, I., and Bonaventure, G. 15.02.10. 9th IMPRS Symposium, Jena, Germany.

Curriculum vitae

- "Early transcriptional targets of the FAC signal transduction pathway in N.attenuata: a SuperSage approach". **Gilardoni, P.A.**, Baldwin, I., and Bonaventure, G. 02-03.03.09. 8th Biannual IMPRS Symposium. Max Planck Institute for Chemical Ecology. Jena.
- "Gene expression analysis after FAC elicitation in Nicotiana attenuata plants by SuperSAGE". **Gilardoni, P.A.**, Baldwin, I., and Bonaventure, G. 24-26.08.09. Utrecht Summerschool on Environmental Signalling. Utrecht. The Netherlands.
- "Early transcriptional targets of the FAC signal transduction pathway in N.attenuata: a SuperSage approach". **Gilardoni, P.A.**, Baldwin, I., and Bonaventure, G. 25-26.09.08. Institute Symposium 2008 and 1st MPICE Alumni Meeting. Max Planck Institute for Chemical Ecology. Jena.
- "Identification of the early transcriptional targets of the FAC signal transduction pathway". **Gilardoni, P.A.**, Baldwin, I., and Bonaventure, G. 25-26.02.08. 7th IMPRS Symposium, Jena, Germany.
- "Mecanismo de regulación de la expresión de la enzima CTP:FOSFOCOLINA CITIDILTRANSFERASA isoforma β"- **Gilardoni, P.A.**, and Banchio C. VII Congress and XXV Annual Meeting of the Biology Society of Rosario. Rosario, Argentina. 12-14 December 2005.
- "Transcriptional Regulation of Ctp: Phosphocholine Cytidylyltransferase Beta". **Gilardoni, P.A.**, and Banchio C. X Congress of the Panamerican Association for Biochemistry and Molecular Biology (PABMB), the XLI Annual Meeting of the Argentine Society for Biochemistry and Molecular Biology (SAIB) and the XX Annual Meeting of the Argentine Society for Neurochemistry (SAN). Pinamar, Argentina. 3-6 December 2005.

Paola Gilardoni

Jena, den 05 Juli 2011

Selbständigkeitserklärung

Entsprechend der geltenden, mir bekannten Promotionsordnung der Biologisch-Pharmazeutischen Fakultät der Friedrich-Schiller-Universität Jena erkläre ich, daß ich die vorliegende Dissertation eigenständig angefertigt und alle von mir benutzten Hilfsmittel und Quellen angegeben habe. Personen, die mich bei der Auswahl und Auswertung des Materials sowie bei der Fertigstellung der Manuskripte unterstützt haben, sind am Beginn eines jeden Kapitels genannt. Es wurde weder die Hilfe eines Promotionsberaters in Anspruch genommen, noch haben Dritte für Arbeiten, welche im Zusammenhang mit dem Inhalt der vorliegenden Dissertation stehen, geldwerte Leistungen erhalten. Die vorgelegte Dissertation wurde außerdem weder als Prüfungsarbeit für eine staatliche oder andere wissenschaftliche Prüfung noch als Dissertation an einer anderen Hochschule eingereicht.

Paola Gilardoni

Jena, den 05 Juli 2011